VISCOSITIES AND DENSITIES OF METHANE, PROPANE AND THEIR MIXTURES AT LOW TEMPERATURES AND HIGH PRESSURES

by 829

Edward T. S. Huang
B.S. in Ch.E., Taiwan Cheng Kung University, 1958
M.S. in Ch.E., University of Kansas, 1963

Submitted to the Department of Chemical and Petroleum Engineering and the Faculty of the Graduate School of the University of Kansas in partial fulfillment of the requirements for the degree of Doctor of Philosophy.

Advisory Committee:

Redacted Signature

Chairman

Redacted Signature

Redacted Signature

Redacted Signature

Redacted Signature

March, 1966

ACKNOWLEDGEMENTS

The National Science Foundation Grant No. GP-386 provided for the purchase of a major portion of the equipment and certain of the hydrocarbons, and the Phillips Petroleum Company furnished certain of the hydrocarbons used in this research. The University of Kansas Research Fund provided the financial assistance for the author, and the University of Kansas Computer Center donated the computer time. The assistance and donations of these organizations are sincerely appreciated.

The author is greatly indebted to Dr. Fred Kurata, advisor to this research, for his continuous interest, encouragement and guidance which led to the success of this project.

The author is also indebted to Dr. G.W. Swift for his constant helpful advice and consultation during the course of this research. Special appreciation is expressed to him for his close guidance and valuable criticisms which made the completion of this project possible in the absence of Dr. Kurata.

Sincere thanks are given to Mr. Morris Teplitz, the Research Chemist of the Department of Chemical and Petroleum Engineering, the University of Kansas, who loaned laboratory equipment and unselfishly gave ideas on the equipment problems.

Dr. N.S. Nahman, the director of the Electronic Research Laboratory, the University of Kansas, generously allowed the author the use of the equipment in his laboratory. He and Mr. B.D. Pradham were of invaluable assistance in designing the transistorized temperature control unit for this research. Mr. Warren Legler of the Department of Electrical Engineering was kind enough to design the electrical timing circuit used in this study.

Mr. J.G. McCreary is appreciated for his assistance in the construction of the equipment, the calibration of the mass injection cylinder, and his generosity in letting the author use his linear regression computer program.

Dr. D.L. Schindler assisted the author in the analysis of methane and propane used in this study by gas chromatograph. Mr. C.R. Clark provided the information concerning the experimental compressibility data

on "pure grade methane" determined by the technique of low temperature direct weighing. Messrs. R.K. Geery, D.L. Johnson and G. Pfantz assisted in the construction of the accessory experimental equipment. Mr. Gilbert Suazo fabricated the falling cylinders.

In general, the support of the faculty and staff of the Department of the Chemical and Petroleum Engineering is very much appreciated.

Special appreciation is expressed to the author's wife, Susan, for her constant encouragement, assistance and patience.

TABLE OF CONTENTS

TABLE OF CONTENTS (Cont.)

TABLE OF CONTENTS (Cont.)

APPENDIXES

LIST OF FIGURES

LIST OF FIGURES (Cont.)

LIST OF TABLES

LIST OF TABLES (Cont.)

SUMMARY

The purpose of this study was to determine experimentally the viscosity and density data for methane, propane and the mixtures of methane and propane at low temperatures and high pressures, and to test the applicability of the existing empirical viscosity correlations to the data of this study.

In order to achieve this purpose, a viscometer and the auxiliary equipment capable of determining experimentally these data were needed. Therefore, an experimental apparatus consisting of the following units was designed and constructed:

(1) A high pressure falling cylinder viscometer for viscosity and density determination.

(2) A low temperature differential pressure indicator for pressure measurement in the investigation of liquid mixtures at low temperatures to prevent changes in the composition of the mixture in the viscometer.

(3) A low temperature bath, for maintaining a constant temperature environment for the viscometer and the low temperature differential pressure indicator.

(4) A high temperature bath containing high pressure equipment for the displacement of the fluids into the viscometer (density determination), the preparation of mixtures, and the generation of high pressures.

Since the viscometer used in this study is a relative instrument, the viscometer has to be calibrated. Three falling cylinders, each falling in the same viscometer tube, were calibrated for the viscosity determination in this study. The calibration data were then correlated by the following relationship,

$$\beta_{red} = \beta_{p,t}/\beta_{calc} = f(N_{Re}) = f(D_e s\rho/\bar{\mu}\theta) \qquad (1)$$

where,

$$\beta_{p,t} = \bar{\mu}s/(\sigma-\rho)\theta$$

$$\beta_{calc} = gD_e^2(1-\kappa)^2(1-\kappa^2)^4/\{32\kappa^6(1+\kappa^2)[(1+\kappa^2)\ln(1/\kappa)-(1-\kappa^2)]\}$$

$$D_e = 2\kappa^4 D_t[(1+\kappa^2)\ln(1/\kappa)-(1-\kappa^2)]/[(1-\kappa)(1-\kappa^2)^2]$$

$$k = D_c/D_t$$

Equation (1) is similar to that developed by Lohrenz[1]. After observing the viscometer calibration plot, β_{red} versus $\log(N_{Re})$, a transition Reynolds number where the linear and non-linear portions of the curve met, was selected for each falling cylinder, and the functional relationship, Equation (1), was represented by two empirical equations:

$$\beta_{red} = A_o + A_1 \log(N_{Re}) \qquad (2)$$

for the flow regime where the Reynolds number was less than the transition value, and

$$\beta_{red} = B_o + B_1 \log(N_{Re}) + B_2[\log(N_{Re})]^2 \qquad (3)$$

for the flow regime where the Reynolds number was greater than the transition value. The viscometer calibration data in each flow regime were fitted to a appropriate equation by regression analysis, and the deviations between experimental β_{red} and those computed from the regression analysis were within $\pm 0.85\%$.

The mixtures investigated in this study were prepared in the high temperature bath by the volumetric displacement of predetermined amounts of pure components at known pressure and temperature conditions into the mixture make up cylinder. The composition of the mixture was then computed from the volumes of pure components transferred and the literature densities of pure components at the appropriate displacement condition of pressure and temperature. The maximum uncertainty in the composition of the mixture obtained from this technique is estimated to be 0.001 mole fraction.

The viscosity and density data for methane, propane and the three mixtures of these were determined experimentally and the recommended values for these fluids are presented in tabular form for the temper-

[1] Lohrenz, J., Ph. D. Thesis, The University of Kansas, Lawrence, Kansas (1960).

ature and pressure ranges shown below:

	Mole % Methane				
	0.0	22.1	50.0	75.3	100.0
Temp. range(°C.)	0 to -100	37.78 to -120	37.78 to -120	37.78 to -150	0 to -170
Press. range	From 100 psia to 5,000 psia				

Density data for methane, except the low temperature vapor data, were not determined in this study, since these data are available in the literature[2,3]

The maximum estimated error in the viscosity for pure components is ±3.4%, and for mixtures is ±3.8%. The reproducibility of viscosity measurements on the average was ±1.2%, and the agreement of viscosities of this study with those from the literature was, for the most part, within ±2.0%. The maximum estimated error in density for pure components is ±0.6% and for mixtures is ±1.2%. Density data of mixture are subject to systematic errors caused by impurities in methane of at most 0.6% higher than the probable true values, while those of methane are subject to 0.8% higher than the probable true values. The agreement of densities of this study with those from the literature for propane was within ±0.1%, and for methane and mixtures was within ±1.2%.

The residual viscosity, that is the difference between the viscosity at any given temperature and pressure and the viscosity at the same temperature and low pressure, has been demonstrated by several investigators to be a function of density only, and the correlation has been used to test the consistency of the experimental viscosity data at low densities. The viscosity and the density data of this study in the high density region were used to construct residual viscosity versus density plots. For the data of methane and propane, the residual viscosity was shown to be a function of density only, but for the data of

[2] Kvalnes, H.M., and Gaddy, V.L., J. Am. Chem. Soc., 53, 394 (1931).
[3] van Itterbeek, A., Verbeke, O., and Staes, K., Physica, 29, 742 (1963).

mixtures, the residual viscosity seemed to depend not only on density but also on temperature. The existing residual viscosity versus density correlations as generalized for the application to the different pure components and mixtures were also tested for their applicability to the current data for methane-propane system in the high density region. Of all the correlations tested, that of Agaev and Golubev[4] was found to be the best.

One general shortcoming of the residual viscosity versus density correlation in the high density region is that the slope of the curve is so steep that the correlation requires highly accurate density data in order to interpolate the viscosity with good accuracy. Therefore, this type of correlation is not very practical for the viscosity prediction of high density fluids. For example, in case of light hydrocarbons at low temperatures, density data of which are almost nonexistent, it is impossible to predict the viscosity of these hydrocarbons from this correlation. A viscosity correlation for the fluid in the high density region not depending on the density would be more practical, and so the Andrade equation for liquid viscosity correlation was used.

The viscosity data in the liquid region for methane, propane and each of the three mixtures studied were well correlated by the Andrade equation. However, the correlation of all the viscosity data for methane-propane system in terms of a modified Andrade equation, based on the principle of corresponding states,

$$\ln \mu_r = (D_o+D_1P_r)+(D_2+D_3P_r)/T_r \qquad (4)$$

was not successful. The current viscosity data for each constant composition fluid in the following region were used to compute the coefficients of Equation (4) by regression analysis:

$$\rho_r \geq 2.2$$

$$1.2 \leq 1/T_r \leq 2.1$$

$$P_r \leq 8.1$$

[4] Agaev, N.A., and Golubev, I.F., Gazovaya, 8, No. 5, 45 (1963).

This equation and the coefficients computed can be used to interpolate the viscosity of methane, propane or each of the three mixtures respectively in the above mentioned region with average deviations of $\pm$2.3%.

In short, the viscosity and density data for methane-propane system at temperatures below 37.78°C. and pressures to 5,000 psia were determined, and the recommended viscosity and density values are presented. These data in the high density region were correlated by the conventional viscosity correlation, i.e., the residual viscosity versus density correlation. Of all the correlations tested, that of Agaev and Golubev[4] was the best. However, it was found that this type of correlation is not practical in the high density region for the viscosity prediction of light hydrocarbons at low temperatures, since the correlation requires highly accurate density data. The present viscosity data for each pure component or each constant composition mixture were well correlated by the density independent Andrade equation respectively. However, the generalized correlation of all the viscosity data for methane-propane system in terms of the Andrade equation and the principle of corresponding states was not successful.

CHAPTER I

INTRODUCTION

Due to the recent developments in cryogenic technology, there has been an increasing interest in the low temperature processing, shipping and storing of natural gas in the petroleum and natural gas industry. As the result of this, there is more emphasis on the extension of the measurements of physical properties of light hydrocarbons (such as transport properties) at low temperatures. One of the important transport properties is viscosity.

A survey presented by Liley (45) on the theoretical and experimental viscosity studies on gases and liquefied gases at temperatures less than 500°K. shows a lack of systematic investigation of viscosities for pure light hydrocarbons and their mixtures at low temperatures. Therefore there is a need for studies of the viscosity behavior of light hydrocarbons and their mixtures at low temperatures.

Lim, et al. (46) investigated the low pressure liquid viscosities of the methane-propane, methane-n-butane and ethane-n-butane systems at low temperatures. Since the equipment they used was inadequate for the study of mixtures, their data were subject to question. The present study, a continuation of the work of Lim, et al., was initiated to thoroughly investigate one of the binary systems mentioned above, using improved equipment to determine the viscosity data over wide ranges of temperature and pressure. The systematic investigation of such a system will provide valuable information regarding the viscosity dependence on temperature, pressure and composition, so that a correlation of these variables can be developed.

Methane, propane and the mixtures of these were selected for the investigation at temperatures below 37.78°C. and pressures to 5,000 psia, because:

(a) methane being a predominent component in natural gas, a binary system containing methane would be of value,

(b) the phase behavior information of this system (2,58,62) from the critical temperature of propane to -130°C. is available; these

data are necessary to insure that the experimental measurements on viscosity at low pressures are in the liquid phase, and they are needed for the extrapolation of the high pressure viscosity data to the bubble point condition so as to define the saturated liquid viscosity data.

Literature Survey on the Viscosity for the Methane-Propane System

A literature survey was undertaken to search for work pertinent to the viscosities for the methane-porpane system. In the superambient temperature region, a number of investigations have been conducted on methane (4,6,7,14,17,20,27,64) and propane (4,7,13,20,27,71,73,75,76), and two papers (7,27) reported data on the viscosity of mixtures of methane and propane. At low temperatures, very little work has been done. Rossini, et al. (65) reported a compilation of the atmospheric pressure viscosity data for the pure, light paraffin hydrocarbons at temperatures below their normal boiling points, and Swift and coworkers (75,76) investigated the liquid viscosities for methane, ethane, propane and n-butane at temperatures above their normal boiling points. Pavlovich and Timrot (55) reported the viscosity for methane at temperatures to -161°C. and pressures to 2,940 psia; Ross and Brown (67) and Barua, et al. (6) reported the viscosity data for methane at temperatures down to -50°C. and at pressures to 10,000 psia and 2,576 psia respectively. For mixtures at low temperatures, no data have been reported except for those of Lim, et al. (46).

Equipment Needed to Study the Proposed System

To obtain the viscosity for the proposed system, it is necessary to develop a viscometer and the related equipment. Swift and coworkers (75,76) used a falling cylinder viscometer satisfactorily for the determination of liquid viscosity at low temperatures and pressures to 800 psia. This viscometer is a relative instrument and has the advantage of being able to measure viscosity and density concurrently. This falling cylinder viscometer was further improved after Lohrenz and coworkers (47,48,49) had developed the theory for the falling cylinder

viscometer and presented an accurate method for correlating the viscometer calibration data. In order to utilize the theoretical and experimental developments of these investigators, a falling cylinder viscometer modified for high pressures was used in this investigation.

In the determination of viscosity using a falling cylinder viscometer, the viscosity is computed from the following equation (47,75):

$$\bar{\mu} = \beta_{p,t}(\sigma-\rho)\theta/s \qquad \text{(I-1)}$$

where $\beta_{p,t}$ is the viscometer calibration constant, σ is the density of the falling cylinder, θ is the time required for the falling cylinder to traverse the distance s, and ρ is the density of fluid at the condition where θ is determined. It should be noted from Equation (I-1) that density is necessary for the computation of the viscosity from the experimentally determined fall time, θ. A search of the literature for the density data of the methane-propane system shows that except for the density data for methane (40,78), those for propane and the mixtures of methane and propane are not available at low temperatures and high pressures. Therefore the density data for propane and for the mixtures of methane and propane was included as a part of this study.

In viscosity and density determinations of mixtures containing light hydrocarbons at low temperatures, the experimental problems encountered are more complex than those for investigating pure components. This additional complexity was not properly treated by Lim, et al. (46) in their experimental study. They used a Heise bourdon tube gage to measure directly the pressure of the mixtures in the viscometer operating at low temperatures. Referring to Figure I-1, when the cricondentherm temperature of the mixture studied, T_{cc}, is higher than ambient temperature, T_2, and the pressure, P_1, of the mixture in the viscometer is lower than the bubble point

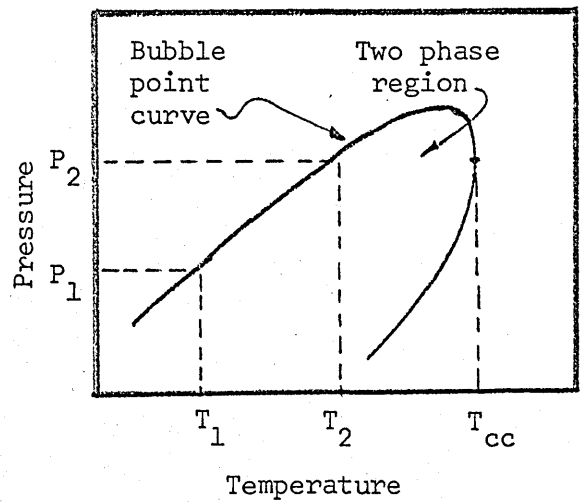

Figure I-1 P-T Diagram for A Mixture

pressure, P_2, of the mixture at ambient temperature, composition changes in the experimental system occur since two phases exist in the bourdon tube. One way to solve this problem is to enclose completely the mixture to be investigated at a low temperature, T_1, at which the viscometer is operated. The pressure of the mixture is then transmitted by some mechanical separation device such as a bellows (a low temperature differential pressure indicator) to an inert fluid on the other side of the separation device so that the pressure of the mixture can be determined indirectly with a Heise bourdon tube gage.

Additional Literature Survey and Analysis of Viscosity and Density Data for the Calibration of the Viscometer

Since the viscometer used in this study is a relative instrument, it was necessary to select reliable and consistent values of viscosity and density for the viscometer calibration. A survey of literature showed that viscosity data for light paraffin hydrocarbons were reported by numerous investigators. Especially in the last few years, several investigators had devoted much effort to systematic and extensive studies of the viscosities for the pure, light paraffin hydrocarbons. In the following analysis of the literature, only those works published systematically in the last few years will be discussed because these later works are considered to have better agreement. Table I-1 shows a summary of the reported viscosity data, the investigators, the types of instrument used, and the reported temperature and pressure range.

Ellington and coworkers (23,25,41,42,73) using a capillary viscometer, reported the viscosity data for ethane, propane, n-butane, n-pentane and n-decane over considerable pressure and temperature ranges. For the purpose of establishing confidence in the reported viscosity data, Sage and coworkers (13,14,15,16,60) used an entirely different instrument, a rotating cylinder viscometer, to determine the viscosity data for methane, ethane, propane, n-butane and n-pentane at selected isotherms for comparison. Within the temperature and pressure ranges concerned with the viscometer calibration of this study, i.e., at pres-

Table I-1

Viscosity Values for Pure Normal Paraffin Light Hydrocarbons near Ambient Temperatures and to High Pressures

Fluid	Investigators	Type of Viscometer	Temp. range °F.	Press. range psia
C_2H_6	Eakin,Starling,Dolan,Ellington(25)	Capillary	70 to 460	to 10,000
C_3H_8	Starling,Eakin,Ellington(73)	Capillary	70 to 460	to 8,000
nC_4H_{10}	Dolan,Starling,Lee,Eakin,Ellington	Capillary	100 to 460	to 10,000
nC_5H_{12}	Lee and Ellington(41) (23)	Capillary	100 to 340	to 3,000
$nC_{10}H_{22}$	Lee and Ellington(42)	Capillary	100 to 460	2,000 to 8,000
$C H_4$	Carmichael,Berry,Sage(14)	Rotating cylinder	40 to 400	to 5,000
C_2H_6	Carmichael,Sage(15)	Rotating cylinder	80 to 400	to 5,000
C_3H_8	Carmichael,Berry,Sage(13)	Rotating cylinder	40 to 400	to 5,000
nC_4H_{10}	Carmichael and Sage(16)	Rotating cylinder	40 to 320	to 5,000
nC_5H_{12}	Reamer,Cokelet,Sage(60)	Rotating cylinder	100 to 280	to 5,000
$C H_4$	Baron,Well,Roof(4)	Capillary	125 to 275	to 8,000
C_2H_6	Baron,Well,Roof(4)	Capillary	125 to 275	to 8,000
C_3H_8	Baron,Well,Roof(4)	Capillary	125 to 275	to 8,000
nC_5H_{12}	Agaev and Golubev(1)		77 to 527	to 7,350
$C H_4$	Giddings(27)	Capillary	50 to 280	to 8,000
C_3H_8	Giddings(27)	Capillary	40 to 220	to 8,000
$C H_4$	Barua,Afzal,Flynn,Ross(6)	Capillary	-58 to 302	to 2,576

sures below 5,000 psia and at temperatures below 190°F., the viscosity data for ethane, propane and n-butane of Sage and coworkers agree with those of Ellington and coworkers for the most part within ±1%. The data for propane from these sources also agree well with those reported by Giddings (27). The viscosity data for ethane and propane of Baron, et al. (4) at 175°F. agree well with these data, but are high by as much as 6% at 125°F. Viscosity data for methane, published by Sage and coworkers (14), are in good agreement with those reported by Barua, et al. (6), Giddings (27) and Baron, et al. (4). Methane viscosity data reported by Barua, et al. (6) cover a wide temperature range, and are considered to be consistent with the data for ethane, propane and n-butane reported by Ellington, et al., because the data of Barua, et al. are consistent with those reported by Sage and coworkers.

The data for n-pentane from different sources are inconsistent. Those of Sage and coworkers (60) are about 10% higher than those of Ellington and coworkers (41), and Agaev and Golubev (1). The data of the latter two sources deviate from each other by about 2.5% at 5,000 psia and the deviations at different isotherms (100 and 190°F.) are not in the same direction.

For the heavier paraffin hydrocarbons at low pressure, the compilation of Rossini, et al. (65) reports atmospheric pressure viscosity and density data below the normal boiling points. For the density data for all the paraffin hydrocarbons mentioned above, values are available in the monograph reported by Sage and Lacey (66). Kvalnes and Gaddy (40) also reported density data for methane from -70 to 200°C. These data are in good agreement with those reported by Sage and Lacey.

In short, the viscosity data for methane reported by Barua, et al. (6), those for ethane, propane, n-butane and n-decane reported by Ellington and coworkers (23,25,42,73), the density data for methane reported by Kvalnes and Gaddy (40), those for the paraffin hydrocarbons reported by Sage and Lacey (66), and the atmospheric pressure liquid viscosity and density data of the paraffin hydrocarbons reported by Rossini, et al. (65) were considered consistent for calibrating the viscometer.

Review of Viscosity Correlations

While searching the viscosity data, many empirical viscosity correlations were found. The principle of corresponding states had been applied to the generalized correlation for different fluids for a long time. Lately much attention has been devoted to the residual viscosity versus density correlation.

Several investigators used the principle of corresponding states to construct the generalized viscosity correlations for gas and dense gas by expressing the reduced viscosity as a function of reduced temperature and reduced pressure. The reduced temperature, T_r, was generally defined as the ratio of temperature to critical temperature, the reduced pressure, P_r, as the ratio of pressure to critical pressure, and the reduced viscosity, μ_r, as the ratio of viscosity to a characteristic parameter I. I was defined differently by different investigators. It was defined by Uyehara and Watson (77) to be critical viscosity, by Comings, et al. (20) to be atmospheric pressure viscosity, and by Smith and Brown (71) to be the square root of the molecular weight. Grunberg and Nissan (30) correlated μ_r as a function of T_r and reduced density, ρ_r, where I is the atmospheric pressure viscosity and ρ_r is the ratio of density to critical density. These correlations are basically similar. Each investigator attempted to define the most convenient characteristic parameter to define the reduced viscosity. These correlations could also be used for the prediction of the liquid viscosity. Because of the general nature of these correlations, the prediction of viscosity from these correlations is subject to errors as large as 20%.

For the correlation of liquid viscosity Brush (12) in his review on the theories of liquid viscosity, pointed out that the simplest and the most frequently used empirical equation is the so called Andrade equation,

$$\ln \mu = a + b/T \qquad \text{(I-2)}$$

Several investigators (3,5,9,31,79) have used this equation with some success to express low pressure liquid viscosity as a function of temperature.

In the past few years, attention has been given to the correlation of residual viscosity as a single function of density. The residual viscosity is defined as the difference between the viscosity at any given temperature and pressure and the viscosity at the same temperature and low pressure (or atmospheric pressure). The validity of this type of correlation has been established in the low density region by several investigators. Thodos and coworkers (10,69) applied this concept to correlate the viscosity of monoatomic and diatomic gases. Most of the viscosity data for each pure, light paraffin hydrocarbon in the superambient temperature region cited earlier were also correlated using this technique. This technique has become so popular that it is now used by most investigators for (a) the internal consistency test of the experimental viscosity data, (b) the interpolation and extrapolation of the viscosity data, and (c) the estimation of the critical viscosity from the knowledge of the critical density.

In an effort to develop a residual viscosity versus density correlation applicable to the viscosity prediction of all the pure components, Jossi, et al. (38) developed a correlation for the prediction of viscosities of several substances in the dense gaseous, and liquid regions, where the residual viscosity, multiplied by a group of critical constants, was shown to be a function of reduced density only. Using a similar approach, Golubev and Agaev (29) developed a correlation for the pure, light paraffin hydrocarbons by plotting the reduced residual viscosity versus reduced density. Eakin and Ellington (24) developed an analytical equation for the prediction of viscosities of methane, ethane, propane and n-butane by expressing the residual viscosity as a function of density and molecular weight.

The development of correlations for the prediction of the viscosities of pure components and mixtures has also been attempted. Dean and Stiel (21) extended the correlation of Jossi, et al., for the prediction of the viscosities of dense gas mixtures. Giddings and Kobayashi (27,28) reported viscosities of methane, propane and mixtures of these and showed that the residual viscosity was a function only of density for each mixture, and developed a correlation for pure components and mixtures

by graphically expressing the residual viscosity as a function of reduced density and molecular weight. Lee, et al. (43), using the viscosity data of pure, light paraffin hydrocarbons reported by Ellington and coworkers (23,25,73) and the methane-n-butane mixture of Dolan and Ellington (22), developed an equation with a method slightly different from the residual viscosity correlation for the calculation of viscosities of these hydrocarbons and their mixtures. They expressed viscosity as a function of density, molecular weight and temperature.

Most of the correlations mentioned thus far were developed primarily on the basis of viscosity and density data for fluids at superambient temperatures. It would be advantageous to test the applicability of these correlations to the high pressure, low temperature liquid viscosity and dnesity data for light hydrocarbons if such data are available. A viscosity correlation applicable to the liquefied light hydrocarbons should be very useful for the prediction of their viscosities and could reduce the experimental work if it is suitable for interpolation.

Restatement of the Scope of This Study

Before proceeding to the next chapter, the scope of the present study is restated as follows:

(a) to construct a viscometer and auxiliary equipment suitable for determining viscosity and density of the pure light hydrocarbons and their mixtures at temperatures to -170°C. and pressures to 5,000 psia,

(b) to determine the viscosities for methane, propane and their mixtures at temperatures below 37.78°C. and pressures to 5,000 psia, and the densities for propane, and mixtures of methane and propane over the same temperature and pressure ranges as those over which the viscosities were determined, and

(c) to test the applicability of the existing empirical viscosity correlations to the low temperature, high pressure data of this study.

CHAPTER II

THEORY AND METHOD OF THE VISCOMETER CALIBRATION

Review of the Theory Pertinent to the Viscometer Calibration

The method for calculating the theoretical viscometer constant for a falling cylinder viscometer and the method for correlating experimental viscometer calibration data in terms of the theory for Newtonian fluids have been developed by Lohrenz and coworkers (47, 48,49).

In the development of the equation for the prediction of the theoretical viscometer constant β_{lsf}, Lohrenz (47) considered that a falling cylinder (see Figure II-1) with density σ and volume V ($\pi D_c^2 L_e/4$) was placed concentrically in a vertical tube which had an inner diameter D_t and was filled with a Newtonian fluid of density ρ and viscosity $\bar{\mu}$. He assumed that the body was falling at terminal velocity v_T, that the fluid flowing through the annulus between the cylinder and the tube was in fully developed laminar flow, and that all friction losses other than the laminar skin friction (lsf) on the cylinder were negligible. With these assumptions, he obtained the following expression for the theoretical prediction of the viscometer constant:

$$\beta_{lsf}=[gL_e(D_{eL})^2/8L_c][\ln(1/\kappa)-(1-\kappa^2)/(1+\kappa^2)] \qquad \text{(II-1)}$$

where κ is the ratio of D_c to D_t, L_c is the length of the cylindrical portion of the falling cylinder, L_e is the equivalent length of the cylinder* and D_{eL} is an equivalent

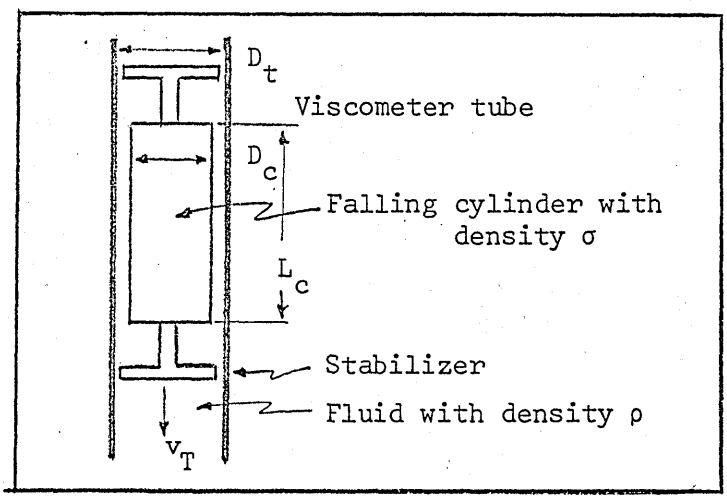

Figure II-1 A schematic Diagram of A Falling Cylinder Viscometer

* L_e is defined as the ratio. of the volume of falling cylinder including stabilizers to the cross-sectional area of the cylindrical portion(Fig.II-1).

diameter defined as,

$$D_{eL} = \kappa D_t \sqrt{2[\ln(1/\kappa) - (1-\kappa^2)/(1+\kappa^2)]} \qquad \text{(II-2)}$$

Equation (II-1) expresses β_{lsf} as a function of D_c, D_t, L and L_e, the physical dimensions of the viscometer. For the calculation of β_{lsf}, the dependence of D_c and D_t on temperature and pressure has to be considered. The temperature and pressure effects on L_c and L_e would cancel each other since L_c and L_e appear on both denominator and numerator. The temperature effect can be predicted from the coefficient of thermal expansion, and the pressure effect can be obtained by assuming a thick walled cylinder of infinite length for both the falling cylinder and the viscometer tube (47). If the linear coefficient of thermal expansion, Young's modulus and Poisson's ratio are assumed to be constant, the following equations may be used to calculate D_c and D_t where temperature and pressure effects are assumed to be independent of one another:

$$D_{c(t,p)} = D_{c(25,0)}[1+\alpha_c(t-25)][1-P(1-\nu_c)/E_c] \qquad \text{(II-3)}$$

$$D_{t(t,p)} = D_{t(25,0)}[1+\alpha_t(t-25)] \left\{1 + \frac{P}{E_t}\left[\frac{D^2_{to(t,0)}+D^2_{t(t,0)}}{D^2_{to(t,0)}-D^2_{t(t,0)}} + \nu_t\right]\right\} \qquad \text{(II-4)}$$

where t is in centigrade and P is in psia. The coefficient of thermal expansion (α), Young's modulus (E) and Poisson's ratio (ν) are given in Table II-1.

Table II-1

Mechanical Properties of the Viscometer Materials of Construction

	Stainless steel (Lyman)(50)	Aluminum (Popov)(56)
Coefficient of thermal expansion 1/°C.	1.602×10^{-5}	2.340×10^{-5}
Young's modulus psi	0.290×10^{8}	0.103×10^{8}
Poisson's ratio	0.26	0.333

Therefore, by substituting Equations (II-3) and (II-4) into Equation (II-1), β_{lsf} at any pressure and temperature for a given viscometer can be calculated. Since this viscometer is used as an relative instrument, it must be calibrated with fluids of known viscosity and density where the experimental viscometer constant, $\beta_{p,t}$, is computed from Equation (I-1) with the experimentally determined fall time θ at pressure P and temperature T.

With this information, Lohrenz showed that a plot of the ratio of the experimental viscometer constant, $\beta_{p,t}$, to the calculated viscometer constant, β_{lsf}, versus Reynolds number, $D_{eL}v_T\rho/\mu$ resulted in an unique curve, i.e.,

$$\beta_{p,t}/\beta_{lsf} = f(D_{eL}v_T\rho/\mu) \qquad \text{(II-5)}$$

This equation takes into account the effects due to temperature, pressure and flow regime. He further concluded that this plot was the most accurate method of calibrating the viscometer.

Modification of the Variables for the Correlation of Viscometer Calibration Data

In the present study, the method of correlating the viscometer calibration data developed by Lohrenz, et al. (47,48,49), will be used with a slight modification. In the develpment of the viscometer calibration method, Lohrenz defined his Reynolds number in terms of an arbitrarily defined equivalent diameter, D_{eL}. The accuracy of the calibration plot would not be effected by how the equivalent diameter is defined. The equivalent diameter used in this study will be defined according to a more conventional method. According to Bird, et al. (8), the friction factor, f, of the fluid flowing through the annulus between the tube and the falling cylinder is related to a force F_k, a characteristic area A and a characteristic kinetic energy per volume K by the relationship,

$$f = F_k/(AK) \qquad \text{(II-6)}$$

$$F_k = \Delta P(\pi D_t^2/4)(1-\kappa^2)$$

$$A = \pi D_t(1+\kappa)L_c$$

$$K = \rho\langle v\rangle^2/2$$

where $\langle v_z \rangle$ is the average velocity of the fluid flowing through the annulus, and P is the pressure drop across the cylinder. Since the over-all flow of the fluid flowing through the annulus of the falling cylinder viscometer is,

$$q = v_T(\pi D_c^2/4)$$

the average velocity is,

$$\langle v \rangle = q/[\pi(D_t^2-D_c^2)/4]$$

$$= \kappa^2 v_T/(1-\kappa^2) \qquad \text{(II-7)}$$

According to Lohrenz (47),

$$\Delta P = 16\bar{\mu}L_c v_T/\{D_t^2[(1+\kappa^2)\ln(1/\kappa)-(1-\kappa^2)]\} \qquad \text{(II-7a)}$$

Substituting Equations (II-7) and (II-7a) into Equation (II-6) and rearranging the equation,

$$f = \frac{8\bar{\mu}}{\rho v_T} \frac{(1-\kappa)(1-\kappa^2)^2}{D_t\kappa^4[(1+\kappa^2)\ln(1/\kappa)-(1-\kappa^2)]} \qquad \text{(II-8)}$$

By convention,

$$f = 16/N_{Re} \qquad \text{(II-9)}$$

for laminar flow where N_{Re} is the Reynolds number. Therefore, by combining Equations (II-8) and (II-9)

$$N_{Re} = D_e s\rho/\bar{\mu}\theta \qquad \text{(II-10)}$$

where

$$D_e = \frac{2\kappa^4 D_t[(1+\kappa^2)\ln(1/\kappa)-(1-\kappa^2)]}{(1-\kappa)(1-\kappa^2)^2} \qquad \text{(II-11)}$$

It should be noted that D_e defined by Equation (II-11) is such that the relationship between the Reynolds number and the friction factor is in conventional form, i.e., Equation (II-9), when the fluid flow is laminar. Equation (II-1) is rearranged and expressed in terms of κ and the newly defined equivalent diameter D_e, to give

$$\beta_{calc} = gD_e^2/8[\ln(1/\kappa)-(1-\kappa^2)/(1+\kappa^2)]$$

$$= \frac{gD_e^2(1-\kappa)^2(1-\kappa^2)^4}{32\kappa^6(1+\kappa^2)[(1+\kappa^2)\ln(1/\kappa)-(1-\kappa^2)]} \qquad \text{(II-12)}$$

β_{calc} instead of β_{lst} is used here to differentiate β used in this

study and β used by Lohrenz. L_e/L_c is deleted in Equation (II-1) since this ratio is almost unity for the type of falling cylinder used in this study (see Figure III-2). With these rearrangements and modifications, the functional relationship, equivalent to Equation (II-5) for representing viscometer calibration data in this study will be:

$$\beta_{red} = \beta_{p,t}/\beta_{calc} = f(N_{Re}) \qquad \text{(II-13)}$$
$$= f[D_e s\rho/(\bar{\mu}\theta)]$$

where β_{calc}, $\beta_{p,t}$ and D_e are defined by Equations (II-12), (I-1) and (II-11).

Treatment of the Viscometer Calibration Data

The type of viscometer used in this study as will be described in Chapter III is such that the fall time, θ, is that measured for the falling cylinder to traverse the distance s, which is the distance between the two electrical leads (O in Figure III-2), located near the terminal ends of the viscometer tube, less the length of the falling cylinder. When using this method of fall time determination, the effects due to the acceleration and the deceleration which cause s/θ term to deviate from the terminal velocity have to be considered. The correction due to the acceleration has been shown mathematically (Appendix K) to be inversely proportional to the square of the viscosity of fluid under investigation. Since the fluid investigated in this study generally is in the dense fluid or liquid state (save for a few cases where methane vapor phase viscosity was determined), this correction is shown to be negligible. In the worst case (gaseous methane), this correction term amounts to 1%, but it is smaller than the uncertainty in the experimental measurement of θ (Appendix H). For the deceleration as the cylinder approaches the bottom end of the viscometer tube, no mathematical relationship has been determined. However, the viscometer was designed so that the cylinder is stopped by the electrical lead which extends approximately 2" from the actual bottom of the tube (Figure III-2). The outside

diameter of this electrical lead is 3/32" as compared to the viscometer tube internal diameter of 5/16". Since (a) the cross-sectional area of the electrical lead is about 9/100 of the inner cross-sectional area of the viscometer tube, and (b) this lead is extended about 2" from the end of the viscometer tube, the bottom effect was considered negligible. Therefore, the terminal velocity was, in all cases, considered to be equal to the total distance of fall divided by the total time of fall.

After the fall time, θ, is determined in the calibration of the viscometer, $\beta_{p,t}$ can be computed from Equation (I-1) and the physical properties of the calibration fluid, the density of the falling cylinder, and the distance of fall in the viscometer. The distance of fall is calculated from the following relationship,

$$s = (s_{25} + L_{25})[1+\alpha_t(t-25)] - L_{25}[1+\alpha_c(t-25)] \qquad \text{(II-14)}$$

to account for the temperature effect on s, while the pressure effect is so small that it is neglected. Here t is temperature in centigrade, and the subscript 25 means that the fall distance s and the cylinder length L are measured at 25°C.

β_{calc} and D_e are functions of pressure and temperature. By substituting Equations (II-3) and (II-4) into Equations (II-12) and (II-11) (keeping in mind that κ is the ratio of D_c to D_t), β_{calc} and D_e at any given pressure and temperature can be calculated for a given viscometer. Computer Program 510 (Appendix R) was written to perform this calculation. β_{calc} and D_e were calculated for each falling cylinder using a common viscometer tube. The calculated β_{calc} and D_e corresponding to the temperature and pressure conditions of the experimental runs are shown in Appendixes P and Q. β_{calc}, D_e, and s are expressed as functions of temperature and pressure(47) so that all calibration data, expressed in terms of Equation(II-13), are independent of temperature and pressure effects, i.e., β_{red} is a function only of the flow regime prevailing in the viscometer.

In the treatment of the experimental calibration data in the form of Equation (II-13), it is expected that the viscometer calibration will cover a wide Reynolds number range including both the truly laminar flow region and the transition region between laminar flow and fully developed turbulence. The functional relationship should be linear in the laminar region and non-linear in the transition region. In order

that the results of the viscometer calibration can be handled by a digital computer, the calibration data are curve fitted by the empirical equations. A first order equation of the form,

$$\beta_{red} = A_o + A_1 \log(N_{Re}) \qquad \text{(II-15)}$$

should fit the experimental calibration data in the laminar region, while a second order equation of the form,

$$\beta_{red} = B_o + B_1 \log(N_{Re}) + B_2[\log(N_{Re})]^2 \qquad \text{(II-16)}$$

should fit the data in the transition region, where more weight is assigned to the function between laminar and transition regions (the transition point) so that these two equations will match.

CHAPTER III
DESCRIPTION OF EQUIPMENT

It has been already mentioned in Chapter I that the viscosities and densities of methane, propane and the mixtures of these at temperatures to -170°C. and pressures to 5,000 psia will be investigated in this study. 5,000 psia was selected as the upper pressure limit of this study, because this was the maximum pressure limit of the available Heise bourdon tube gages in the Low Temperature Laboratory, Chemical and Petroleum Engineering Department, The University of Kansas.

Since suitable experimental equipment was not available, a viscometer and related equipment capable of achieving the purpose of this study had to be developed. A low temperature bath which could maintain a constant temperature environment for the viscometer at any temperature level in the temperature range considered in this study and a high temperature bath containing high pressure equipment to meter fluids into the viscometer for density determination were to be constructed. The problem was to develop a viscometer which could be operated at high pressures and also be suitable for the study of mixtures without encountering the problem of composition changes as experienced by Lim, et al. (46). It was already mentained in Chapter I that a high pressure falling cylinder viscometer and a low temperature differential pressure indicator were finally used in this study. However before the development of this viscometer, other viscometer designs had been considered. A brief description of the development of viscometers during the course of this study will be given here.

Lim, et al. (46) used the same equipment developed by Swift (75) to investigate the low pressure liquid viscosities of light hydrocarbon binary mixtures. However, this equipment, using a Pyrex glass tube as a viscometer tube, was primarily developed for the study of pure components and the maximum operating pressure of the Pyrex tube was 1,000 psia. For this viscometer to be operated at pressures higher than 1,000 psia, it would be necessary to enclosed the glass viscometer tube (C) in a high pressure stainless steel vessel (A & B in Figure

III-1-a) such that an equalizing pressure could be brought to bear on the outside of the glass wall. The difficulties inherent in this type of design for operation at the extremes of pressure and temperature are:(1) if the interior of the high pressure vessel is designed to be one chamber having the interior and exterior of the glass tube open to each other, there is difficulty in achieving sufficient mixing of fluid for the study of mixtures, (2) whereas the above mentioned problem could be solved if the vessel is designed to be two chambers (having no pressure communication) by making a glass-to-metal seal between the glass tube (C) and the vessel head (A), and using the interior of the tube (C) as a viscometer cell, with a second fluid counter balancing the pressure in the annular space, no satisfactory glass-to-metal seal has been found that is suitable for long-term operation at low temperatures (less than -50°C.).

The development of a falling sleeve viscometer (see Figure III-1-b) was then initiated to circumvent the problems discussed above. This viscometer consists of a high pressure stainless steel vessel (B) having a Pyrex glass tube (C) aligned concentrically with the inner bore of the vessel, and a doughnut shape sleeve (S) falling in the annular space between the vessel (B) and the glass tube (C). The fluid to be investigated fills the annular space. The interior of the glass tube is exposed to the atmospheric air. The feature of this type of viscometer is that the following information can be obtained in the same experimental run.

1. The determination of viscosity by measuring the fall time required for the sleeve (S) in the annular space to traverse through a fixed distance.
2. The determination of density data, using a specially designed high pressure, low temperature miniature valve (V) (74) and a sensitive differential pressure indicator (D) (52) for the pressure measurement so that the fluid under investigation is completely isolated in the experimental temperature and pressure environment. (This design eliminates the possibility of change in the composition of mixtures mentioned in Chapter I).

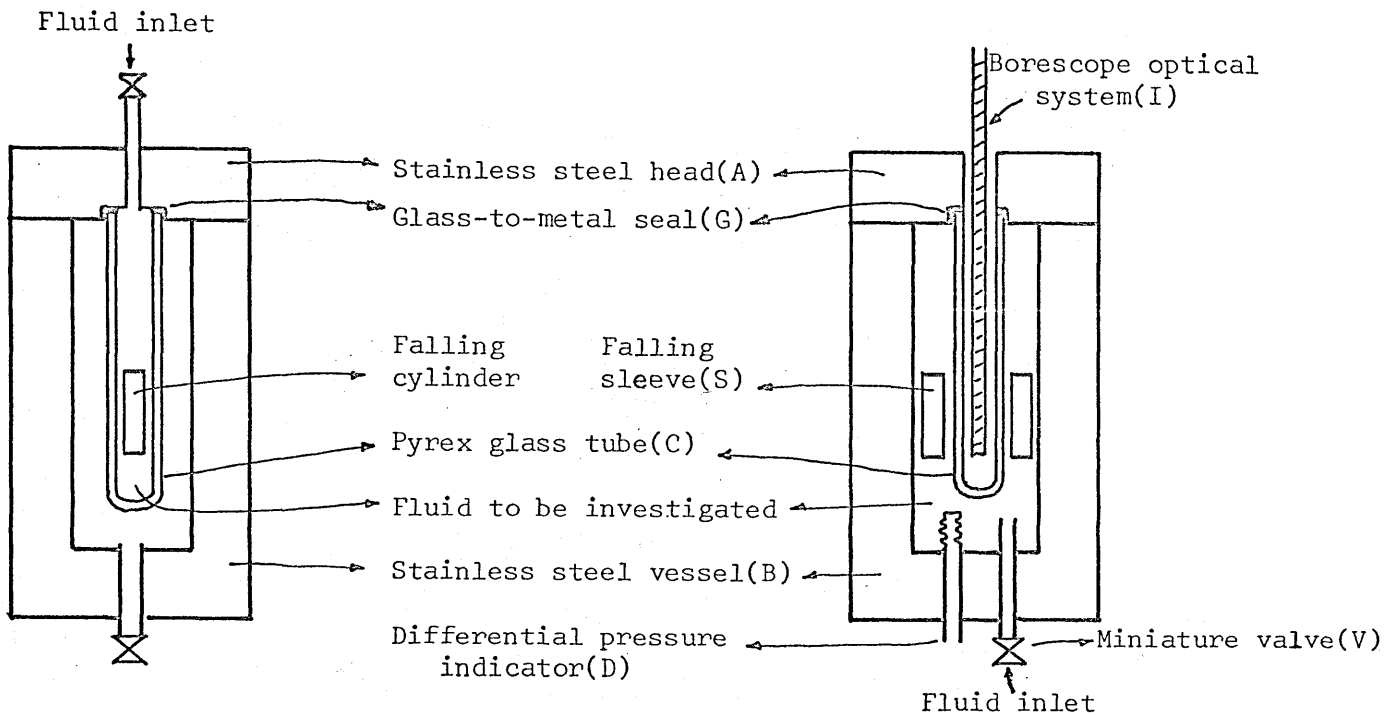

(a) A Falling Cylinder Viscometer

(b) A Falling Sleeve Viscometer

Figure III-1 Schematic Diagrams for the Earlier Viscometer Designs

3. The determination of phase behavior study by the method of dew point and bubble point observation by inserting a borescope optical (I) system into the glass tube.

Furthermore, since the theoretical prediction of the annular sleeve viscometer parallel to that of the falling cylinder viscometer developed by Lohrenz (47) had been derived (74), this information made the calibration of the falling sleeve viscometer possible. Because this design made concurrent phase, volumetric and viscometric studies possible, and allowed for adequate stirring of the contents of the vessel, this viscometer was constructed and a high pressure, low temperature glass-to-metal seal (36) was developed to seal between cap (A) and glass tube (C) using resilient epoxy glue as a pressure seal. The results of the test runs from the operation of the viscometer showed that the reproducibility of the fall time was better than that for the falling cylinder. However, because: (1) the glass-to-metal seal (36) developed was not a permanent seal (it worked satisfactorily in a short period after the preparation of the seal), and (2) there was no method of insuring the same alignment between the glass tube (C) and the vessel (B) whenever the viscometer was reassembled (the calibration of the viscometer changed every time when the parts were disassembled for maintenance service), it was finally decided to postpone work on this viscometer design until such time as additional developmental work concerning points (1) and (2) above could be undertaken.

After the unsuccessful tests of the viscometer design discussed above, it was finally decided to design and construct a falling cylinder viscometer using a stainless steel tube (similar to the one reported by Bridgman (11)) instead of Pyrex glass tube, so that the viscometer could be operated at high pressures. The key to the successful design of this viscometer was the successful test of the electrical lead assembly (C and D in Figure III-2) at low temperature and high pressure. The problem concerning the composition changes mentioned earlier was also solved by installing a DPI to the viscometer for the pressure measurement.

In the following sections, the following will be discussed:

(1) Viscometer, timing mechanism and low temperature differential pressure indicator, (2) Low temperature bath, and (3) High temperature bath.

Viscometer, Timing Mechanism and Low Temperature Differential Pressure Indicator

Since the viscometer used in this study, a stainless steel tube viscometer, is different from that developed by Swift (75), a Pyrex glass tube viscometer, the method of determining the fall time by inductence coil as reported by Swift is no longer applicable. In this new design, the time that required for the falling cylinder to drop from the top to the bottom of the viscometer tube was determined as the fall time. Thus it was necessary to develop a new timing mechanism to initiate and terminate a time interval meter to count the fall time. The timing mechanism consists of a simple RC circuit (Figure III-3) designed by Mr. Warren Legler.

The viscometer consists of a falling cylinder, one nipple*, one coupling*, one tee* and three modified plugs (see Figure III-2). Two of the modified plugs have electrical leads (O) insulated from the plug (M). The electrical lead assembly, which is a part of the RC timing circuit, is illustrated by C and D in Figures III-2 and III-3, and a detailed design drawing is shown in Figure S-1 of Appendix S. The stainless steel leads (O) is about 2" long and 3/32" in outer diameter. The extension (P) of lead (O) makes a non-conducting, unsupported area pressure seal with shoulder (Q) of a modified stainless steel plug (M) via a 0.010" thick Mylar gasket (N) as suggested by Weitzel, et al. (80). The insulator (L), made of fiber wool impregnated phenolic resin, spaces the electrical lead (O) through the port in plug (M) to prevent short circuiting. Washer (K) and lock nut (J) hold the assembly together and are tightened to effect the initial (zero load) pressure seal between electrical lead (O) and plug (M). No leakage through the electrical lead assembly (C or D) was found even when the assembly was tested at liquid nitrogen temperature and 8,000 psia.

*Cat. Numbers, CNX99012, 15FX-9966 and CTX-9990 from Bulletin No. 502 of Autoclave Engineers, Inc.

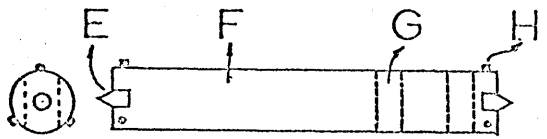

Falling cylinder, A

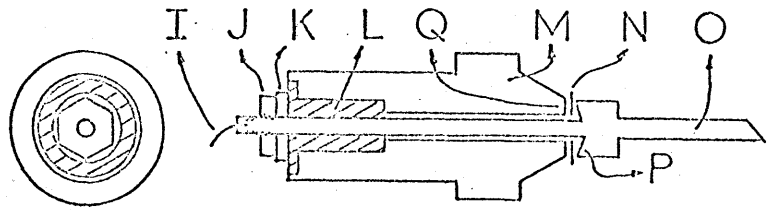

Electrical lead assembly, C&D

Falling cylinder viscometer

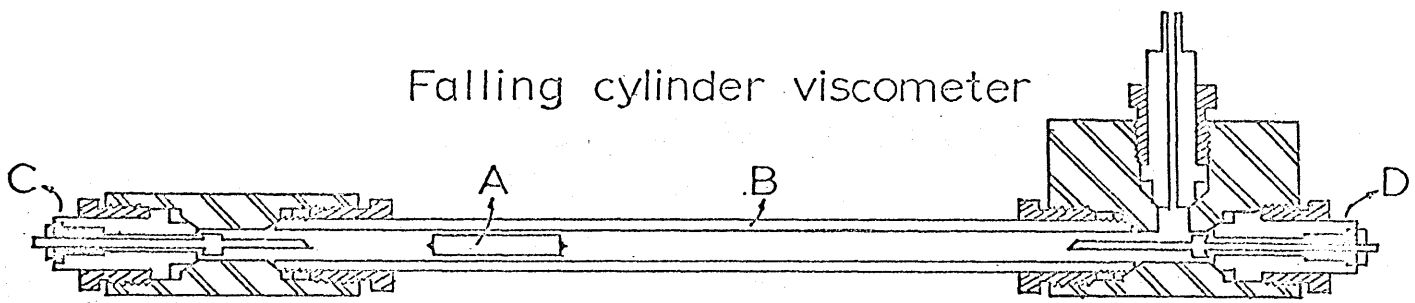

A Falling cylinder
B Precision bore ss tube
C Top elec. lead assembly
D Bottom elec. lead assembly
E ss protrusion
F Aluminum body
G Mild steel rod
H Alignment pin
I Electrical wire
J Lock nut
K Steel washer
L Non-metallic insulator
M ss plug
N Mylar gasket
O ss electrical lead

(SS: AISI 316 STAINLESS STEEL)

Figure III-2 Diagram of Viscometer Assembly

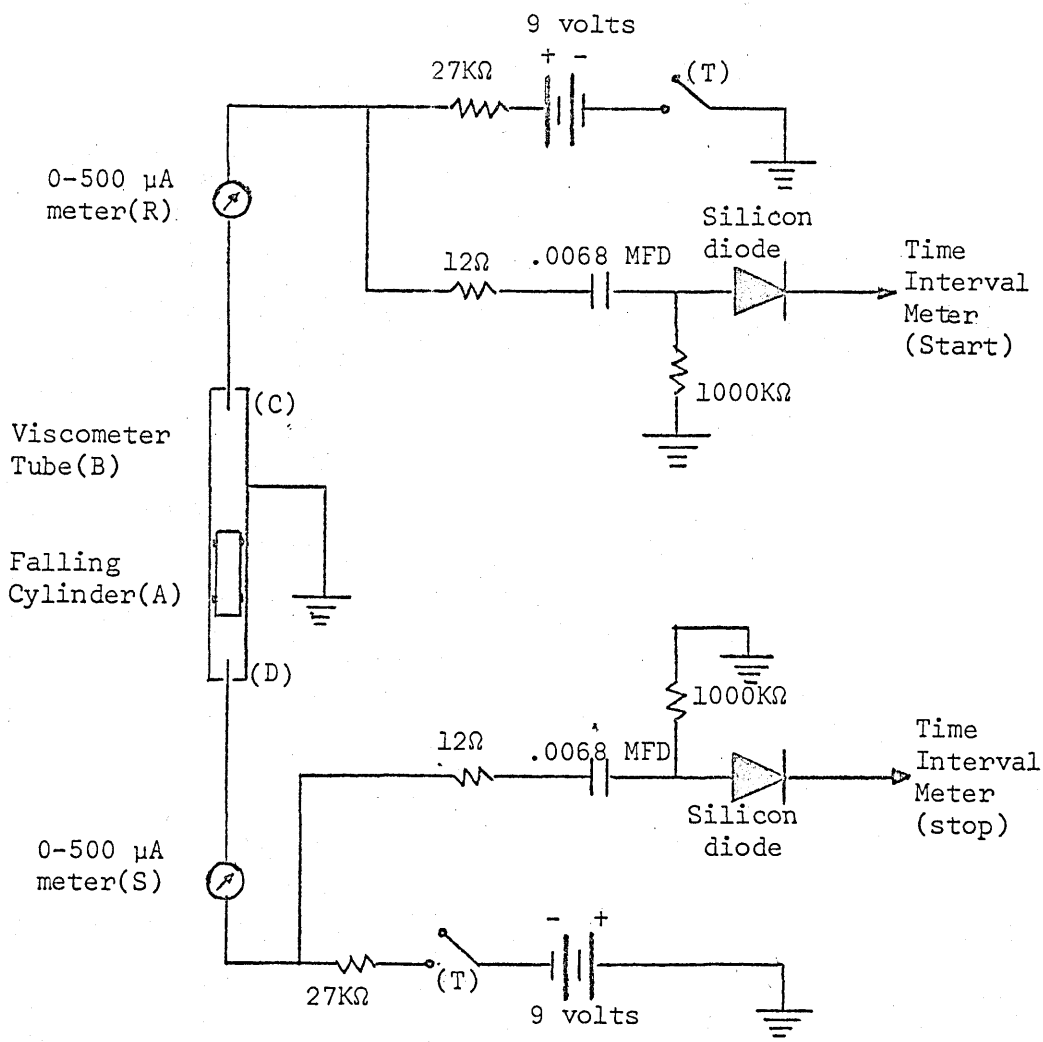

Figure III-3 Electric Timing Circuit

The inner bore of the high pressure nipple was reamed and polished to a diameter of 0.3140 inches. The falling cylinders used in this study are similar to those described by Swift (75). A schemetic drawing of a typical falling cylinder is shown in Figure III-2 and a detailed design drawing is shown in Figure S-2 of Appendix S. It is a right circular cylinder fabricated from aluminum (A) with metallic pins (H) for aligning the cylinder (A) concentrically within the vertically positioned tube (B). Two mild steel rods (G) are imbedded in the lower part of the falling cylinder so that the cylinder (A) can be elevated when acted upon by the magnetic field of a magnet mounted externally to the tube (B). Two stainless steel protrusions (E), one at each end of the cylinder (A), are provided (1) to give a hard surface so that the aluminum cylinder will not be damaged when it drops and (2) to make a better electrical contact with the tapered end of the electrical lead (O).

In the actual operation of the viscometer (see Figures III-2 and III-3), the cylinder (A) is raised to the top of the tube (B) by the action of a magnet mounted externally to the tube (B). As upper protrusion (E) on the cylinder (A) comes into contact with electrical lead (O) of the top electrical lead assembly (C), ammeter (R) will show a reading to indicate that cylinder (A) is at the top. Then following a further elevation of magnet, the cylinder (A) is disengaged from the magnetic field and falls through the fluid confined in the tube (B). The breaking of the electrical contact between upper protrusion (E) on the cylinder (A) and the electrical lead (O) of the top electrical lead assembly (C) initiates a time count on the time interval meter. The making of the electrical contact between lower protrusion (E) on the cylinder (A) and the electrical lead (O) of the bottom electrical lead assembly (D) terminates the time count. At this time the ammeter (S) will show a reading to indicate that the cylinder (A) is at the bottom. The tube (B) forms the ground side of the circuit in both initiation and termination steps of the time count.

Since liquid mixtures at low temperatures were to be investigated in this study, it would be necessary on occasion to measure the pres-

sure of a given mixture in the viscometer in a pressure range between the bubble point pressure at ambient temperature and that at the temperature of the viscometer (see Figure I-1). If constant composition in the viscometer is to be maintained under these conditions, the mixture can not be exposed to ambient temperature, since that portion so exposed would exist in two phases (vapor and liquid). This reasoning precluded the measurement of the pressure of the mixture directly with Heise bourdon gage. A low temperature differential pressure indicator (LT DPI) was used to isolate the liquid mixture in the viscometer at the temperature of the low temperature bath and yet retain pressure communication. This DPI is a modified version of the one described by McCreary and Swift (52). A schematic diagram is shown in Figure III-4 and the detailed diagram of the parts are shown in Figure S-3 of Appendix S.

The active element (pressure communicator) of the DPI is a nickel bellows (E) (Servometer Corp., Passaic, N.J.), having an outer diameter of 0.250", inner diameter of 0.150", wall thickness of 0.002" and 24 convolutions totaling 0.775" long. One end of the bellows (E) is soft-soldered to a 1/4" tube (C) and the other to an end cap (F). The cap (F) is connected to a transformer core (J) by a stainless steel extension rod (G), and the whole assembly is enclosed in a 1/4" stainless steel tube (C). A transformer (I) (Model 6234A-03-K-01-XK, supplied by Automatic Timing and Controls, Inc., King of Prussia, Pa.) is press-fitted to a brass holder (K) which is mounted externally on the 1/4" tube (C) and screwed into a nut (M). The position of the transformer can be easily adjusted by turning the holder (K) against the nut (M). The core (J) connected to the cap (F) by rod (G) is free to move and its position is sensed by the differential transformer (I) and then transmitted to the transformer excitation-device (Model 6101EIX, supplied by Automatic Timing and Controls, Inc., King of Prussia, Pa.). Two ammeters, one having a maximum reading of $\pm$500 μA and the other $\pm$50 μA, are connected in parallel to the readout device. The $\pm$500 μA meter is used for course adjustment of the DPI, while the $\pm$50 μA meter is used for final fine adjustment.

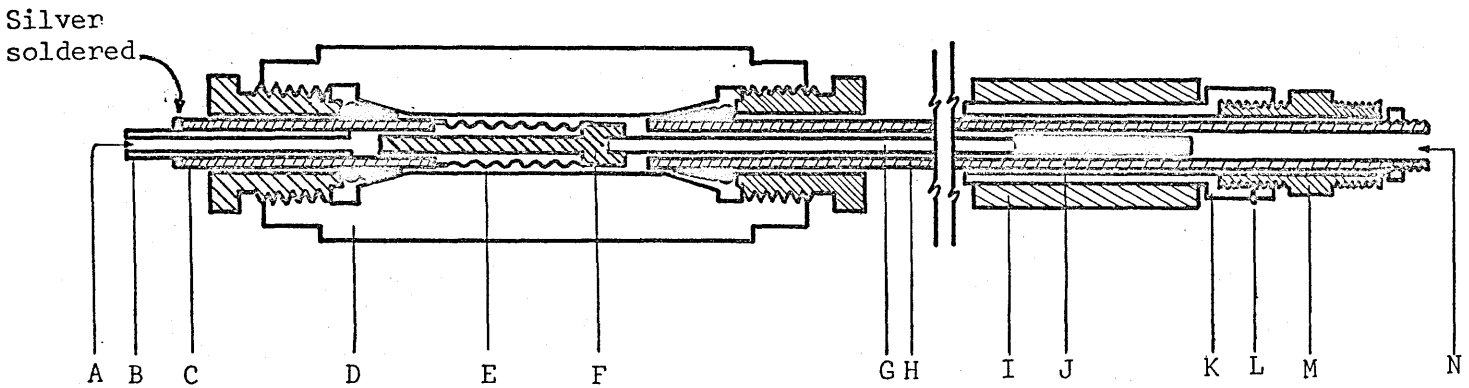

A	System fluid inlet	H	1/4" stainless steel tubing
B	1/8" stainless steel tube	I	ATC Differential transformer(Type 6234)
C	1/4" stainless steel tube	J	Transformer core
D	Bellows housing	K	Transformer holder
E	Bellows	L	Set screw
F	Movable end cap	M	Nut
G	Extension rod	N	LPG inlet

Figure III-4 Low Temperature Differential Pressure Indicator Assembly

In the installation of the assembly for operation, the bellows housing (D) is kept inside the low temperature bath, while the transformer (I) is exposed to ambient temperature. The system fluid fills the interior of the bellows (E) via port (A), and liquefied propane gas (LPG) fills the space between the DPI housing and the bellows (E) via port (N) to balance the pressure of the system fluid through the bellows. The fluid (or the mixture) is isolated in the low temperature bath and never exposed to ambient temperature. By balancing the readout device to the null point, the pressure of the LPG, which is measured by a 5,000 psi Bourdon gage, is the pressure of the mixture in the viscometer.

This DPI has a sensitivity of $\pm$10 psi (see Appendix A) which is considered to be sufficient for the determination of liquid viscosity, since the liquid viscosity is not sensitive to the change in pressure (10 psi change in pressure causes a change in liquid viscosity less than 0.1%). The design of this DPI is such that it can stand a larger over pressure than that reported by McCreary and Swift, because, (a) a bellows having a larger wall thickness is used and, (b) as is shown in Figure III-4, the movable cap (E), is confined by an 1/8" stainless steel tube (O) and an 1/4" stainless steel tube (H) so that only approximately 1/8" is allowed for the movement of bellows in each direction. This type of DPI can be subjected to 1,000 psi over-pressure without damaging the bellows.

The density determination is made by transferring a known amount of fluid into the viscometer, the volume of which has been calibrated. In the determination of the liquid density of mixtures, the low temperature DPI has to be used for the pressure determination of the mixtures in the viscometer. It is expected that there would be more error in density determination for the mixture, due to the insensitivity of the DPI in the pressure measurement. However, as will be shown in Chapter V, density data of high accuracy for the computation of the viscosity data are not required so the error introduced by the DPI is not considered serious.

Low Temperature Bath

The low temperature bath described here is a modified version of the one described by Sinor (70). Figure III-5 shows a schematic diagram of the bath. It consists of a stainless steel dewar flask (P) having an inner diameter of 5" and a depth of 18" and a phenolic cover (O), which is assembled from eight 1/2" thick fiber wool impregnated phenolic resin plates, one 1/8" aluminum plate, one 1/8" brass plate, and six 1/4" nylon rods to bind all the plates together. The fiber wool impregnated phenolic resin and the nylon rod, being good insulators as well as possessing the necessary structural strength, provide an insulated cover and a rigid platform for mounting the instruments. This cover (O) simplifies the top layer of Sinor's bath design (70) which is complicated by aluminum plates, plastic insulation forms and a heat exchanger.

For the achievement and maintenance of a certain low temperature, liquid nitrogen was injected directly into the bath by passing liquid nitrogen (at a pressure slightly above atmospheric pressure) through the tube (N) and vaporizing it in the liquid nitrogen evaporator (M). Evaporator (M) is a copper can containing copper gauze to provide more heat transfer surface. Small holes at the upper end of (M) allow the gaseous nitrogen to flow into the bath. The gaseous nitrogen, circulated by a high speed blower (E) powered by the air motor (D) which is mounted on the cover (O) by a rubber collar (S), flows in the bath as indicated by arrows in Figure III-5. The rubber collar (S) absorbs most of the vibration of the air motor even at high speed. Nitrogen gas is vented to the atmosphere through the hollow shaft (F) of the air motor which is tempered by the exhausting heat transfer medium. The injection rate of liquid nitrogen is controlled by the back pressure valve (C). The gap between (O) and (P) is sealed by the rubber sleeve (V) to prevent blow-by of the nitrogen gas. This is necessary to obtain effective control of the nitrogen flow rate, and to have good control of the bath temperature. An electrical resistance wire heater (L) provides the amount of heat necessary to offset the liquid nitrogen vaporization load at a preset temperature level. The resistance

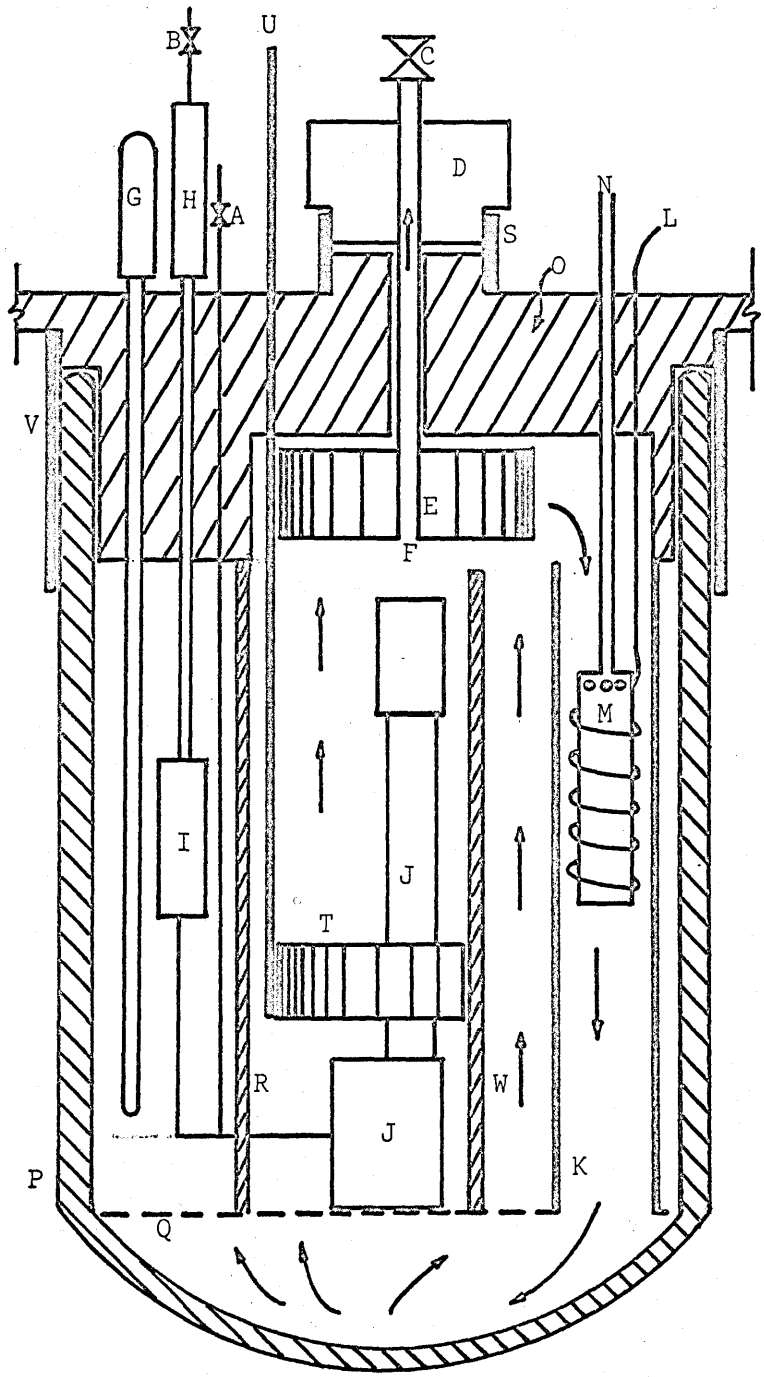

A system valve
B LPG valve
C N_2 controlled valve
D Air motor
E Blower
F Hollow shaft
G Pt resistance thermometer
H ATC transformer
I Low temp. DPI
J Viscometer
K Copper down comer
L Heater
M LN_2 evaporator
N LN_2 injection tube
O Phenolic cover
P Stainless steel dewar flask
Q N_2 distributor
R Stainless steel support rod
S Rubber collar
T Magnet
U Magnet elevating rod
V Rubber sleeve
W Mild steel guide rod for magnet

Figure III-5 Low Temperature Bath

setting on the bridge of a platinum resistance thermometer (G)-Mueller bridge-DC null detector system sets the temperature level in the bath. A signal from the DC null detector reflecting the difference between thermometer temperature and set-point temperature is fed to a solid state temperature control device which in turn proportionally controls the voltage drop across the resistance wire heater. The solid state temperature control device has been described by Schindler (68). Temperature measurement and control at the temperatures down to -170°C. were within ±0.01°C. (slightly more at the extreme low end of the temperature range). Temperature differences between thermometer and various points on the viscometer were less than 0.1°C. as measured by thermocouples whose reference junctions were mounted on the sensing element of the thermometer. Because liquid nitrogen was injected directly into the bath as a coolant, the liquid nitrogen was used efficiently, and the fabrication of the top cover (O) was greatly simplified. Only one tube is required for the injection of liquid nitrogen, and the exhaust gas is vented through the hollow shaft of the air motor. By minimizing the number of metal tubes going through the cover (O), the heat leak through the cover is considerably reduced. The viscometer (J) is mounted on the gaseous nitrogen distributor (Q) which in turn is supported by four stainless steel rods (R) hung down from the phenolic cover (O). The viscometer is mounted concentrically with the blower (E), so that the flow of gaseous nitrogen is uniformly distributed around the viscometer. The falling cylinder inside the viscometer is elevated by a U shape magnet (T), which is held against two mild steel rods (W) mounted vertically in the bath, one on either side of the viscometer (J). The magnet is held between two 1/8" aluminum plates and a 3/16" stainless steel rod (U) is attached to the upper aluminum plate so that the magnet can be easily moved up or down by pushing or pulling on rod (U). The mild steel rods (W) serve as a guide for the magnet assembly. A small O-ring serves as a seal between the rod (U) and the 1/8" hole through the cover (O). This prevents the formation of frost inside the hole (which would impair the movement of the rod (U)). The O-ring also reduces the blow-by of gaseous nitrogen from the bath. An

O-ring is also used to seal the gap between the platinum resistance thermometer (G) and its hole on the cover (O) to eliminate nitrogen blow-by.

This bath can also be operated at superambient temperature by simply injecting the exhaust air from the air motor into the bath through the tube (N). However if the air motor is operated at high temperature (say 90°C.) for a long time, the bottom shaft seal of the air motor wears out and causes the compressed air to leak into the bath. Then, when the bath is operated again at low temperature, the moisture in the air freezes in the back pressure valve (C) and upsets the temperature controlled system. When this happens, it is only necessary to replace a lower shaft seal.

In short, the features of the modified bath which give improved performence are:

(1) Direct injection of liquid nitrogen, with a single valve controlling the flow, uses the liquid nitrogen more efficiently and simplifies the operation of the temperature control system. Also the bath can be cooled more rapidly.

(2) The source of heat leak through the phenolic cover is reduced because there are fewer metal connections passing through the cover, and the motor shaft is tempered since the exhausting heat transfer medium passed through it.

(3) The air motor is mounted on the phenolic cover by a thick rubber collar which absorbs most of the vibration even when the motor runs at high speed.

High Temperature Bath

The high temperature bath is an oil bath containing high pressure equipment to generate and maintain high pressures (as high as 10,000 psia). The equipment maintained in the high temperature bath is used to displace the fluid into the viscometer for density determinations, and to prepare mixtures. Figure III-6 shows the schematic diagram of this equipment and its relationship to the other parts of the apparatus. This high temperature bath and the high pressure cylinders, which are

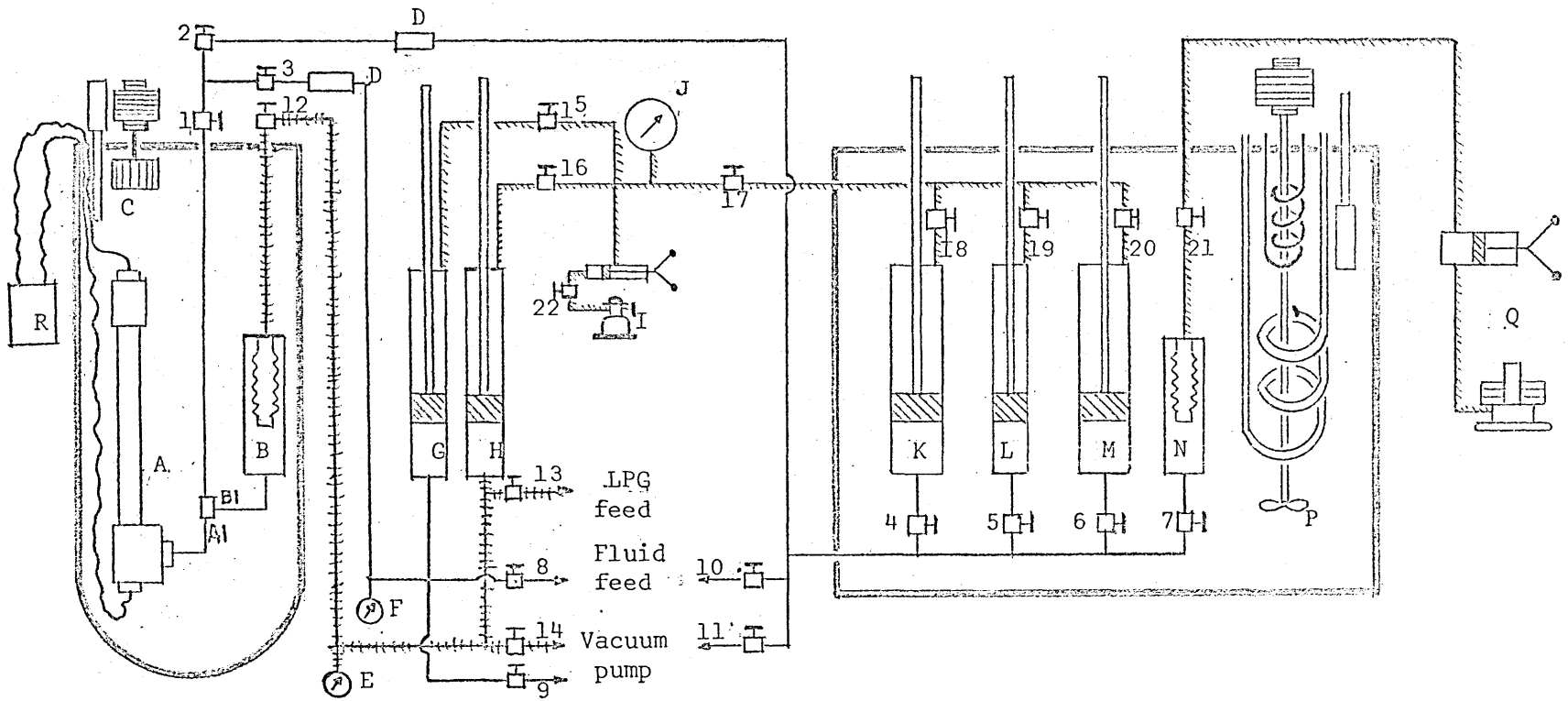

A	Viscometer	G,K,L	Mass injection cylinder(MIC)
B	Low temp.DPI	M	Mixture make up cylinder(MMC)
C	LTB temp.controlled system	N	High temp.DPI
D	Filter	P	HTB temp.controlled system
E,F	Heise gage(0-5000 psia)	Q	Ruska dead weight pressure tester
H	LPG intensifier for DPI	R	Timing mechanism unit
I	Sprague pump	1,2,3,4,5,6,7,8,9,10,11	Fluid system's valves
J	Heise gage(0-15000 psia)	12,13,14	LPG system's valves
		15,16,17,18,19,20,21,22	Oil system's valves

Figure III-6 Flow Diagram for the Apparatus

rated for 12,000 psi working pressure at -10 to 400°F., are essentially identical to those described by Gupta (32). A brief description will be given here to illustrate the function of each part of the equipment.

The high temperature bath consists of an eight gallon stainless steel vacuum jacketed flask filled with kerosene, three high pressure cylinders (K, L, M), a high temperature differential pressure indicator (N) and a temperature control system (P). Each of the high pressure cylinder is a high pressure vessel containing a movable, O-ring sealed piston (see Figure S-5 of Appendix S) separating the experimental fluid from the hydraulic oil which is used to move the piston. The movable piston has three Buna-N O-rings acting as pressure seals between experimental and hydraulic fluids. A 1/8" stainless steel rod is attached to the hydraulic oil side of the piston and the other end of the stainless steel rod is passed through a "stuffing box" (32) (see Figure S-5 of Appendix S) to the atmosphere so that the position of the piston can be measured. Hydraulic oil pressure is generated by a Sprague air-over-oil diaphram pump. The action of hydraulic oil pressure on the movable piston in the cylinder in turn pressurizes the experimental fluid. The pressure of the experimental fluid is measured by the Ruska dead weight tester through a high temperature DPI (see Figure S-4 of Appendix S). The active element of the DPI is a nickel alloy bellow, 0.25" in diameter, 1.25" in length with 24 convolutions, fabricated from alloy of 0.001" thickness. Detailed information on the DPI has been published by McCreary and Swift (52). In the present study the cylinder M is used as a reservoir for the preparation of mixtures and it will be called a mixture make up cylinder (MMC) throughout the text. Cylinders K and L are used to meter the fluid into the viscometer and they will be called mass injection cylinders (MIC). MIC-K has an inner diameter of 1.250" with a full capacity of approximately 200cc., while MIC-L has an inner diameter of 0.288" with a full capacity of approximately 10cc. The latter, having a smaller diameter, gives a better resolution for the injection of small amounts of mass. The temperature controlled system consists of an air cooling coil, a heating wire, a stirrer to agitate the heat transfer fluid, and a Bayley temperature controller, which

regulates the amount of current passing through the heater wire. The temperature in the bath is measured by copper-constantan thermocouples. All valves, fittings and tubing in Figure III-6 except valve 1 are rated for 12,000 psi working pressure. Valve 1, a Hoke "Millimite" valve (Model No. 1325S 2Y), is designed for fine metering purpose and is rated for 5,000 psi working pressure.

In the present study, the injection of the experimental fluid into the viscometer and the pressurization of this fluid were achieved by using cylinders MIC-K and MIC-L. Since the pistons in these cylinders are not absolutely leak proof, there could be a trace amount of hydraulic oil leaked into the experimental fluid side of the cylinders and eventually into the viscometer. To check on how much oil would leak through this piston, one of the cylinders was subjected to severe tests by enclosing a constant amount of methane in the cylinder and moving the piston back and forth to simulate the actual experimental operation of the cylinder. At the end of the 60th cycle, almost no trace of oil could be detected on the methane side of the cylinder, although particles of O-ring material were noted. At the end of the 100th cycle, O-ring particles and only a slight trace of oil could be found on the methane side of the cylinder. This test indicated that, as long as O-rings were not used for too many compression cycles, the amount of oil leaked through the piston would not be detectable.

The following evidence further supports this finding:

(1) No difficulty was encountered in the elevation, release, or fall of the falling cylinder at -170°C. using methane which was pumped by cylinders MIC-K and MIC-L.

(2) Reproducibility of fall time of No. 1 falling cylinder using propane at 37.78°C. and 300 psia indicated no significant difference in fall time between runs using fresh propane from the propane supply cylinder and a run using propane which had been compressed and decompressed in MIC-L (Appendix H).

From the tests mentioned above, it is concluded that any traces of hydraulic oil in the system should have no effect on the experimental data of this study.

Before proceeding to the next section, one other thing should be mentioned. Figure III-6 shows the diagram of the entire apparatus used in this study. The apparatus is designed such that the high temperature bath unit (the square box) and the rest of the equipment can be separated into two self-contained units simply by closing valves 2 and 17. The high temperature bath unit, being identical to the one described by Gupta (32), can be used to perform high temperature PVT measurements. The other unit can be used to perform viscosity and density measurements with MIC-G serving the same function as MIC-K or MIC-L. The high pressure intensifier (HPI) H is an intensifier for the liquid propane (LPG) and is used to balance the pressure of the system fluid in the viscometer through the low temperature DPI (B). It should be noted that MIC-G is exposed to room temperature, thus for the density determination of more compressible fluids, a mass injection cylinder, which has a larger capacity and is in a constant temperature environment, such as MIC-K in high temperature bath, is necessary to obtain accurate density data.

MIC-G and HPI-H are modified from high pressure nipples (Autoclave Engineers, Cat. No. CNX99012) and have inner diameters of 5/16". A detailed designed diagram of the stuffing box and the dynamic piston is shown in Figure S-6 of Appendix S.

CHAPTER IV

PURE MATERIALS USED AND THE PREPARATION OF MIXTURES

Purification and Analyses of Methane and Propane

The materials employed in this investigation were Phillips pure grade methane with a stated minimum purity of 99 mole percent and instrument grade propane with a stated minimum purity of 99.5 mole percent. To remove water and carbon dioxide from the materials as received, methane was passed through tubes filled with ascarite and phosphorus pentoxide, and propane, from the vapor space of the supply cylinder, was passed through tubes filled with silica gel, ascarite and phosphorus pentoxide. These purified materials were analyzed using a F & M Model 720 Chromatograph with a silica gel column. The results of the analyses are given in Table IV-1.

Table IV-1

Purity Analyses for Methane and Propane

	Mole Percent				
	CH_4	C_2H_6	C_3H_8	$n\text{-}C_4H_{10}$	N_2
Methane	99.31	0.15	0.01	--	0.53
Propane	trace	--	99.97	0.03	trace

Preparation of the Mixtures

The mixtures were prepared in MMC-M (cylinder M) of the high temperature bath (see Figure III-6) at a controlled temperature of 37.8°C. The bath temperature was measured with calibrated copper-constantan thermocouples to an uncertainty of $\pm$0.1°C., and the pressure of the system was measured with a Ruska dead weight tester to an uncertainty of $\pm$1 psia. A volumetric displacement of material from MIC-K (cylinder K) to MMC-M determined the amount of material placed into MMC-M. The detailed procedure for preparing mixture will be described in Chapter V.

The original data for the preparation of the mixtures are presented

in Appendix I. The compositions for the mixtures studied in this investigation were:

22.1 mole% CH_4 - 77.9 mole% C_3H_8

50.0 mole% CH_4 - 50.0 mole% C_3H_8

75.3 mole% CH_4 - 24.7 mole% C_3H_8

After preparation, all mixtures were maintained for at least 33 hours at a pressure above 1,500 psia (the maximum possible cricondenbar pressure for the methane-propane system). This time for equilibration was found sufficient for the establishment of a homogeneous composition state for the methane-propane mixtures because:

(a) at the end of this equilibration period, the system was at constant volume for at least one hour while the pressure remained constant,

(b) in Table VII-2 (P. 78) the viscosity data for run 1 in Group I were taken just after the mixture was equilibrated for 33 hours, and the viscosity data for run 3 were taken after approximately 150 hours from the same batch of mixture. The agreement of these data is a strong indication that the mixture had achieved a homogeneous state after 33 hours.

CHAPTER V

OPERATION AND CALIBRATION OF EQUIPMENT

Preliminary Procedures

(1) Temperature measurement

A platinum resistance thermometer (No. 281) was used to measure the temperature of the low temperature bath to an uncertainty of ±0.01°C. This thermometer was calibrated against a standard platinum resistance thermometer which in turn had been calibrated directly by the National Bureau of Standards against fixed points on the International Temperature Scale. The detailed calibration of this thermometer is discussed in Appendix B.

The temperature in the high temperature bath was measured by copper-constantan thermocouples to an uncertainty of ±0.1°C. These thermocouples were calibrated against platinum resistance thermometer No. 281. The calibration of the thermocouples is shown in Appendix B.

(2) Pressure measurement

The pressure in the low temperature bath was measured with one 5,000 psi Heise bourdon tube gage for the study of the pure components to an uncertainty of ±5 psi and with another 5,000 psi Heise bourdon tube gage via a low temperature DPI for the study of mixtures to an uncertainty of ±15 psi (this uncertainty includes that due to the low temperature DPI). These gages were calibrated against a Ruska dead weight tester-high temperature DPI combination, which is accurate to ±1 psi. The results of the calibration are shown in Appendix A. The pressure of the high pressure unit in the high temperature bath was measured with a Ruska dead weight tester-high temperature DPI combination to an uncertainty of ±1 psi.

(3) Measurements of physical dimensions of the viscometer

In this study three falling cylinders were used in one viscometer tube. A detailed diagram of the cylinder is shown in Figure S-2 of Appendix S. The outer diameter of the falling cylinder was measured with a micrometer to an uncertainty of 0.0001 inches. The measured diameters for the three falling cylinders are presented in Table V-1.

The outer diameter of the stainless steel viscometer tube, which is 12" long, was measured to be 0.5619 inches. The inner diameter was measured by a machinist to be 0.3140" using a feeler gage. It was estimated that the inner diameter of the tube is known within 0.0005 inches.

The distances of fall for the falling cylinders to fall from the top to the bottom of the viscometer tube, were measured with a method described in Appendix F. These distances for each falling cylinder are shown in Table V-1.

(4) Determination of density of the falling cylinders

The volume of the falling cylinder was determined by two methods: (a) Using Archimedes' principle; and (b) Using a pycnometer. The density of the falling cylinder was obtained by dividing the mass of the cylinder by the average value of volumes determined experimentally (Appendix E).

The densities so determined for each falling cylinder are given in Table V-1 with an estimated precision of $\pm$0.05 percent.

(5) Accuracy of the time counting mechanism

A Beckman Time Interval Meter (Model 5230R-4), part of the experimental apparatus, was compared with a new Beckman Time Interval Meter (Model 5230R) to determine the accuracy of the counting mechanism. Appendix G gives the results of the comparison. The difference between the same time recorded on both instruments was never more than 0.0033 seconds out of 27.8 seconds. This deviation was not considered to be significant, since the overall reproducibility from day to day of the fall time of the viscometer is $\pm$0.6% for No. 1 falling cylinder and $\pm$1.1% for No. 2 falling cylinder (Appendix H).

(6) Cleaning of viscometer and installation of the viscometer in the low temperature bath

The existence of solid particles in the viscometer is detrimental to repeatable operation. Therefore high pressure filters (AE Cat.No. 12F2200) are installed between the viscometer and the mass injection cylinders to keep solid particales from entering the viscometer. However, since there are valves between the viscometer and the filters, fragments of packing materials in the valves could enter the viscometer after repeated operation of the equipment and cause poor reproducibility of fall

time determinations. Therefore, the viscometer was dismantled periodically to remove these solid particles. The viscometer was dismantled from the low temperature bath assembly by (a) disconnecting the electrical lead wires at both ends of the viscometer, (b) disconnecting the 1/8" tubing of the viscometer from the 1/8" tee at A1 (Figure III-6), (c) disconnecting the bath medium distributing plate (Q in Figure III-5) from the support rod (R in Figure III-5) of the low temperature bath assembly so that the plate, and the attached viscometer can be removed from the low temperature bath.

To clean the interior of the viscometer, it is disassembled by disconnecting the high pressure nipple from the tee and coupling. The falling cylinder and the interiors of the tube, tee and coupling are cleaned thoroughly with acetone. Then after the parts are dried, the viscometer is reassembled and remounted in the low temperature bath.

It is important that the viscometer tube be mounted as near to a vertical position as possible. Otherwise error from sliding contact of the cylinder to the tube will occur. The vertical alignment of the viscometer tube is adjusted by manipulating the four leveling screws underneath the low temperature bath assembly until a bulls-eye level mounted on the outside of the viscometer tube indicates that the tube is vertical.

General Procedure of Operation

This section describes the operating procedures for: (1) The high temperature bath unit, (2) The low temperature bath unit, and (3) The preparation of mixtures. In the description of the operating procedures, reference should be made to the schematic diagram of Figure III-6.

(1) The high temperature bath unit

The high temperature bath is used to displace fluid into the viscometer for density determinations and also to prepare mixtures. This bath was generally run at 37.8°C. where bath temperature was controlled by a Bayley temperature controller. Once the experimental program had been started, this unit was maintained at constant temperature continuously. The operation of the bath and the procedure for the displace-

ment of fluid from the mass injection cylinder (MIC) into other cylinders are as follows:

1. Supply fresh ice to the thermocouple reference junction thermos bottle, check the bath temperature and readjust the Bayley temperature controller, if the set point on the temperature controller has changed because of drift in electronic components.
2. Check the null point of the high temperature DPI by exposing both sides of DPI to atmospheric pressure. Adjust DPI if necessary.
3. Evacuate the viscometer (for viscosity and density determinations) or MMC-M (for preparation of a mixture).
4. Evacuate MIC (MIC-K or MIC-L), and then introduce the fluid to be investigated into MIC.
5. Compress the fluid to a predetermined reference pressure and record the position of the piston and the reference pressure. This reference pressure must be higher than the bubble point pressure of the fluid at the bath temperature. When taking a piston position measurement, one should always approach the reference pressure from a lower pressure so that the O-rings of the dynamic piston will seat in their grooves in a consistent manner. This eliminates volume error due to random seating of the O-rings.
6. Slowly displace the fluid into the viscometer (or MMC-M) from MIC. The pressure in MIC should always be higher than the reference pressure to prevent the transfer of so much fluid from MIC that it would be impossible to restore the pressure in MIC to the reference pressure.
7. At the end of displacement, adjust the pressure in MIC to the reference pressure. Be sure the final position of the piston is obtained in the same manner as that described in step 5.
8. Record the position of the piston. The change in the position of the piston multiplied by the crossectional area of MIC gives the volume, ΔV of the fluid, displaced into the viscometer at that reference pressure and bath temperature. The amount of mass displaced is computed by multiplying ΔV by the density of the fluid at the temperature and pressure of displacement.

9. Repeat the same procedure if additional displacements are needed.

10. After completion of a run, bring the pressure on both sides of the DPI to atmospheric pressure, check the null point of the DPI again. Reset the DPI null point if necessary. If the DPI has been overpressurized to the point of damaging the bellows, replace the defective bellows.

(2) The low temperature bath unit

During the course of the experiment, the null detectors for the temperature measurement systems, and the DPI excitation-readout devices for pressure measurement system were never turned off. Upon initiating a particular experimental run, the time interval meter was turned on at least 30 minutes before taking data.

Before admitting fluid into the viscometer, the falling cylinder was elevated to the top of the viscometer tube. This is important, since, if the viscometer is at a lower pressure than the displacement system and the falling cylinder is at the bottom of the viscometer, sudden introduction of material into the viscometer by opening valve 1 drives the falling cylinder to the top of the viscometer causing damage to the falling cylinder and the stainless steel extension of the top electrical lead assembly (see E and O in Figure III-2).

The procedure for low temperature bath operation will be described in general in subsection (a). Particular aspects of operation pertaining to making viscosity and density measurements on pure components and on mixtures will be discussed in subsections (b) and (c) respectively. Finally, the particulars of low temperature bath operation in making routine reproducibility tests will be covered in subsection (d).

(a) Start-up and equilibration of low temperature bath

1. Raise the stainless steel dewar flask into place, put the rubber sleeve (V in Figure III-5) in position to prevent the blow-by of the heat transfer medium, and start the air motor.

2. Set the resistance on the Mueller bridge at a value equivalent to the desired temperature of operation.

3. Remove the back-pressure control valve from the top of the air motor to allow maximum flow of the coolant (heat transfer medium).

4. For superambient temperature operation, heat the bath to approximately the desired temperature using the bath heating wire with a variac. This wire is disconnected from the temperature control system(a platinum resistance thermometer-Mueller bridge-DC null detector system) and plugged into the variac to obtain efficient heating during the bath warmup period.

5. Turn off the variac, plug the bath heating wire back to the temperature control system, feed the air motor exhaust air into the bath as a coolant, and activate the temperature control system to control the temperature.

6. For subambient temperature operation, cool the bath down to a desired temperature by injecting liquid nitrogen from a 100 liter liquid nitrogen supply dewar into the bath.

7. As the temperature is approaching the desired temperature, mount the back-pressure valve on the exhaust line to cut down the exhaust flow rate of the gaseous nitrogen and hence the injection rate of liquid nitrogen.

8. Set the pressure in the liquid nitrogen supply dewar to a normal operating pressure of approximately 2 psig by adjusting a self-relieve valve mounted on the top of the dewar; then activate the temperature control system to control the bath temperature.

(b) Viscosity and density measurements for pure materials (without low temperature DPI)

1. Disconnect low temperature DPI(B) from the viscometer, and plug the hole at B1.

2. Evacuate the viscometer.

3. Turn on the battery switch of timing mechanism (Figure III-3). A reading on either top or bottom ammeter indicates that the falling cylinder is either at the top or the bottom of the viscometer. (The falling cylinder should be at the top at this time.)

4. Displace the fluid from MIC-K or MIC-L (or MIC-G if high temperature bath unit is not used) into the viscometer until the pressure of the fluid in the viscometer reaches the desired pres-

sure as indicated by the Ruska dead weight tester (or Heise gage F). (From here on, the statement of "a displacement of the fluid from MIC into the viscometer" implies the precedure performed according to that described in the operation of high temperature bath (steps 5 to 8) so that the amount of mass transferred can be determined.)

5. Drop the falling cylinder several times to agitate the fluid in the viscometer, and allow at least 30 minutes after the bath temperature is controlled at the desired set point temperature to achieve thermal equilibrium.

6. Check the pressure again, and transfer more fluid from MIC into the viscometer if necessary.

7. Record the set resistance on the Mueller bridge, the pressure reading of the Ruska dead weight tester (or Heise gage F), and drop the falling cylinder to determine the fall time at that temperature and pressure conditions. In the calibration of the viscometer, five consecutive fall times are determined at each operating condition. In the viscosity determination, 10 consecutive fall times are determined at each operating condition. The number of fall times determined is reduced if (1) the fall time exceeds 40 seconds; or (2) the operating pressure is at 5,000 psia.

8. Repeat steps 4 to 7, after the operating pressure or temperature condition has been changed. Generally, the operation is started from the highest temperature and a low pressure (if the temperature is below the critical temperature of the fluid, the operation is started at a pressure 200 to 300 psi higher than the bubble point pressure). The subsequent data are taken at pressures of the lowest multiple of 1,000 psia above the bubble point pressure, and thereafter in 1,000 psi increments to 5,000 psia. After the completion of an isotherm, the temperature is decreased to other temperatures in 20°C. temperature increments.

9. After the completion of a run, vent the fluid from the viscometer, elevate the falling cylinder to the top of the visco-

meter, and turn off the electrical switch of the timing mechanism.

10. Warm the bath to ambient temperature, if the bath has been operated at subambient temperatures. If the bath is allowed to warm by heat leak only, condensation of moisture on the eletrical leads of the viscometer occurs and causes short-circuiting between the electrical leads and the viscometer tube, thereby requiring the removal of the stainless steel dewar flask to wipe off the moisture before the next run.

11. Leave the hydrocarbon fluid in the viscometer under atmospheric pressure instead of allowing air to enter. This prevents oxidation of the aluminum falling cylinder.

(c) Viscosity and density measurements for mixtures (with low temperature DPI)

The viscometer operation for viscosity and density measurements of mixtures is the same as that described for the pure materials, except for the operation of the low temperature DPI(B). The operation pertinent to DPI is described as follows:

1. Assemble DPI(B) to the viscometer at B1 (Figure III-6). With both sides of the DPI at atmospheric pressure, adjust the null point of the DPI on the readout ammeter to a value of zero. Since there are two readout ammeters (ranges $\pm$50 μA and $\pm$500 μA), zero the $\pm$50 μA ammeter and then switch to the $\pm$500 μA ammeter to protect the $\pm$50 μA ammeter from overload.

2. Evacuate the viscometer through valve 3 and evacuate the LPG system.

3. Close valves 3, 9, 14.

4. Open valves 2 and 13 simultaneously to introduce the mixture into the viscometer and propane vapor into DPI. The flow of the fluids should be controlled closely by valves 2 and 13 such that the DPI remains close to the null position.

5. Close these valves when the Heise gage (E) shows a reading of approximately 150 psia (the vapor pressure of propane at ambient temperature).

6. Charge the LPG system with liquid propane through valve 13

until it is filled with liquid propane at the saturation pressure. Then close valve 13.

7. Compress the mixture in the viscometer to a desired pressure by opening valves 2 and 15 alternately, keeping the DPI under a differential pressure of less than ±100 psi. This unbalance of pressure corresponds approximately to the maximum free movement of the bellows in the DPI housing.

8. During the displacement of the mixture from MIC-K or MIC-L into the viscometer, care should be taken to keep the pressure in the high temperature bath above the bubble point pressure of the mixture at the temperature of the high temperature bath to prevent composition change.

9. After allowing at least another 30 minutes for the mixture to achieve thermal equilibrium, adjust the pressure reading in gage (E) to the desired pressure by changing the pressures on both sides of the DPI while keeping the DPI at the null point.

10. As the pressure approaches the desired pressure, switch the current from the ±500 μA ammeter to the ±50 μA ammeter for fine adjustment of the DPI. The desired pressure in the viscometer is finally reached when the gage (E) shows this pressure reading and the ±50 μA ammeter is at the null point.

11. Record the Mueller bridge resistance setting and the pressure reading of the Heise gage (E), and then switch the current in the DPI readout from the ±50 to the ±500 μA ammeter.

12. After the completion of fall time determination, care must be taken to prevent the over pressurization of the DPI when changing the pressure and temperature conditions.

13. After completing a run, vent the mixture in the viscometer and the LPG in the LPG system simultaneously to keep the DPI balanced. The null point of the DPI is checked after the run and reset if necessary.

(d) Routine reproducibility test of the fall time.

To check the timing circuitry, condition of the falling cylinder, and the cleanliness of the viscometer system, a routine reproducibility

test was established so that improper functioning of the viscometer for any of the reasons cited could be detected and remedied before too much faulty experimental data were taken.

A series of fall times using propane at 300 psia and 37.78°C. were taken between experimental runs at three to four day intervals during the course of the experimental work on pure methane and pure propane to check the reproducibility of fall time for the No. 1 falling cylinder. The results are shown in Appendix H. The reproducibility of fall time was computed to be ±0.8% based on 98% confidence limits. It should be noted that the fall times of No. 1 falling cylinder at the reference condition decreased about 2% between runs 1P-1 and 1P-13. This decrease in fall time was probably caused by erosion of the brass alignment pins of the falling cylinder after repeated falls in the viscometer tube. Because of the change in the calibration of No. 1 falling cylinder, No. 2 falling cylinder, having stainless steel alignment pins, was used for the determination of the viscosities of the mixtures. The results of the routine reproducibility test for No. 2 falling cylinder using propane at 37.78°C. and 1,000 psia are presented in Appendix H. The reproducibility of the fall time for No. 2 falling cylinder was computed to be ±1.1% based on 98% confidence limits.

(3) The preparation of mixtures

Mixtures were prepared by volumetric displacement of each of the pure materials from MIC-K into the mixing cylinder, MMC-M. The detailed procedure is as follows:

1. Compute the moles of propane to be transferred from MIC-K to MMC-M. This requires information on the volume of MMC-M, the composition of the mixture desired, and the density of the mixture at the temperature and pressure conditions of the mixture as it will exist after mixing is completed. The volume of propane, ΔV_2, displaced from MIC-K is then computed, knowing the density of propane at the temperature and pressure of the displacement (reference) condition. The ratio of ΔV_2 to the cross-sectional area of MIC-K is the piston displacement, ΔH_3, that must take place to

transfer the proper quantity of propane in MMC-M.

2. Evacuate MIC-K and MMC-M, and transfer a sufficient amount of propane into MIC-K with the valve (valve 6 in Figure III-6) between MIC-K and MMC-M closed.

3. Open valve 6 and displace propane from MIC-K into MMC-M such that the piston of MIC-K moves a distance ΔH_2 (recalling the procedure of displacing fluid from MIC-K into MMC-M described in P. 44).

4. Close valve 6, vent the propane from MIC-K and evacuate MIC-K.

5. Compute the exact volume of methane, ΔV_1, required to make the mixture of the desired composition, X_1, from the methane density at the temperature and pressure of the displacement (reference) condition and the following relationship,

$$\Delta V_1 = \Delta V_2 M_1 X_1 \rho_2 / (M_2 X_2 \rho_1) \qquad \text{(V-1)}$$

The ratio of ΔV_1 to the cross-sectional area of MIC-K is the length of displacement, ΔH_1, that is necessary to transfer the proper quantity of methane from MIC-K into MMC-M.

6. Transfer a sufficient amount of methane into MIC-K.

7. Open valve 6 and displace methane from MIC-K to MMC-M such that the piston of MIC-K moves ΔH_1.

8. Close valve 6 and compress the fluids in MMC-M and MIC-K to a pressure above the maximum cricondenbar of the system studied. Fluids on both sides of valve 6 are compressed to the same pressure to prevent differential leakage across valve 6 from MMC-M to MIC-K.

9. After approximately ten hours, vent methane from MIC-K, evacuate MIC-K and then transfer the mixture from MMC-M to MIC-K. It is necessary to transfer the mixture from MMC-M to MIC-K, because MIC-K is the displacement cylinder used for density determinations. The mixture is again pressurized to the pressure mentioned in step 8 for equilibration.

10. The composition of methane expected, X_1, should check with the value computed from the following equation,

$$X_1 = (\rho_1 \Delta V_1 / M_1) / (\rho_1 \Delta V_1 / M_1 + \rho_2 \Delta V_2 / M_2) \qquad \text{(V-2)}$$

Determination of Density

This section is divided into three parts: (1) Calibration of the mass injection cylinders; (2) Calibration of the viscometer volumes; and (3) Computation of density from the experimentally determined volumetric displacement data.

(1) Calibration of the mass injection cylinders

The mass injection cylinders (MIC-K, MIC-L and MIC-G) were calibrated to determine the consistency of the cross-sectional area of the cylinders at different distances along the cylinder lengths and to determine "best" values for the cross-sectional areas. Distilled water was used as the calibration fluid where the density data of water were taken from the literature (34,39). The procedure of operation is as follows:

1. Fill the MIC with distilled water.
2. Displace water at a known temperature and pressure from the MIC into a beaker.
3. Record the change in the position of the piston (ΔH) and weigh the amount of water displaced from MIC (ΔW).
4. Compute the average cross-sectional area over the length the piston moved by dividing ($\Delta W/\Delta H$) by the density of water at the reference temperature and pressure condition. This gives the number ($\Delta V/\Delta H$) reported in Appendix C.

The errors in ($\Delta V/\Delta H$) reported in Appendix C were computed based on 95% confidence limits if there were more than two replicated runs available. If there were only two replicated runs, the error was reported for the percent difference for the two values. The error in displacing a complete cylinder load of fluid for MIC-K is $\pm$0.08%, for MIC-L is $\pm$0.06% and for MIC-G is $\pm$0.04%. The error in injecting approximately 10% of a complete cylinder load at random starting points of the fluid for MIC-K is $\pm$0.27%, for MIC-L is $\pm$0.94% and for MIC-G is $\pm$0.26%. The reason that the partial injection has a larger error than the full injection is probably due to: (a) Poorer resolution in the height measurement, (b) Non-uniformity of the inner bore of the cylinder with length, (c) Hysteresis in the high temperature DPI.

The pressure effect on the inner bore of the MIC up to 5,000 psia

was predicted from Equations (II-3) and (II-4) and the mechanical properties of the stainless steel shown in Table II-1. For all the cylinders calibrated, the pressure effect on the diameter was estimated to be less than 0.07% at 5,000 psia. Since the MIC's were generally operated at pressures lower than 5,000 psia, this effect was neglected.

(2) Calibration of viscometer volumes

Methane was used as the fluid for the calibration of viscometer volume. Methane density was taken from the data of Sage and Lacey (66), Kvalnes and Gaddy (40) and van Itterbeek, et al. (78). The densities of Sage and Lacey are reported for superambient temperatures, those of Kvalnes and Gaddy cover the range from -70 to 200°C., and the pressure range for data reported from these two papers is from one atmosphere to pressures in excess of 5,000 psia. van Itterbeek, et al. (78) presented methane density data over a temperature range of -160 to -85°C. and at pressures to 4,500 psia. The data of the first two sources agree within 0.3% and the data of later two sources matched smoothly when they were plotted on a large-scale graph paper. The composite data cover the complete pressure and temperature ranges of interest to the present investigation.

In the calibration, the volume of the viscometer and the temperature and pressure dependence of the volume were determined. The procedure for the determination of viscometer volume without the low temperature DPI is as follows:

1. Place a falling cylinder in the viscometer and assemble the low temperature bath unit.
2. Run the low temperature bath at the same temperature as that of high temperature bath (37.8°C.).
3. Charge methane into MIC-K, set the pressure of methane in MIC-K to a reference pressure, and record the position of the piston.
4. After evacuating the viscometer, transfer methane into the viscometer until the pressure in both the viscometer and MIC-K are at the original reference pressure.
5. Record the position of the piston. The difference in the position of the piston multiplied by the cross-sectional area

of MIC-K is the volume of the viscometer at that temperature.

The procedure for the determination of temperature dependence of the viscometer volume was similar to that just described, except that the low temperature bath was operated at several different low temperatures. The viscometer volume at any low temperature was computed by multiplying the volume of methane transferred at the reference condition, ΔV, by the ratio of the methane density at the reference condition to that at low temperature and reference pressure. The temperature coefficient of the viscometer, α_v, (the slope on a plot of viscometer volume versus temperature) was computed by a least squares method. The procedure for the volume calibration of the viscometer including low temperature DPI was the same as that described above, except that care was taken to operate the DPI according to the procedure mentioned in P. 45.

The results of the calibration are presented in Appendix D. The appendix shows the calibrated volumes of the viscometer with different falling cylinders and with or without low temperature DPI. The error in these volumes is less than $\pm 0.2\%$.

The temperature coefficient, α_v, for the viscometer assembly without the DPI, was calculated theoretically from the linear coefficients of thermal expansion of the stainless steel and aluminum (Table II-1) to be 4.1×10^{-5}/°C. This value agreed reasonably well with the experimental value of α_v for the assembly without the DPI (4.87×10^{-5}/°C.) and that for the assembly with No. 1 DPI (5.35×10^{-5}/°C.) (see Appendix D). The temperature coefficient, α_v, for the assembly with No. 2 DPI had a larger value. This was probably due to the inconsistency of the density data between those of van Itterbeek, et al. (78) and those of Kvalnes and Gaddy (40), since for this calibration run, one density value of van Itterbeek, et al. was used at the temperature of -138.82°C.

To determine the pressure dependence of the viscometer volume, a run was made by compressing the fluid in the viscometer to 5,000 psia with the mass injection cylinder. However, no significant change in volume could be detected. Therefore no correction for the pressure effect on the viscometer volume was made in the calculation of the experimental density.

(3) Computation of Density from the Experimentally Determined Volumetric Displacement Data

The density of the fluid at the temperature and pressure conditions of viscometer was computed from the literature density at the reference condition, ρ_{rc}, and the following relationship,

$$\rho = \rho_{rc} \frac{\Delta V}{V_{vm}} \qquad \text{(V-4)}$$

Determination of Viscosity

This section is divided into three parts: (1) Selection of the fluids for calibration of the viscometer; (2) Calibration of the viscometer, and (3) Computation of viscosity from the experimentally determined fall time.

(1) Selection of the Fluids for Calibration of the Viscometer

The fluids used in the calibration of the viscometer, based on the analysis of available data in Chapter I, were methane, propane, n-butane, n-hexane and n-octane (n-decane was not used, because the viscosity data of n-decane (42) was not published at the time when the viscometer was calibrated).

For methane, the viscosity data used were those of Barua, et al. (6), and the density data used were those reported by Kvalnes and Gaddy (40). For propane and n-butane, the data of Ellington and coworkers (23,73) were used for viscosity and those of Sage and Lacey (66) were used for density. The composite data of Rossini, et al. (65) for both viscosity and density were used for n-hexane and n-octane.

(2) Calibration of the Viscometer

Three falling cylinders, each falling in the same viscometer tube, were calibrated with methane, propane, n-butane, n-hexane and n-octane. The calibration constants for the viscometer were computed from fall time data using Computer Program 604 (Appendix R). A complete tabulation of the calibration data are presented in Appendix M.

Figure V-1 shows a plot of β_{red} versus $\log(N_{Re})$ for the three falling cylinders calibrated. From this plot, a transition point for each falling cylinder was selected by inspection for each cylinder.

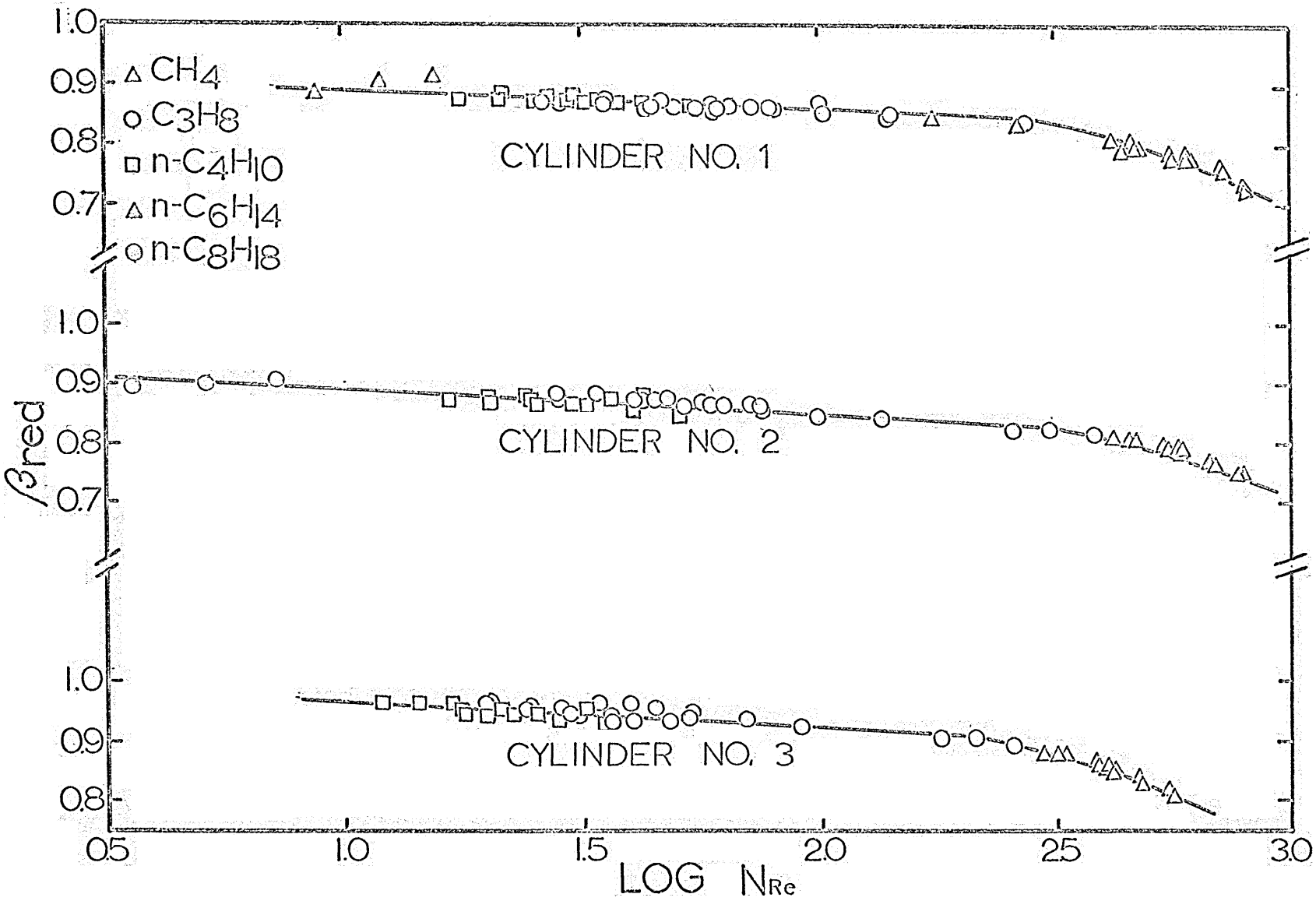

Figure V-1 Viscometer Calibration Plot

The logarithm of the transition Reynolds number [$\log(N_{Re})_{trans}$] for each falling cylinder is shown in Table V-1. By regression analysis, Equation (II-15) was fitted to all the points in the laminar region [$\log(N_{Re}) < \log(N_{Re})_{trans}$], and Equation (II-16) was fitted to all the points in the transition region [$\log(N_{Re}) > \log(N_{Re})_{trans}$], where more weight was assigned in each equation to the transition point so that the β_{red}'s computed from these two equations at the transition Reynolds numbers agreed to within 0.38%. The coefficients for the equations and the transition Reynolds number for each falling cylinder are reported in Table V-1.

Table V-1 also shows the maximum $\log(N_{Re})$ covered in the calibration, and the average deviations of β_{red} from the equations for each falling cylinder in laminar and transition regions. The average deviations in both laminar and transition regions are within $\pm 0.85\%$.

It should be noted that in this study the upper pressure limit of the viscometer calibration is 5,000 psia, while that of Lohrenz was 600 psia (47). Thus the experimental calibration data of this study show that the viscometer calibration method developed by Lohrenz is applicable to high pressures.

In Figure V-1, β_{red} in all cases is less than 1. This is because the friction due to entrance and exit losses, etc., which was encountered in the experimental calibration of the viscometer, was neglected in the theoretical derivation of viscometer constant. It is also noticed in Figure V-1 that those calibration data using the viscosity and density data reported by Rossini, et al. (65) appear to deviate more from the solid line representing Equation (II-15). This seems to imply that the data of Rossini, et al. may not be consistent with those reported by Ellington and coworkers for propane and n-butane.

(3) Computation of Viscosity from the Experimentally Determined Fall Time

After the fall time θ in the fluid at a given temperature and pressure conditions was determined, the viscosity was computed from the following equations:

Table V-1

Physical Dimensions, Densities, Estimates of Error, and Coefficients for Equations(II-15) and (II-16) for the Falling Cylinders Used In This Investigation

Falling Cylinder No.	Cylinder Diameter in.	Cylinder Density g/cc.	Distance of Fall in.	Length of Cylinder in.	Transition[a] $\log(N_{Re})$	Maximum[b] $\log(N_{Re})$
1	0.3077	3.0058	5.064	2.099	2.446	2.917
2	0.3078	2.9996	5.044	2.120	2.488	2.904
3	0.3087	3.0073	5.065	2.098	2.327	2.750

Cylinder No.	Coefficient for Equation(II-15) A_o	A_1	% error in β_{red}[c] in the laminar region
1	0.9351	-0.03870	±0.61
2	0.9353	-0.04462	±0.85
3	1.0207	-0.04888	±0.81

Cylinder No.	Coefficient for Equation(II-16) B_o	B_1	B_2	% error in β_{red}[c] in the transition region
1	0.3633	0.5441	-0.1427	±0.81
2	-0.6431	1.2495	-0.2656	±0.83
3	-0.3075	1.1564	-0.2730	±0.65

Notes: (a) The transition $\log(N_{Re})$ is the point where Equations (II-15) and (II-16) meet.

(b) The maximum $\log(N_{Re})$ is the largest $\log(N_{Re})$ covered in the calibration of viscometer.

(c) Percent errors in β_{red} are reported as

$$S_m = 100\left[\sum_{1}^{n}\frac{\left|(X_{exp}-X_{calc})\right|}{X_{exp}}\right]/n$$

where n is the number of data points.

$$\bar{\mu} = \beta_{p,t}(\sigma-\rho)\theta/s \qquad \text{(I-1)}$$

$$\beta_{p,t} = \beta_{red}(\beta_{calc}) \qquad \text{(II-13)}$$

$$\beta_{red} = A_0 + A_1\log(N_{Re}) \qquad N_{Re} < (N_{Re})_{trans} \qquad \text{(II-15)}$$

$$\beta_{red} = B_0 + B_1\log(N_{Re}) + B_2[\log(N_{Re})]^2 \qquad N_{Re} > (N_{Re})_{trans} \qquad \text{(II-16)}$$

$$\beta_{calc} = (gD_c^2/8)[\ln(1/\kappa) - (1-\kappa^2)/(1+\kappa^2)] \qquad \text{(II-12)}$$

$$D_e = 2\kappa^4 D_t[(1+\kappa^2)\ln(1/\kappa) - (1-\kappa^2)]/[(1-\kappa)(1-\kappa^2)^2] \qquad \text{(II-11)}$$

$$s = (s_{25}+L_{25})[1 + \alpha_t(t-25)] - L_{25}[1 + \alpha_c(t-25)] \qquad \text{(II-14)}$$

and the following steps:

a. β_{calc}, D_e and s were computed for the temperature and pressure at which the experiment was conducted.

b. A trial value of β_{red} was assumed, and $\beta_{p,t}$ was calculated. $\bar{\mu}$ was computed from Equation (I-1) using the experimentally determined fall time, θ, the density, ρ, at the temperature and pressure of the experiment (either from literature or experiment), $\beta_{p,t}$, s and σ.

c. The Reynolds number, N_{Re}, was then computed.

d. The appropriate regression relationship [Equation (II-15) or (II-16) for the falling cylinder being used] was selected for N_{Re} computed in step c above, and β_{red} was computed to compare with the assumed β_{red} in step b.

e. This iterative procedure was continued until the assumed and computed values of β_{red} agree to within an assigned tolerance. This procedure was performed by Computer Program 703.

In the experimental investigation, methane at most and propane at all of the temperature and pressure covered were in the liquid or dense fluid state such that the Reynolds numbers were below the transition value. Certain of the low pressure methane viscosity data were obtained at Reynolds numbers above the transition value. However, the highest $\log(N_{Re})$ value encountered in this case was 2.992 so that only modest extrapolation of the calibration was required.

Error Analysis

The experimental data reported in this study are expected to be subject to systematic errors and random errors. The systematic errors will be discussed first.

(1) Systematic Errors in the Experimental Results due to the Impurities in the Materials Used

(a) Density data

In the computation of the experimental density from Equation (V-4), ρ_{rc} used in the calculation was obtained from the literature (66). For the methane used in this study, which contained 0.69 mole% impurities, the literature density values (66) were used to calculate the experimental densities. Since the "Direct Determination of Mass by Weighing in a Cryogenic Environment" technique (19,37, 59) for the determination of the compressibility factor (Z) of gases was not well established in the Low Temperature Laboratory of the Department of Chemical and Petroleum Engineering, The University of Kansas, until near the end of this study, the effect of nitrogen, ethane and propane impurities on Z of the methane used (0.69 mole% total impurity) is treated as a systematic error.

To estimate the effect on Z due to these impurities, the results of the experimentally determined Z from the "Progress Report on API Project 69-C" (59) were used. The Z for pure grade methane at 99.7°F. and 997.2 psia having impurities of 0.12% ethane and 0.62% nitrogen was determined by the low temperature direct weighing technique. This methane was from a different cylinder than that used in this study, but the analysis was almost the same. The experimental Z was determined to be 0.914, which was 0.8% higher than the literature value, Z=0.907, reported by Sage and Lacey (66) at 100°F. and 1,000 psia for methane containing impurities less than 0.02 mole% (54). In other words, the literature density of methane was 0.8% larger than the true density of the methane used at 100°F. and 1,000 psia. In the computation of the experimental density for this study, the literature values at the other pressures up to 5,000 psia were also used. Since only the experimental Z value at 100°F. and 1,000 psia was available, it was assumed that the same deviation in density

also existed at the other pressures of this study. Therefore, from Equation (V-4), it should be obvious that the experimental densities for methane obtained in this study are approximately 0.8% higher than the probable true values. This systematic error can be corrected from the reported original density data (Appendix O) when the experimental density data of pure grade methane used in this study at 100°F. and pressures to 5,000 psia are determined.

For the propane used in this study, because it contains less than 0.005 mole% impurities (Table IV-1), the use of densities reported by Sage and Lacey (66) should not introduce significant error.

The error due to impurities in the mixtures was estimated by taking the molar average of the errors in the two pure components. As a result, a maximum error of 0.6% was estimated for the worst case, i.e., the 75.3 mole% methane mixture. The experimental densities for mixtures would be higher than the probable true values by 0.6% at the most.

(b) Viscosity data

The propane used in this study contains 0.03 mole% of impurities (Table IV-1). The effect of this amount of impurities on the propane viscosity is considered to be negligible. The methane used in this study contains 0.67 mole% impurities. To estimate the effect of these impurities on the viscosity of methane, methane and nitrogen viscosities reported by Ross and Brown (64) were used. They reported the viscosity data of these materials at temperatures between 25 and -50°C. and at pressures to 10,000 psia. It was assumed that all of the impurities could be represented as nitrogen, since nitrogen was the major impurity in the methane used. The percent deviations between the viscosities for methane and nitrogen at the same temperatures and pressures reported by Ross and Brown are within 45% so that the effect of 0.7 mole% nitrogen on the methane viscosity would be 0.3%, assuming that the molar average rule for the calculation of the viscosity for the mixture of nitrogen and methane applies. Since the reproducibility of the fall time is $\pm$0.8% for No. 1 falling cylinder and $\pm$1.1% for No. 2 falling cylinder,

the effect due to the impurities (0.3%) was not considered significant. The same reasoning also applied to the data for mixtures of this study.

(c) Composition

In the computation of the composition, there is an error due to the use of methane density data of Sage and Lacey (66) in the conversion of the volumetric data to mass data. The effect of this error on the composition is small, since this density appears in both denominator and numerator. By taking into account the 0.8% correction on the methane data, it is estimated that 50.0 mole% methane mixture should be 0.002 mole fraction richer in propane, and the 22.1 and 75.3 mole% methane mixtures should be 0.001 mole fraction richer in propane (Appendix J).

(2) Random Errors

The maximum random errors in the composition, density and viscosity reported in this study are estimated by the method described by Mickley, et al. (53) as applied to the following equations:

$$X_1 = (\rho_1 \Delta V_1/M_1)/(\rho_1 \Delta V_1/M_1+\rho_2 \Delta V_2/M_2) \qquad (V-2)$$

$$\rho = \rho_{rc} \Delta V/V_{vm} \qquad (V-4)$$

$$\bar{\mu} = \beta_{calc} \beta_{red} (\sigma-\rho)\theta/s \qquad (V-3)$$

Appendix J shows the error analysis on X_1, ρ and μ based on these equations. In the following sections, the error in composition will be estimated first, and then the errors in density and viscosity will be analyzed.

(a) Error analysis on composition

In the preparation of the mixtures, the pressure was measured with the Ruska dead weight tester to an uncertainty of ± 1 psi and the temperature of the bath was measured with the calibrated copper-constantan thermocouples to an uncertainty of ± 0.1°C. These measurements are sufficiently precise to eliminate the error from these sources. The uncertainty of density data for methane and propane is stated to be within ± 0.1% by its investigators (54,66) and the error of the volume determination using MIC-K is estimated to be ± 0.27%

(Appendix C). The maximum error is then estimated to be ±0.005 mole fraction (Appendix J).

(b) Error analysis on density and viscosity data

Table V-2 presents the sources of errors and the maximum estimated errors in the density and viscosity data for methane, propane and mixtures of these. The sources of error in the density data are:

1. The error in V_{vm} (Appendix D).
2. The error in ΔV (Appendix J).
3. The error in ρ_{rc} from the literature density (54,66,67).
4. Pressure measurements of the fluids in high temperature bath in all cases were made by the Ruska dead weight tester to an uncertainty of ±1 psi. Therefore there is no appreciable error in ρ_{rc} due to the pressure measurement. The error in ρ_{rc} due to the change in reference temperature is considered negligible for those densities measured with MIC-L, since MIC-L was in the high temperature bath. The density of the mixture is subject to uncertainty of ±0.5% in ρ_{rc} due to the uncertainty in the composition. Propane density was determined with MIC-G which was exposed to room temperature. Hence an uncertainty of ±0.25% is estimated for the ρ_{rc} of propane due to 2°C. change in room temperature.
5. The temperature and pressure measurements in the low temperature bath (P. 38) was precise enough to eliminate errors from these sources. The pressure measurement for the mixtures using Heise gage-DPI system is reported (P. 38) to have an uncertainty of ±15 psi. However, since the mixtures existed in liquid state at the conditions of this study, the uncertainty of ±15 psi in the pressure does not have a significant effect on the liquid density.

By summing up all the error terms, the maximum estimated error in the density for each fluid is shown in Table V-2.

For the viscosity data, the effects of the uncertainties in the temperature and pressure measurements are the same as those described for the density. The other errors different from those of density data are:

Table V-2

Summary of Error Analysis on
Density and Viscosity Data

(a) Density calculated from, $\rho = \rho_{rc}\ \Delta V/V_{vm}$, is subject to the following errors.

Fluid	Error in % Methane	Propane	Mixtures
MIC used	MIC-L	MIC-G	MIC-L
(1) $\Delta(V_{vm})$	0.16	0.16	0.18
(2) $\Delta(\Delta V)$	0.35	0.11	0.35
(3) $\Delta(\rho_{rc})$ reported by investigators	0.10	0.10	0.13
(4) $\Delta(\rho_{rc})$ due to ΔT & ΔX	0.00	0.25	0.50
Total $\Delta(\rho)$	$\pm$0.61	$\pm$0.62	$\pm$1.16

(b) Viscosity calculated from, $\mu = \beta_{calc}\ \beta_{red}(\sigma-\rho)\theta/s$, is subject to the following errors,

Fluid	Error in % Methane & Propane	Mixtures
(1) $\Delta(\theta)$	0.8	1.1
(2) $\Delta(s)$	0.1	0.1
(3) $\Delta(\sigma-\rho)$	0.2	0.3
(4) $\Delta(\beta_{red})$	0.8	0.8
(5) $\Delta(\beta_{calc})$	1.5	1.5
Total $\Delta(\bar{\mu})$	$\pm$3.4	$\pm$3.8

1. The error in the determination of distance of fall, s, is estimated to be 0.004" out of a total distance of 5 inches.
2. The error in θ is reported in Appendix H (No. 1 falling cylinder for pure components and No. 2 falling cylinder for mixtures).
3. The error in $(\sigma-\rho)$ is shown in Appendix J.
4. The error in β_{red} is from Table V-1.
5. The error in β_{calc} according to Equation (II-12) depends on the uncertainty in κ, the ratio of the outer diameter of the falling cylinder to the inner diameter of the viscometer tube. Since the uncertainty in κ is estimated to be $\pm 0.1\%$, which corresponds to an uncertainty of ± 0.0003" out of 0.314", there would be approximately $\pm 1.5\%$ change in β_{calc} at -170°C. relative to β_{calc} at ambient temperature.

By summing up these error terms, the estimated maximum errors in the viscosity for pure components and mixtures are shown in Table V-2.

CHAPTER VI

PRESENTATION OF EXPERIMENTAL RESULTS

The viscosity and density data were determined experimentally for methane, propane and three mixtures of methane and propane. The original experimental data and the calculated data are shown in Appendixes N and O for density and in Appendixes P and Q for viscosity. The viscosities presented in Appendixes P and Q were calculated by Computer Program 703 (Appendix R). Since these calculated viscosities have more significant figures than are justified by the accuracy of the experimental measurements, all the experimental values reported in the text have been rounded to three significant figures.

The recommended values of viscosity and density for methane, propane and three mixtures of methane and propane based upon these data and the low pressure methane viscosity data of Barua, et al. (6), are presented in this chapter. These values were obtained from smoothed curves of the viscosity (or density) as a function of pressure with temperature as a parameter.

Table VI-1 presents the recommended viscosity data for methane in the single phase region at temperatures from -170 to 0°C. and at pressures to 5,000 psia. Table VI-2 presents the recommended density data for vapor methane at temperatures below -80°C. Table VI-3 presents the recommended viscosity and density data for propane in the liquid region at temperatures from -100 to 0°C. and at pressures to 5,000 psia. The recommended viscosity and density data for the mixtures of methane and propane in the dense fluid regions are presented in Tables VI-4 and VI-5 for 22.1 and 50.0 mole% methane mixtures respectively at temperatures from -120 to 37.78°C. and pressures to 5,000 psia, and in Table VI-6 for 75.3 mole% mixture at temperatures from -150 to 37.78°C. at pressures to 5,000 psia.

Table VI-1

Recommended Viscosity Values for Liquid, Vapor and Fluid Methane

Pressure psia	Temperature °C.					
	0	-25	-50	-60	-70	-80
			Viscosity, Micropoise			
14.7	101*	93*	85*	83	80	76
600	111*	103*	96*	92	90	94
800	115*	108*	104*	103	113	235
1000	120	116	118	127	185	288
1500	138	144	184	229	280	345
2000	161	182	244	287	333	391
3000	214	256	330	364	403	453
4000	263	314	386	420	456	508
5000	305	361	432	463	501	555
	-100	-120	-140	-150	-160	-170
14.7	71	64	58	55	52	1440
D.P. [1]	75	66	58	55	52	50
B.P. [1]	385	542	767	940	1140	1440
600	405	570	810	990	1190	1510
1000	438	599	840	1020	1230	1560
1500	477	631	878	1070	1280	1620
2000	512	664	917	1110	1330	1680
3000	573	727	990	1200	1420	1810
4000	627	788	1060	1290	1520	1930
5000	676	847	1140	1370	1620	2060

Notes: (1) Dew point and bubble point pressures are from literature (51).
(2) Values with asterisk are obtained from the data of Barua, et al (6).
(3) These data were determined by No. 1 falling cylinder.
(4) The vapor phase viscosities at temperatures below -140°C. were extrapolated from the higher temperature data.

Table VI-2

Recommended Density Values for Vapor Methane

Pressure psia	Temperature, °C. -80	-100	-120	-140
		Density, g/cm		
D.P.	--	0.047	0.020	0.007
100	0.007	0.008	0.009	
200	0.016	0.019		
300	0.026	0.031		
400	0.038			
600	0.070			
800	0.228			
1000	0.252			

Note: (1) Density values at dew point pressures are from literature (51).

Table VI-3

Recommended Viscosity and Density Values for Liquid Propane

Pressure psia	Temperature °C.					
	0		-20		-40	
	Viscosity Micropoise,	Density g/cc.	Viscosity Micropoise,	Density g/cc.	Viscosity Micropoise,	Density g/cc.
B.P.[1]	1260	0.528	1550	0.554	1940	0.578
1000	1380	0.540	1670	0.564	2070	0.587
2000	1490	0.551	1800	0.573	2210	0.594
3000	1600	0.561	1910	0.582	2340	0.602
4000	1710	0.569	2030	0.589	2470	0.608
5000	1810	0.576	2150	0.595	2600	0.613
	-60		-80		-100	
B.P.[1]	2450	0.602	3160	0.624	4290	0.646
1000	2600	0.608	3320	0.630	4520	0.651
2000	2750	0.616	3500	0.636	4760	0.655
3000	2910	0.622	3680	0.641	5020	0.660
4000	3060	0.627	3880	0.645	5270	0.663
5000	3220	0.632	4060	0.651	5540	0.669

Notes: (1) Bubble point pressure values are from literature (33).
(2) Viscosity data were determined by No. 1 falling cylinder.

Table VI-4

Recommended Viscosity and Density Values for 22.1 mole% Methane-77.9 mole% Propane

Pressure psia	Temperature °C.							
	37.78		0		-20		-40	
	Viscosity Micropoise,	Density g/cc.	Viscosity Micropoise,	Density g/cc.	Viscosity Micropoise,	Density g/cc.	Viscosity Micropoise,	Density g/cc.
B.P.[1]	640	0.410	970	0.470	1190	0.497	1450	0.524
500	--	--	--	--	1200	0.500	1470	0.527
1000	676	0.421	1020	0.482	1250	0.510	1530	0.535
2000	785	0.451	1110	0.500	1350	0.525	1630	0.548
3000	870	0.467	1200	0.512	1440	0.535	1730	0.556
4000	949	0.482	1290	0.521	1540	0.542	1830	0.563
5000	1020	0.495	1380	0.530	1630	0.549	1930	0.569
	-60		-80		-100		-120	
B.P.[1]	1820	0.550	2340	0.576	3140	0.600	4580	0.625
500	1860	0.554	2390	0.580	3210	0.604	4700	0.628
1000	1930	0.560	2460	0.585	3290	0.608	4830	0.631
2000	2050	0.571	2610	0.593	3480	0.616	5090	0.637
3000	2170	0.577	2750	0.598	3660	0.620	5350	0.641
4000	2300	0.583	2900	0.605	3850	0.625	5620	0.644
5000	2420	0.588	3040	0.609	4040	0.629	5890	0.649

Notes: (1) Bubble point pressure values are from literature(2,58,62).
(2) Density data at 37.78°C. are from Sage and Lacey(66).
(3) Viscosity data were determined by No. 2 falling cylinder.

Table VI-5

Recommended Viscosity and Density Values for 50.0 mole% Methane-50.0 mole% Propane

Pressure psia	Temperature °C.							
	37.78		0		-20		-40	
	Viscosity Micropoise	Density g/cc.	Viscosity Micropoise	Density g/cc.	Viscosity Micropoise	Density g/cc.	Viscosity Micropoise	Density g/cc.
B.P.[1]	315	0.275	560	0.350	735	0.396	910	0.432
500	--	--	--	--	--	--	--	--
1000	--	--	--	--	740	0.400	935	0.440
2000	438	0.338	670	0.403	840	0.435	1020	0.464
3000	538	0.379	760	0.427	920	0.453	1100	0.478
4000	611	0.403	830	0.445	1000	0.467	1180	0.490
5000	676	0.420	890	0.458	1070	0.478	1260	0.499
	-60		-80		-100		-120	
B.P.[1]	1120	0.469	1450	0.499	1900	0.529	2710	0.557
500	--	--	1460	0.500	1930	0.532	2780	0.560
1000	1150	0.477	1510	0.507	1990	0.537	2860	0.562
2000	1240	0.492	1610	0.518	2110	0.545	3030	0.568
3000	1320	0.503	1700	0.527	2230	0.550	3200	0.573
4000	1400	0.512	1800	0.535	2350	0.557	3380	0.578
5000	1480	0.520	1900	0.541	2470	0.562	3550	0.582

Notes: (1) Bubble point pressure values are from literature(2,58,62).
(2) Density data at 37.78°C. are from Sage and Lacey(66).
(3) Viscosity data were determined by No. 2 falling cylinder.

Table VI-6

Recommended Viscosity and Density Values for 75.3 mole% Methane-24.7 mole% Propane

Pressure psia	Temperature °C.									
	37.78		0		-20		-40		-60	
	Viscosity Micropoise	density g/cc.	Viscosity Micropoise	Density g/cc.	Viscosity Micropoise	Density g/cc.	Viscosity Micropoise	Density g/cc.	Viscosity Micropoise	Density g/cc.
B.P.[1]	--	--	245	0.226	330	0.280	445	0.328	600	0.372
500	113	0.035	--	--	--	--	--	--	--	--
1000	131	0.083	--	--	--	--	--	--	615	0.380
2000	220	0.193	305	0.277	400	0.325	530	0.368	680	0.404
3000	296	0.264	395	0.329	480	0.364	600	0.393	750	0.421
4000	365	0.302	460	0.356	550	0.383	660	0.408	810	0.433
5000	430	0.326	520	0.375	605	0.398	710	0.422	870	0.444
	-80		-100		-120		-140		-150	
B.P.[1]	740	0.418	960	0.446	1330	0.478	1920	0.507	2440	0.522
500	745	0.410	975	0.429	1360	0.482	1980	0.510	2510	0.526
1000	785	0.422	1020	0.455	1410	0.487	2050	0.514	2600	0.529
2000	860	0.437	1090	0.467	1510	0.495	2190	0.520	2760	0.533
3000	930	0.448	1170	0.474	1600	0.500	2330	0.525	2930	0.537
4000	990	0.458	1250	0.482	1690	0.506	2460	0.530	3100	0.542
5000	1060	0.467	1320	0.490	1780	0.513	2600	0.535	3280	0.546

Notes: (1) Bubble point pressure values are from literature(2,58,62).
(2) Density data at 37.78°C. are from Sage and Lacey(66).
(3) Viscosity data were determined by No. 2 falling cylinder.

CHAPTER VII

DISCUSSION OF EXPERIMENTAL RESULTS

Discussion of Experimental Density Data

(1) Density Data of Methane and Propane

Figure VII-1 compares the experimental vapor density data for methane with the values from the literature. The figure shows that the data of this study at -80 and -100°C. are consistent with the saturated vapor densities of Matthews and Hurd (51) and the high temperature densities of Kvalnes and Gaddy (40).

Figure VII-2 compares the experimental liquid density data for propane with values obtained by other investigators at various temperatures and pressures. The low pressure liquid density data for propane agree with those of Rossini, et al. (65) to within ±0.1% (see Table VII-1), and the high pressure data extrapolate smoothly to those reported by Sage and Lacey (66). The comparison indicates that the average error for the propane density data of this study is less than the maximum error of ±0.6% predicted from error analysis (P. 61).

The recommended data in the single phase region and on the vapor-liquid boundary presented in Tables VI-2 and VI-3 are the smoothed values from large scale density-temperature plots where the original data of this study (Appendix N) and those from the literature (65,66) were plotted. The smoothed values agree with the original data points within 1%.

Table VII-1

Comparison of Low Pressure Propane Densities of This Study and the Literature

	Density(g/cc.)			
Temperature(°C.)	-20	-40	-60	-80
Rossini, et al.(65)	0.5541	0.5784	0.6017	0.6241
This study	0.554	0.578	0.602	0.624
% Deviation	-0.02	-0.07	0.05	-0.02

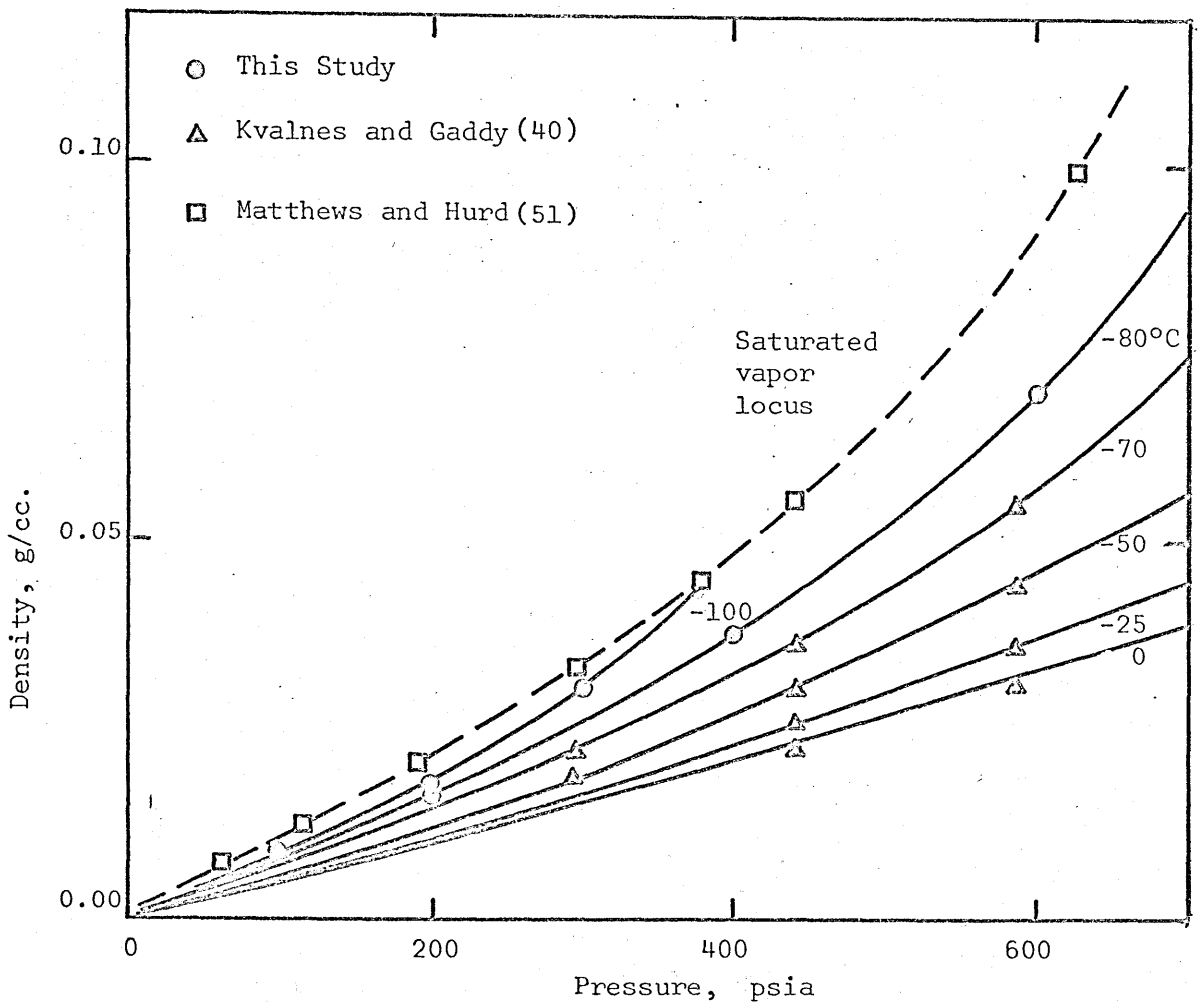

Figure VII-1 Vapor Density vs. Pressure Diagram for Methane

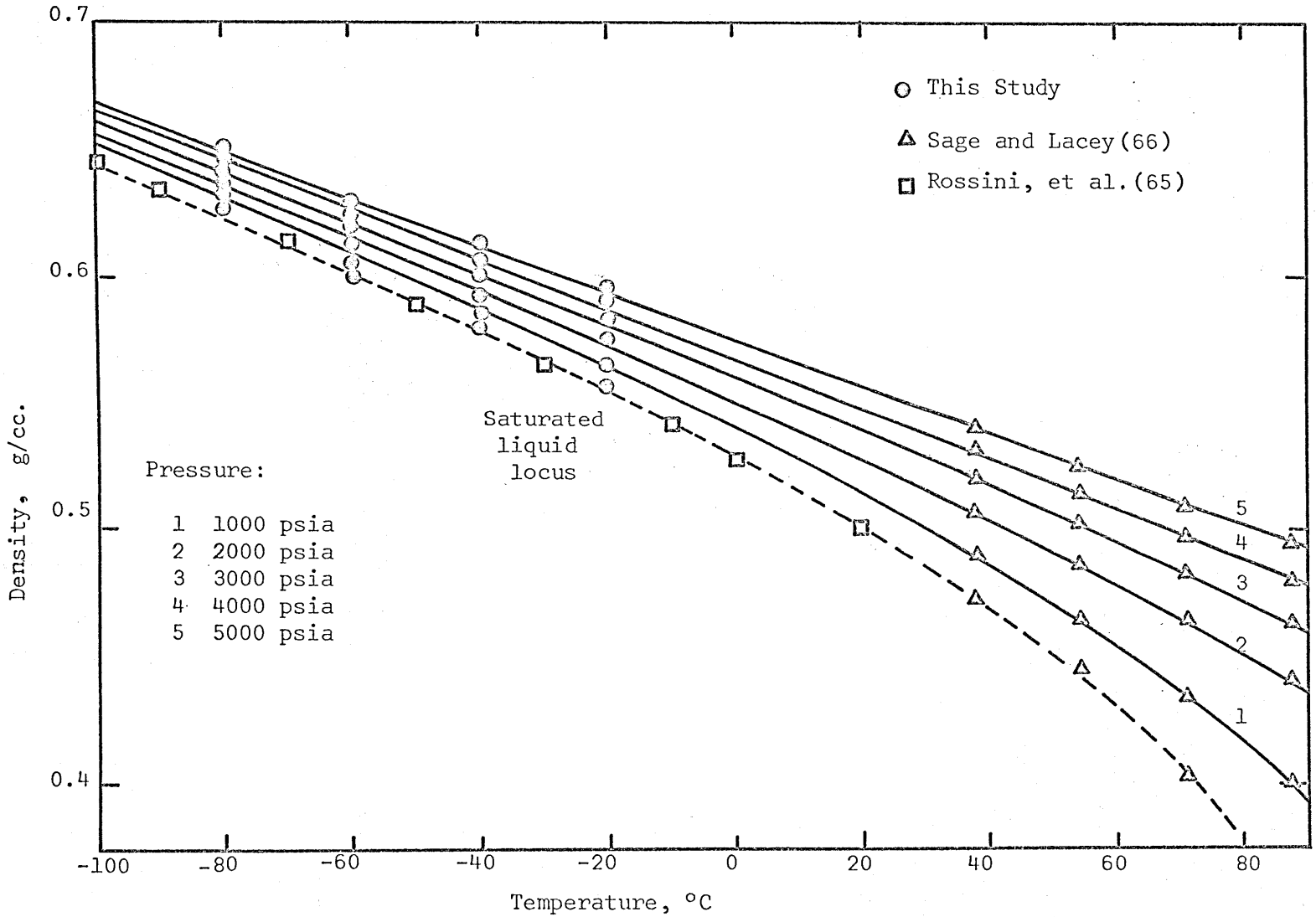

Figure VII-2 Density vs. Temperature Diagram for Propane

(2) Density Data for the Mixtures

The density data for mixtures as a function of temperature with pressure as a parameter are shown in Figures VII-3, VII-4 and VII-5. The experimental density data at pressures higher than 2,000 psia are shown to extrapolate smoothly to the high temperature data of Sage and Lacey (66). The two phase boundary for each mixture studied was obtained by extrapolating the isothermal high pressure density data on a density-pressure plot to the bubble point pressures which were obtained from the literature (2,58,62).

Density as a function of composition with temperature as a parameter at constant pressures of 2,000 and 5,000 psia is shown in Figure VII-6. These figures show the internal consistency of the density data for the methane-propane system.

The recommended density data in the single phase region and on the vapor-liquid boundary presented in Tables VI-4, VI-5 and VI-6 are the smoothed values from large-scale plots where the original data of this study (Appendix O) and those from the literature (66) were plotted. These smoothed data are in agreement with the original data points within 1% excepting those data at pressures lower than 2,000 psia. These low pressure data are obtained by extrapolating the high pressure density data (2,000 to 5,000 psia) to the bubble point pressures (2,58,62) using the data of Sage and Lacey (66) at 37.78°C. as a guide.

Table VII-2 shows the reproducibility of the density data for mixtures. Comparison is made between the data of the different runs from the same batch of mixture and between those of the runs from different batches of the same composition mixtures. The comparison shows that the reproducibility is better than 0.8%.

Huang (35) reported liquid densities for binary mixtures of methane and propane at low temperatures and low pressures. These data were taken concurrently with the viscosity determinations of Lim, et al. (46). Table VII-3-a compares the saturated liquid densities of Huang (35) with those of this study (interpolated to the compositions of Huang's work). The comparison between these data is very good for the 76.7 mole% methane mixture, but is poor for the 27.9 mole% methane mixture. The

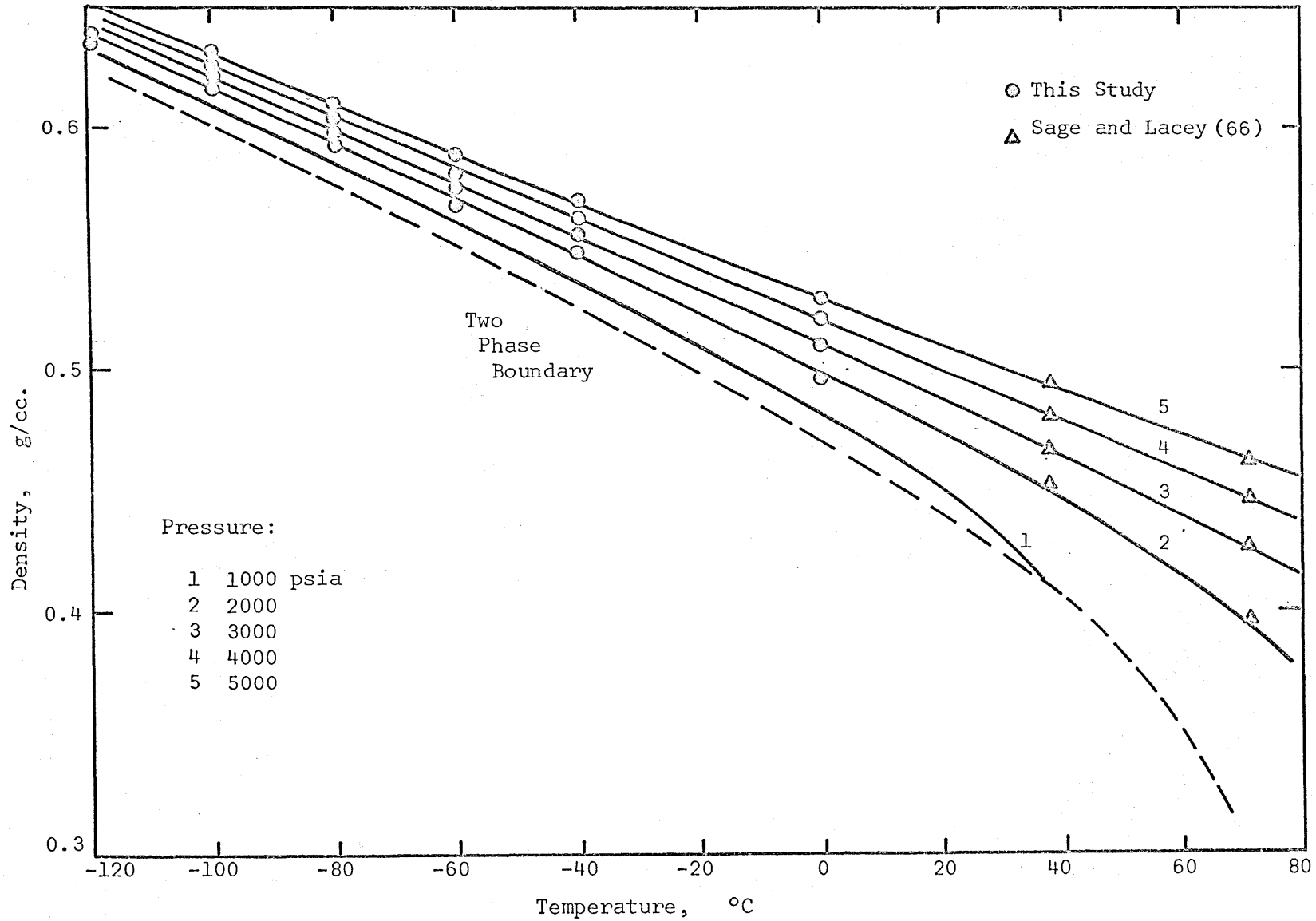

Figure VII-3 Density vs. Temperature Diagram for a 22.1 mole % CH_4-77.9 mole % C_3H_8 Mixture

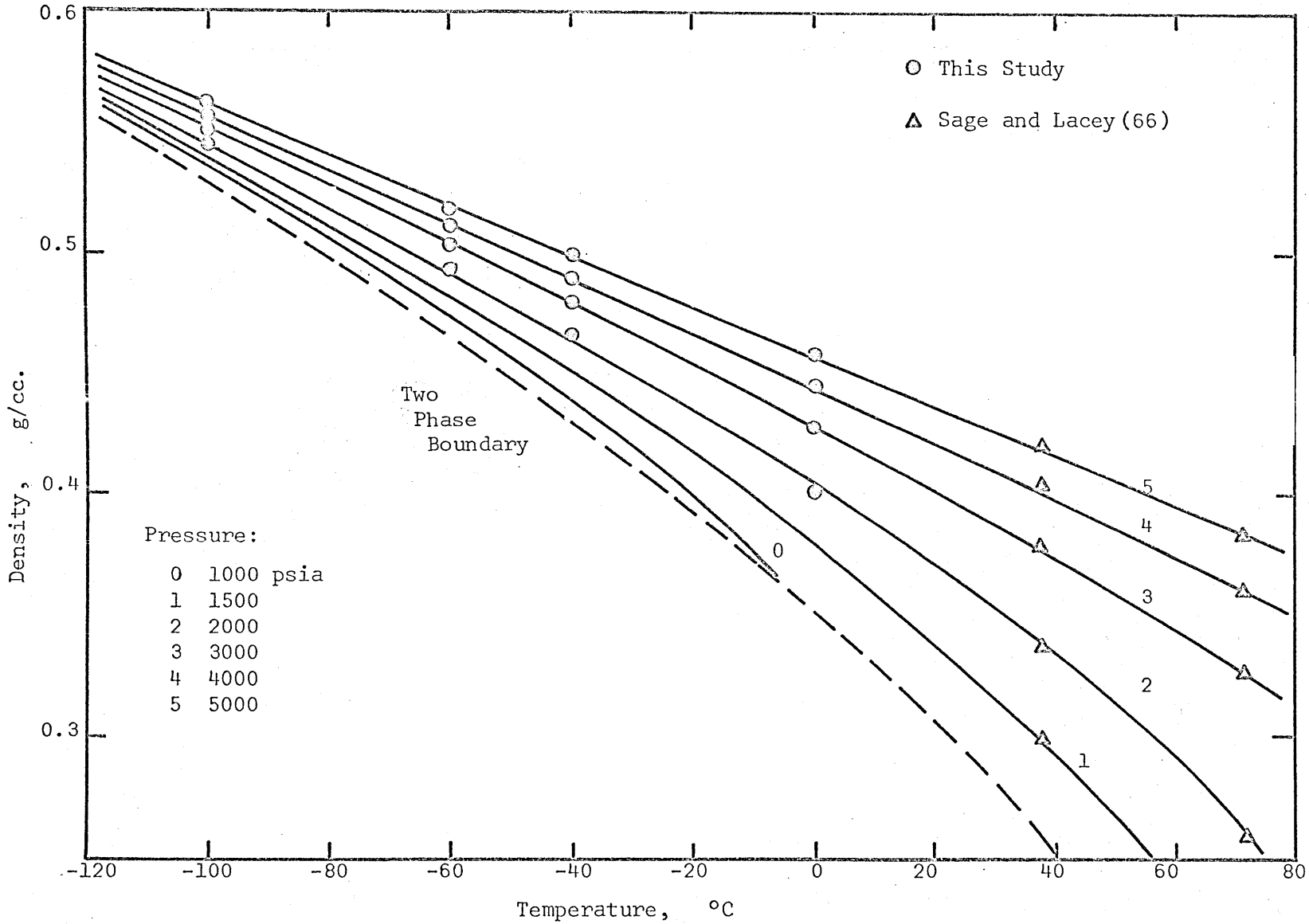

Figure VII-4 Density vs. Temperature Diagram for 50.0 mole % CH_4-50.0 mole % C_3H_8 Mixture

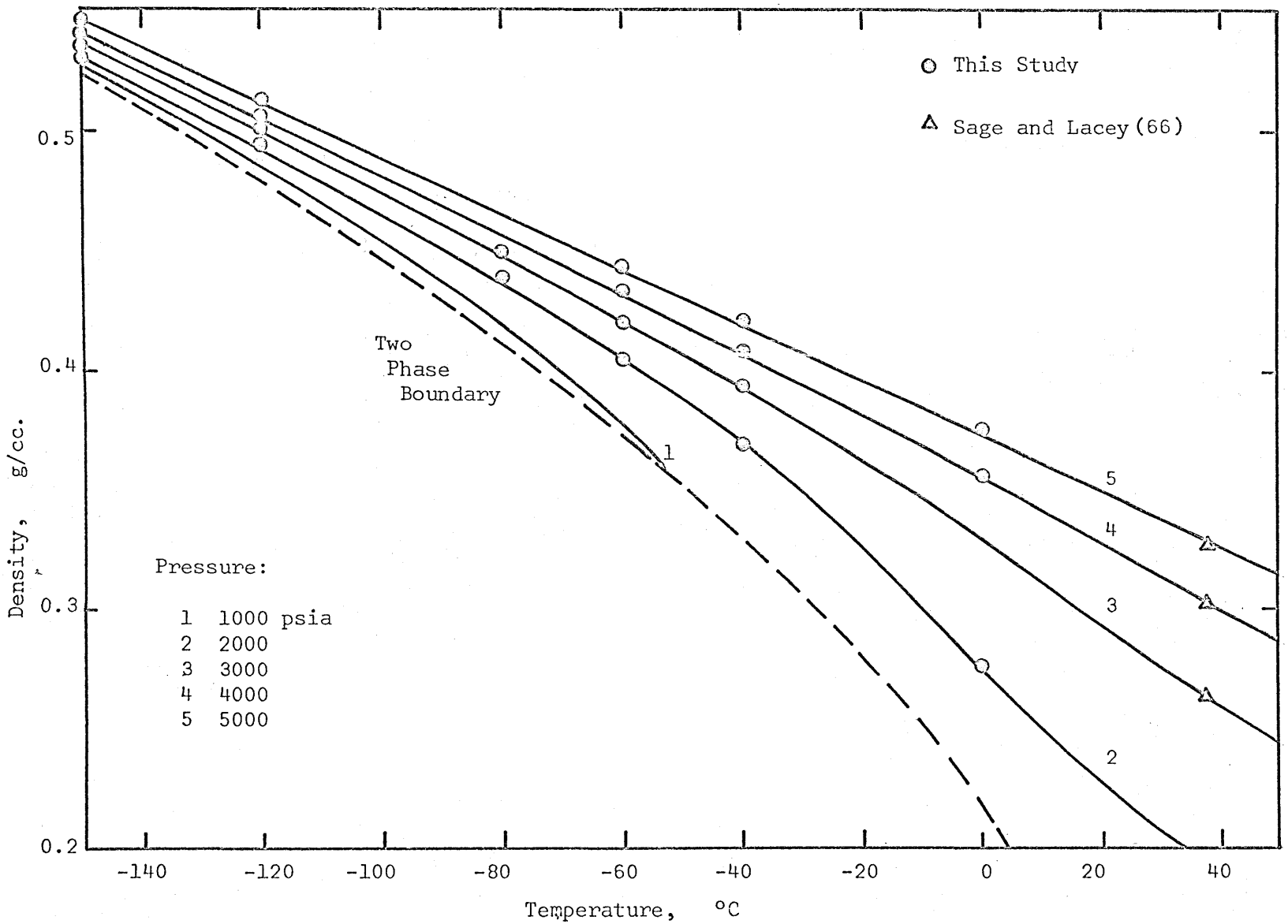

Figure VII-5 Density vs. Temperature Diagram for a 75.3 mole % CH_4-24.7 mole % C_3H_8 Mixture

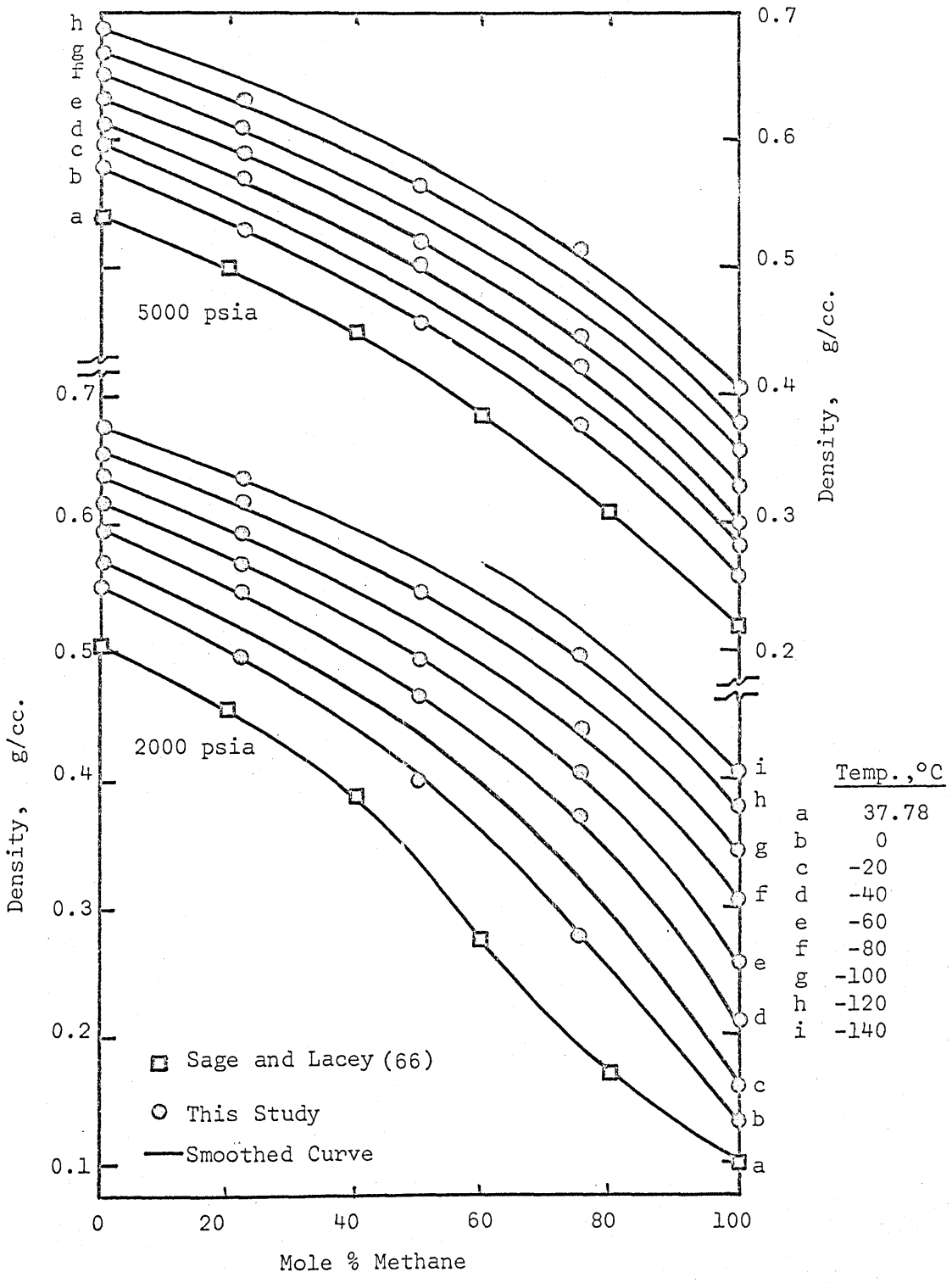

Figure VII-6 Density vs. Composition Diagram for CH_4 -C_3H_8 System at 2000 psia and 5000 psia

Table VII-2

Reproducibility of Viscosity and Reproducibility of Density from Different Runs and Different Batches of Mixtures

Group No.	Temp. °C.	Press. psia.	First Mixture Viscosity(Density) Micropoise g/cc.		Second Mixture Viscosity(Density) Micropoise g/cc.		% Dev. of Viscosity
I	0	2000	1 1110				0.0*
	0	2000	3 1110				
II	0	2000	4 685	(0.400)	5 683	(0.397)	0.3
	0	3000	4 760	(0.427)	5 758	(0.425)	0.3
	0	4000	4 823	(0.444)	5 829	(0.442)	-0.7
	0	5000	4 891	(0.457)	5 890	(0.455)	0.1
	-60	930	2 1140		5 1140		0.0
	-60	2000	2 1230		5 1230		0.0
	-60	3000	2 1320		5 1340		-1.5
	-100	2000			5	(0.545)	
	0	2000			6	(0.397)	
	-100	2000			6	(0.545)	
III	0	2000	1 308	(0.277)	5 314	(0.278)	-1.9
	-80	910	1 779		5 766		1.7
	-80	2000	1 860	(0.439)	5 866	(0.439)	-0.7

Notes: (1) Group numbers I, II, III represent respectively the data for 22.1, 50.0, 75.3% methane mixtures.
(2) The number with underline stands for run number corresponding to the last number in the code number mentioned in P. 168.
(3) * is the deviation of the two fall times in group I.

Table VII-3

Comparison of Density Data for Mixtures of
This Study and Other Investigators

(a) Saturated liquid densities at low temperatures

Temperature °C.	Mole % Methane 27.9 This study	Huang (35)	% Dev.	76.7 This study	Huang (35)	% Dev.
-80	0.560	0.538	3.9	--	--	--
-100	0.587	0.573	2.4	0.440	0.438	0.5
-120	0.613	0.604	1.5	0.472	0.473	-0.2

(b) Dense fluid densities at 37.78°C.

Pressure psia	Mole % Methane 75.3 This study	Sage & Lacey(66)	% Dev.
2000	0.195	0.193	1.0
3000	0.265	0.264	0.4
4000	0.304	0.302	0.7
5000	0.330	0.326	1.2

Note: Density is expressed in g/cc.

data of the present work are considered more accurate because of improvements in the experimental equipment, e.g., the installation of a low temperature DPI for pressure measurement in the viscometer (P. 25). In the earlier experimental work (35), a Heise bourdon tube gage was used directly for pressure measurement where the bourdon tube was exposed to ambient temperature. For the 76.7 mole% methane mixture the cricondentherm is below ambient temperature, therefore the mixture in the bourdon tube existed in a single phase condition, and the composition of the liquid mixture in the viscometer was always the same as that reported. This explains the agreement between the data of the earlier work and this study. In the case of the 27.9 mole% methane mixture, since the cricondentherm of the mixture is higher than ambient temperature, the mixture in the bourdon tube existed in two phases. This would cause the composition of the mixture in the viscometer to be different from that analyzed in the storage reservoir which was maintained above the cricondentherm, and explains the discrepancy between the data of the earlier work and this study.

The densities of this study for the 75.3 mole% methane mixture at 37.78°C. were compared with those of Sage and Lacey (66). Table VII-3-b shows that the data of this study are consistently higher than those reported by Sage and Lacey. The deviations are probably due to the error in the methane density used in the density computation because of the presence of nitrogen and ethane (P. 57). If the 0.6% correction for the impurity in the methane is made, the data of this study will agree with those of Sage and Lacey within $\pm$0.6%.

The maximum error of the density data for mixtures is estimated to be within $\pm$1.2% (P. 61). The reproducibility of the density determination and the deviations between the density data from this study and the other works cited (except for the 27.9 mole% methane mixture of Huang) are within this maximum estimate of error.

Discussion of Experimental Viscosity Data

(1) Viscosity Data of Methane and Propane

Methane viscosity behavior as a function of pressure near the critical region is depicted in Figure VII-7, where the solid lines representing the isotherms link the data points of this study and those of Barua, et al. (6). The saturated liquid and saturated vapor loci represented by the dotted line are defined by the data of Swift (75) and by the data extrapolated from the low temperature vapor viscosities of this study to the vapor pressures. Figure VII-8 presents methane viscosity as a function of pressure to 5,000 psia, showing the isothermal data from 0 to -170°C. with the data of Swift defining the saturated liquid locus. Figure VII-9 gives the viscosity as a function of temperature with pressure as parameter, and the dotted curve defines the saturated vapor and saturated liquid loci.

Propane viscosity data as a function of pressure with temperature as a parameter are shown in Figure VII-10 and the same data as a function of temperature with pressure as parameter are shown in Figure VII-11. The saturated liquid locus is defined by the data of Swift (75) and Rossini, et al. (65).

The smoothed values from large-scale viscosity-pressure plots, with temperature as a parameter constructed from the original data (Appendix P), are reported as recommended viscosity data for methane and propane in the single phase region and on the vapor-liquid boundary in Tables VI-1 and VI-3. These smoothed values are in agreement with the original data points within 1%. Table VI-1 also presents methane viscosity values at atmospheric pressure which were extrapolated from the low pressure data of this study and those of Barua, et al. (6).

The data of this study were compared with the data in the literature whenever possible. For methane data in the low temperature region, the only data available for comparison are those of Rossini, et al. (65), Swift (75) and Pavlovich and Timrot (55).

Table VII-4 compares the low pressure liquid viscosity data for methane with those from the literature. The data of this study agree within 1.4% with the data of Rossini, et al. (65) but are somewhat higher than those reported by Swift (75), showing a trend of increasing dis-

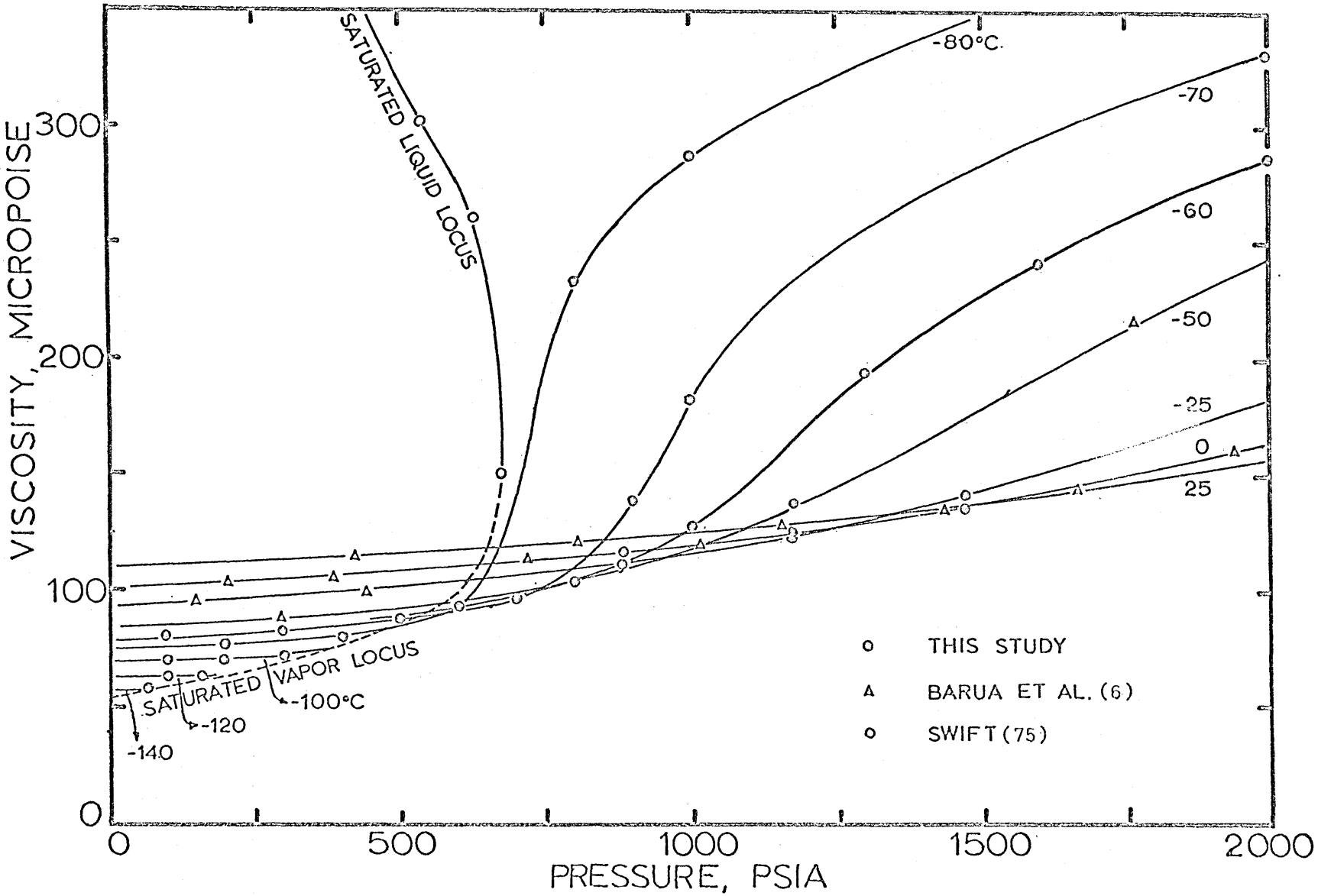

Figure VII-7 Viscosity vs. Pressure Diagram for Methane at Low Pressures

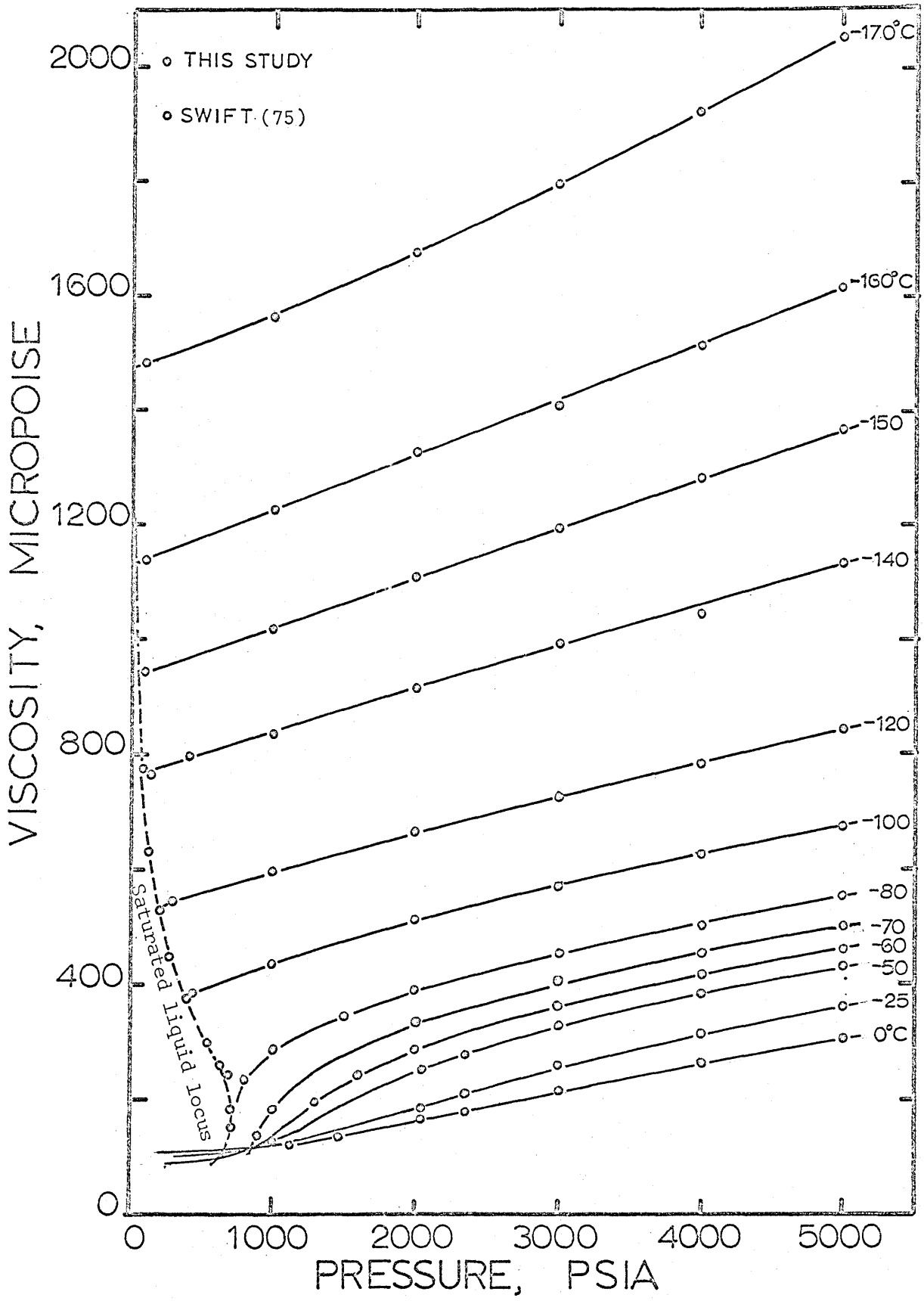

Figure VII-8 Viscosity vs. Pressure Diagram for Methane

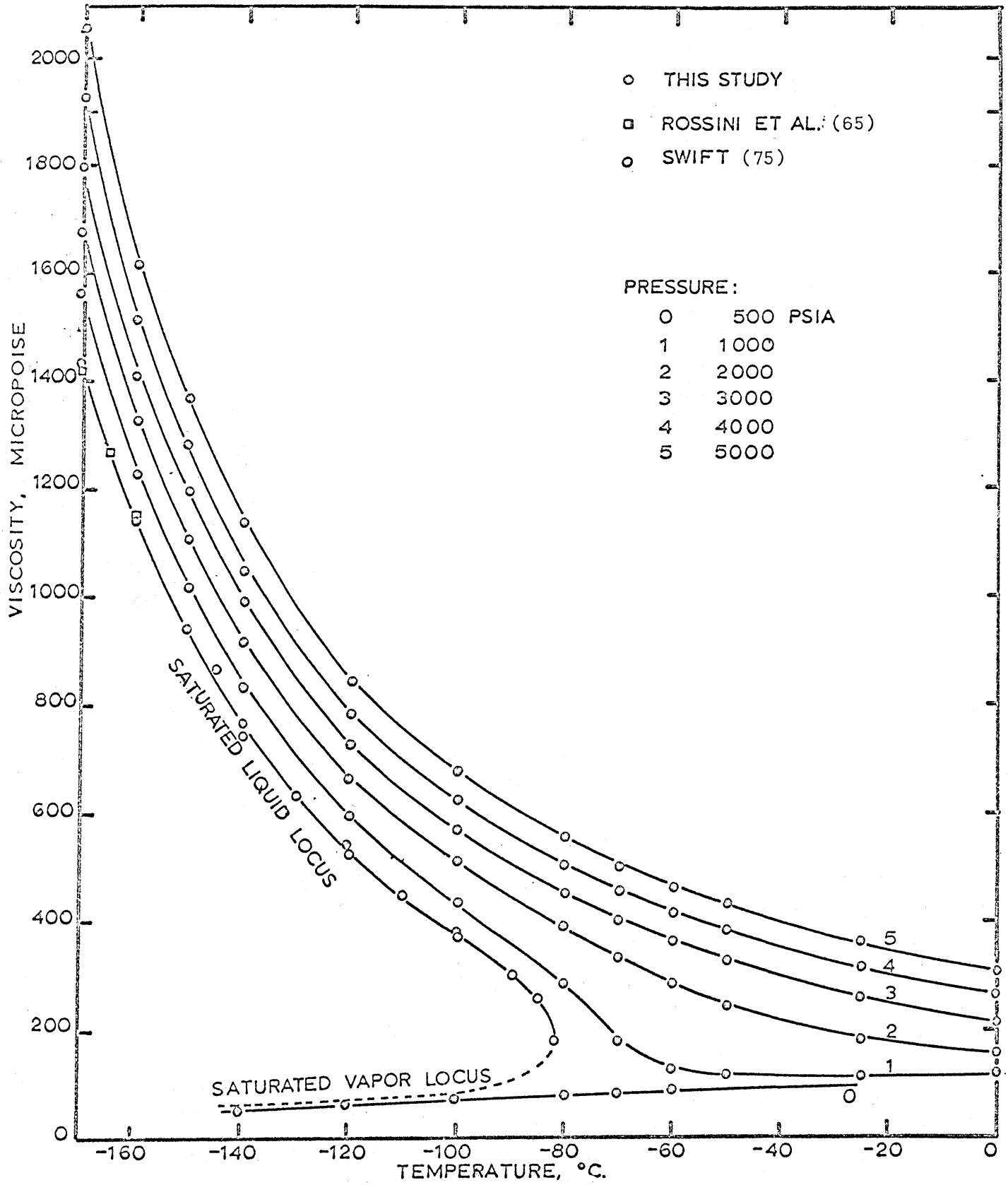

Figure VII-9 Viscosity vs. Temperature Diagram for Methane

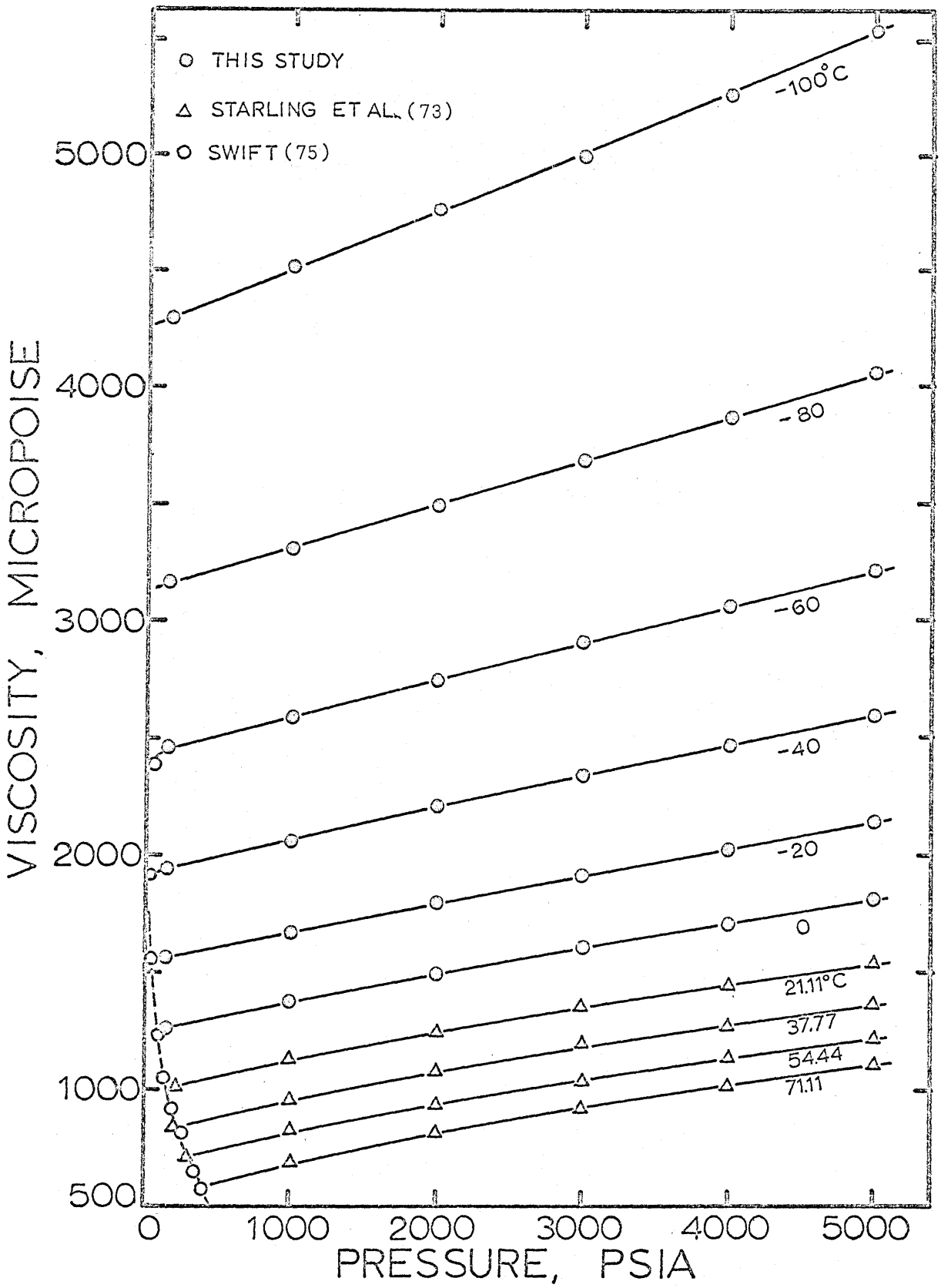

Figure VII-10 Viscosity vs. Pressure Diagram for Propane

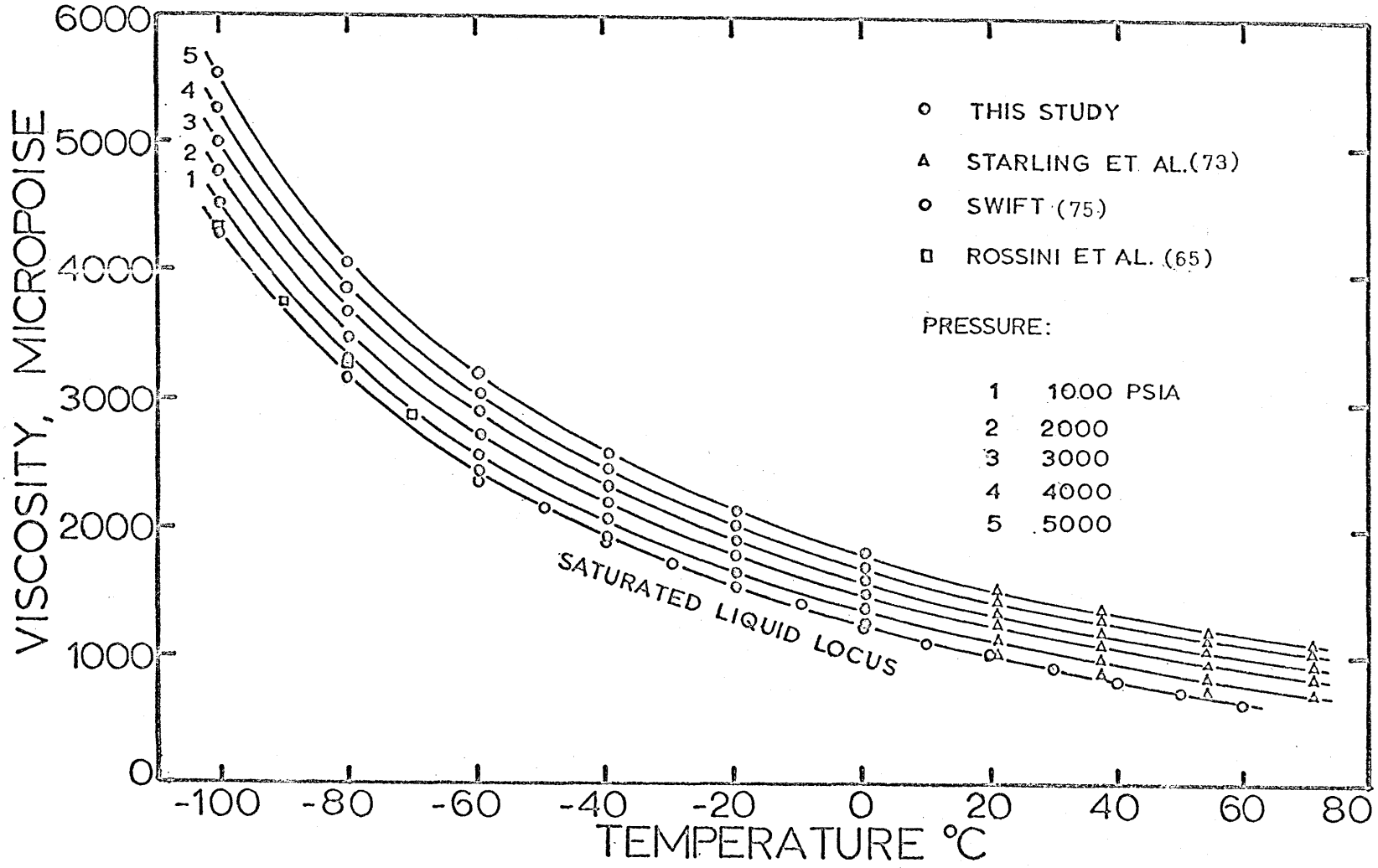

Figure VII-11 Viscosity vs. Temperature Diagram for Propane

Table VII-4

Comparison of Low Pressure Viscosity Data for Methane and Propane in the Liquid Phase

Substance	Temp. °C.	This study	Rossini, et al. (65)	Percent Dev.	Swift (75)	Percent Dev.
			Viscosity, Micropoise			
Methane	-100	385	--	--	376(400)	2.3
	-120	542	--	--	531(195)	2.0
	-140	767	--	--	742(85)	3.3
	-160	1140	1150	-0.9	-- --	--
	-170	1440	1420	1.4	-- --	--
Propane	0	1260	--	--	1240(100)	1.6
	-20	1550	--	--	1570(50)	-1.3
	-40	1940	2050	-5.7	1920(40)	1.0
	-60	2450	2560	-4.5	2390(40)	2.5
	-80	3160	3270	-3.5	-- --	--
	-100	4290	4330	-0.9	-- --	--

Notes: (1) The data of this study are reported at bubble point pressure.
(2) The data of Rossini, et al are reported at the atmospheric Pressure.
(3) The data of Swift are reported at the pressure (psia) in parenthesis.

crepancy with decreasing temperature. Swift assumed that the viscometer calibration constant was a linear function of temperature whereas theoretical calculations (see P. 15) show that it is a non-linear function where both the first and the second derivatives of the viscometer calibration constant with respect to temperature are negative. Since the non-linear temperature dependence of the viscometer calibration constant was taken into account in the computation of the viscosity in this investigation, the trend of increasing deviation between the data of this study and those of Swift with decreasing temperature is to be expected. The agreement of the present data with those of Rossini, et al. (65) at -160 and -170°C. indicates the validity of the calibration method used in the present study. The data of this study are considered more accurate than those reported by Swift (75), because of the improvement in the method of calibrating the viscometer.

Pavlovich and Timrot (55) reported some viscosity data for methane at low temperatures and high pressures. Their data are not considered to be reliable, since (a) they are not self-consistent and (b) the data are considerably higher than the data of this investigation and those of Rossini, et al. (65). At -161.4°C. and 20 atmospheres for example, their reported viscosity value is about 40% higher than the values of this study and Rossini, et al. (keep in mind that the effect of 20 atmospheres on the viscosity of a liquid should be negligible).

In the high temperature region Barua, et al. (6) reported viscosity data at temperatures to -50°C. and pressures to 2,576 psia, while Ross and Brown (64) investigated the viscosity at temperatures down to -50°C. and pressures to 10,000 psia. Several other investigators (4,14,27) also published methane viscosity data at temperatures above 0°C. and high pressures. A graphical comparison between these data is shown in Figure VII-12. The present results are in good agreement with those of Barua, et al. (6) which is to be expected since they were used in the calibration of the falling cylinder viscometer used in the present investigation. The present data extrapolate smoothly to the high temperature data reported by Carmichael, et al. (14), Giddings (27), and Baron, et al. (4). The data of Ross and Brown (64) are consistently

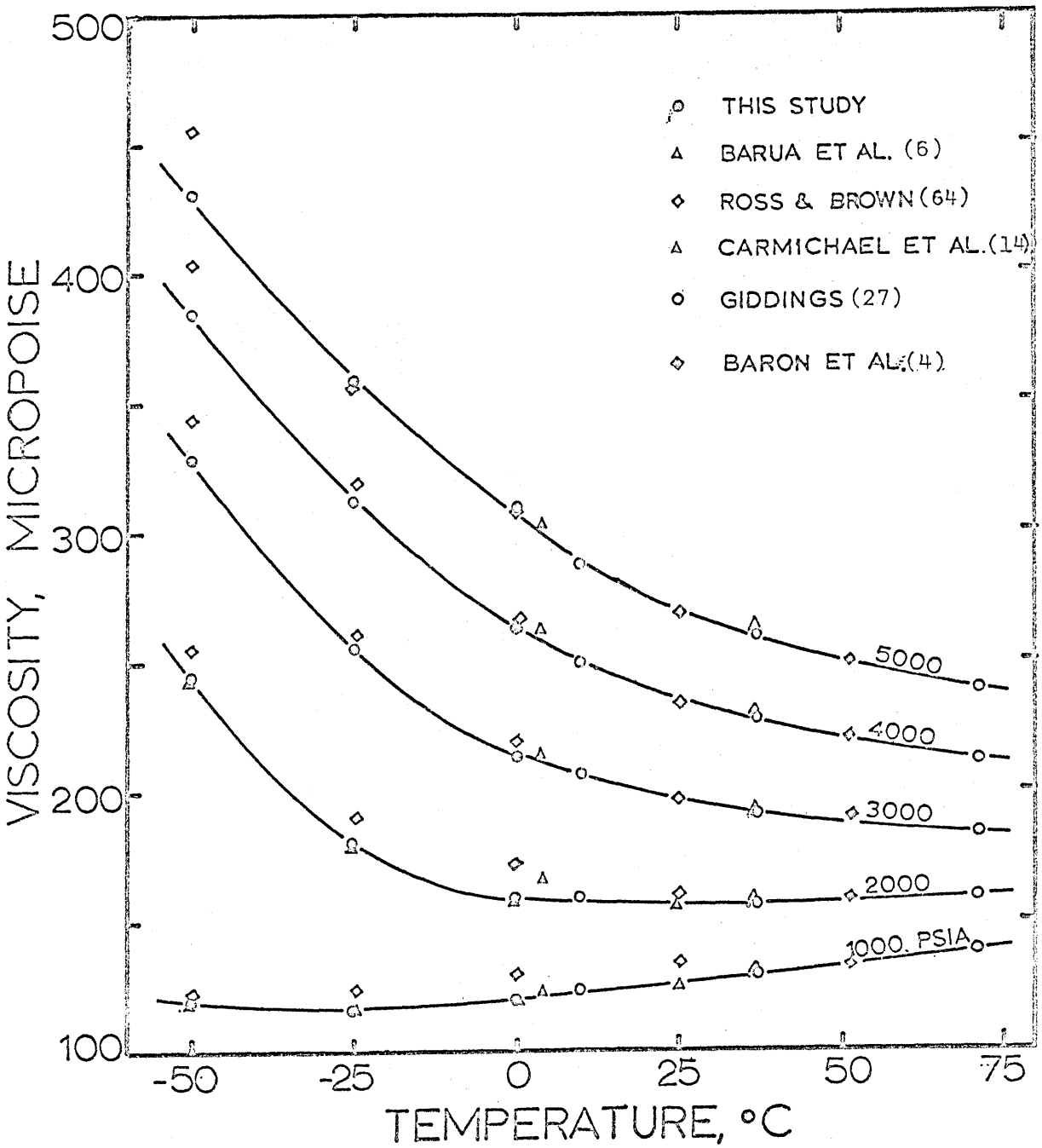

Figure VII-12 Comparison of Viscosity Data for Methane from Several Investigators

higher than the smooth curves which were constructed by inspection to represent the best fit of all other data including those of this investigation.

Figure VII-11 shows that the propane data of this study extend smoothly to the data of Starling, et al. (73) at the superambient temperatures. This is to be expected since the data of Starling, et al. were used in the calibration of the viscometer. Table VII-4 compares the low pressure liquid propane viscosity data of this investigation and those of Swift (75) and Rossini, et al. (65). The present viscosity data are higher than those reported by Swift because of the non-linear temperature dependence of the viscometer constant used in this study. A good agreement with the value reported by Rossini, et al. at -100°C. shows again the validity of the method used to correct the calibration constant for the temperature change. At temperatures above -100°C. the viscosity data of Rossini, et al. appear to be higher than those of this study and of Swift (75). However, the data of this study at higher temperatures are believed to be more reliable than the compilation data of Rossini, et al., because the data reported by two independent investigators, the author and Swift (75) have better agreement and both are shown to be smaller than those of Rossini, et al. The average deviation between the data of this study and those of Swift (75) and of Rossini, et al. (65) is, for the most part, within $\pm$2.0%.

Viscosity data for methane and propane were determined by No. 1 falling cylinder. Tables VII-5 and VII-6 show a comparison of methane and propane viscosity data obtained from three different falling cylinders According to the results shown in this table, the precision of the viscosity with respect to temperature and pressure is random and does not correlate with temperature or pressure. The precision of the viscosity measurements as determined with different falling cylinders, reported as the average of all the percent errors listed in Tables VII-5 and VII-6 is $\pm$1.2% for methane and $\pm$1.1% for propane respectively.

(2) Viscosity Data of Mixtures

The viscosity data for the three mixtures were determined using No. 2 falling cylinder because the calibration of No. 1 falling cylinder

Table VII-5

Comparison of Methane Viscosities Obtained from Different Falling Cylinders

Temp. °C.	Press. psia	No. 1 Falling Cylinder	No. 2 Falling Cylinder	No. 3 Falling Cylinder	Average	% Error*
		Viscosity, Micropoise				
0	880	117	117	117	117	0.0
	1175	125	125	125	125	0.0
	1470	135	135	135	135	0.0
	2060	161	162	163	162	0.6
	2350	179	177	179	178	0.6
	3000	214	211	211	212	0.9
	4000	263	260	--	261	0.8
	5000	305	300	295	300	1.7
-25	880	111	113	111	112	0.9
	1175	123	124	123	123	0.8
	1470	141	142	143	142	0.7
	2060	187	186	188	187	0.5
	2350	211	208	211	210	1.0
	3000	256	251	250	252	1.6
	4000	314	301	--	308	2.3
	5000	361	344	345	350	3.1
-50	880	110	110	108	109	0.9
	1175	137	136	136	136	0.7
	1470	--	182	184	183	0.6
	2060	251	250	248	250	0.8
	2350	280	275	275	277	1.1
	3000	330	318	320	323	2.1
	4000	386	372	--	379	1.8
	5000	432	414	414	420	2.9
-70	1000	185	193	--	189	2.1
	3000	403	401	--	402	0.3
	5000	501	498	--	500	0.4
-80	1000	288	--	278	283	1.8
	3000	453	--	440	447	1.6
	5000	555	--	535	545	1.8
-120	1000	599	597	599	598	0.2
	3000	728	718	725	724	0.8
	5000	847	--	836	841	0.7

Note: *Computed on basis of absolute value of maximum deviation between the average value and any value.

Table VII-6

Comparison of Propane Viscosities Obtained from Different Falling Cylinders

Temp. °C.	Press. psia	No. 1 Falling Cylinder	No. 2 Falling Cylinder	No. 3 Falling Cylinder	Average	% Error*
		Viscosity, Micropoise				
0	160	1270	--	1290	1280	0.8
	1000	1380	--	1390	1385	0.4
	3000	1600	--	1610	1605	0.3
	5000	1810	--	1810	1810	0.0
-40	150	1940	--	2000	1970	1.5
	1000	2070	2100	2110	2093	1.1
	3000	2340	2360	2370	2357	0.7
	5000	2600	2620	2630	2617	0.6
-80	1000	3320	--	3530	3425	3.1
	5000	4060	--	4300	4180	2.9

Note: *Computed on basis of absolute value of maximum deviation between the average value and any measured value.

had changed after the completion of the viscosity determinations for methane and propane. The precision of viscosity determination obtained from different falling cylinders has been shown in the preceding section, where the average precision is ±1.2%, and the maximum deviation is ±3.1%. Therefore, the viscosity data for the mixtures are believed to be consistent with those for the pure components to within ±1.2% on the average.

The recommended viscosity data in the single phase region and on the vapor-liquid boundary presented in Tables VI-4, VI-5 and VI-6 are the smoothed values from large-scale viscosity-temperature plots of the original data (Appendix Q). These smoothed data are in agreement with the original data points within 1%.

The viscosities for 22.1, 50.0 and 75.3 mole% methane mixtures are shown as a function of pressure with temperature as the parameter in Figures VII-13, VII-14 and VII-15 respectively. Smoothed solid curves were drawn through the isothermal data points and extrapolated to the bubble point pressures to define the bubble point locus which is represented by the dotted curve. The phase behavior information on these figures was obtained from the literature (2,58,62). These figures show the pressure effect on the isothermal viscosity data, and this effect becomes more significant as the temperature decreases. Figures VII-16, VII-17 and VII-18 show the viscosity data from this study as a function of temperature with pressure as the parameter. The data of Giddings (27) in the high temperature region are also shown in these figures. Curves were drawn through all the isobaric data points, and then were extended smoothly from the low temperature data of this study to the high temperature data of Giddings (27). In Figures VII-13, VII-14 and VII-15, a loop is also shown for the two phase boundary (dotted curve) for each mixture at the cricondentherm which is estimated from the literature phase behavior data (2,58,62).

The experimental viscosity data for pure components and mixtures are plotted versus composition in Figure VII-19 indicating that the data obtained from No. 1 falling cylinder for the pure components and

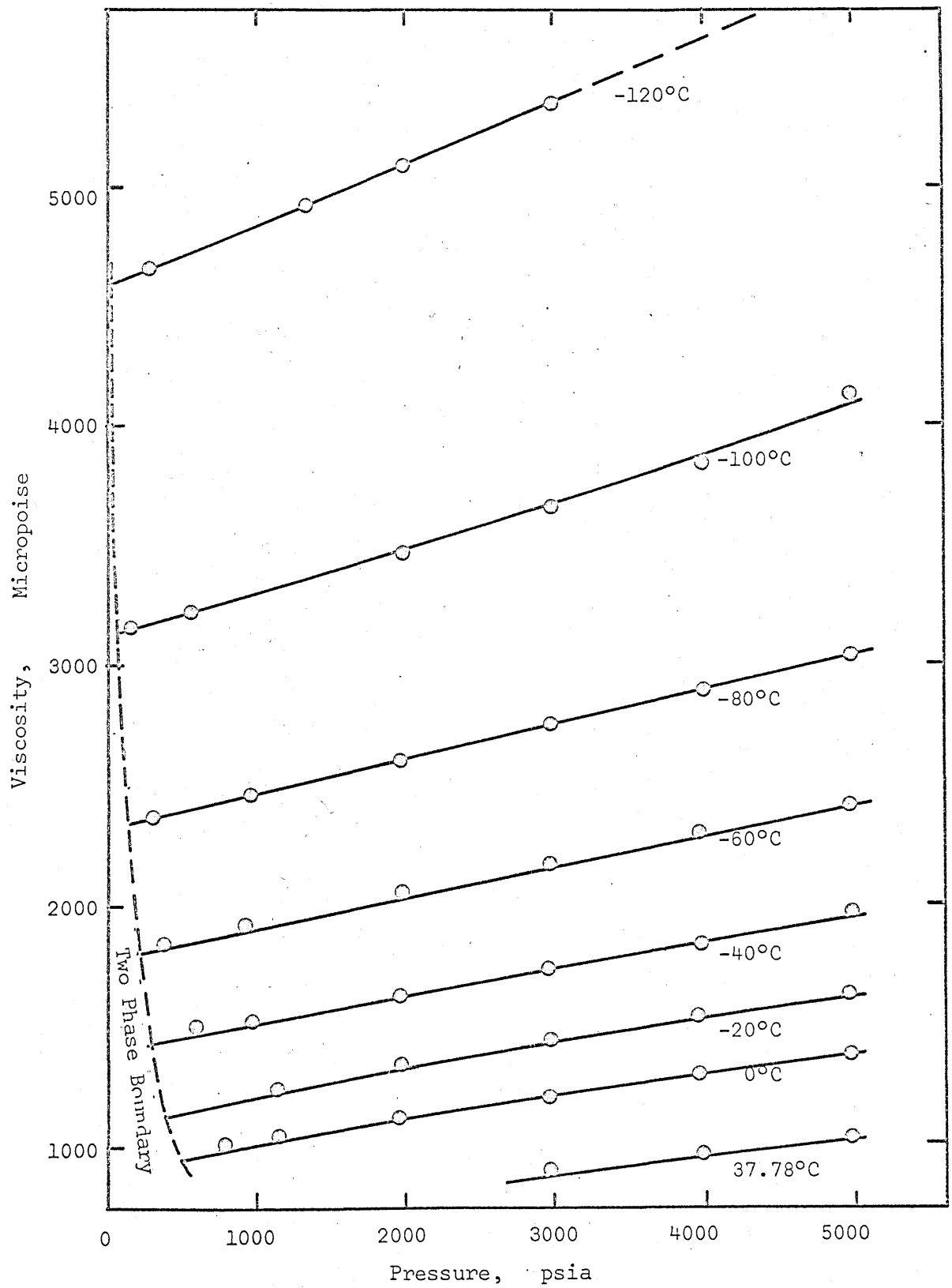

Figure VII-13 Viscosity vs. Pressure Diagram for a 22.1 mole % CH_4-77.9 mole % C_3H_8 Mixture

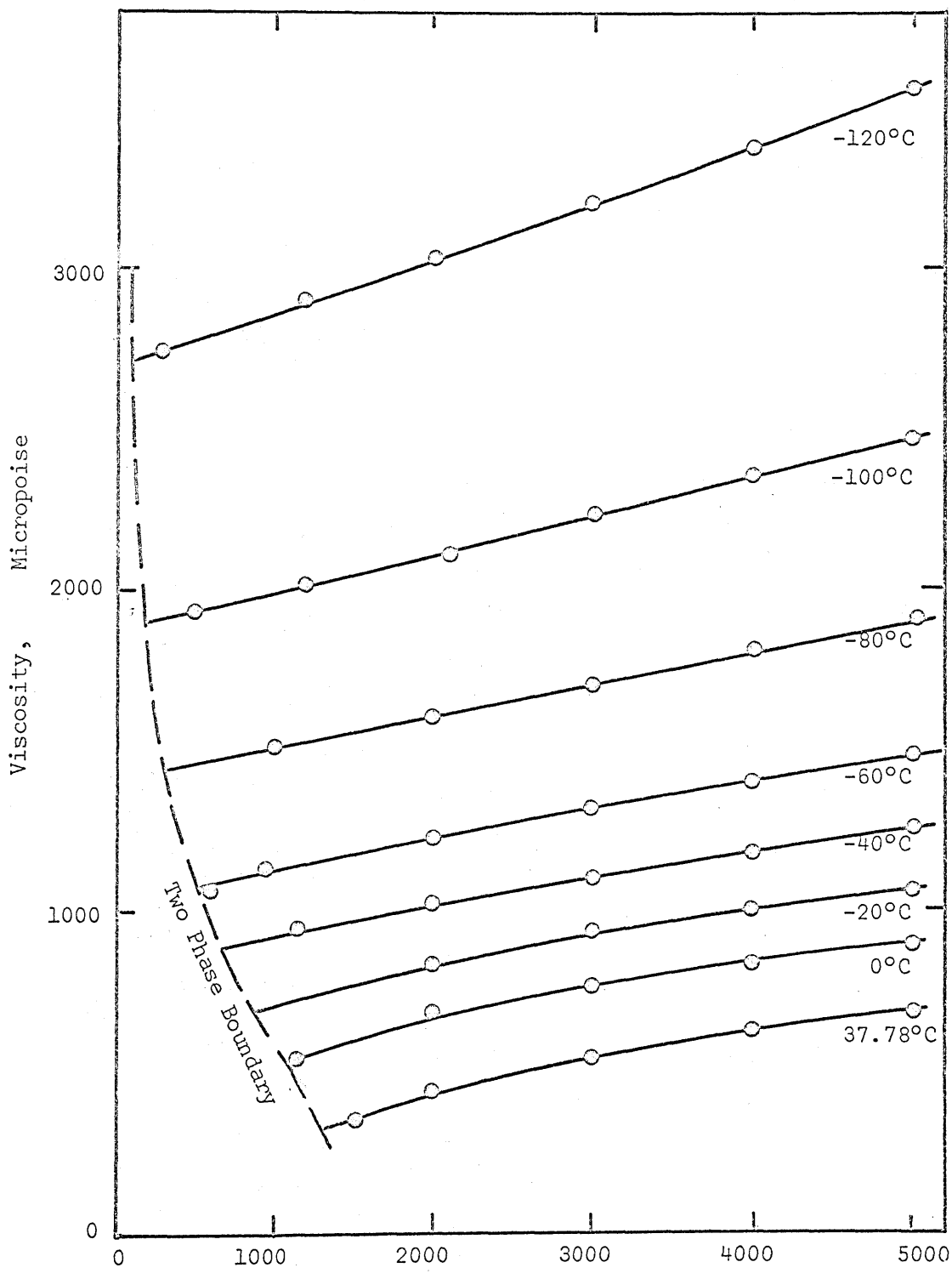

Figure VII-14 Viscosity vs. Pressure Diagram for a 50.0 mole % CH_4-50.0 mole % C_3H_8 Mixture

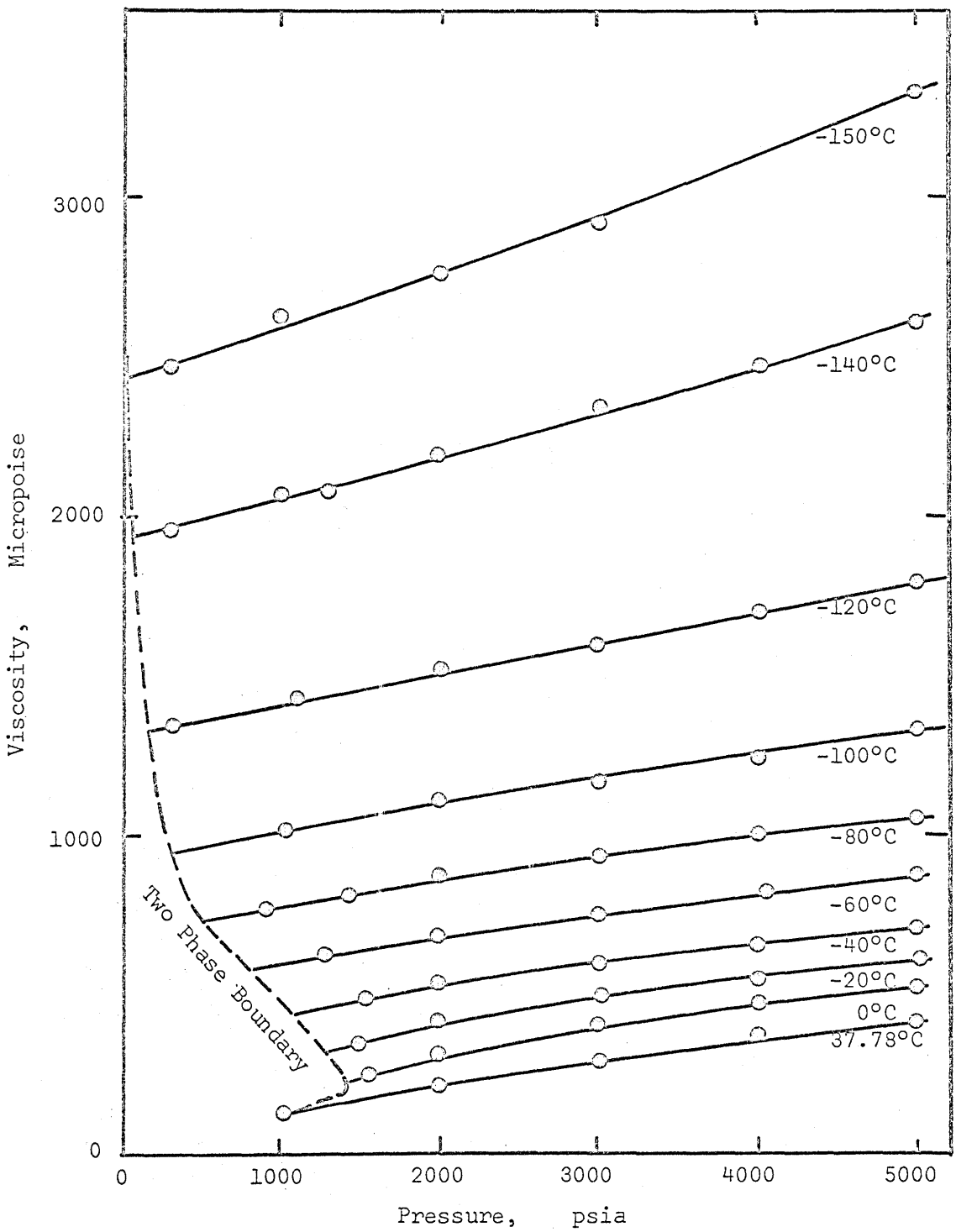

Figure VII-15 Viscosity vs. Pressure Diagram for a 75.3 mole % CH_4-24.7 mole % C_3H_8 Mixture

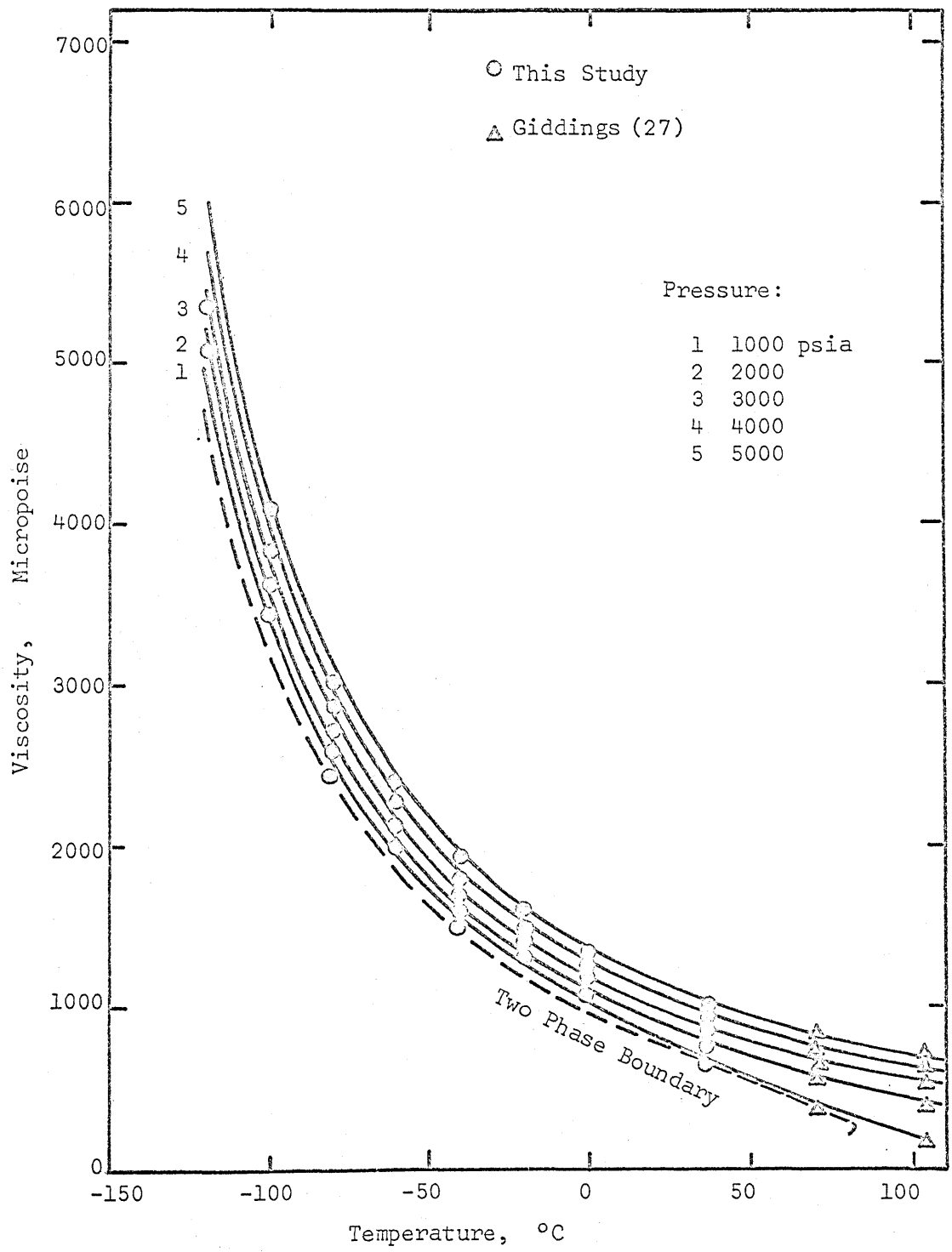

Figure VII-16 Viscosity vs. Temperature Diagram for a 22.1 mole % CH_4-77.9 mole % C_3H_8 Mixture

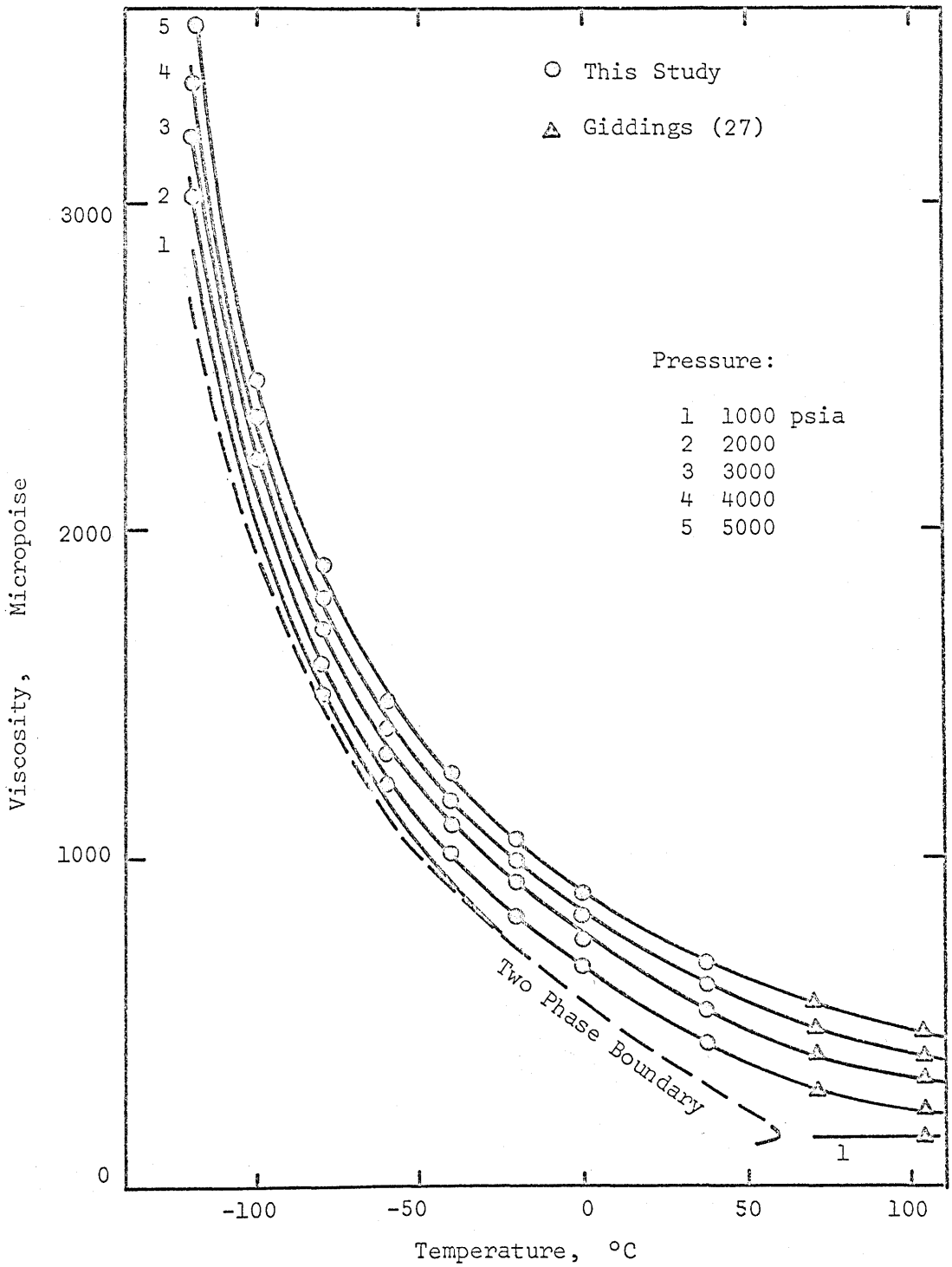

Figure VII-17 Viscosity vs. Temperature Diagram for a 50.0 mole % CH_4-50.0 mole % C_3H_8 Mixture

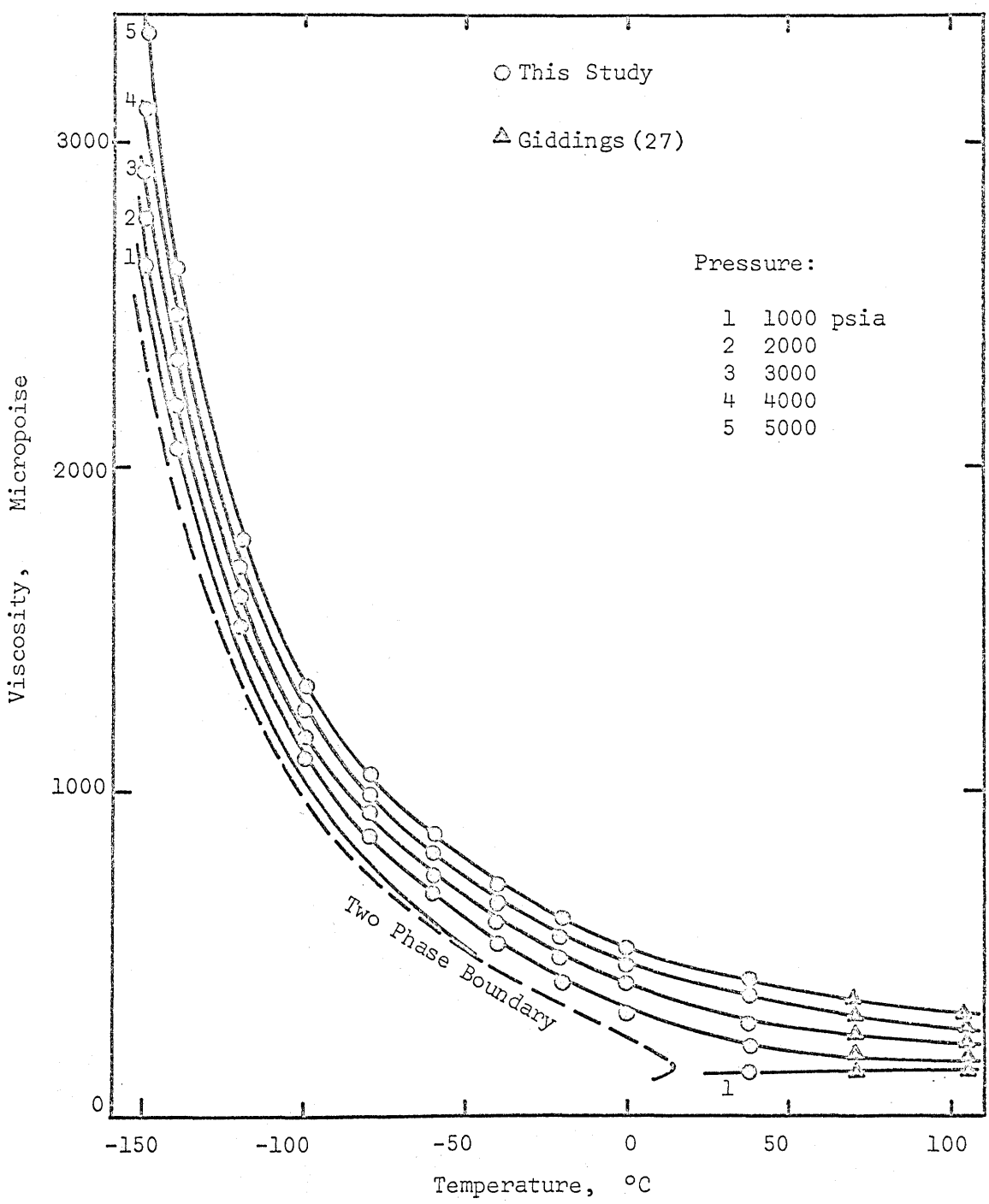

Figure VII-18 Viscosity vs. Temperature Diagram for a 75.3 mole % CH_4-24.7 mole % C_3H_8 Mixture

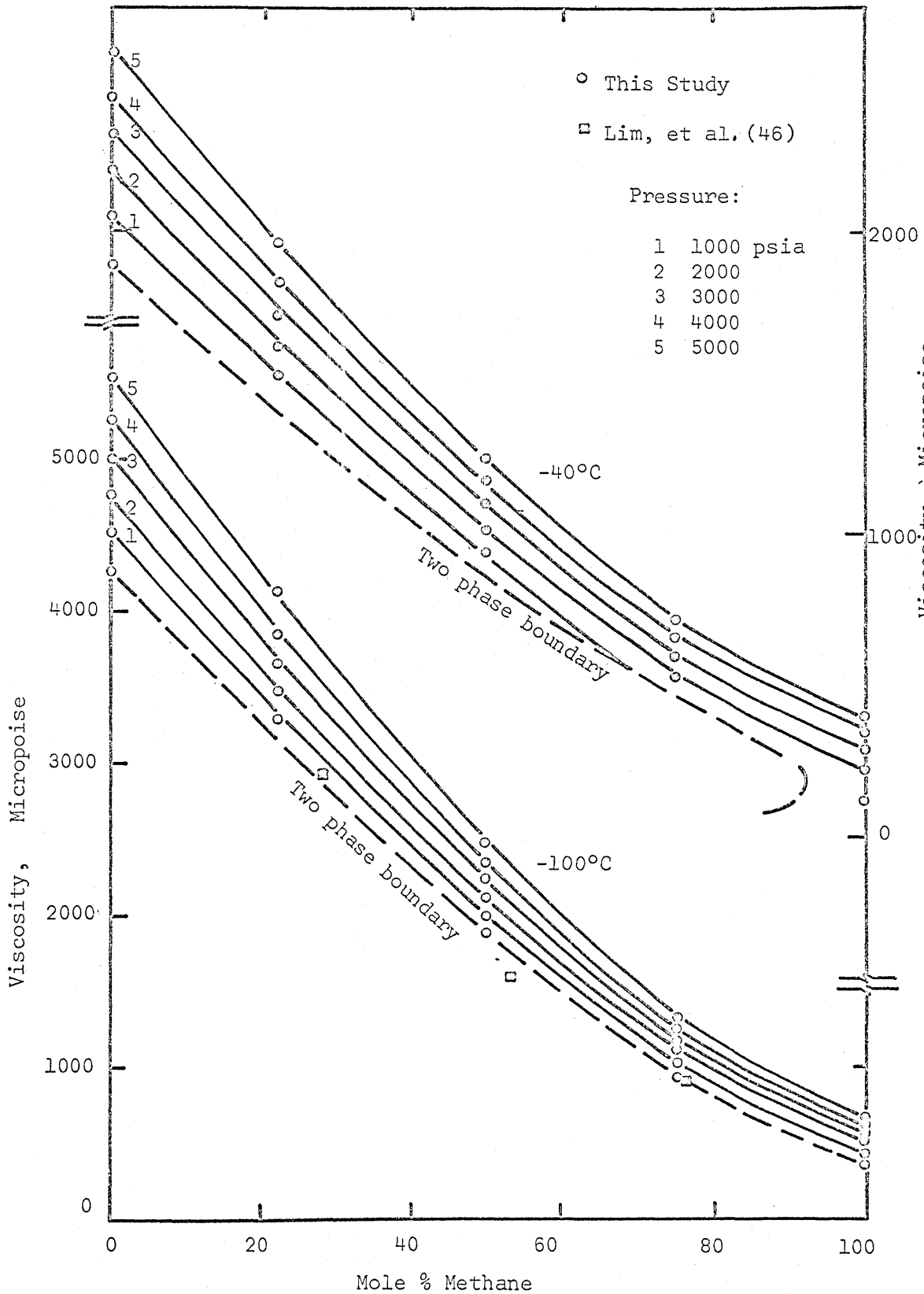

Figure VII-19 Viscosity vs. Composition Diagram for CH_4-C_3H_8 System at -40°C. and -100°C.

those obtained from No. 2 falling cylinder for the mixtures are consistent. The dotted curves are the estimated vapor-liquid boundaries. At -100°C. the temperature is below the critical temperature of methane and the two phase boundary (saturated liquid locus) is continuous from 0 to 100 mole% methane. At -40°C. the temperature is higher than the critical point of methane and the two phase boundary no longer goes all the way across the composition axis but loops back. The exact location of this boundary is questionable beyond the 75.3 mole% methane point because of lack of data.

The low pressure data of Lim, et al. (46) at -100°C. are also shown in Figure VII-19 to give a comparison with the saturated liquid viscosity of this study. The point for the 76.7 mole% methane mixture agrees well with the value of this study, that for the 53.6 mole% methane mixture is about 10% lower and that for the 27.9 mole% methane mixture is about 3% higher than the data of the present study. The deviations can be explained in the same manner as the explanation for the density data for mixtures (P. 73). Good agreement for the 76.7 mole% methane mixture is expected because the cricondentherm of this mixture is lower than ambient temperature. The comparison for the other two mixtures is poor because the cricondentherms of these two mixtures are higher than ambient temperature.

Table VII-7 compares the viscosity data at 37.78°C. of this study and those of Giddings (27) interpolated to the compositions of the present study. The viscosity data for 50.0 mole% methane mixture from the two sources agree well, while those for 75.3 mole% methane mixture show the largest deviation. The average absolute deviation is computed to be $\pm$1.8%. The data of Bicher and Katz (7) obtained from a rolling ball viscometer were also compared with those of this study. Their data are consistently low, and the maximum deviation amounts to 15%.

Table VII-2 shows the reproducibility of the viscosity determination for the mixtures studied. The table indicates that the repeatability is better than 2%. The maximum error of the viscosity data for the mixtures is estimated to be within $\pm$3.8% (P. 61). Thus the reproducibility of the viscosity determination and the deviations between the viscosity

data from this study and the Giddings (27) are within this maximum estimate of error.

Table VII-7

Comparison of Viscosity Data for Mixtures of This Study and Giddings at 37.78°C.

	Mole % Methane								
	22.1			50.0			75.3		
Press. psia	This study	Giddings (27)	% Dev.	This study	Giddings (27)	% Dev.	This study	Giddings (27)	% Dev.
	Viscosity, Micropoise								
1000	676	655	3.1	--	--	--	131	139	-6.1
2000	785	778	0.9	438	436	0.5	220	220	0.0
3000	870	876	-0.7	538	532	1.1	296	307	-3.7
4000	949	962	-1.4	611	605	1.0	363	372	-2.5
5000	1020	1040	-2.0	676	680	-0.6	425	430	-1.2
Abs. ave. % dev.			1.6			0.8			2.7

Treatment of Experimental Data by the Residual Viscosity Versus Density Correlation

(1) Methane and Propane

The experimental viscosity data of this study were used to plot residual viscosity against molar density. The atmospheric pressure viscosity data for methane are from Table VI-1 and the data for propane at atmospheric pressure which were calculated from the Sutherland equation (24) are presented in Appendix T. The calculated values for propane compare well with the literature atmospheric pressure viscosity data (13,27,73).

A plot of residual viscosity as a function of molar density for methane in the low density region is shown in Figure VII-20. Methane viscosity data reported by other investigators are also shown in Figure VII-20 for comparison. There is good agreement between the data of this study and those of the other investigators (4,6,14,27) except for

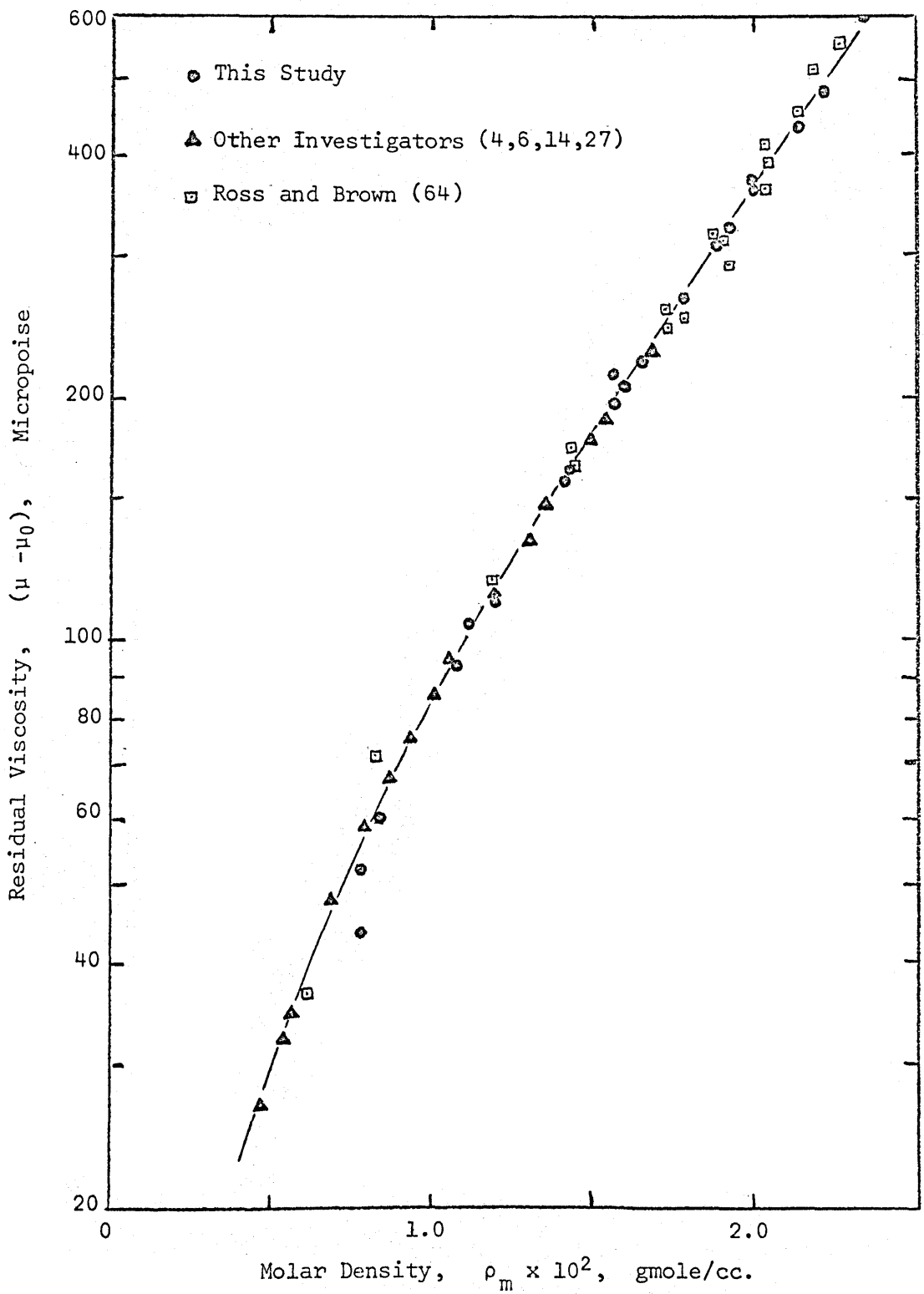

Figure VII-20 Residual Viscosity vs. Molar Density for Methane at Low Density Region

the data of Ross and Brown (64). The residual viscosity versus molar density plot in the high density region is shown in Figure VII-21, where the points of Group V represent methane data and those of Group I represent propane data. Molar density instead of weight density is used to construct these plots since this coordinate gives a better presentation, in a single diagram, of the data for each fixed composition. Figure VII-21 shows that the methane and propane residual viscosities are functions of density only. Note also that this figure shows good agreement between the propane data of this study and those of other investigators (4,27,73).

(2) Mixtures

The atmospheric pressure viscosity data for the mixtures at low temperatures were calculated from the following equation:

$$\mu_{om} = (\sum_{1}^{2} X_i \sqrt{M_i} \mu_{oi}) / (\sum_{1}^{2} X_i \sqrt{M_i}) \qquad \text{(VII-2)}$$

which has been shown to accurately predict the atmospheric viscosity data for mixtures at superambient temperatures (18). The data calculated from this equation for methane-propane system are shown in Appendix T. The residual viscosity versus density plot for the data of the mixtures determined in this study are shown in Figure VII-21, where the data of 22.1, 50.0 and 75.3 mole% methane mixtures are represented by Groups II, III and IV respectively.

Figure VII-21 shows that the data points for each constant composition mixture plotted as residual viscosity versus molar density form a band. In the high density region, the residual viscosity is very sensitive to slight changes in the density. Since the experimental densities of this study are estimated to have a maximum random error of $\pm$1.2%, if the scatter of the data for each constant composition mixture is due to this error, the data points in the band should be randomly distributed. However, with a careful examination of the data for each constant composition mixture, it is found that the points are not randomly distributed, but that all the isothermal points form a single curve as shown by the solid curves of Group IV in Figure VII-21. This phenomenon seems to show that, the data for mixtures in the high density

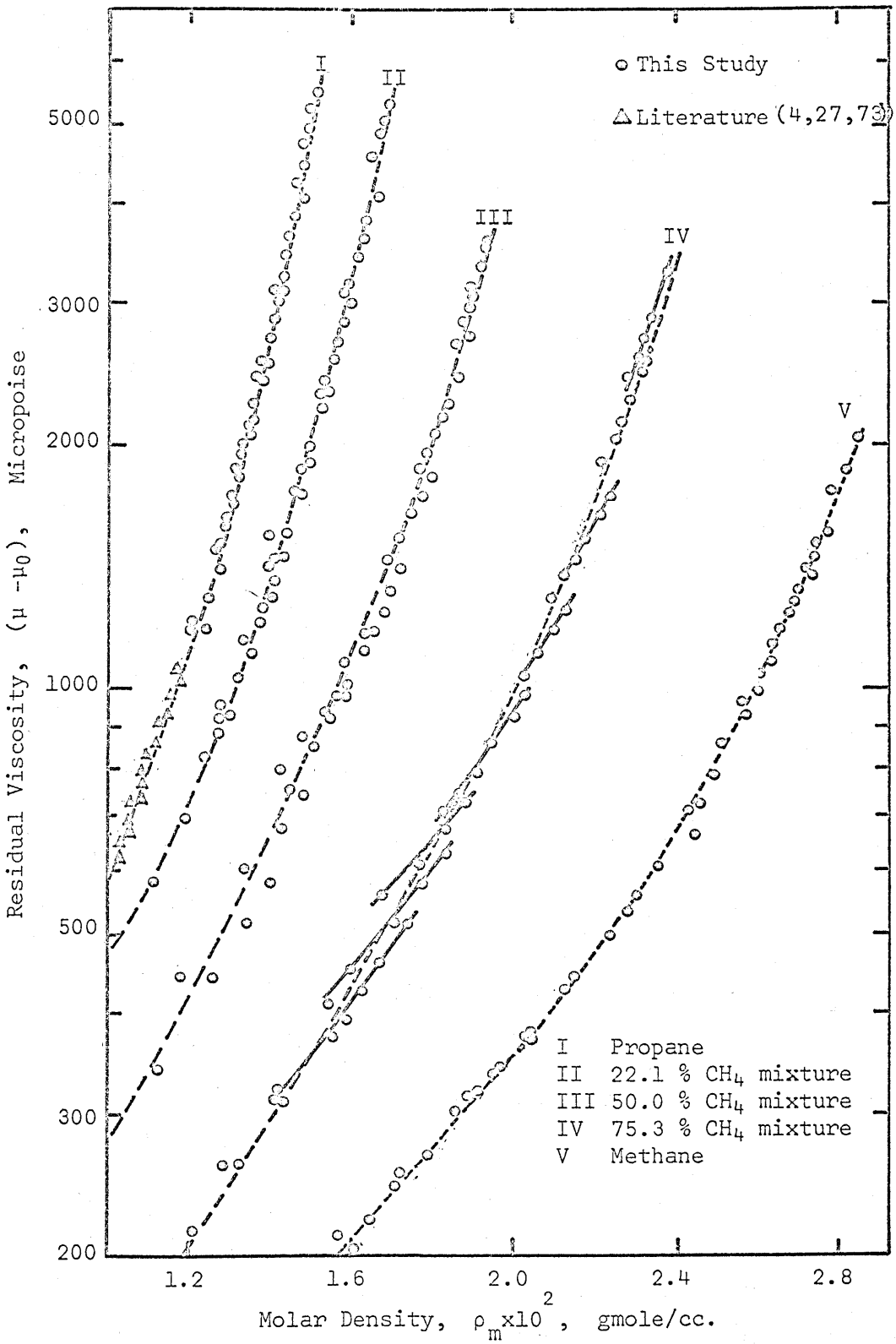

Figure VII-21. Residual Viscosity vs. Molar Density for the CH_4-C_3H_8 System

region depend on temperature as a second independent parameter. This temperature effect seems to be present in all the mixture data.

The temperature effect might be less noticeable if the density values at high pressure on each isotherm were lower. This seems to imply that if there was a pressure effect correction for the viscometer volume in the computation of the density data, the data would be improved insofar as the residual viscosity concept is concerned. However, as mentioned before, no pressure effect was detected in the viscometer volume calibration. It is concluded that with the data presently available it seems impossible to determine if the temperature effect on the residual viscosity correlation is actually a variable to consider when studying mixtures in the high density region. More accurate density data are needed to establish this point. However, it has been demonstrated that the residual viscosity concept is applicable to compressed liquefied methane and propane.

CHAPTER VIII

CORRELATION OF EXPERIMENTAL RESULTS

Residual Viscosity versus Density Correlation

In Chapter VII, the low temperature, high pressure viscosity and density data for methane, propane and the mixtures of these were used to construct residual viscosity versus density plots in high density region. It was shown that the residual viscosity versus density correlation was applicable to the pure component data but that no definite conclusion concerning the validity of this correlating technique could be obtained from the mixture data, because of the observable temperature dependency of these data, when plotted as residual viscosity versus density.

In this section, the applicability of the existing generalized correlations to the present low temperature viscosity data of methane and propane in hgih density region will be tested and then a qualitative test of the validity of these correlations to the data of the mixtures of this study will be attempted.

(1) Generalized Correlations for pure components

(a) Residual viscosity modulus versus reduced density

Jossi, et al. (38) developed a correlation for the prediction of viscosities of pure substances in the dense gaseous and liquid phases. They expressed the residual viscosity modulus, i.e., the residual viscosity multiplied by a group of critical constants[$T_c^{1/6}/(M^{1/2}P_c^{2/3})$], as a single function of reduced density. Figure VIII-1 shows the smoothed curve (Curve 1) of Jossi, et al. (38) which was constructed from the viscosity and density data from different investigators for non-hydrocarbons and hydrocarbons including methane. Dean and Stiel(21) reconstructed the correlation of Jossi, et al. using the consistent viscosity data for argon, neon, nitrogen, ethane, propane and n-butane (23,25,26,73) which were not available at the time the study of Jossi, et al. was conducted. This correlation is represented by the dotted curve (Curve 2) in Figure VIII-1.

The data of this study for methane and propane are also shown on

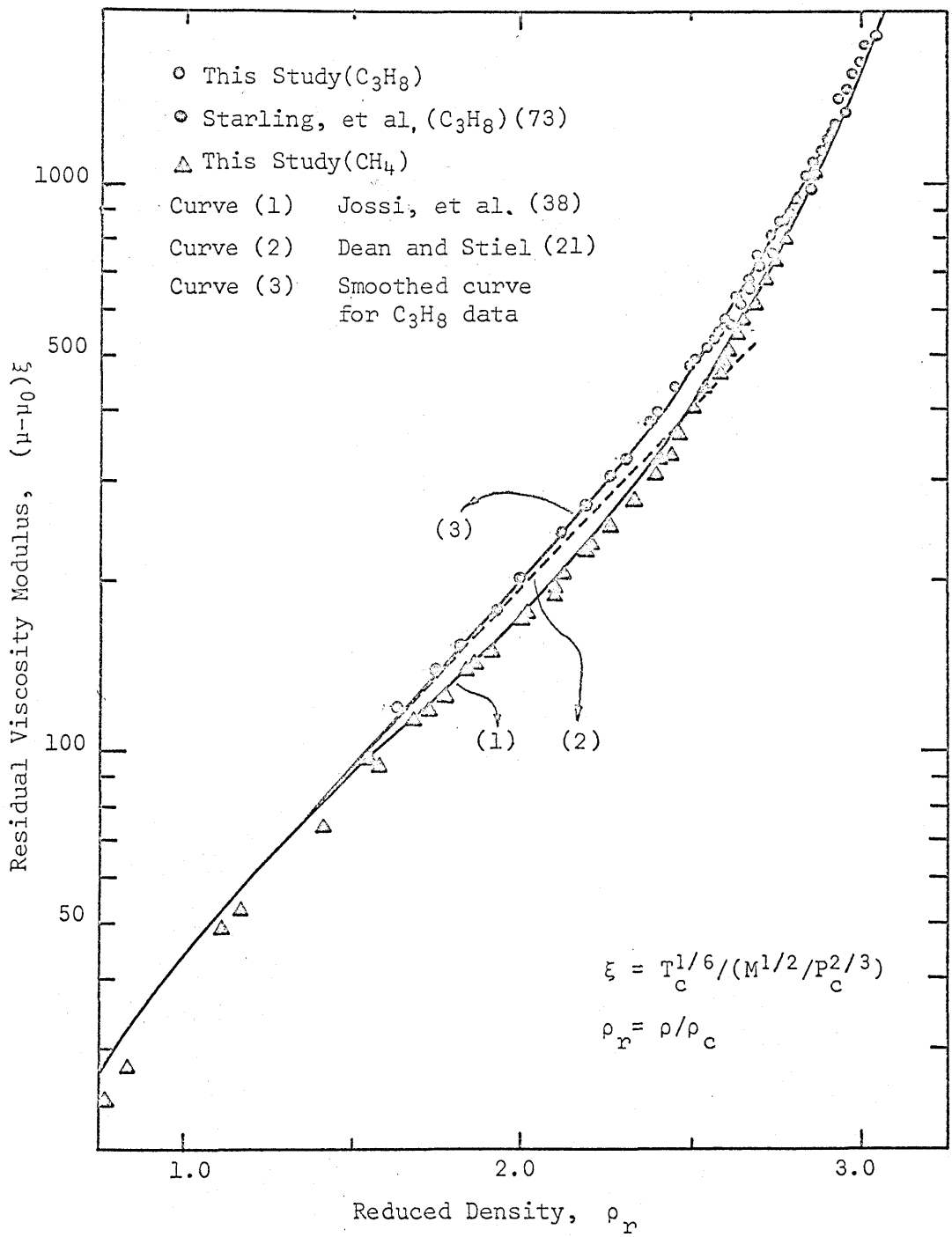

Figure VIII-1 Residual Viscosity Modulus vs. Reduced Density Diagram for Pure Components

Figure VIII-1 by triangles and circles respectively. The critical constants used to correlate the data are given in Appendix U. The methane data of this study, represented by triangles, follow the trend of the smoothed curve of Jossi, et al. (Curve 1). The propane data of this study, represented by solid circle, fall on this curve in the higher density region, and depart from the curve as the density decreases. The data of Starling, et al. (73), represented by open circles, are also shown in the figure to indicate the trend of the propane data in the lower density region. Curve 3 is the best curve by inspection representing the data of propane.

It should be noted that the correlation represented by Curve 2 was constructed from viscosity data excluding those for methane while the correlation represented by Curve 1 was based on data including those for methane. The disagreement between the two correlations shows that methane behaves abnormally in this type of correlation. Methane, then, can not be well correlated with the other normal paraffin hydrocarbons using this technique.

(b) Reduced residual viscosity versus reduced density

Another type of generalized viscosity correlation was developed by Golubev and Agaev (29) for the prediction of viscosities of pure normal paraffin hydrocarbons from methane to n-octane. They showed that a reduced residual viscosity, i.e., the residual viscosity divided by the residual viscosity at the critical temperature, is a single function of reduced density for all the substances they investigated.

Figure VIII-2 shows a Golubev and Agaev type plot (29) which was constructed from the methane and propane data of this study. The critical constants used for the construction of the plot are the same as those used in the preceding section. The methane and propane data were reasonably well correlated using this technique. Curve 2 represents the best curve by inspection of the data of this study. The points for methane and propane appear to be slightly higher than the smoothed solid curve given by Golubev and Agaev (Curve 1). However, the agreement is reasonable considering that Curve 1 is a generalized correlation for eight normal paraffin hydrocarbons.

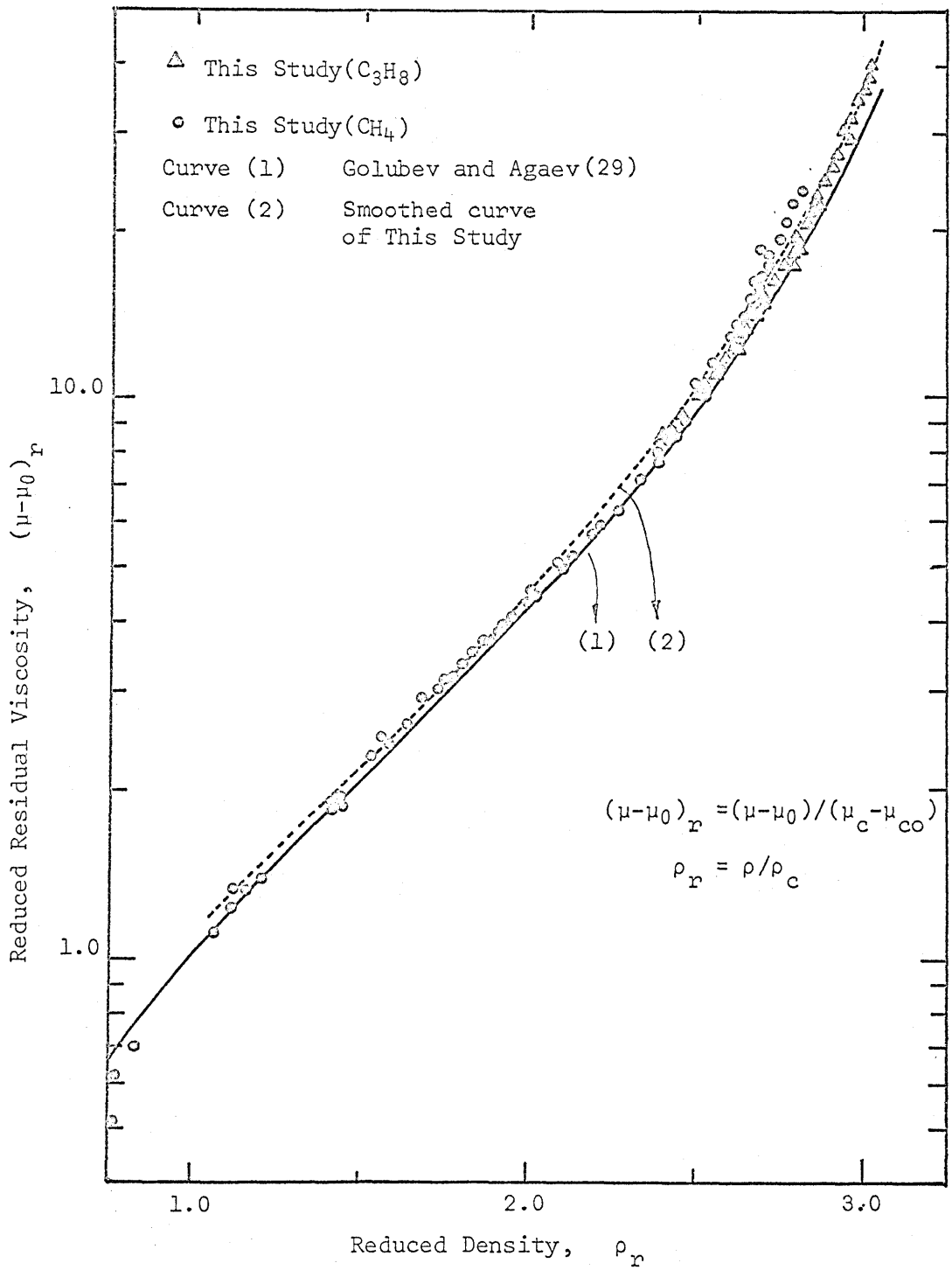

Figure VIII-2 Reduced Residual Viscosity vs. Reduced Density Diagram for Pure Components

In the high density region, the points for methane are higher than those for propane. This is probably because the freezing point of methane is being approached so that viscosity increases more rapidly than would be expected.

(c) Empirical equations for the prediction of viscosities

Based on the residual viscosity concept, Eakin and Ellington (24) developed the following equation for the prediction of viscosities of methane, ethane, propane and n-butane:

$$\mu-\mu_0 = A(e^{7.237\rho}-e^{-45.9\rho^2}) \qquad \text{(VIII-1)}$$

$$A = 32.80-0.1637M$$

$$\mu_0 = BT^{3/2}/(T+S)$$

where B and S are the Sutherland constants (24). Viscosities for methane and propane at all the conditions investigated in this study were calculated from Equation (VIII-1) and compared with the experimental values. The average deviations for all the points tested for methane and propane are shown in Table VIII-1-a. The results show that this equation fails to predict the sudden increase in viscosity in the high density region.

Lee, et al. (43) developed the following equation for the prediction of the viscosity for light paraffin hydrocarbons and their mixtures:

$$\mu = K(T,M)\ \exp[X(T,M)\rho^{Y(T,M)}] \qquad \text{(VIII-2)}$$

where, K and Y are the functions of temperature and molecular weight.

Equation (VIII-2) was used to calculate the viscosities for methane and propane at all conditions investigated in this study. Table VIII-1-a shows the average deviations between the calculated and experimental values. Although Equation (VIII-2) predicts the experimental data of this study better than Equation (VIII-1), the degree of correlation is still poor.

(2) Generalized Correlations Extending to Mixtures

(a) Residual viscosity modulus versus reduced density

Dean and Stiel (21) extended their correlation (P. 107), to the prediction of viscosity of several dense fluid mixtures including the superambient temperature data of the methane-propane system (7,27).

Table VIII-1

Comparison of Viscosities Determined Experimentally in This Study and Those Calculated from Equations (VIII-1) and (VIII-2)

(a) Pure components

	Average % Deviation	
Equation No.	Methane	Propane
(VIII-1)	24.5	21.5
(VIII-2)	14.9	13.1
n	97	36

(b) Mixtures

Equation No.	22.1% CH_4	50.0% CH_4	75.3% CH_4
(VIII-2)	9.09	6.79	4.07
n	44	42	53

Notes: (1) Average % Deviation $= 100\left[\frac{\sum^{n}[(\mu_{exp}-\mu_{calc})/\mu_{exp}]^2}{n-1}\right]^{\frac{1}{2}}$

(2) n is the number of data points tested.

They used the method of Prausnitz and Gunn (57) to calculate the pseudo-critical properties of mixtures. For the data of the nine different mixtures, including the data for the mixtures of methane and propane (7,27), which they tested, they claimed that they were able to predict the viscosities with an average deviation of 3.7%. However, it should be recalled from section (1-a) that this correlation was constructed without using the viscosity data of methane.

Since the data of pure propane and those of methane-propane mixtures at temperatures above ambient were well correlated by Dean and Stiel, an attempt was made to apply their correlation technique to the data for the mixtures of this study in the high density region (Figure VIII-3). Curve 1 represents the correlation of Jossi, et al. (38) for pure components and Curve 2 represents that of Dean and Stiel (21) which has been applied to both pure components and mixtures in the low density region. The mixture data of this study form a band that superimposes on Curve 3 of the propane data from Figure VIII-1. This result shows that for the correlation of viscosity data of the methane-propane mixtures in the higher density region, the critical properties used by Dean and Stiel in the lower density region are not appropriate. Some other definition of pseudo-critical properties may improve the correlation of the mixture data of this study in the higher density region in terms of the Dean and Stiel correlation.

(b) Residual viscosity versus reduced density with molecular weight as a parameter

Giddings and Kobayashi (28) expressed the residual viscosity as a function of reduced density and molecular weight in a graphical form for the prediction of light paraffin hydrocarbons and their mixtures up to a reduced density of 2.0. They used the method of Leland and Mueller (44) to calculate the pseudo-critical density for the mixtures. Although most of the viscosity data of the current study are at reduced densities greater than 2.0, an attempt was made to correlate these data using the technique of Giddings. No significant correlation using this technique was obtained.

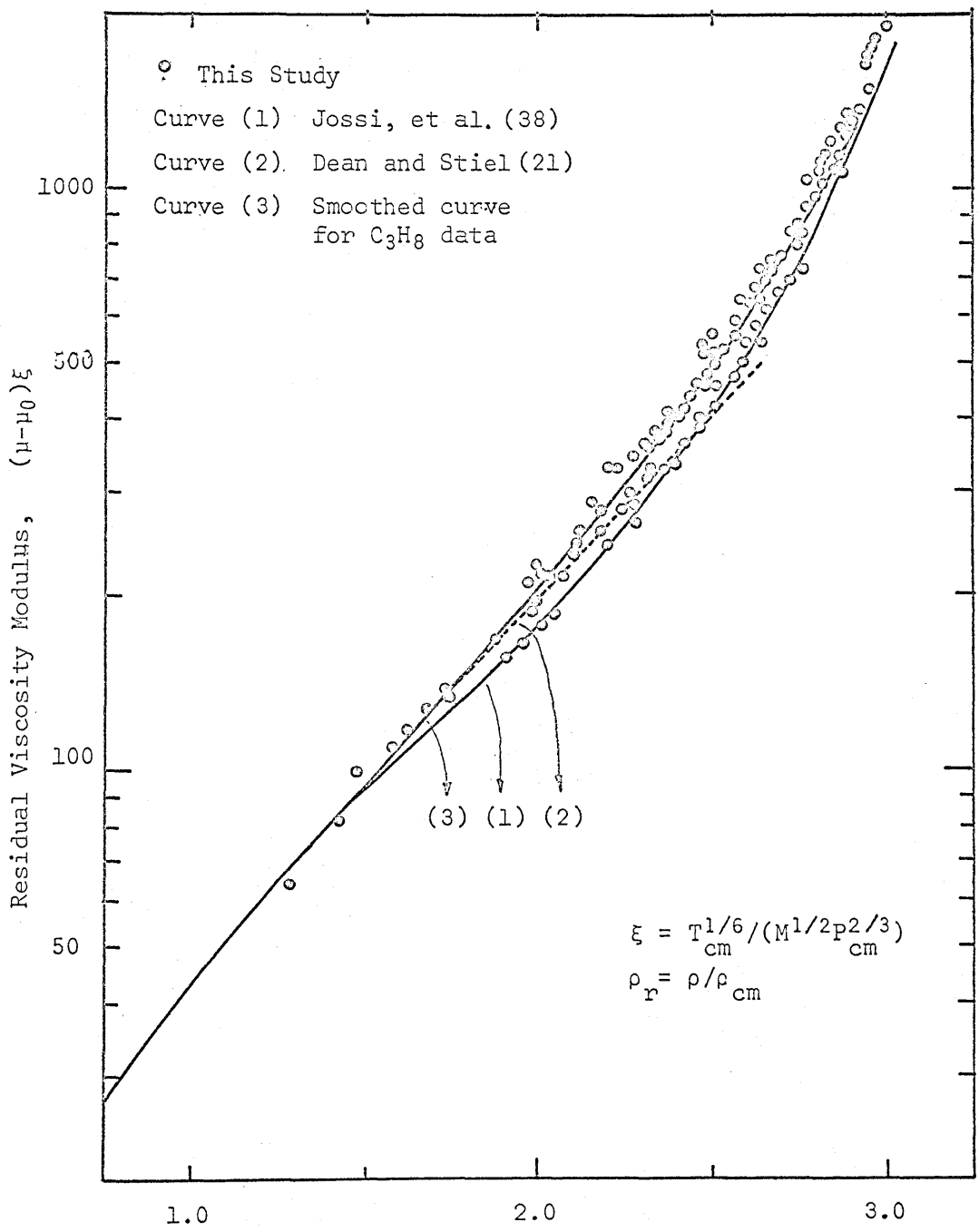

Figure VIII-3 Residual Viscosity Modulus vs. Reduced Density Diagram for Mixtures

(c) Empirical equation of Lee, et al. (43)

The viscosities for the mixtures investigated in this study were calculated using Equation (VIII-2) and compared with the experimental data of this study. The average deviations are shown in Table VIII-1-b. It is seen that Equation (VIII-2) predicts the viscosities for mixtures better than those for the pure components, but the agreement is still poor.

(d) Reduced residual viscosity versus reduced density

The data for the mixtures of this study were used to test the applicability of the correlation of Golubev and Agaev (29) for mixtures. The critical densities used for the mixtures were the same as those used by Dean and Stiel(21), while the pseudo-critical temperature residual viscosities for mixtures were defined as the molar average values of the risidual viscosities for the pure components at their critical temperatures, i.e.,

$$(\mu_c-\mu_{co})_m = \sum_1^2 X_i(\mu_{ci}-\mu_{coi}) \qquad \text{(VIII-3)}$$

Figure VIII-4 is a Golubev and Agaev type plot constructed using the mixture data of this study. All the points again form a band and are consistently higher than the smoothed solid curve of Golubev and Agaev (Curve 1) and the dotted curve (Curve 2) representing the smoothed curve of methane and propane data from Figure VIII-2. This implies that another means of evaluating the pseudo-critical properties for the mixtures may better correlate mixture data relative to those for the pure components.

In short, of all the correlations tested, that of Golubev and Agaev (29) seems best for the present low temperature, high pressure data for methane, propane, and the mixtures thereof. Some better definition of the critical residual viscosity for mixtures would seem to be in order.

One general shortcoming of the residual viscosity versus density correlation in the higher density region is that the slope of the curve is so steep that the residual viscosity is very sensitive to a slight change in density. Therefore the correlations require extremely accurate density data in the high density region in order to interpo-

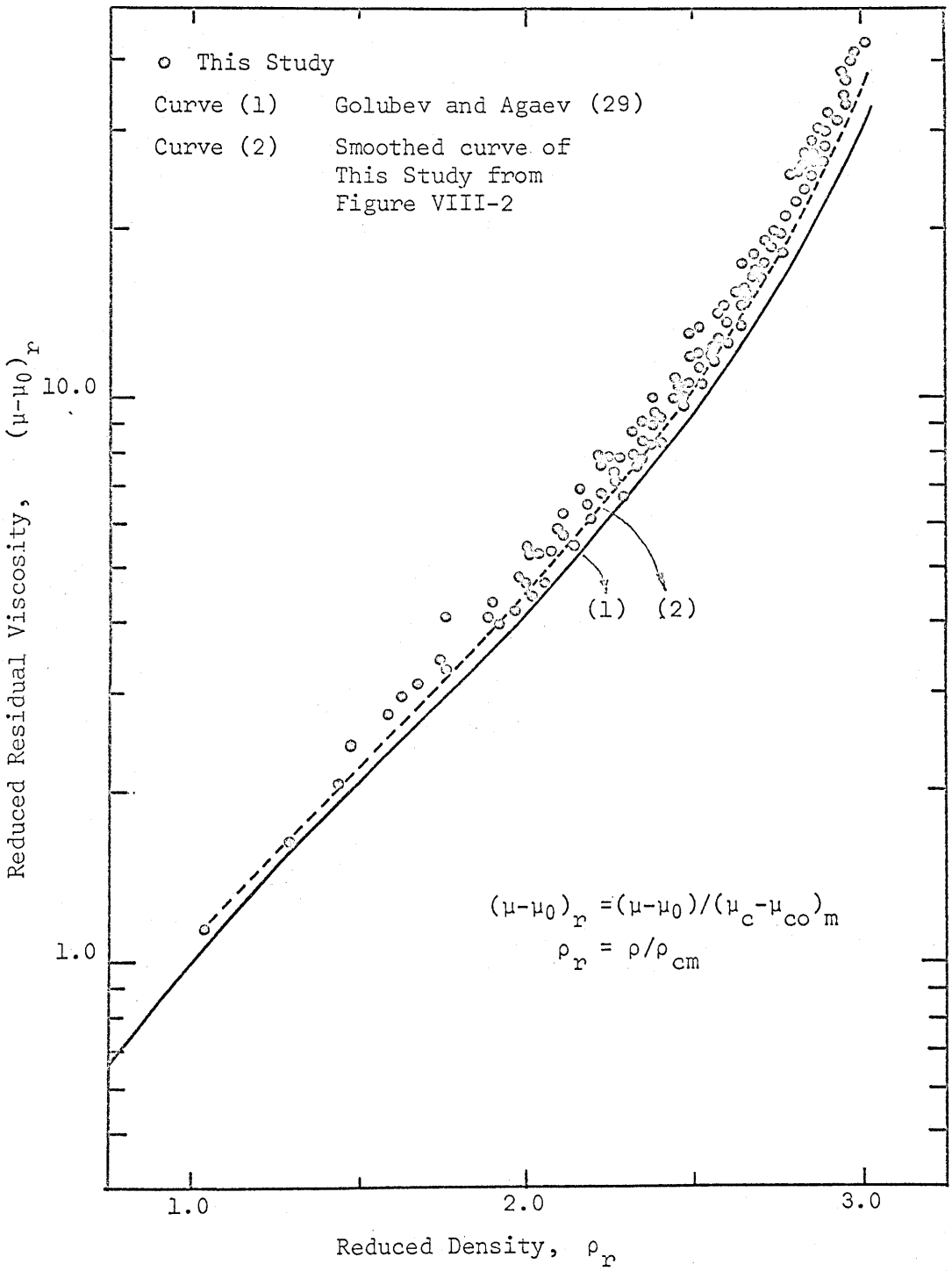

Figure VIII-4 Reduced Residual Viscosity vs. Reduced Density Diagram for Mixtures

late the viscosity data with good accuracy. In fact, the use of such a correlation is highly questionable at high densities since the indication is that a condition, such that viscosity is independent of density, is being approached. Low temperature, high pressure density data are seldom available for light hydrocarbons and even if the density data could be estimated from other density correlations, it is improbable that the estimated density would be of sufficient accuracy to use for the estimation of viscosity. Therefore, it would be almost impossible to predict the viscosity data for such fluids even if a reliable correlation was available. A different approach to the problem of correlating viscosity, one which does not rely upon density, will be discussed in the next section.

Modified Andrade Equation

For the calculation of liquid viscosity, the simplest and the most frequently used empirical equation is,

$$\ln \mu = a + b/T \qquad \text{(I-2)}$$

Since several investigators (3,5,9,31,79) have used this equation to express low pressure liquid viscosity as a function of temperature with some success, this equation is used to correlate the low temperature, high pressure viscosity data for the methane-propane system. In the development of the correlation, the viscosity data of this study will be treated in the following manner:

(1) The viscosity data for each pure component and for each mixture will be correlated using Equation (I-2).

(2) A generalized Andrade equation will be developed using the principle of corresponding states as applied to the viscosity data for methane and propane.

(3) This generalized equation will be extending to the viscosity data for mixtures, using pseudo-critical parameters.

Five plots of log μ versus 1/T (one for each pure component and one for each mixture) were constructed. Constant pressure data, plotted in this way, demonstrated the validity of Equation (I-2), except for those data near the critical region. The slopes and the intercepts for

each isobar appeared to be linear functions of pressure, and, within the temperature range investigated, the viscosities for each of the pure components and for each of the constant composition mixtures are reasonably well represented by a modified Andrade equation,

$$\ln \mu = (\bar{D}_0+\bar{D}_1P) + (\bar{D}_2+\bar{D}_3P)/T \qquad \text{(VIII-4)}$$

The data were then plotted on a reduced coordinate system to examine the possibility of developing generalized correlation in terms of the principle of corresponding states. The reduced form of Equation (VIII-4) can be written as,

$$\ln \mu_r = (D_0+D_1P_r) + (D_2+D_3P_r)/T_r \qquad \text{(VIII-5)}$$

A plot (Figure VIII-5) for reduced viscosity, μ_r, versus reciprocal reduced temperature, $1/T_r$, with reduced pressure, P_r, as a parameter was constructed using the propane data. These data were then used to establish the coefficients of Equation(VIII-5) by regression analysis, excluding those data points at temperatures above 0°C. and/or having reduced densities less than 2.2. A reduced density of 2.2 is determined as a criterion for rejection since at reduced densities of less than 2.2, the reduced viscosity decreases so rapidly that the Andrade equation is no longer valid. This criterion is also found to be applicable to the other fluid analyzed later in this study. The coefficients and the deviations between the experimental and calculated points are presented in Table VIII-2. The six isobars (P0,P1,P2,P3,P4, and P5) shown in Figure VIII-5 represent those computed from Equation (VIII-5) using the propane coefficients. The six isobars are almost parallel as expected, since the slopes of the lines are only slightly pressure dependent.

Next, the coefficients of Equation(VIII-5) for methane were determined by regression analysis, observing the same rejection criterion as for propane. The coefficients and the deviation are shown in Table VIII-2. The computed isobar for methane at reduced pressure of 1.62 is shown on Figure VIII-5(isobar C1). The other isobars for methane are again almost parallel but not shown here to preserve clarity of presentation. It should be noted that the isobar C1 is almost parallel with the isobar P1 but not superimposed on it. This implies that the viscosity data for methane and propane can not be correlated as an universal function of reduced temperature and reduced pressure. The failure of this correlation is probably due to the abnormal

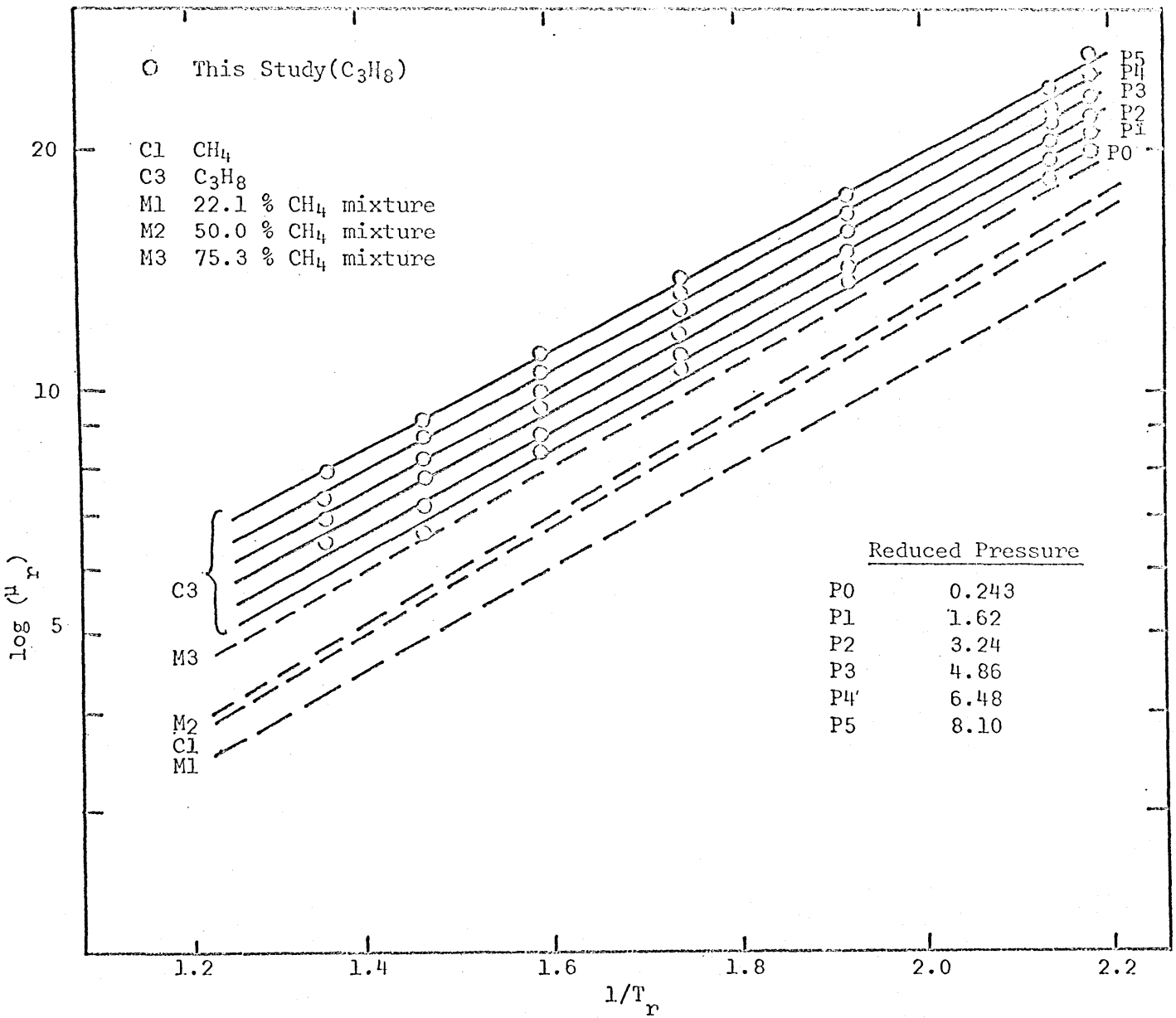

Figure VIII-5 Graphical Representation of Modified Andrade Equation

Table VIII-2

Coefficients for Empirical Equations and Average Percent Deviations between the Experimental and Calculated Viscosities

Coeff. for equations	Mole % Methane				
	0.0	22.1	50.0	75.3	100
(a) Equation (VIII-5)					
D_0	-0.2526	-0.4024	-0.6631	-0.6375	-0.6337
D_1	0.05001	0.05625	0.06951	0.05136	0.05832
D_2	1.4905	1.5149	1.5862	1.4770	1.5398
D_3	-0.00877	-0.01170	-0.01777	-0.00563	-0.00404
% Dev.	± 1.6	± 1.9	± 1.1	± 1.0	±2.3
n	36	41	32	33	34
(b) Equation (VIII-6)					
C_0	12.776	10.875	14.361	10.962	9.909
C_1	-1228.3	-867.0	-1146.6	-656.4	-473.7
C_2	62953.	43120.	42756.	22548.	13796.
% Dev.	± 2.9	± 4.5	± 4.3	± 4.3	± 2.0
n	36	41	32	33	34

Note: Percent standard deviation computed for n data points is defined as:

$$\% \text{ Dev.} = 100 \sqrt{\frac{\sum_{1}^{n} [(\mu_{exp} - \mu_{calc})/\mu_{exp}]^2}{n-1}}$$

behavior of methane.

Treatment of the data for the mixtures was considered next. Different definitions of critical temperature and pressure for the mixture were tried in the construction of these reduced plots. It was found that the experimental critical temperature and the molar average critical pressures for the mixtures gave the most compatible representation of mixture data on the reduced plot. Molar average values of the critical viscosities of pure components were used to reduced the viscosity data of the mixtures, since the magnitude of the pseudo-critical viscosity for the mixture is immaterial insofar as the slope of a given isobar in a $\log\mu_r$-T_r plot is concerned. The coefficients of Equation(VIII-5) were then determined by regression analysis for each of the mixtures using the same rejection criterion as for propane. The coefficients and deviations for the data of each mixture are presented in Table VIII-2. The computed isobars (M1,M2 and M3) for the three mixtures (22.1, 50.0 and 75.3 mole % methane) at a reduced pressure of 1.62 are also shown in Figure VIII-5. Most of the data points obtained in this study fall between 1.2 and 2.1 along $1/T_r$ axis. These five isobars (P1,C1,M1,M2 and M3) almost have the same slope but they are not in order with respect to the methane content in the mixture.

It is possible to make a vertical translation of the isobars by dividing the isobaric viscosities for each mixture by a pseudo-critical viscosity instead of a molar average critical viscosity such that the intercept for each isobar (M1,M2 and M3) will be a molar avarage value of the intercepts of the isobars (C1 and P1). This idea was tested but, since there did not appear to be any simple functional relationship between pseudo-critical viscosity and composition, no further effort was made to develop a generalized correlation in terms of the reduced properties.

To compare the viscosity correlation using Equation(VIII-5) and that based on the residual viscosity versus density correlation, the same data points used in the evaluatin of the coefficients for Equation (VIII-5) were used to determine the coefficients of the following empirical equation by regression analysis:

$$\ln (\mu-\mu_0) = C_0 + C_1\rho_m + C_2\rho_m^2 \qquad \text{(VIII-6)}$$

The computed coefficients of Equation(VIII-6) for the data of constant composition and the deviations between the calculated and the experimental viscosities are presented in Table VIII-2-b. It is clear from this table that the modified Andrade equation correlates the low temperature, high pressure viscosity data of the methane, propane and mixtures of these somewhat better than the correlation based on the residual viscosity concept, if Equation(VIII-6) is conceded to be the proper functional relationship for the residual viscosity correlation. Of all the constant composition data tested using Equation(VIII-5), the average deviation between the experimental points and the points calculated from Equation(VIII-5) is less than $\pm$2.3%, while for Equation (VIII-6), the corresponding deviation is less than $\pm$4.5%.

The results of this section are briefly summarized as follows:

(a) The modified Andrade equation, Equation(VIII-5), expressed in reduced variables, can be used to correlate the high pressure, low temperature liquid viscosity data for methane, propane, and the mixtures of methane and propane of the study to within $\pm$2.3% using the coefficients presented in Table VIII-2-a. This equation does not require density or atmospheric pressure viscosity as does the residual viscosity versus density correlation for the calculation of viscosity. The present correlation is recommended for interpolation of the viscosity data of this study in the following region:

$$\rho_r \geq 2.2$$
$$1.2 \leq 1/T_r \leq 2.1$$
$$P_r \leq 8.1$$

where for the mixtures, the critical properties are defined for density by $(\sum_1^n X_i M_i / \sum_1^n X_i V_{ci})$, for temperature by the experimental critical temperature, and for pressure by molar average critical pressure.

(b) The existing residual viscosity versus density correlation is recommended for the interpolation of the viscosities of pure components and mixtures at $\rho_r < 2.2$.

(c) An attempt to develop a single equation for the prediction of viscosities of methane, propane and any mixture of methane and propane, based upon the modified Andrade equation and the principle of corres-

ponding states, was not successful.

(d) It is expected that Equation(VIII-5) would also apply to other similar light hydrocarbons and their mixtures within the parameter ranges specified under (a) above. If this is true, the amount of data required in future experimental investigations of such hydrocarbons and their mixtures could be greatly reduced.

CHAPTER IX

CONCLUSIONS

(1) Experimental equipment, including a falling cylinder viscometer, a low temperature differential pressure indicator, a low temperature bath unit, and a high temperature bath unit, capable of determining the viscosity and density of pure components and mixtures thereof over the temperature range from +100 to -170°C. and at pressures to 5,000 psia, has been designed, constructed, calibrated, and operated. The high temperature bath containing the high pressure equipment was used to: (a) meter fluids into the viscometer for density determinations; (b) prepare mixtures; and (c) generate high pressures. The temperature and the pressure of this unit were measured to an uncertainty of $\pm$0.1°C. and $\pm$1 psi respectively. The low temperature bath, a modified version of Sinor's bath (70), was used to maintain a constant temperature environment for the viscometer at any temperature level from +100 to -170°C. to within $\pm$0.01°C. The falling cylinder viscometer was used to determined the viscosity and density concurrently, using a 5,000 psi Heise gage to determine the pressure to an uncertainty of $\pm$5 psi. The low temperature DPI, a modified version of the one described by McCreary and Swift (52), and a Heise gage were installed to measure pressure when experimenting with mixtures of methane and propane. In this case the pressure was measured to an uncertainty of $\pm$15 psi. The upper operating pressure limit for all equipment can be extended to 12,000 psia if (a) a 12,000 psia valve is installed in place of valve 1 (Hoke Millimite valve) of Figure III-6, and (b) 12,000 psia pressure gages are installed.

(2) The method of correlating viscometer calibration data developed by Lohrenz (47) was used in this investigation with a slight modification of the variables. The functional relationship for this viscometer calibration method, $\beta_{red} = f(N_{Re})$, has been represented by two empirical equation, Equations (II-15) and (II-16).

(3) Three falling cylinders, each falling in the same viscometer tube, were calibrated and used to determine the viscosity in this

study. The calibration data for each falling cylinder and the viscometer tube in the laminar region were fitted to a linear equation, Equation (II-15), and those in the transition region were fitted to a second order equation, Equation (II-16). The transition $\log(N_{Re})$ is about 2.45 for all three falling cylinders and the maximum $\log(N_{Re})$ calibrated is 2.917 (Table V-1). The average deviations of β_{red} from the equations in both regions are within $\pm$0.85%.

(4) A technique for preparing mixtures by the volumetric displacement of known amounts of pure components into a mixture make up cylinder has been developed in this study. The maximum error in the composition of mixtures prepared by this technique is estimated from an error analysis to be $\pm$0.005 mole fraction. The actual errors in the compositions are expected to be less than $\pm$0.005 mole fraction. Because of the use of literature densities for the computation of compositions, the reported compositions are subject to a maximum systematic error of +0.002 mole fraction propane. This error is caused by the error in methane density due to impurities present in the methane used, and will vary with mixture composition.

(5) The viscosity and density data for methane, propane and the three mixtures of these were determined, and the recommended values for these fluids are presented in Tables VI-1 to VI-6 for the temperature and pressure ranges shown below:

	Mole % Methane				
	0.0	22.1	50.0	75.3	100.0
Temp. range(°C.)	0 to -100	37.78 to -120	37.78 to -120	37.78 to -150	0 to -170
Press. range	From 100 psia to 5,000 psia				

Density data for methane, except the low temperature vapor data, were not determined in this study, since these data are available in the literature (40,78).

The maximum estimated error in the viscosity for pure components was ±3.4% and for mixtures was ±3.8%, while the maximum estimated error in density for pure components was ±0.6% and for mixtures was ±1.2%. The density data for mixtures were subject to a systematic error of, at most, +0.6%, and those for methane were subject to a systematic error of +0.8%. The reproducibility of viscosity determination was on the average ±1.2%, and the agreement of the viscosities of this study with those from the literature was, for the most part, ±2.0%. The agreement of densities of this study with values from the literature was ±0.1% for propane and ±1.2% for methane and mixtures of methane and propane.

(6) The conventional method of testing the viscosity data by employing residual viscosity versus density correlation was used to test the experimental data of this study. For the data of methane and propane in the high density region, the residual viscosity was shown to be a function of density only. However, for the data of mixtures, no definite conclusion was obtained because of an observable temperature effect when the data were plotted as residual viscosity versus density.

(7) The existing residual viscosity versus density correlations, as generalized for application to different pure components and their mixtures, were tested using the data of the methane-propane system in the high density region investigated in this study. The correlation of Golubev and Agaev (29) was found to be the best of all the correlations tested. However, it should be emphasized that any type of residual viscosity correlation is not particularly suitable for the correlation of viscosity in high density region since, in this region, the slope of the curve in the residual viscosity versus density plot is so steep that a slight change in density causes a significant change in the residual viscosity.

(8) The modified Andrade equation, Equation (VIII-5), and the coefficients listed in Table VIII-2-a were developed for the interpolation of the liquid viscosities of methane, propane, and the three

mixtures investigated in this study with an average deviation of ±2.3%. This equation does not require density or atmospheric pressure viscosity as does the residual viscosity versus density correlation for the calculation of viscosity. The present equations are suitable for interpolation of viscosity data of the system studied in the following region:

$$\rho_r \geq 2.2$$

$$1.2 \leq 1/T_r \leq 2.1$$

$$P_r \leq 8.1$$

where, for the mixtures, the critical properties are defined for (a) density, by $(\sum_{1}^{2} X_i M_i / \sum_{1}^{2} X_i V_{ci})$, (b) temperature, by the experimental critical temperature, and (c) pressure, by molar average critical pressure. The residual viscosity versus density correlation is suitable for the interpolation of viscosities of the pure components and mixtures of this investigation at reduced densities less than 2.2.

(9) The correlation of the current viscosity data for methane, propane and the mixtures of methane and propane by a single equation based on the modified Andrade equation and the principle of corresponding states was not successful.

(10) Since Equation (VIII-5) [or Equation (VIII-4)] has been demonstrated to correlate the compressed liquid viscosities well for each pure component and each constant composition mixture of the methane-propane system at $1/T_r$ greater than 1.2, it is expected that this equation would also apply to other similar light hydrocarbons and their mixtures. If this is true, the amount of experimental data required in future investigations could be reduced appreciably in the range of parameters given in (8) above.

CHAPTER X

RECOMMENDATIONS

(1) The current experimental equipment can be operated at a maximum pressure of 12,000 psia, if a 12,000 psia valve and 12,000 psia Heise pressure gages are substituted for valve 1 and the current pressure gages respectively. It is recommended that use be made of the maximum capability of this equipment in future studies of viscosity and density by installing the valve and pressure gages suitable for operation at pressures to 12,000 psi.

(2) From the results of the treatment of the current data by the residual viscosity versus density plot, it was found that more accurate density data for mixtures are necessary to test the validity of the residual viscosity versus density correlation for light paraffin hydrocarbon liquid mixtures in the high density region. To improve the density measurement, the following suggestions are made:

(a) Use the low temperature direct weighing technique (37) to determine the reference condition density data for the fluids containing impurities. This should eliminate systematic errors in density data. For mixtures, this would eliminate the uncertainty in ρ_{rc} due to the uncertainty in the composition.

(b) Use an isochoric process to take density data rather than the isothermal process used in this study. This would minimize the error due to the frequent reading of height gages for the determination of piston position in the mass injection cylinder.

(c) Replace the high temperature DPI in the high temperature bath by a Ruska DPI (Model 2416.1, Ruska Instrument Corporation, Houston, Texas). It was suspected that there was hysterisis in the high temperature DPI. The Ruska DPI has better sensitivity and no measureable hysterisis and should, therefore, improve the metering technique.

(d) Place a more sensitive bellows in the low temperature DPI to improve the sensitivity in the pressure measurement for the study

of mixtures.

(3) To improve the viscosity measurement, the following suggestions are made:

(a) Use the viscosity data for n-decane reported by Lee and Ellington (42) for the extension of the viscometer calibration to the low Reynolds number region. The calibration points of this study in the low Reynolds number region using the data of Rossini, et al. (65) appear to have larger deviations from the "best" line than those of other calibration fluids used. This could possibly be due to the inconsistency of the viscosity data between those of Rossini, et al. and those of Ellington and coworkers.

(b) The inner bore of the viscometer tube should be more precisely machined and polished to obtain better reproducibility of fall times. Further, the method for measuring the inner diameter of the viscometer tube should be improved to decrease the uncertainty in the calculation of β_{calc}.

(c) No correction on the fall time due to the bottom effect of the viscometer was made in this study, since the bottom configuration of the viscometer was such that the bottom effect was considered negligible. However, in order to improve the accuracy of the viscosity determination, a study to determine the parameters affecting "bottom" corrections to time of fall should be undertaken.

(4) For future investigations of the viscosities in the high density-low temperature region, studies on other light hydrocarbons, and binary or ternary mixtures thereof are suggested. By using other paraffins, the applicability of the modified Andrade equation for interpolation of liquid viscosities can be tested.

NOMENCLATURE

Symbol	Definition	Unit
Latin Symbols		
A	characteristic area$[\pi D_t(1+\kappa)L_c]$ defined for Equation(II-6)	$cm.^2$
A,B,C,D	constants in Callendar-Van Dusen equation, Equation(B-1)	
A_0, A_1	constants in Equation(II-15)	
B_0, B_1, B_2	constants in Equation(II-16)	
C_0, C_1, C_2	constants in Equation(VIII-6)	
D_0, D_1, D_2, D_3	constants in Equation(VIII-6)	
$\overline{D}_0, \overline{D}_1, \overline{D}_2, \overline{D}_3$	constants in Equation(VIII-4)	
D_c	outer diameter of the viscometer falling cylinder	cm.
$D_{c(t,p)}$	outer diameter of the viscometer falling cylinder at t°C. and p lb./sq.in.abs.	cm.
D_e	equivalent diameter of the falling cylinder viscometer defined by Equation(II-11)	cm.
D_{eL}	equivalent diameter of the falling cylinder viscometer defined by Equation(II-2)	cm.
D_t	internal diameter of the viscometer tube	cm.
$D_{t(t,p)}$	internal diameter of the viscometer tube at t°C. and p lb./sq.in.abs.	cm.
$D_{to(t,p)}$	outer diameter of the viscometer tube at t°C.and p lb./sq.in.abs.	cm.
E_0, E_1, E_2, E_3	sonstants in Equation(B-2)	
E_c	Young's modulus for the material of the viscometer falling cylinder	lb./sq.in.
EMF	dependent variable in Equation(B-2)	millivolt
E_t	Young's modulus for the material of the viscometer tube	lb./sq.in.
F_g	gravitational force on the viscometer falling cylinder	$g.cm./sec.^2$
F_k	force $[\Delta P(\pi D_t^2/4)/(1-\kappa^2)^2]$ defined for Equation(II-6)	$g.cm./sec.^2$

Symbol	Definition	Unit
F_{lsf}	force on the viscometer falling cylinder due to friction of laminar flow along the cylindrical surface	g.cm./sec^2
$F_{\Delta p}$	force on the viscometer falling cylinder due to pressure drop	g.cm./sec^2
ΔH	change in height of the piston in the mass injection cylinder	inch
K	characteristic kinetic energy per volume $[\rho\langle v\rangle^2/2]$ defined for Equation(II-6)	g./(cm.sec^2)
L	total length of the falling cylinder	cm.
L_{25}	total length of the falling cylinder measured at 25°C.	cm.
L_c	length of the cylindrical portion of the falling cylinder	cm.
L_e	volume equivalent length$[V/(\pi D_c^2/4)]$ of the falling cylinder defined by Lohrenz(47)	cm.
M	molecular weight	
M_i	molecular weight of component i	
N_{Re}	Reynolds number defined by Equation(II-10)	dimensionless
P	pressure	lb./sq.in.abs.
P_c	critical pressure	lb./sq.in.abs.
P_{cm}	critical pressure of the mixture	lb./sq.in.abs.
P_r	P/P_c, reduced pressure	
R_t	resistance in Callendar-Van Dusen equation	ohm
T	temperature	°K.
T_c	critical temperature	°K.
T_{cm}	critical temperature of mixture	°K.
T_r	T/T_c, reduced temperature	
V	volume of the falling cylinder	cu.cm.
V_c	critical molar volume	cu.cm./g-mole
V_{ci}	critical molar volume of component i	cu.cm./g-mole
V_{cm}	critical molar volume of mixture	cu.cm./g-mole
V_{vm}	vomule of the viscometer(pycnometer)	cu.cm.

Symbol	Definition	Unit
W	mass of the fluid	g.
X	mole fraction	
X_i	mole fraction of component i of a mixture	
a	acceleration of a falling cylinder	cm./sec.^{2}
a,b	constants in Andrade equation, Equation(I-1)	
f	friction factor defined by Equation(II-6)	
g	local acceleration of gravity	cm./sec.^{2}
log	logarithm to the base 10	
ln	logarithm to the base e	
q	volumetric flow rate of fluid flowing through the annulus of a falling cylinder viscometer	cu.cm./sec.
s	distance of fall	cm.
s_i	distance of fall defined by Equation(K-10)	cm.
s_{25}	distance of fall measured at 25°C.	cm.
$\bar{s}$	distance of fall defined by Equation(K-8)	cm.
t	temperature	°C.
$\bar{v}$	velocity defined by Equation(K-5)	cm./sec.
<v>	average velocity of the fluid flowing through the annulus of the falling cylinder viscometer	cm./sec.
v_T	terminal velocity of a falling cylinder	cm./sec.

Symbol	Definition	Unit
Greek Symbols		
α_c	coefficient of thermal expansion of the material of the viscometer falling cylinder	1/°C.
α_t	coefficient of thermal expansion of the materail of the viscometer tube	1/°C.
α_v	temperature coefficient of the viscometer volume	1/°C.
β_{calc}	viscometer constant defined by Equation(II-12)	cu.cm./sec^2.
$\beta_{p,t}$	viscometer constant defined by Equation(I-1)	cu/cm./sec^2.
β_{red}	$\beta_{p,t}/\beta_{calc}$, reduced viscometer constant	
ΔP	pressure drop	g.force/sq.cm.
ΔV	volume of fluid displaced from the mass injection cylinder into the viscometer	cu.cm.
θ	time of fall	sec.
κ	D_c/D_t, ratio of outer diameter of the falling cylinder to internal diameter of the viscometer tube	
$\bar{\mu}$	viscosity	poise
μ	viscosity	micropoise
μ_{calc}	viscosity calculated from the empirical equation	micropoise
μ_{exp}	viscosity determined from the experiment	micropoise
μ_0	atmospheric pressure viscosity	micropoise
μ_{0i}	atmospheric pressure viscosity of component i	micropoise
μ_c	critical viscosity	micropoise
μ_{co}	atmospheric pressure viscosity at critical temperature	micropoise
μ_{cm}	critical viscosity for mixture	micropoise
μ_{ci}	critical viscosity of component i	micropoise
μ_{coi}	μ_{co} of component i	micropoise
μ_r	μ/μ_c, reduced viscosity	

Symbol	Definition	Unit
ν_c	Poisson's ratio for the material of the falling cylinder	
ν_t	Poisson's retio for the material of the viscometer tube	
ξ	$T_c^{1/6} / (M^{1/2} P_c^{2/3})$	
π	3.14159.....	
ρ	density of fluid	g./cu.cm.
ρ_c	critical density	g./cu.cm.
ρ_{ci}	critical density of component i	g./cu.cm.
ρ_{cm}	critical density of mixture	g./cu.cm.
ρ_m	molar density	g-mole/cu.cm.
ρ_r	ρ/ρ_c, reduced density	
ρ_{rc}	density of fluid at a reference condition	g./cu.cm.

LITERATURE CITED

1. Agaev, N.A., and Golubev, I.F., "Viscosity of n-Pentane," Gazovaya, 8, No. 5, 45 (1963).

2. Akers, W.W., Burns, J.F., and Fairchild, W.R., "Low Temperature Phase Equilibria Methane-Propane System," Ind. Engr. Chem., 46, 2531 (1954).

3. Andrade, E.N. da C., "The Viscosity of Liquids," Endeavour, 13, 117 (1954).

4. Baron, J.D., Roof, J.G., and Wells, F.W., "Viscosity of Nitrogen, Methane, Ethane and Propane at Elevated Temperature and Pressure," J. Chem. Engr. Data., 4, 283 (1959).

5. Barrer, R.M., "Viscosity of Pure Liquid, I. Polymerized and non-Polymerized Fluids," Trans. Faraday Soc., 39, 48 (1943).

6. Barua, A.K., Afzal, M., Flynn, G.P., and Ross, J., "Viscosity of Hydrogen, Deuterium, Methane and Carbon Monoxide from -50 to 150°C.," J. Chem. Phys., 41, 374 (1964).

7. Bicher, L.B.,Jr., and Katz, D.L., "Viscosity of the Methane-Propane System," Ind. Engr. Chem., 35, 754 (1943).

8. Bird, R.B., Stewart, W.E., and Lightfoot, E.N., Transport Phenomena,P.181, John Wiley and Sons,Inc., New York,1960.

9. Bondi, A.,"Viscosity of Nonassociating Liquids, Initial Correlation," Ind. Engr. Chem. Fundamentals, 2, No. 2, 95 (1963).o

10. Brebach, W.J., and Thodos, G., "Viscosity - Reduced State Correlation for Diatonic Gases," Ind. Engr. Chem., 50, 1095 (1958).

11. Bridgman, P.W., The Physics of High Pressure, P. 333, G. Bell and Sons, Ltd., London, 1949.

12. Brush, S.G., "Theories of Liquid Viscosity," Chemical Review, 62, No. 6, 513 (1962).

13. Carmichael, L.T., Berry, V.M., and Sage, B.H., "Viscosity of Hydrocarbons Propane," J. Chem. Engr. Data, 9, 411 (1964).

14. Carmichael, L.T., Berry, V.M., and Sage, B.H., "Viscosity of Hydrocarbons Methane," J. Chem. Engr. Data, 10, 57 (1965).

15. Carmichael, L.T., and Sage, B.H., "Viscosity of Ethane at High Pressures," J. Chem. Engr. Data, 8, 94 (1963).

16. Carmichael, L.T., and Sage, B.H., "Viscosity of Hydrocarbons. n-Butane," J. Chem. Engr. Data, 8, 612 (1963).

17. Carr, N.L., "Viscosity of Natural Gas Components and Mixtures," Institute of Gas Technology Research Bulletin 23, Chicago, Ill. (1953).

18. Carr, N.L., Parent, J.D., and Peck, R.E., "Viscosity of Gases and Gas Mixtures at High Pressures," Chem. Engr. Prog. Symposium Series, 51, No. 16, 91 (1955).

19. Clark, C.R., Private Communication.

20. Comings, E.W., Mayland, B.J., and Egly, R.S., "The Viscosity of Gases at High Pressure," University of Illinois Engr. Exptl. Station Bulletin, Serial 354 (1944).

21. Dean, D.E., and Stiel, L.I., "The Viscosity of Nonpolar Gas Mixtures at Moderate and High Pressures," A.I.Ch.E. Journal, 11, 526 (1965).

22. Dolan, J.P., Ellington, R.T., and Lee, A.L., "Viscosity of Methane-n-Butane Mixtures," J. Chem. Engr. Data, 9, 484 (1964).

23. Dolan, J.P., Starling, K.E., Lee, A.L., Eakin, B.E. and Ellington, R.T., "Liquid Gas and Dense Fluid Viscosity of n-Butane," J. Chem. Engr. Data, 8, 396 (1963).

24. Eakin, B.E., and Ellington, R.T., "Predicting the Viscosity of Pure Light Hydrocarbons," J. Petro. Tech., 210, February(1963).

25. Eakin, B.E., Starling, K.E., Dolan, J.P., and Ellington, R.T., "Liquid, Gas and Dense Fluid Viscosity of Ethane," J. Chem. Engr. Data, 7, 33 (1962).

26. Flynn, G.P., Hanks, R.V., LeMaire, N.A., and Ross, J., "Viscosity of Nitrogen,Helium,Neon and Argon from -78.5 to 100°C. below 200 Atmosphereres," J.Chem.Phys.,38, 154(1963).

27. Giddings, J.G., "The Viscosity of Light Hydrocarbon Mixtures at High Pressures: The Methane-Propane System," Ph. D. Thesis, Rice University, Houston, Texas (1963).

28. Giddings, J.G., and Kobayashi, R., "Correlation of the Viscosity of Light Paraffin Hydrocarbons and Their Mixtures in the Liquid and Gaseous Regions," J. Petro. Tech., 679, June(1964).

29. Golubev, I.F., and Agaev, N.A., "A Generalization of the Data on the Viscosities of Saturated Hydrocarbons at Various Temperatures and Pressures," Doklady Akademii Nauk SSSR, 151, No. 4, 875 (1963).

30. Grunberg, L., and Nissan, A.H., "Viscosity of Highly Compressed Fluids," Ind. Engr. Chem., 42, 885 (1950).

31. Grunberg, L., and Nissan, A.H., "The Viscosity of Hydrocarbons," Third World Petroleum Congress, The Hague, Proceedings, Section VI, P. 279 (1951).

32. Gupta, P.C., "A Study of the P-V-T Behavior of Mixtures of Methane with Different Types of Heavy Hydrocarbons with the Composition of the Heavy Fraction as a Controlled Variables," M.S. Thesis, The University of Kansas, Lawrence, Kansas (1965).

33. Hanson, G.H., "Thermodynamic Properties of Saturated Propylene, Propane, i-Butylene and n-Butane," Trans. A.I.Ch.E., 42, 959 (1946).

34. Hodgman, C.D., Editor, Handbook of Chemistry and Physics, 39th. ed., Chemical Rubber Publishing Company, Cleveland, Ohio, 1958.

35. Huang, T.S., "Saturated and Subcooled Liquid Densities of Light Paraffin Hydrocarbons and their Mixtures," M.S. Thesis, The University of Kansas, Lawrence, Kansas (1963).

36. Huang, T.S., Swift, G.W., and Kurata, F., "High Pressure Low Temperature Glass-to-Metal Seal," Rev. Sci. Instr., 35, 637 (1964).

37. Johnson, D.L., "Direct Determination of Mass by Weighing in a Cryogenic Environment," Interim report submitted to the Dept. of Chem. & Petro. Engr., The University of Kansas, Lawrence, Kansas (1964).

38. Jossi, J.A., Stiel, L.I., and Thodos, G., "The Viscosity of Pure Substances in the Dense Gaseous and Liquid Phases," A.I.Ch.E. Journal, 8, 59 (1962).

39. Keenan, J.H., and Keyes, F.G., Thermodynamic Properties of Steam, John Wiley & Sons, Inc., New York, 1936.

40. Kvalnes, H.M., and Gaddy, V.L., "The Compressibility Isotherms of Methane at Pressure to 1,000 Atmospheres and at Temperatures from -70 to 200°C.," J. Am. Chem. Soc., 53, 394 (1931).

41. Lee, A.L., and Ellington, R.T., "Viscosity of n-Pentane," J. Chem. Engr. Data, 10, 101 (1965).

42. Lee, A.L., and Ellington, R.T., "Viscosity of n-Decane in the Liquid Phase," J. Chem. Engr. Data, 10, 346 (1965).

43. Lee, A.L., Starling, K.E., Dolan, J.P., and Ellington, R.T., "Viscosity Correlation for Light Hydrocarbon Systems," A.I.Ch.E. Journal, 10, 694 (1964).

44. Leland, T.W., and Mueller, W.H., "Applying the Theory of Corresponding States to Multicomponent Systems," Ind. Engr. Chem., 51, 597 (1959).

45. Liley, P.E., "Survey of Recent Work on the Viscosity, Thermal Conductivity, and Diffusion of Gases and Liquefied Gases Below 500°K.," Progress in International Research on Thermodynamic and Transport Properties, J.G. Masi, Editor, ASME, Academic Press, New York, 1962.

46. Lim, B.S., Huang, T.S., VandenBoom, J.L., Swift, G.W., and Kurata, F., "Liquid Viscosity of Binary Mixtures of Methane, Ethane, Propane and n-Butane," Paper presented at the 29th. Annual Chemical Engineering Symposium on Thermodynamic and Transport Properties of Fluids, Division of Industrial and Engineering Chemistry of ACS, Rice University, Houston, Texas (Dec., 1962).

47. Lohrenz, J., "An Experimentally Verified Theoretical Analysis of the Falling Cylinder Viscometer," Ph.D. Thesis, The University of Kansas, Lawrence, Kansas (1960).

48. Lohrenz, J., and Kurata, F., "Design and Evaluation of a New Body for Falling Cylinder Viscometers," A.I.Ch.E. Journal, 8, 190 (1962).

49. Lohrenz, J., Swift, G.W., and Kurata, F., "An Experimentally Verified Theoretical Study of the Falling Cylinder Viscometer," A.I.Ch.E. Journal, 6, 547 (1960).

50. Lyman, T., Editor, Metals Handbook, 8th. ed., Am. Soc. of Metals, Metals Park, Ohio, 1961.

51. Matthews, C.S., and Hurd, C.O., "Thermodynamic Properties of Methane," Trans. A.I.Ch.E., 42, 55 (1946).

52. McCreary, J.G., and Swift, G.W., "High Pressure, Low Temperature Differential-Pressure Probe," Rev. Sci. Instr., 35, 1366 (1964).

53. Mickley, H.S., Sherwood, T.K., and Reed, C.E., Applied Mathematics in Chemical Engineering, McGraw-Hill, New York, 1957.

54. Olds, R.H., Reamer, H.H., Sage, B.H., and Lacey, W.N., "Volumetric Behavior of Methane," Ind. Engr. Chem., 35, 922 (1943).

55. Pavlovich, N.V., and Timrot, D.V., Teploenergetika, 5, No. 8, 61 (1958).

56. Popov, E.P., Mechanics of Materials, P. 36, Prentice Hall, Englewood Cliff., New Jersey, 1958.

57. Praushitz, J.M., and Gunn, R.D., "Volumetric Properties of Non-polar Gaseous Mixtures," A.I.Ch.E. Journal, 4, 430 (1958).

58. Price, A.R., and Kobayashi, R., "Low Temperature Vapor-Liquid Equilibrium in Light Hydrocarbon Mixtures: Methane-Ethane-Propane System," A.I.Ch.E. Journal, 4, 40 (1959).

59. Progress Report on API Project 69-C: "A Systematic Study of the P-V-T Behavior of Gaseous Mixtures Comprised of Methane and Heavy Paraffinic, Napthenic and Aromatic Components in Varying Ratio,"Low Temperature Laboratory,the Univ.of Kansas(Nov.1965).

60. Reamer, H.H., Cokelet, G., and Sage, B.H., "Viscosity of Fluids at High Pressures; Rotating Cylinder Viscometer and the Viscosity of n-Pentane," Anal. Chem., 31, 1422 (1959).

61. Reamer, H.H., Sage, B.H., and Lacey, W.N., "Phase Equilibria in Hydrocarbon Systems: Volumetric Behavior of Methane," Ind. Engr. Chem., 41, 482 (1949).

62. Reamer, H.H., Sage, B.H., and Lacey, W.N., "Phase Equilibria in Hydrocarbon Systems: Volumetric and Phase Behavior of the Methane-Propane System," Ind. Engr. Chem., 42, 534 (1950).

63. Roark, R.J., Formulas for Stress and Strain, P. 276, McGraw-Hill, New York, 1943.

64. Ross, J.F., and Brown, G.M., "Viscosity of Gases at High Pressures," Ind. Engr. Chem., 49, 2026 (1957).

65. Rossini, F.D., et al., Selected Values of the Properties of Hydrocarbons and Related Compounds, Carnegie Institute of Technology, Pittsbury, Pa., 1958.

66. Sage, B.H., and Lacey, W.N., Thermodynamic Properties of Lighter Paraffin Hydrocarbons and Nitrogen, American Petroleum Institute, New York, 1950.

67. Sage, B.H., Lacey, W.N., and Schaafsma, J.G., "Phase Equilibria in Hydrocarbon Systems: II Methane-Propane System," Ind. Engr. Chem., 26, 214 (1934).

68. Schindler, D.L., "The Heterogeneous Phase Behavior of the Helium-Propane, Nitrogen-Propane and Helium-Nitrogen-Propane System," Ph. D. Thesis, The University of Kansas, Lawrence, Kansas (1966).

69. Shimotake, H., and Thodos, G., "Viscosity: Reduced State Correlation for the Inert Gases," A.I.Ch.E. Journal, 4, 257 (1958).

70. Sinor, J.E., "The Solubility, Partial Molal Volume and Diffusivity of Helium in Liquid Methane," Ph. D. Thesis, The University of Kansas, Lawrence, Kansas (1965).

71. Smith, A.S., and Brown, G.G., "Correlating Fluid Viscosity," Ind. Engr. Chem., 35, 705 (1943).

72. Starling, K.E., Eakin, B.E., Dolan, J.P., and Ellington, R.T., "Critical Region Viscosity Behavior of Ethane, Propane and n-Butane," Progress in International Research on Thermodynamic and Transport Properties, J. F. Masi, Editor, ASME, Academic Press, New York, 1962.

73. Starling, K.E., Eakin, B.E., and Ellington, R.T., "Liquid Gas and Dense-Fluid Viscosity of Propane," A.I.Ch.E. Journal, 6, 438 (1960).

74. Swift, G.W., Private Communication.

75. Swift, G.W., "Liquid Viscosities Above the Normal Boiling Point for Methane, Ethane, Propane and n-Butane," Ph. D. Thesis, The University of Kansas, Lawrence, Kansas (1959).

76. Swift, G.W., Lohrenz, J. and Kurata, F., "Liquid Viscosities Above the Normal Boiling Point for Methane, Ethane, Propane and n-Butane," A.I.Ch.E. Journal, 6, 415 (1960).

77. Uyehara, O.A., and Watson, K.M., "Generalized Correlation of Viscosity," National Petroleum News, Tech. Section 36, 764 (Oct. 4, 1944).

78. van Itterbeek, A., Verbeke, O., and Staes, K., "Measurements on the Equation of State of Liquid Argon and Methane up to 300 Kg/cm^2," Physica, 29, 742 (1963).

79. Ward, A.G., "The Viscosity of Pure Liquids," Trans. Faraday Soc., 33, 88 (1937).

80. Weitzel, D.H., Robbins, R.F., Bopp, G.R., and Bjorklund, W.R., "Elastomers for Static Seals at Cryogenic Temperatures," Advances in Cryogenic Engr., P. 219, Vol. 6, K.D. Timmerhaus, Editor, Plenum Press, Inc., New York, 1961.

APPENDIXES

Appendix A

Calibration of Heise Pressure Gages and Characteristics of Low Temperature Differential Pressure Indicator

(A) Calibration of Heise Pressure Gages

Heise pressure gage H10788 was calibrated against a Ruska dead weight pressure tester [Model 5000.10(M-238), Serial Numbers 11516(gage) and 11687(weight)] and a high temperature differential pressure indicator combination. Heise pressure gage H3065 and the low temperature DPI(P.25) were calibrated against the Ruska dead weight tester and the high temperature DPI combination.

Ruska reading psia	Gage H10788 reading psia	Ruska reading psia	Gage H3065 reading psia
249.2	250	0.0	15
498.9	500	199.4	210
748.6	749	399.1	409
998.3	1000	598.9	609
1247.9	1249	798.6	810
1497.6	1495	998.3	1010
1747.3	1748	1397.8	1405
1997.0	1998	1697.4	1701
2246.7	2248	1997.0	1998
2496.4	2499	2995.8	3000
2746.1	2745	3994.5	4000
2995.8	2991	4993.3	5000
3245.4	3245		
3495.1	3502		
3744.8	3742		
3994.5	3992		
4244.3	4242		
4494.0	4492		
4743.7	4747		
4993.4	4992		

(B) Characteristics of Low Temperature Differential Pressure Indicator

In order to show the performance characteristics of the low temperature differential pressure indicators, the read out (micro-amperes), the position of the core relative to the null point and the corresponding differential pressure are shown for No. 2 DPI.

Read out (μA)	ΔH (cm)	ΔP (psi)
150	0.20	65
100	0.13	45
50	0.06	25
10	0.01	5
0	0.00	0
10	0.02	10
100	0.15	55
150	0.22	75
200	0.28	95

ΔP vs. ΔH is almost linear in the range reported, and the slope, ΔP/ΔH is 350 psi/cm. The sensitivity of the DPI of the bellow is $\pm$20 μA (or $\pm$10 psia).

Appenidx B

Calibration of Platinum Resistance Thermometer and Copper-Constantan Thermocoulpes

(A) Calibration of Platinum Resistance Thermometer

The platinum resistance thermometer used in this study for the temperature measurement of the low temperature bath was from the American Instrument Company marked "C. H. Meyers 281". This thermometer was calibrated against a platinum resistance thermometer from the American Instrument Company marked "C. H. Meyers 252", which in turn was calibrated by the National Bureau of Standards. The calibration of No. 281 thermometer was conducted in a special thermometer calibration bath using isopentane as bath fluid when calibrating at temperatures below 20°C. and using kerosene as bath fluid when calibrating at temperatures between 20 and 100°C. The bath temperature was controlled by the same temperature control system used in this study. The resistance of the No. 281 thermometer was measured by a Rubicon Mueller bridge, serial number 83628, operated with a continuous thermometer current of 3 milliamperes and the null point was observed on a L & N DC null detector. The resistance of the No. 252 thermometer was measured by a Rubicon Mueller bridge, serial number 113539, and the null point was observed on another L & N DC null detector. The thermometer and the Mueller bridge were operated with a continuous thermometer current of 2 milliamperes which was the value of current used by the National Bureau of Standards in the calibration of No. 252 thermometer. The No. 281 thermometer was calibrated with the mercury commutator of the Mueller bridge set at the normal position.

The temperatures at which the thermometer was calibrated and the experimental values of the resistances of both No. 252 and No. 281 thermometers are shown in Table B-1. In Table B-1, R_{252} is the resistance of the No. 252 thermometer (the standard thermometer), and R_{281} is the resistance of the No. 281 thermometer. The experimental calibration data, i.e., R_{281} versus T, for the No. 281 thermometer were then fitted by the Callendar-Van Dusen equation,

$$R_t = A + Bt + C(1-t/100)(t/100) + D(1-t/100)(t/100)^3 \quad \text{(B-1)}$$

where R_t is the resistance in ohms and t is the temperature in °C.

The coefficients computed from the regression analysis were,

$$A = 25.4762$$
$$B = 0.100023$$
$$C = 0.147104$$
$$D = 0.0116603$$

The resistances computed from the regression analysis, R_{281c}, were also shown in Table B-1. The maximum deviation between the experimental and computed resistances was 0.0015 ohms corresponding to about 0.015°C., and the standard deviation of the difference between the experimental and the computed resistances was 0.0007 ohms corresponding to about 0.007°C.

(B) Calibration of Copper-Constantan thermocouples

The copper-constantan thermocouples were used in this study to measure the temperature of the high temperature bath which contains mass injection cylinders. These thermocouples were calibrated against the No. 252 platinum resistance thermometer in the thermometer calibration bath using kerosene as bath fluid, and a Bayley temperature controller to control the bath temperatures. The electromotive force of the thermocouples was measured by a Rubicon High Precision Type B Potentiometer, Model 2780, and the null point was observed on a L & N DC null detector. The agreement of the readings from these thermocouples were within 0.02°C. The calibration data of one particular thermocouple are presented in Table B-2, where R_{252} is the resistance of No. 252 platinum resistance thermometer and EMF is the millivolts read from the potentiometer. These data were fitted by the following equation,

$$EMF = E_o + E_1 t + E_2 t^2 + E_3 t^3 \quad \text{(B-2)}$$

where EMF is in millivolt and t is in°C. The coefficients computed from the regression analysis were,

$$E_o = -0.00089$$
$$E_1 = 0.038960$$
$$E_2 = 0.3980 \times 10^{-4}$$
$$E_3 = 0.6212 \times 10^{-9}$$

The millivolts computed from the regression analysis(EMF_c) are also shown in Table B-2. In this study, these thermocouples were used to measured the temperature between 20 to 40°C. In this temperature range, the deviation between the experimental and computed data was less than 0.0016 m.v. corresponding to about 0.05°C.

Table B-1

Platinum Resistance Thermometer Calibration

Temp. °C.	R_{252} Ohms	R_{281} Ohms	R_{281c} Ohms	$R_{281}-R_{281c}$ Ohms
100.00	35.4722	35.4786	35.4785	0.0001
80.00	33.4959	33.5020	33.5027	-0.0007
60.00	31.5077	31.5147	31.5139	0.0008
40.00	29.5076	29.5124	29.5128	-0.0004
20.00	27.4955	27.5015	27.5002	0.0013
0.00	25.4699	25.4747	25.4762	-0.0015
-20.00	23.4355	23.4403	23.4403	0.0000
-60.00	19.3241	19.3301	19.3296	0.0005
-80.00	17.2460	17.2518	17.2518	0.0000
-100.00	15.1504	15.1564	15.1564	0.0000
-120.00	13.0350	13.0405	13.0408	-0.0003
-140.00	10.8967	10.9019	10.9019	0.0000
-155.00	9.2761	9.2806	9.2805	0.0001

Table B-2

Copper-Constantan Thermocouple Calibration

Temp. °C.	R_{252} Ohms	EMF m.v.	EMF_c m.v.	$EMF-EMF_c$ m.v.
10.00	26.4850	0.3917	0.3927	-0.0010
20.00	27.4955	0.7933	0.7942	-0.0009
30.01	28.5045	1.2028	1.2044	-0.0016
40.00	29.5076	1.6210	1.6213	-0.0003
50.00	30.5087	2.0458	2.0464	-0.0006
60.01	31.5087	2.4815	2.4806	0.0009
70.00	32.5032	2.9234	2.9239	-0.0005
80.00	33.4959	3.3744	3.3709	0.0035
90.00	34.4855	3.8324	3.8283	0.0041
100.00	35.4722	4.2982	4.2937	0.0045
110.00	36.4558	4.7699	4.7670	0.0029
120.00	37.4368	5.2498	5.2485	0.0013

Appendix C

Calibration of Mass Injection Cylinders

Run No.	Height inch	ΔW g	(ΔV/ΔH) cc./in.	Percent error of (ΔV/ΔH)	Overall (ΔV/ΔH)oa	Percent error of (ΔV/ΔH)oa	Ave. of (ΔV/ΔH)oa
Calibration of mass injection cylinder K							
K-1	13.152						
	12.032	22.3630	20.02	0.26	20.112	0.08	20.120
	10.753	25.7225	20.16				
	9.483	25.5022	20.13				
	6.181	66.2817	20.12				
	3.622	51.3368	20.11				
K-2	12.620						
	9.397	64.7794	20.15	0.27	20.129		
	6.183	64.4847	20.11				
	3.585	52.1645	20.13				
Calibration of mass injection cylinder L							
L-1	11.922						
	1.502	11.0229	--		1.0603	0.06	1.0604
L-2	12.058						
	1.594	11.0751	--		1.0610		
L-3	11.988						
	1.525	11.0735	--		1.0608		
L-4	11.845						
	1.609	10.8178	--		1.0594		
L-5	11.982						
	10.382	1.6825	1.054	0.94	1.0604		
	8.859	1.6012	1.054				
	7.315	1.6225	1.053				
	6.014	1.3617	1.049				
	4.764	1.3361	1.072				
	3.413	1.4360	1.066				
	1.653	1.8865	1.075				
L-6	11.921						
	10.623	1.3766	1.063	0.92	1.0603		
	8.747	1.9738	1.055				
	7.113	1.7050	1.046				
	5.742	1.4586	1.067				
	3.870	1.9772	1.059				
	2.598	1.3674	1.078				
	1.569	1.0918	1.064				

Run No.	Height inch	ΔW g	(ΔV/ΔH) cc./in.	Percent error of (ΔV/ΔH)	Overall (ΔV/ΔH)oa	Percent error (ΔV/ΔH)oa	Ave. of (ΔV/ΔH)oa
Calibration of mass injection cylinder G							
G-1	11.678						
	10.983	0.8707	1.256	0.26	1.2642	0.04	1.2640
	10.205	0.9760	1.258				
	9.467	0.9301	1.263				
	8.426	1.3109	1.262				
	7.612	1.0294	1.268				
	6.757	1.0772	1.263				
	5.230	1.9280	1.266				
	4.346	1.1138	1.263				
	3.355	1.2532	1.268				
	2.692	0.8408	1.271				
	2.251	0.5592	1.271				
G-2	11.699						
	10.602	1.3840	1.264	0.18	1.2637		
	8.909	2.1317	1.261				
	7.566	1.6938	1.264				
	6.378	1.5004	1.265				
	5.298	1.3604	1.262				
	4.205	1.3754	1.261				
	3.227	1.2381	1.264				
	2.231	1.2572	1.268				

Notes: (1) Mass injection cylinders K and L were calibrated in high temperature bath with distilled water at 100°F. and 1500 psia. Density of water at this condition is 1.0024 g/cc. (39). Mass injection cylinder G was calibrated with distilled water at ambient temperature (23°C.) and atmospheric pressure. Density of water at this condition is 0.99756 g/cc. (34).

(2) Runs K-1 to L-4 were run by J. G. McCreary.

(3) Percent error is computed on 95% probability using "t" statistics. When only two data points are available, percent error is the difference of the two values divided by the mean value and then multiplied by 100.

Appendix D

Calibration of Viscometer Volumes

LTB Temp. °C.	LTB Press. psia	HTB Press. psia	Volume transferred cc.	Viscometer volume cc.	Percent error	Average viscometer volume cc.	$\alpha_V \times 10^5$ $(°C)^{-1}$
Viscometer tube and No. 1 falling cylinder (No DPI).							
23.	1,500	1,500	12.012	12.024	±0.20	12.024*	
	1,000	1,000	12.036				
Viscometer tube and No. 2 falling cylinder (No DPI).							
37.78	1,500	1,500	11.987	11.987	±0.16	11.998	4.87
			11.976	11.976			
			12.008	12.008			
			11.998	11.998			
			12.019	12.019			
-70.00	1,470	1,470	42.441	11.943	±0.13	11.935	
			42.387	11.928			
					Ave. error		
					±0.16		
Viscometer tube, No. 2 falling cylinder and No. 1 DPI.							
37.78	1,500	1,500	12.641	12.641	±0.15	12.646	5.35
			12.670	12.670			
			12.654	12.654			
			12.638	12.638			
			12.626	12.626			
-70.00	1,470	1,470	44.715	12.583	±0.16	12.573	
			44.644	12.563			
Viscometer tube, No. 2 falling cylinder and No. 2 DPI.							
37.78	1,500	1,500	12.670	12.670	±0.10	12.687	7.88
			12.699	12.699			
			12.693	12.693			
			12.692	12.692			
			12.682	12.682			
-25.00	1,470	1,500	19.960	12.607	±0.38	12.636	
			20.040	12.657			
			20.020	12.645			
-70.00	1,470	1,500	43.742	12.576	±0.20	12.584	
			43.742	12.576			
			43.823	12.599			
138.82	1,500	1,500	68.267	12.520	±0.11	12.512	
			68.209	12.510			
			68.189	12.506			
					Ave. error		
					±0.18		

Appendix D (Continued)

Notes: (1) *This run was conducted with propane as a calibration fluid and the mass injection cylinder G was used to meter mass into viscometer (α_v used in the correction of temperature effect is $4.87 \times 10^5 (°C)^{-1}$).
(2) Percent error is computed on 95% probability using "t" statistics.
(3) The density at 37.78°C. is from Sage and Lacey(66), that at -138.82°C. is from van Itterbeek, et al.(78) and those at -25 and -70°C. are from Kvalnes and Gaddy(40).

Appendix E

Density of Falling Cylinders

Two methods were used to determine the volume of the falling cylinders:

Method A: Using Archimedes'principle
Method B: Using a pycnometer

Method A	No.1 cylinder	No.2 cylinder	No.3 cylinder
Wt. of cylinder and wire	7.3227	7.3548	7.3769
Wt. of cylinder and wire in water(g)	4.8938	4.9137	4.9325
Boyancy force(g)	2.4289	2.4411	2.4444
Density of water(g/cc.) at temp.(°C.)	0.99717 (24.5°C.)	0.99574 (29.7°C.)	0.99691 (25.5°C.)
Volume of body(cc.)	2.4357	2.4515	2.4520
Method B			
Wt. of pycnometer, water and cylinder(g)	61.6224	61.5851	61.6484
Wt. of pycnometer and water(g)	56.7355	56.6723	56.7172
Boyancy force(g)	2.4358	2.4420	2.4457
Density of water at temp.(°C.)	0.99717 (24.5°C.)	0.99583 (29.4°C.)	0.99668 (26.4°C.)
Volume of body(cc.)	2.4367	2.4522	2.4539
Average cylinder volume(cc.)	2.4362	2.4519	2.4530
Wt. of cylinder(g)	7.3227	7.3548	7.3769
Density of cylinder(g/cc.)	3.0058	2.9996	3.0073

Appendix F

Determination of Distance of Fall

The distance of fall, s, which the falling cylinder traversed was determined by an indirect method as described in this appendix.

Refer to the figures, the lengths of the falling cylinder (L_c), viscometer tube (L_t) and auxiliary rod (L_r) were first measured with a "machinist precision height gage". Then the distance A was measured by assembling the coupling, the viscometer tube, the falling cylinder and the auxiliary rod as shown in Figure (I); and the distance B was measured by assembling the tee, the viscometer tube, the falling cylinder and the auxiliary rod as shown in Figure (II). The distance of fall was then computed by,

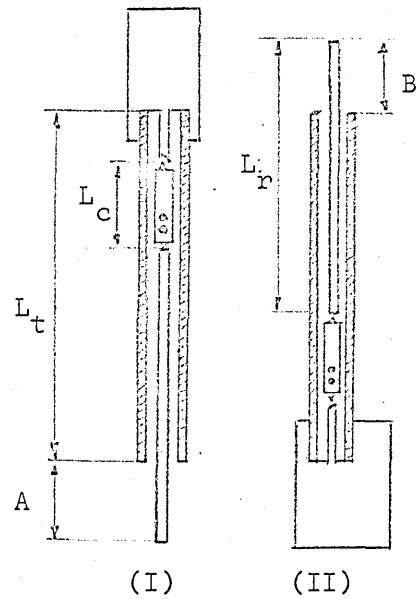

$$s = (L_r - B) + (L_r - A) + L_c - L_t.$$

Table F-1 shows these measurements and the computed distances of fall.

Table F-1

Determination of Distance of Fall

Falling Cylinder No.	L_c	L_r	L_t	A	B	S
1	2.099	10.269	9.993	4.280	3.300	5.064
	2.099	10.269	9.993	4.280	3.297	5.067
2	2.120	10.269	9.993	4.293	3.330	5.044
3	2.098	10.269	9.993	4.275	3.303	5.065

Note: The unit of these numbers is in inches.

Appendix G

Comparison of Time Interval Meters

Beckman Time Interval Meter, Model 5230R, Serial Number, 148, the one used in this study, was compared with a new Beckman Time Interval Meter, Model 5230R, Serial Number 408 which was purchased in 1965. The test was made on October 4, 1965, using a stainless steel viscometer tube, Number 2 falling cylinder and instrument grade propane at 100°F. and 1,000 psia. The same starting and stopping signals were fed to the both time meters.

M 5230R-4 θ_1(sec.)	M 5230R θ_2(sec.)	$(\theta_2-\theta_1)$ (sec.)
27.8905	27.8913	0.0008
27.9325	27.9358	0.0033
27.8912	27.8930	0.0018
28.0107	28.0116	0.0009
27.8890	27.8902	0.0012
27.9859	27.9875	0.0016
27.8833	27.8865	0.0032
27.9624	27.9633	0.0009
27.8658	27.8666	0.0008
27.8313	27.8327	0.0014

Appendix H

Reproducibility of the Fall Time of Falling Cylinders

(a) Fall times of No. 1 cylinder in the research and the pure grade propane at 100°F. and 300 psia.

Run No.	Fall time sec.	% error	Remarks
1P-1	24.58	0.11	Instrument grade C_3H_8. (Fresh C_3H_8 from supply cylinder)
1P-2	24.66	0.13	Instrument grade C_3H_8.
1P-6	24.60	0.06	The same instrument grade C_3H_8 used in the viscosity measurement of the three isotherms at low temperatures.
1P-9	24.48	0.20	Research grade C_3H_8. (Fresh C_3H_8 from supply cylinder)
1P-10	24.40	0.17	Research grade C_3H_8. (Fresh C_3H_8 from supply cylinder)
1P-10	24.31	0.14	Instrument grade C_3H_8.
1P-12	24.43	0.41	Instrument grade C_3H_8. Teflon fragments were found in the viscometer after the run. (believed to be fragments of Hoke valve seat)
1P-13	24.09	0.26	Instrument grade C_3H_8.
1P-13	26.42		Fall time at 1000 psia.

Overall percent error = $\pm$0.8%

(b) Fall times of No. 2 cylinder in the instrument grade propane at 100°F. and 1000 psia.

Run No.	Fall time sec.	% error	Remarks
2P-1	28.40	0.07	Calibration datum of the viscometer.
2P-3	27.91	0.14	After run 2X2-4.
2P-4	27.91	0.18	After run 2X2-4.
2P-5	28.35	0.73	After run 2X3-3.
2P-6	27.97	0.51	Before run 2X3-5.
2P-7	28.05	0.12	Before run 2X1-1.

Overall percent error = $\pm$1.1%

Notes: (1) All the percent errors are computed on the 98% probability using "t" statistics.
(2) Run 1P-13 at 1000 psia was excluded in the computation of overall percent error for No. 1 falling cylinder.

Appendix I

Original Data for the Preparation of Mixtures

The mixtures were prepared in the mixture make up cylinder M (MMC-M), which was in the high temperature bath controlled at 100°F., by transferring a known amount of pure components from the mass injection cylinder K into MMC-M. The original data are as follows:

Sequence No.	Fluid	Reference Press.* psia	Difference in Height in.	No. of g-mole	Calculated mole %
1	CH_4	1,500	8.683	0.7998	50.0
	C_3H_8	1,000	3.574	0.7997	50.0
2	CH_4	2,500	7.629	1.2087	75.3
	C_3H_8	1,000	1.767	0.3954	24.7
3	CH_4	2,500	7.627	1.2080	75.3
	C_3H_8	1,000	1.767	0.3954	24.7
4	CH_4	1,500	4.801	0.4423	22.1
	C_3H_8	1,000	6.980	1.5617	77.9
5	CH_4	1,500	7.394	0.6811	50.0
	C_3H_8	1,000	3.043	0.6808	50.0

Notes: (1) *These numbers are the apparent weight from Ruska dead weight tester. The actual pressures are 0.17% smaller than the reported values.

(2) Sequence numbers in this table indicate the squence in which the mixtures were prepared and studied.

Appendix J

Error Analysis

The relationship between the maximum probable error in an experimental result and the fractional errors for the type of formula, i.e.,

$$Q = q_a^a \, q_b^b \ldots\ldots q_n^n$$

according to Mickley, et al. (53) is,

$$\frac{\Delta Q}{Q} = a \frac{\Delta q_a}{q_a} + b \frac{\Delta q_b}{q_b} + \ldots\ldots + n \frac{\Delta q_n}{q_n}$$

In the following, the relationships between the total error and the fractional errors for the computed composition, density and viscosity are shown (all the negative signs in a, b etc. are changed to positive signs to propagate the error), and an example of computing error is shown for each case.

(1) Composition

(a) Random error: From Equation (V-2), the maximum error in the composition is (note ρ_{im} is used instead of ρ_i/M_i),

$$\frac{dX_1}{X_1} = \frac{d(\rho_{1m}\Delta V_1)}{\rho_{1m}\Delta V_1} + \frac{d(\rho_{1m}\Delta V_1 + \rho_{2m}\Delta V_2)}{\rho_{1m}\Delta V_1 + \rho_{2m}\Delta V_2}$$

$$= \frac{d\rho_{1m}}{\rho_{1m}} + \frac{d(\Delta V_1)}{\Delta V_1} + \frac{[\rho_{1m}\Delta V_1(\frac{d\Delta V_1}{\Delta V_1} + \frac{d\rho_{1m}}{\rho_{1m}}) + \rho_{2m}\Delta V_2(\frac{d\Delta V_2}{\Delta V_2} + \frac{d\rho_{2m}}{\rho_{2m}})]}{(\rho_{1m}\Delta V_1 + \rho_{2m}\Delta V_2)}$$

Since the absolute errors in methane and propane densities are reported to be the same, i.e.,

$$\frac{d\rho_{1m}}{\rho_{1m}} = \frac{d\rho_{2m}}{\rho_{2m}}$$

and the injections of the methane and propane were made from the same cylinder, i.e.,

$$\frac{d\Delta V_1}{\Delta V_1} = \frac{d\Delta V_2}{\Delta V_2}$$

The error $(\Delta X_1/X_1)$ can then be rewritten as,

$$\frac{dX_1}{X_1} = 2\left(\frac{d\rho_{1m}}{\rho_{1m}} + \frac{d\Delta V_1}{\Delta V_1}\right)$$

Since $d\rho_{1m}/\rho_{1m} = 0.1\%$, $d\Delta V_1/\Delta V_1 = 0.27\%$ (Appendix C)

then, $dX_1/X_1 = 2(3.7) = 0.74\%$

Therefore the relative error in the composition is ± 0.74, and the maximum absolute error is $\pm 0.5\%$ (=0.74x0.753), i.e., ± 0.005 mole fraction.

(b) Systematic error: The systematic error due to the error of 0.8% in the methane density (see P. 57) is estimated for the composition of each mixture studied:

Computed CH_4 composition(%) X_1	Corrected CH_4 composition(%) $X_{1c} = \frac{X_1(1-0.008)}{1-X_1(0.0008)}$	Absolute error in the composition(%) $\Delta X = X_1 - X_{1c}$
75.3	75.2	0.1
50.0	49.8	0.2
22.1	22.0	0.1

(2) Density: From Equation(V-4),

$$\Delta\rho/\rho = \Delta\rho_{rc}/\rho_{rc} + \Delta(\Delta V)/\Delta V + \Delta(V_{vm})/V_{vm}$$

For methane using MIC-L, $\Delta\rho/\rho = 0.1\%$, $\Delta(\Delta V)/\Delta V = 0.35\%$, $\Delta(V_{vm})/V_{vm} = 0.16\%$,

therefore, $\Delta\rho/\rho = \pm 0.61\%$

The error in ΔV is estimated as follows: In the determination of density, one full load displacement and one half load displacement of fluids (Appendixes N and O) were transferred into the viscometer on the average. The errors in ΔV for full load displacement and half load displacement are reported in Appendix C. Based on this one and half load displacement of fluid, the error in ΔV when MIC-L was used is,

$$\Delta V/V = [1(0.06) + 0.5(0.94)]/1.5 = 0.35\%$$

and the error in ΔV when MIC-G was used is,

$$\Delta V/V = [1(0.04) + 0.5(0.27)]/1.5 = 0.11\%$$

(3) Viscosity: From Equation(V-3),

$$\Delta\mu/\mu = \Delta\beta_{calc}/\beta_{calc} + \Delta\beta_{red}/\beta_{red} + \Delta(\sigma-\rho)/(\sigma-\rho) + \Delta\theta/\theta + \Delta s/s$$

For methane, $\Delta\beta_{calc}/\beta_{calc} = 1.5\%$, $\Delta\beta_{red}/\beta_{red} = 0.8\%$, $\Delta(\sigma-\rho)/(\sigma-\rho) = 0.2\%$

$\Delta\theta/\theta = 0.8\%$, $\Delta s/s = 0.1\%$

Therefore, $\Delta\mu/\mu = \pm 3.4\%$

To estimate the error in $(\sigma-\rho)$, the error in the density of the falling cylinder is estimated to be less than 0.1% (Appendix E), and the error in the density of fluid is $\pm 0.6\%$ for pure components ($\pm 1.2\%$ for mixtures). The error associated with the difference between the densities of the falling cylinder and the fluid is then estimated to be $\pm 0.2\%$ for pure components ($\pm 0.3\%$ for mixtures). It is clear from these numbers that the uncertainty in density is always decreased in the computation of viscosity from Equation (V-3), and so high precision density data are not required in the computation of the viscosity.

Appendix K

Effect of the Acceleration on the Fall Time

Consider the viscometer assembly shown in Figure II-1 where a falling cylinder is falling inside a viscometer tube. Two types of fall are considered in this appendix:

(1) The falling cylinder is dropped from a static position and traverses a distance s in θ seconds;

(2) The falling cylinder is falling at a terminal velocity v_T and traverses a distance s_1 in θ seconds.

It will be shown in this appendix that, for the conditions of the fluids investigated in this study, there is negligible difference between these two distances.

Consider a falling cylinder falling from a static position inside the viscometer tube. Before the falling cylinder reaches the terminal velocity v_T, the falling cylinder is falling at a transient velocity $\bar{v}$ with an acceleration a. A force balance on this non-steady fall of the cylinder, with an assumption that only laminar skin friction occurs on the cylindrical surface of the cylinder, is,

$$F_g = V(\sigma-\rho)g = (V\sigma)a + F_{\Delta p} + F_{lsf} \qquad (K\text{-}1)$$

where F_g is the gravitational force on cylinder, $F_{\Delta p}$ is the force on the cylinder due to pressure drop and F_{lsf} is the force on the cylinder due to friction on laminar flow along the cylindrical surface. Equation (K-1) is the same as Equation (45) in Lohrenz's thesis (47) except for the extra transient force term $(V\sigma)a$. By substituting Equations (17) and (44) from Lohrenz's thesis into Equation (K-1), and rearrenging, the following relationship is obtained,

$$F_g = V(\sigma-\rho)g = (V\sigma)a + \frac{2\,\bar{\mu}\,\bar{v}\,L_e\,\pi}{\ln(1/\kappa)-(1-\kappa^2)/(1+\kappa^2)} \qquad (K\text{-}2)$$

By combining Equations (K-2) and (II-12), and recalling that V equals $(\pi/4)D_c^2L_e$,

$$(\sigma-\rho)g = \sigma a + \bar{\mu}\bar{v}g/\beta_{calc} \qquad (K\text{-}3)$$

Since $a = \frac{d\bar{v}}{dt}$,

$$\frac{d\bar{v}}{dt} + [\frac{g\bar{\mu}}{\sigma\beta_{calc}}]\bar{v} = \frac{(\sigma-\rho)g}{\sigma} \qquad (K-4)$$

and, solving Equation (K-4) for $\bar{v}$,

$$\bar{v} = (\sigma-\rho)\frac{\beta_{calc}}{\bar{\mu}}[1 + \exp(-\frac{\bar{\mu}gt}{\sigma\beta_{calc}})] \qquad (K-5)$$

Recalling that β_{calc} is derived for a cylinder falling at a terminal velocity, v_T, we have,

$$v_T = (\sigma-\rho)\beta_{calc}/\bar{\mu} \qquad (K-6)$$

Then Equation (K-5) can be rewritten as,

$$\bar{v} = \frac{d\bar{s}}{dt} = v_T[1 - \exp(-\frac{\bar{\mu}gt}{\sigma\beta_{calc}})] \qquad (K-7)$$

Integrating Equation (K-7) with respect to t,

$$\bar{s} = v_T t\{1 - \frac{\sigma\beta_{calc}}{\bar{\mu}gt}[1 - \exp(-\frac{\bar{\mu}gt}{\sigma\beta_{calc}})]\} \qquad (K-8)$$

Equation (K-8) expresses the instantaneous position $\bar{s}$ of the cylinder in the tube as a function of the time t that required for the cylinder to fall from a static position. If θ seconds are required for the falling cylinder to traverse a distance of s, (case 1), by substituting θ in Equation (K-8), the total distance of fall s is related to θ by,

$$s = v_T\theta\{1 - \frac{\sigma\beta_{calc}}{\bar{\mu}g\theta}[1 - \exp(-\frac{\bar{\mu}g\theta}{\sigma\beta_{calc}})] \qquad (K-9)$$

Since s_i, as already defined (case 2), is

$$s_i = v_T\theta \qquad (K-10)$$

Furthermore, Equation (K-6) can be rewritten as,

$$\bar{\mu} = \frac{(\sigma-\rho)\beta_{calc}}{v_T} = (\sigma-\rho)\beta_{calc}(\theta/s_i) \qquad (K-11)$$

By substituting Equations (K-10) and (K-11) into Equation (K-9), and rearranging the equation,

$$\Delta s = s - s_i = \frac{\sigma(\sigma-\rho)\beta^2_{calc}}{\bar{\mu}^2 g}\{1 - \exp[-\frac{\bar{\mu}^2 g s_i}{\sigma(\sigma-\rho)\beta^2_{calc}}]\} \quad (K\text{-}12)$$

Here, since β_{calc} for the viscometer used in this study is about 2×10^{-4} cm^3/sec^2, σ is 3 g/cc., ρ is 0.5 g/cc., g is 980 cm/sec^2, and $\bar{\mu}$ is between 0.00006 to 0.005 poises, the exponential term is small compared to 1, therefore, Equation (K-12) is reduced to,

$$\Delta s = \sigma(\sigma-\rho)\beta^2_{calc}/(\bar{\mu}^2 g) \quad (K\text{-}13)$$

Since for a given viscometer, σ and β_{calc} are about constant, and $(\sigma-\rho)$ is also almost constant (because $\sigma >> \rho$), $\bar{\mu}^2$ is the only variable affecting Δs according to Equation (K-13). Δs is inversely proportional to the $\bar{\mu}^2$; this term $(\Delta s)_\Lambda$ would almost be zero for the highly viscous fluids. The fluids investigated in this study, at most parts, existed in the liquid or dense fluid state, therefore, Δs is negligible. For the worst cases encountered in this study however (methane vapor at -140°C. and 70 psia, see Appendix P), $(\Delta s/s)$ is determined from Equation (K-13) to be 0.009. This value shows that if the falling cylinder is falling at v_T from the beginning of fall (case 2), it would fall (0.009)s further than s, the total actual distance of fall (case 1) in θ seconds. This indicates that there is approximately 1% error between the experimentally determined fall time, θ, and the ideal fall time, s/v_T. This error is tolerable in view of the fact that the reproducibility of fall time of the falling cylinders used in this study is not better than $\pm$0.8% (Appendix H). Therefore, it is concluded that, the effect of the acceleration on the time of fall determined experimentally in this study is negligible.

Appendix L

Sample Calculations

Calculation of Viscometer constant and Equivalent Diameter

β_{calc} and D_e as functions of temperature and pressure were calculated from Equations(II-12), (II-11), (II-3) and (II-4) using Computor Program 510 (see Appendixes M,P and Q). Double precision (16 significant figures) was specified in this program, since the calculations involved the difference of almost identical numbers. The following sample calculation was done with a desk calculator and the logarithms were obtained from "Table of Natural Logarithm"* containing sixteen decimal place values of the natural logarithm of the numbers.

β_{calc} and D_e for No.1 falling cylinder and the viscometer tube at 0°C. and 4,000 psia are calculated. The diameters of the falling cylinder and the viscometer tube at 25°C. are,

$$D_c = 0.3077"$$
$$D_t = 0.3140"$$
$$D_{to} = 0.5619"$$

From Equation(II-3),

$$D_{c(0,4000)} = 2.54(0.3077)[1+2.34\times10^{-5}(0-25)][1-\frac{4000}{0.103\times10^{8}}(1-0.33)]$$
$$= 0.7810 \text{ cm.}$$

From Equation(II-4),

$$D_{t(0,0)} = 0.3140[1+1.602\times10^{-5}(0-25)] = 0.3139"$$
$$D_{to(0,0)} = 0.5619[1+1.602\times10^{-5}(0-25)] = 0.5617"$$
$$D_{t(0,4000)} = 2.54(0.3139)[1+\frac{4000}{0.29\times10^{8}}(\frac{0.5617^2+0.3139^2}{0.5617^2-0.3139^2}+0.26)]$$
$$= 0.7974 \text{ cm.}$$
$$\kappa = D_{c(0,4000)}/D_{t(0,4000)} = 0.979433157$$
$$\kappa^2 = 0.95928930903$$

Equation(II-12) gives,

$$\beta_{calc} = (gD_c^2/8)[\ln(1/\kappa) - (1-\kappa^2)/(1+\kappa^2)]$$

* Lowan, A.N., Director,"Table of Natural Logarithms", Vol.III, Federal Works Agency Work Projects Administration for the City of New York(1941).

$$1+\kappa = 1.979433157$$

$$1-\kappa = 0.020566843$$

$$\frac{1-\kappa^2}{1+\kappa^2} = \frac{(1.979433157)(0.020566843)}{(1.959289309)} = 0.020778295$$

From "Table of Natural Logarithms":

$$\ln(1/\kappa) = \ln D_t - \ln D_c$$
$$= \ln(0.7974) - \ln(0.7810)$$
$$= 0.22639884403$$
$$-0.24718012914$$
$$= 0.02078128510$$

$$\beta_{calc} = (980/8)(0.7810)\ (0.000002990) = 2.234 \times 10^{-4}\ \text{cc./sec}^2$$

From Equation(II-11),

$$D_e = 2\kappa^4 D_t[\ln(1/\kappa)-(1-\kappa^2)/(1+\kappa^2)](1+\kappa^2)/[(1-\kappa)(1-\kappa^2)^2]$$

$$\ln(1/\kappa) - (1-\kappa^2)/(1+\kappa^2) = 2.990 \times 10^{-6}$$

$$\frac{(1+\kappa^2)}{(1-\kappa)(1-\kappa^2)^2} = \frac{(1.959289309)}{(0.020566843)(0.04071069097)^2} = 5.74796 \times 10^4$$

$$\kappa^4 = 0.9202360$$

$$D_e = 2(0.9202360)(0.7974)(2.990 \times 10^{-6})(5.74796 \times 10^4)$$
$$= 0.2523\ \text{cm.}$$

The values for β_{calc} and D_e calculated here are slightly different from those calculated from Computer Program 510, i.e., $\beta_{calc} = 2.308 \times 10^{-4}$ cc./sec^2 and $D_e = 0.2522$ cm.(see Table P-1 of Appendix P). The difference is due to (a)the different values of $D_{t(0,4000)}$ and $D_{c(0,4000)}$ used in the calculations, (b) the uncertainty in the last significant figure in the value of $(1-\kappa)$ calculated from the desk calculator.

Calculation of Experimental Viscometer Constant

The calibration of a viscometer was conducted by measuring the fall time that was required for a falling cylinder to traverse a known distance of fall in the viscometer which was filled with the fluid of known viscosity and density. From this experimentally determined fall time and the physical properties of the fluid and the viscometer, the experimental viscometer constant, $\beta_{p,t}$, was calculated as demonstrated by the following example(the data are from Appendix M):

Run No.: 1P-3

Falling cylinder: No.1
Fluid: Propane T = 21.111°C. P = 1000 psia

σ = 3.0058 g./cc. ρ = 0.511 g./cc.

s_{25} = 5.064 in. $\bar{\mu}$ = 0.001125 poises

L_{25} = 2.099 in. θ = 31.09 sec.

$\alpha_t = 1.602 \times 10^{-5}$/°C.

$\alpha_c = 2.340 \times 10^{-5}$/°C.

From Equation(II-14),

$$s = (2.54)\{(7.163)[1+1.602\times10^{-5}(21.11-25)] - (2.099)[1+2.340\times10^{-5}(21.11-25)]\}$$

$$= 12.862 \text{ cm.}$$

From Equation(I-1)

$$\beta_{p,t} = 0.001125(12.878)/[(2.4948)(31.09)]$$

$$= 1.866 \times 10^{-4} \text{ cc./sec.}^2$$

Calculation of Composition of the Mixture

The mixture was prepared in MMC-M which was in the HTB controlled at 100°F., by transferring a known amount of pure components from MIC-K into MMC-M. A sample calculation of the composition from the original data is shown as follows(the following data are from Sequence No. 1 of Appendix I):

$(\Delta V/\Delta H)$ for MIC-K = 20.120 cc./in.

ρ for methane at 1500 psia and 100°F., ρ_1 = 0.07344 g./cc.

ρ for propane at 1000 psia and 100°F., ρ_2 = 0.4904 g./cc.

volume of methane displaced, $\Delta H_1(\Delta V/\Delta H)$ = 8.683(20.12) = 174.7 cc.

volume of propane displaced, $\Delta H_2(\Delta V/\Delta H)$ = 3.574(20.12) = 71.91 cc.

g-moles of methane displaced = 174.7(0.07344)/16.04 = 0.7998 g-moles

g-moles of propane displaced = 71.91(0.4904)/44.10 = 0.7997 g-moles

the composition of methane = 100(0.7998)/(0.7998+0.7997) = 50.0 mole %

the composition of propane = 100.0 - 50.0 = 50.0 mole %

Calculation of Density

The experimental density was determined by using a MIC which displaced measured volume of fluid into a viscometer at 100°F. A sample calculation is shown as follows(the following data are from Appendix O):

Run No.: 2X3-1

Fluid: 75.3 mole % methane mixture

volume of viscometer tube, No.2 falling cylinder and No.1 DPI at 100°F. = 12.646 cc.

temperature coefficient, α_v = 5.35 x 10^{-5}/°C.

$(\Delta V/\Delta H)$ for MIC-L = 1.0604 cc./in.

(a) At T = -40°C., and P = 2000 psia

volume of the mixture displaced $\Delta H(\Delta V/\Delta H)$ = 22.692(1.0604) = 24.06 cc.

ρ_{rc} for the mixture at 100°F. and 2000 psia = 0.1925 g./cc.

mass of the mixture displaced = 4.632 g.

V_{vm} at -40°C. = 12.646[1+5.35x10^{-5}(-40-37.8)] = 12.593 cc.

From Equation(V-4),

$$\rho_{-40°C.\ \&\ 2000\ psia} = 0.368\ g./cc.$$

(b) At T = -40°C., and P = 3000 psia

additional volume of the mixture displaced

$\Delta H(\Delta V/\Delta H)$ = 1.076(1.0604) = 1.141 cc.

ρ_{rc} for the mixture at 100°F. and 3000 psia = 0.2630 g./cc.

additional mass of the mixture displaced = 0.2630(1.141) = 0.300 g.

total mass in the viscometer = 4.932 g.

From Equation(V-4),

$$\rho_{-40°C.\ \&\ 3000\ psia} = 0.392\ g./cc.$$

Calculation of Viscosity

The experimental viscosity was determined by measuring the fall time required for a falling cylinder to traverse a known distance of fall in a viscometer which was filled with the fluid of unknown viscosity. The following example shows how the viscosity was calculated from the experimental fall time data (the data are from Table P-1 of Appendix P):

Run No.: 1M-5

Falling cylinder: No.1

Fluid: methane $T = -100°C.$ $P = 5000$ psia

$\sigma = 3.0058$ g./cc. $\rho = 0.378$ g./cc.

$s_{25} = 5.064$ in. $\theta = 14.88$ sec.

$L_{25} = 2.099$ in. $\beta_{calc} = 2.598 \times 10^{-4}$ cc./sec^2.

$\alpha_t = 1.602 \times 10^{-5}/°C.$ $D_e = 0.2513$ cm.

$\alpha_c = 2.340 \times 10^{-5}/°C.$

(a) From Equation(II-14)

$$s = (2.54)\{(7.163)[1+1.062\times10^{-5}(-100-25)] - (2.099)[1+2.340\times10^{-5}(-100-25)]\}$$

$$= 12.842 \text{ cm.}$$

(b) Assume $\beta_{red} = 0.8545$

$$\beta_{p,t} = \beta_{calc}\beta_{red} = (2.598\times10^{-4})(0.8545) = 2.220\times10^{-4} \text{ cc./sec}^2.$$

From Equation(I-1),

$$\bar{\mu} = \beta_{p,t}(\sigma-\rho)\theta/s = 2.220\times10^{-4}(3.0058-0.378)(14.88)/(12.842)$$

$$= 675.9 \times 10^{-6} \text{ poises}$$

(c) $\log(N_{Re}) = \log[0.2513(12.842)(0.378)/\{(675.9\times10^{-6})(14.88)\}]$

$= 2.084$

(d) $\log(N_{Re}) < 2.446$[transition $\log(N_{Re})$], therefore, Equation(II-15) was used to compute β_{red}.

$$\beta_{red} = 0.9351 - 0.03870\{\log(N_{Re})\} = 0.8545$$

Since this β_{red} agrees with the assumed β_{red} in step(b), the value of $\bar{\mu}$ calculated in step(b) is the correct viscosity value at this particular condition.

Note on Appendixes M, N, O, P and Q

Appendixes M, N, O, P and Q present the original experimental data and the calculated data for the viscometer calibration, density and viscosity determinations. Since three falling cylinders (No. 1, 2 and 3) and different fluids were used during the course of experiment, a coding system was developed for all the experimental runs. Each code consists of three sub-codes. The first sub-code indicates the falling cylinder used, i.e.,

1: No. 1 falling cylinder
2: No. 2 falling cylinder
3: No. 3 falling cylinder

the second sub-code indicates the fluid being used, i.e.,

M: methane	X1: 22.1 mole% methane mixture
P: propane	X2: 50.0 mole% methane mixture
B: n-butane	X3: 75.3 mole% methane mixture
H: n-hexane	
O: n-octane	

and the third sub-code indicates the run number of the particular fluid being investigated. For example, run 1B-2 indicates the second run of n-butane series using No. 1 falling cylinder.

The percent errors reported in Appendixes M, P and Q are the errors of the replicated fall time data computed on 98 % confidence using "t" statistics.

Appendix M Viscometer Calibration for Viscosity Determination

Table M-1 Calibration of Viscometer and No. 1 Falling Cylinder

Fluid	RUN NO.	TEMP. °C	PRESS. PSIA.	FALL TIME SEC.	PERCENT ERROR	DENSITY G/CC	VISCOSITY MICRO-POISE	BCALC $X10^4$ CC/SEC^2	EQUI. DIAMETER CM	LOG(N) Re	BPT $X10^4$ CC/SEC^2
CH_4	1M-2	-50.00	880.	2.855	0.35	0.078	108.8	2.281	0.2520	2.908	1.672
		-50.00	1175.	3.618	0.39	0.125	135.3	2.295	0.2520	2.917	1.668
		-50.00	2060.	6.255	0.09	0.234	250.1	2.337	0.2519	2.685	1.854
		-50.00	2350.	6.872	0.19	0.250	273.1	2.352	0.2519	2.635	1.853
	1M-2	-25.00	880.	2.820	0.11	0.059	111.2	2.227	0.2522	2.789	1.720
		-25.00	1175.	3.198	0.13	0.086	123.9	2.240	0.2522	2.849	1.706
		-25.00	1470.	3.692	0.06	0.116	141.4	2.253	0.2522	2.859	1.704
		-25.00	2060.	4.829	0.04	0.173	186.9	2.280	0.2521	2.794	1.757
		-25.00	2350.	5.379	0.10	0.195	208.7	2.295	0.2521	2.751	1.775
	1M-2	0.00	880.	2.947	0.71	0.050	116.7	2.170	0.2524	2.674	1.723
		0.00	1175.	3.207	0.13	0.070	125.4	2.183	0.2524	2.752	1.713
		0.00	1470.	3.524	0.22	0.091	137.0	2.197	0.2524	2.788	1.715
		0.00	2060.	4.245	0.09	0.135	164.1	2.222	0.2523	2.798	1.732
		0.00	2350.	4.658	0.06	0.155	179.5	2.237	0.2523	2.779	1.738
	1M-4	71.11	200.	3.237	0.15	0.008	128.	1.987	0.2529	1.786	1.698
		71.11	600.	3.387	0.15	0.024	133.	2.005	0.2529	2.238	1.692
		71.11	1000.	3.579	0.10	0.041	139.	2.020	0.2528	2.421	1.682
		71.11	3000.	4.842	0.12	0.126	184.	2.105	0.2527	2.661	1.701
		71.11	5000.	6.180	0.17	0.190	239.	2.192	0.2526	2.621	1.766
C_3H_8	1P-3	21.11	200.	28.690	0.08	0.500	1010.	2.092	0.2526	1.749	1.807
		21.11	1000.	31.090	0.03	0.511	1125.	2.128	0.2526	1.676	1.866
		21.11	3000.	35.960	0.06	0.538	1351.	2.216	0.2524	1.556	1.958
		21.11	5000.	39.820	0.15	0.553	1538.	2.305	0.2523	1.467	2.025
	1P-2	37.78	300.	24.660	0.13	0.475	863.0	2.058	0.2528	1.861	1.779
		37.78	1000.	27.000	0.16	0.490	956.0	2.092	0.2528	1.791	1.811
		37.78	3000.	32.220	0.09	0.520	1176.	2.180	0.2526	1.650	1.889
		37.78	5000.	36.060	0.17	0.541	1367.	2.268	0.2525	1.552	1.978
	1P-2	54.44	300.	20.290	0.30	0.449	710.0	2.022	0.2530	2.006	1.761
		54.44	1000.	23.230	0.13	0.465	814.0	2.055	0.2529	1.903	1.775
		54.44	3000.	28.770	0.09	0.502	1037.	2.142	0.2528	1.738	1.853
		54.44	5000.	32.700	0.19	0.525	1220.	2.228	0.2527	1.632	1.935

Table M-1 (Continued)

Fluid	RUN NO.	TEMP. °C	PRESS. PSIA.	FALL TIME SEC.	PERCENT ERROR	DENSITY G/CC	VISCOSITY MICRO-POISE	BCALC X10^4 CC/SEC^2	EQUI. DIAMETER CM	LOG(N_{Re})	BPT X10^4 CC/SEC^2
C_3H_8	1P-2	71.11	400.	16.420	0.13	0.403	562.0	1.987	0.2529	2.153	1.693
		71.11	1000.	19.800	0.30	0.434	682.0	2.020	0.2528	2.020	1.724
		71.11	3000.	25.840	0.11	0.483	922.0	2.105	0.2527	1.819	1.821
		71.11	5000.	29.850	0.07	0.509	1102.	2.192	0.2526	1.702	1.903
	1P-2	87.78	200.	2.679	0.21	0.023	102.0	1.952	0.2532	2.446	1.643
		87.77	600.	13.13	0.44	0.361	454.	1.968	0.2532	2.292	1.682
		87.78	1000.	16.400	0.05	0.400	560.0	1.985	0.2532	2.152	1.687
		87.78	3000.	23.230	0.14	0.463	815.0	2.069	0.2531	1.902	1.776
		87.78	5000.	27.310	0.18	0.494	996.0	2.154	0.2529	1.772	1.869
nC_4H_{10}	1B-1	37.78	200.	41.430	0.08	0.560	1430.	2.058	0.2528	1.488	1.815
		37.78	1000.	44.070	0.14	0.571	1540.	2.092	0.2528	1.437	1.846
		37.78	3000.	49.880	0.27	0.591	1795.	2.180	0.2526	1.331	1.917
		37.78	5000.	54.780	0.05	0.605	2035.	2.268	0.2525	1.246	1.991
	1B-1	54.44	1000.	38.940	0.22	0.552	1335.	2.055	0.2529	1.538	1.798
		54.44	3000.	44.700	0.08	0.575	1590.	2.142	0.2528	1.420	1.883
		54.44	5000.	49.380	0.19	0.592	1820.	2.228	0.2527	1.331	1.965
	1B-1	71.11	1000.	34.320	0.23	0.532	1160.	2.020	0.2528	1.638	1.758
		71.11	3000.	40.300	0.19	0.559	1412.	2.105	0.2527	1.505	1.843
		71.11	5000.	45.040	0.19	0.578	1632.	2.192	0.2526	1.407	1.921
	1B-1	87.78	1000.	30.290	0.21	0.511	1005.	1.985	0.2532	1.738	1.712
		87.78	3000.	36.490	0.21	0.543	1260.	2.069	0.2531	1.585	1.805
		87.78	5000.	41.180	0.13	0.564	1480.	2.154	0.2529	1.479	1.895
nC_6H_{14}	1H-1	30.00	15.	85.02	0.13	0.650	2854.	2.064	0.2527	0.940	1.833
		50.00	15.	71.44	0.06	0.632	2411.	2.021	0.2529	1.077	1.828
		70.00	15.	61.27	0.21	0.610	2050.	1.979	0.2531	1.198	1.800

Table M-2 Calibration of Viscometer and No. 2 Falling Cylinder

Fluid	RUN NO.	TEMP. °C	PRESS. PSIA.	FALL TIME SEC.	PERCENT ERROR	DENSITY G/CC	VISCOSITY MICRO-POISE	BCALC $X10^{4}$ CC/SEC^2	EQUI. DIAMETER CM	LOG(N_{Re})	BPT $X10^{4}$ CC/SEC^2
CH_4	2M-1	-50.00	880.	2.951	0.64	0.078	108.8	2.174	0.2522	2.892	1.615
		-50.00	1175.	3.715	0.08	0.125	135.3	2.188	0.2522	2.904	1.621
		-50.00	2060.	6.481	0.26	0.234	250.1	2.228	0.2521	2.668	1.786
		-50.00	2350.	7.080	0.11	0.250	273.1	2.240	0.2521	2.620	1.795
	2M-1	-25.00	880.	2.959	0.65	0.059	111.2	2.121	0.2524	2.767	1.636
		-25.00	1175.	3.332	0.36	0.086	123.9	2.133	0.2524	2.830	1.634
		-25.00	1470.	3.944	0.13	0.116	141.4	2.146	0.2524	2.840	1.633
		-25.00	2060.	4.997	0.19	0.173	186.9	2.171	0.2524	2.778	1.694
		-25.00	2350.	5.537	0.14	0.195	208.7	2.182	0.2524	2.737	1.721
	2M-1	0.00	880.	3.064	0.15	0.050	116.7	2.065	0.2526	2.655	1.654
		0.00	1175.	3.332	0.16	0.070	125.4	2.078	0.2526	2.734	1.645
		0.00	1470.	3.654	0.25	0.091	137.0	2.091	0.2526	2.771	1.651
		0.00	2060.	4.402	0.26	0.135	164.1	2.117	0.2525	2.781	1.667
		0.00	2350.	4.800	0.34	0.155	179.5	2.129	0.2525	2.765	1.684
	2M-2	37.78	1000.	3.520	0.30	0.047	130.	1.992	0.2530	2.525	1.607
		37.78	1500.	3.883	0.18	0.073	142.	2.035	0.2529	2.635	1.605
		37.78	3000.	5.234	0.13	0.150	193.	2.076	0.2528	2.691	1.662
		37.78	5000.	6.970	0.40	0.218	261.	2.162	0.2527	2.591	1.729
C_3H_8	2P-1	21.11	300.	30.740	0.49	0.500	1025.	1.992	0.2528	1.711	1.709
		21.11	1000.	32.830	0.14	0.511	1125.	2.025	0.2528	1.651	1.764
		21.11	3000.	37.730	0.27	0.538	1351.	2.110	0.2527	1.534	1.863
		21.11	5000.	41.560	0.25	0.553	1538.	2.199	0.2525	1.447	1.938
	2P-1	37.78	200.	25.490	0.19	0.473	848.0	1.960	0.2530	1.851	1.687
		37.78	1000.	28.400	0.07	0.490	956.0	1.992	0.2530	1.768	1.719
		37.78	3000.	33.570	0.27	0.520	1176.	2.076	0.2528	1.630	1.810
		37.78	5000.	37.490	0.39	0.541	1367.	2.162	0.2527	1.533	1.900
	2P-1	54.44	200.	2.562	0.27	0.028	93.0	1.925	0.2532	2.577	1.565
		54.44	1000.	24.620	0.22	0.465	814.0	1.956	0.2531	1.876	1.672
		54.44	3000.	30.220	0.28	0.502	1037.	2.038	0.2530	1.716	1.761
		54.44	5000.	34.140	0.28	0.525	1220.	2.125	0.2529	1.611	1.851

Table M-2 (Continued)

Fluid	RUN NO.	TEMP. °C	PRESS. PSIA.	FALL TIME SEC.	PERCENT ERROR	DENSITY G/CC	VISCOSITY MICRO-POISE	BCALC X10^4 CC/SEC^2	EQUI. DIAMETER CM	LOG(N_{Re})	BPT X10^4 CC/SEC^2
C_3H_8	2P-1	71.11	200.	2.715	0.19	0.025	98.0	1.891	0.2533	2.488	1.556
		71.11	1000.	21.000	0.49	0.434	682.0	1.921	0.2532	1.993	1.623
		71.11	3000.	27.180	0.16	0.483	922.0	2.002	0.2531	1.796	1.728
		71.11	5000.	31.190	0.25	0.509	1102.	2.088	0.2529	1.682	1.819
	2P-1	87.78	200.	2.890	0.23	0.023	102.0	1.857	0.2534	2.411	1.520
		87.78	1000.	17.330	0.11	0.400	560.0	1.887	0.2534	2.126	1.594
		87.78	3000.	24.480	0.27	0.463	815.0	1.968	0.2533	1.877	1.683
		87.78	5000.	28.670	0.28	0.494	996.0	2.052	0.2531	1.749	1.778
nC_4H_{10}	2B-1	37.78	200.	44.410	0.10	0.560	1430.	1.960	0.2530	1.456	1.691
		37.78	1000.	47.280	0.18	0.571	1540.	1.992	0.2530	1.405	1.718
		37.78	3000.	53.050	0.16	0.591	1795.	2.076	0.2528	1.303	1.800
		37.78	5000.	57.950	0.74	0.605	2035.	2.162	0.2527	1.220	1.879
	2B-1	54.44	1000.	41.560	0.26	0.552	1335.	1.956	0.2531	1.509	1.682
		54.44	3000.	47.320	0.36	0.575	1590.	2.038	0.2530	1.394	1.776
		54.44	5000.	51.980	0.27	0.592	1820.	2.125	0.2529	1.307	1.864
	2B-1	71.11	1000.	36.660	0.48	0.532	1160.	1.921	0.2532	1.608	1.644
		71.11	3000.	42.690	0.09	0.559	1412.	2.002	0.2531	1.479	1.738
		71.11	5000.	47.220	0.15	0.578	1632.	2.088	0.2529	1.386	1.829
	2B-1	87.78	1000.	32.400	0.40	0.511	1005.	1.887	0.2534	1.707	1.598
		87.78	3000.	38.700	0.19	0.543	1260.	1.968	0.2533	1.558	1.699
		87.78	5000.	43.300	0.12	0.564	1480.	2.052	0.2531	1.456	1.799
nC_8H_{18}	2O-1	40.00	15.	139.58	0.45	0.687	4368.	1.945	0.2530	0.563	1.738
		60.00	15.	115.49	0.09	0.670	3587.	1.904	0.2532	0.721	1.713
		80.00	15.	97.40	0.07	0.653	3004.	1.863	0.2534	0.860	1.688

Table M-3 Calibration of Viscometer and No. 3 Falling Cylinder

Fluid	RUN NO.	TEMP. °C	PRESS. PSIA.	FALL TIME SEC.	PERCENT ERROR	DENSITY G/CC	VISCOSITY MICRO-POISE	BCALC $X10^{4}$ CC/SEC^2	EQUI. DIAMETER CM	LOG(N$_{Re}$)	BPT $X10^{4}$ CC/SEC^2
CH_4	3M-1	-50.00	880.	4.225	0.24	0.078	108.8	1.388	0.2540	2.741	1.130
		-50.00	1175.	5.357	0.27	0.125	135.3	1.399	0.2540	2.750	1.126
		-50.00	2060.	9.238	0.32	0.234	250.1	1.428	0.2539	2.519	1.255
		-50.00	2350.	10.090	0.19	0.250	273.1	1.438	0.2539	2.471	1.262
	3M-1	-25.00	880.	4.245	0.44	0.059	111.2	1.347	0.2543	2.615	1.142
		-25.00	1175.	4.812	1.35	0.086	123.9	1.357	0.2543	2.676	1.133
		-25.00	1470.	5.592	0.22	0.116	141.4	1.367	0.2543	2.683	1.125
		-25.00	2060.	7.261	0.25	0.173	186.9	1.386	0.2542	2.621	1.168
		-25.00	2350.	8.035	0.46	0.195	208.7	1.396	0.2542	2.580	1.187
	3M-1	0.00	880.	4.438	0.76	0.050	116.7	1.303	0.2545	2.500	1.144
		0.00	1175.	4.842	0.20	0.070	125.4	1.312	0.2545	2.577	1.134
		0.00	1470.	5.321	0.75	0.091	137.0	1.322	0.2545	2.613	1.136
		0.00	2060.	6.430	0.52	0.135	164.1	1.343	0.2544	2.622	1.143
		0.00	2350.	6.995	0.27	0.155	179.5	1.352	0.2544	2.606	1.157
C_3H_8	3P-2	21.11	200.	44.450	0.23	0.500	1010.	1.252	0.2547	1.562	1.166
		21.11	1000.	48.060	0.24	0.511	1125.	1.275	0.2546	1.491	1.206
		21.11	3000.	54.780	0.28	0.538	1351.	1.339	0.2545	1.377	1.285
		21.11	5000.	59.630	0.21	0.553	1538.	1.402	0.2544	1.295	1.352
	3P-2	37.78	200.	37.490	0.36	0.473	848.0	1.228	0.2549	1.688	1.148
		37.78	1000.	41.710	0.25	0.490	956.0	1.250	0.2548	1.606	1.172
		37.78	3000.	48.870	0.35	0.520	1176.	1.312	0.2547	1.472	1.245
		37.78	5000.	53.960	0.22	0.541	1367.	1.377	0.2545	1.380	1.321
	3P-1	54.44	200.	3.758	0.53	0.028	93.0	1.200	0.2550	2.415	1.069
		54.44	1000.	35.830	0.37	0.465	814.0	1.224	0.2550	1.719	1.150
		54.44	3000.	43.630	0.26	0.502	1037.	1.287	0.2549	1.561	1.221
		54.44	5000.	48.940	0.40	0.525	1220.	1.349	0.2547	1.460	1.293

Table M-3 (Continued)

Fluid	RUN NO.	TEMP. °C	PRESS. PSIA.	FALL TIME SEC.	PERCENT ERROR	DENSITY G/CC	VISCOSITY MICRO-POISE	BCALC X10^4 CC/SEC^2	EQUI. DIAMETER CM	LOG(N$_{Re}$)	BPT X10^4 CC/SEC^2
C_3H_8	3P-1	71.11	200.	3.977	0.39	0.025	98.0	1.175	0.2551	2.327	1.064
		71.11	1000.	30.440	0.69	0.434	682.0	1.198	0.2551	1.837	1.121
		71.11	3000.	39.080	0.23	0.483	922.0	1.259	0.2549	1.644	1.203
		71.11	5000.	44.630	0.61	0.509	1102.	1.321	0.2548	1.531	1.272
	3P-1	87.78	200.	4.224	0.22	0.023	102.0	1.150	0.2553	2.252	1.042
		87.78	1000.	25.470	0.75	0.400	560.0	1.172	0.2552	1.964	1.086
		87.78	3000.	35.200	0.25	0.463	815.0	1.232	0.2551	1.725	1.172
		87.78	5000.	40.960	0.13	0.494	996.0	1.294	0.2550	1.599	1.246
nC_4H_{10}	3B-1	37.78	200.	64.840	0.39	0.560	1430.	1.228	0.2549	1.297	1.159
		37.78	1000.	68.490	0.32	0.571	1540.	1.250	0.2548	1.249	1.187
		37.78	3000.	76.260	0.24	0.591	1795.	1.312	0.2547	1.150	1.253
		37.78	5000.	82.050	0.92	0.605	2035.	1.377	0.2545	1.074	1.328
	3B-1	54.44	1000.	60.550	0.65	0.552	1335.	1.224	0.2550	1.350	1.156
		54.44	3000.	68.530	0.71	0.575	1590.	1.287	0.2549	1.238	1.228
		54.44	5000.	74.480	0.23	0.592	1820.	1.349	0.2547	1.156	1.302
	3B-2	71.11	1000.	53.600	0.35	0.532	1160.	1.198	0.2551	1.448	1.125
		71.11	3000.	61.870	0.35	0.559	1412.	1.259	0.2549	1.322	1.200
		71.11	5000.	67.950	0.72	0.578	1632.	1.321	0.2548	1.233	1.273
	3B-2	87.78	1000.	47.410	0.40	0.511	1005.	1.172	0.2552	1.547	1.093
		87.78	3000.	56.260	0.23	0.543	1260.	1.232	0.2551	1.401	1.170
		87.78	5000.	62.330	0.19	0.564	1480.	1.294	0.2550	1.302	1.251

Appendix N

Experimental Density Data for Methane and Propane

Table N-1 Density of Gaseous Methane Determined with No. 1 Falling Cylinder in Viscometer Tube

Volume of viscometer tube and No. 1 falling cylinder at 23°C. = 12.024cc.
Temperature coefficient of viscometer volume = $4.87 \times 10^{-5} (°C.)^{-1}$
Mass injection cylinders used : MIC-K and MIC-L.
Reference density used : Sage and Lacey(66).

Run No.	Temp. °C.	Press. psia	Reference Temp. °F.	Reference Press. psia	Difference in Height in.	Density g/cc.
1M-8	-80	200	74.0	400	9.581	0.016
	-80	400	74.0	600	8.582	0.038
	-80	600	74.0	600	12.498	0.070
1M-9	-80	800	74.0	1000	2.684	0.228
	-80	1000	74.0	1000	0.282	0.252
1M-10	-100	100	78.0	100	22.633	0.009
	-100	200	78.0	200	11.088	0.018
	-100	300	78.0	300	10.592	0.031
	-100	378	78.0	400	8.518	0.045
1M-6	-120	100	75.0	100	10.968	0.009
1M-10	-120	160	78.0	200	21.037	0.017
1M-10	-140	70	77.0	100	17.393	0.007

Note: MIC-K was used in run 1M-9; while all the other runs were conducted with MIC-L.

Table N-2

Density of Liquid Propane Determined with
No. 1 Falling Cylinder in Viscometer Tube

Volume of viscometer tube and No. 1 falling cylinder at 23°C. = 12.024cc.
Temperature coefficient of viscometer volume = $4.87 \times 10^{-5}(°C.)^{-1}$
Mass injection cylinder used : MIC-G.
Reference density used : Sage and Lacey(66).

Run No.	Temp. °C.	Press. psia	Reference Temp. °F.	Reference Press. psia	Difference in Height in.	Density g/cc.
1P-4	-20	150	75.0	1500	10.211	0.557
	-20	1000	73.0	1500	0.611	0.565
	-20	2000	72.0	1500	0.176	0.575
	-20	3000	72.0	1500	0.141	0.583
	-20	4000	72.0	1500	0.145	0.591
	-20	5000	77.5	1500	0.117	0.597
1P-5	-40	150	74.0	1500	10.582	0.580
	-40	1000	74.0	1500	0.134	0.587
	-40	3000	73.5	3500	0.244	0.601
	-40	4000	73.0	3500	0.118	0.607
	-40	5000	73.5	3500	0.117	0.614
	-40	2000	73.5	3500	-0.434	0.593
	-60	150	73.0	1500	0.381	0.601
	-60	1000	73.0	1500	0.100	0.606
	-60	2000	72.5	1500	0.116	0.613
	-60	3000	72.5	3500	0.115	0.620
	-60	4000	72.5	3500	0.105	0.625
	-60	5000	72.5	3500	0.108	0.631
1P-10	-80	150	78.0	1500	11.409	0.627
	-80	1000	80.0	1500	0.088	0.632
	-80	2000	80.0	2000	0.097	0.637
	-80	3000	80.5	3000	0.085	0.642
	-80	4000	80.5	4000	0.083	0.647
	-80	5000	81.0	5000	0.077	0.651

Appendix O

Experimental Density Data for Mixtures

Table O-1 Density of Mixtures Determined with No. 1 DPI and No. 2 Falling Cylinder in Viscometer Tube

Volume of viscometer tube, No. 2 falling cylinder and No. 1 DPI at 37.8°C. = 12.646cc.
Temperature coefficient of viscometer volume = $5.35 \times 10^{-5} (°C.)^{-1}$
Mass injection cylinder used : MIC-L.
Reference density used : Sage and Lacey(66).
HTB was controlled at 37.8°C.

Run No.	Temp. °C.	Press. psia	Reference Press. psia	Difference in Height in.	Density g/cc.
2X2-4	0	1390	1500	14.258	0.358
	0	2000	2000	1.488	0.400
	0	3000	3000	0.869	0.427
	0	4000	4000	0.483	0.444
	0	5000	5000	0.365	0.457
2X3-1	0	1620	2000	14.483	0.235
	0	1760	2000	1.063	0.252
	0	2000	2000	1.498	0.277
	-40	1300	2000	19.799	0.322
	-40	1550	2000	1.604	0.348
	-40	2000	2000	1.289	0.369
	-40	3000	3000	1.076	0.393
	-40	4000	4000	0.618	0.409
	-40	5000	5000	0.450	0.421
	-80	910	2000	0.000	0.422
	-80	1430	2000	0.545	0.431
	-80	2000	2000	0.483	0.439
	-80	3000	3000	0.504	0.450

Table O-2

Density of Mixtures Determined with No. 2 DPI and No. 2 Falling Cylinder in Viscometer Tube

Volume of viscometer tube, No. 2 falling cylinder and No. 2 DPI at 37.8°C. = 12.687cc.
Temperature coefficient of viscometer volume = $7.88 \times 10^{-5} (°C.)^{-1}$
Mass injection cylinder used ; MIC-L.
HTB was controlled at 37.8°C.
Reference density used : Sage and Lacey(66).

Run No.	Temp. °C.	Press. psia	Reference Press. psia	Difference in Height in.	Density g/cc.
2X3-2	37.78	1025	2000	5.181	0.084
	37.78	2000	2000	6.898	0.195
	37.78	3000	3000	3.169	0.265
	37.78	4000	4000	1.546	0.304
	37.78	5000	5000	0.955	0.330
	0	3030	--	0.000	0.331
	0	4000	4000	0.988	0.356
	0	5000	5000	0.689	0.375
2X3-5	0	2000	2000	17.162	0.278
	-80	800	2000	8.497	0.418
	-80	2000	2000	1.253	0.439
	-120	340	2000	2.512	0.481
	-120	1095	2000	0.428	0.488
	-120	2000	2000	0.420	0.495
	-120	3000	3000	0.289	0.501
	-120	4000	4000	0.227	0.507
	-120	5000	5000	0.192	0.513
	-150	280	2000	0.519	0.522
	-150	1320	2000	0.382	0.528
	-150	2000	2000	0.223	0.532
	-150	3000	3000	0.215	0.537
	-150	4000	4000	0.193	0.542
	-150	5000	5000	0.150	0.546
2X3-7	-60	1270	2000	23.604	0.384
	-60	2000	2000	1.306	0.405
	-60	3000	3000	0.754	0.422
	-60	4000	4000	0.488	0.434
	-60	5000	5000	0.367	0.444

Table O-2 (Continued)

Run No.	Temp. °C.	Press. psia	Reference Press. psia	Difference in Height in.	Density g/cc.
2X1-1	0	1180	1500	12.800	0.469
	0	2000	2000	0.719	0.497
	0	3000	3000	0.343	0.510
	0	4000	4000	0.263	0.521
	0	5000	5000	0.206	0.529
	-60	980	2000	0.797	0.562
	-60	2000	2000	0.197	0.569
	-60	3000	3000	0.165	0.576
	-60	4000	4000	0.152	0.582
	-60	5000	5000	0.140	0.588
	-100	180	2000	0.000	0.590
	-100	590	2000	0.416	0.606
	-100	2000	2000	0.312	0.617
	-100	3000	3000	0.120	0.622
	-100	4000	4000	0.107	0.626
	-100	5000	5000	0.100	0.631
2X1-2	-40	1000	2000	13.977	0.530
	-40	2000	2000	0.459	0.548
	-40	3000	3000	0.216	0.556
	-40	4000	4000	0.176	0.563
	-40	5000	5000	0.156	0.570
	-80	345	2000	0.000	0.572
	-80	1000	2000	0.400	0.587
	-80	2000	2000	0.153	0.593
	-80	3000	3000	0.139	0.598
	-80	4000	4000	0.124	0.603
	-80	5000	5000	0.152	0.609
	-120	295	2000	0.417	0.627
	-120	1350	2000	0.136	0.632
	-120	2000	2000	0.068	0.635
	-120	3000	3000	0.096	0.639

Table O-2 (Continued)

Run No.	Temp. °C.	Press. psia	Reference Press. psia	Difference in Height in.	Density g/cc.
2X2-5	0	1340	2000	12.400	0.352
	0	2000	2000	1.592	0.397
	0	3000	3000	0.898	0.425
	0	4000	4000	0.497	0.442
	0	5000	5000	0.367	0.455
	-60	910	2000	0.655	0.476
	-60	1500	2000	0.454	0.489
	-60	2000	2000	0.197	0.494
	-60	3000	3000	0.301	0.504
	-60	4000	4000	0.244	0.512
	-60	5000	5000	0.205	0.519
	-100	290	2000	0.000	0.522
	-100	910	2000	0.538	0.537
	-100	2000	2000	0.267	0.545
	-100	3000	3000	0.185	0.551
	-100	4000	4000	0.162	0.556
	-100	5000	5000	0.162	0.562
2X2-6	0	2000	2000	13.991	0.397
	-40	1340	2000	1.818	0.450
	-40	2000	2000	0.553	0.466
	-40	3000	3000	0.422	0.480
	-40	4000	4000	0.299	0.490
	-40	5000	5000	0.259	0.499
	-100	2000	2000	1.502	0.545

Appendix P Experimental Viscosity data for Methane and Propane

Table P-1 Viscosity data of Methane using No.1 Falling Cylinder

RUN NO.	TEMP. °C	PRESS. PSIA.	FALL TIME SEC.	PERCENT ERROR	DENSITY G/CC	BRED	BCALC X10^4 CC/SEC^2	EQUI DIAMETER CM	LOG(N$_{Re}$)	VISCOSITY MICRO-POISE
1M-2	0.00	880.	2.947	0.71	0.050	0.7985	2.170	0.2524	2.671	117.4
	0.00	1175.	3.207	0.13	0.070	0.7792	2.183	0.2524	2.755	124.5
	0.00	1470.	3.524	0.22	0.091	0.7695	2.197	0.2524	2.794	135.0
	0.00	2060.	4.245	0.09	0.135	0.7666	2.222	0.2523	2.806	161.4
	0.00	2350.	4.658	0.06	0.155	0.7726	2.237	0.2523	2.782	178.5
	0.00	3000.	5.497	0.12	0.194	0.7854	2.263	0.2523	2.729	213.6
	0.00	4000.	6.567	0.05	0.232	0.8055	2.308	0.2522	2.639	263.3
	0.00	5000.	7.391	0.35	0.257	0.8195	2.354	0.2521	2.568	304.8
1M-2	-25.00	880.	2.820	0.11	0.059	0.7705	2.227	0.2522	2.790	110.9
	-25.00	1175.	3.198	0.13	0.086	0.7539	2.240	0.2522	2.854	122.7
	-25.00	1470.	3.692	0.06	0.116	0.7516	2.253	0.2522	2.862	140.5
	-25.00	2060.	4.829	0.04	0.173	0.7693	2.280	0.2521	2.795	186.6
	-25.00	2350.	5.379	0.10	0.195	0.7813	2.295	0.2521	2.746	210.9
	-25.00	3000.	6.371	0.09	0.231	0.8005	2.324	0.2521	2.662	255.8
	-25.00	4000.	7.561	0.13	0.265	0.8213	2.370	0.2520	2.558	313.8
	-25.00	5000.	8.468	0.10	0.286	0.8348	2.414	0.2519	2.481	361.1
1M-2	-50.00	880.	2.855	0.35	0.078	0.7400	2.281	0.2520	2.904	109.8
	-50.00	1175.	3.618	0.39	0.125	0.7382	2.295	0.2520	2.910	137.4
	-50.00	2060.	6.255	0.09	0.234	0.7958	2.337	0.2519	2.683	250.9
	-50.00	2350.	6.872	0.19	0.250	0.8086	2.352	0.2519	2.623	280.3
	-50.00	3000.	7.889	0.18	0.274	0.8261	2.382	0.2518	2.532	330.0
	-50.00	4000.	8.971	0.21	0.298	0.8405	2.430	0.2517	2.444	386.1
	-50.00	5000.	9.893	0.19	0.317	0.8430	2.476	0.2517	2.380	432.1
1M-8	-60.00	500.	2.209	0.10	0.038	0.7701	2.288	0.2519	2.792	89.9
	-60.00	800.	2.707	0.12	0.079	0.7222	2.302	0.2519	2.964	102.5
	-60.00	1000.	3.383	0.11	0.122	0.7223	2.311	0.2519	2.964	126.7
	-60.00	1300.	4.995	0.18	0.188	0.7697	2.325	0.2519	2.793	196.0
	-60.00	1600.	6.078	0.08	0.228	0.7926	2.339	0.2519	2.698	243.6

Note: All the methane densities were from the literature(40,78), except for those with * which were determined experimentally.

Table P-1 (Continued)

RUN NO.	TEMP. °C	PRESS. PSIA.	FALL TIME SEC.	PERCENT ERROR	DENSITY G/CC	BRED	BCALC $X10^{4}$ CC/SEC^{2}	EQUI DIAMETER CM	LOG(N$_{Re}$)	VISCOSITY MICRO-POISE
1M-8	-60.00	2000.	7.022	0.17	0.256	0.8106	2.357	0.2518	2.614	287.1
	-60.00	3000.	8.559	0.09	0.292	0.8345	2.404	0.2517	2.483	362.7
	-60.00	4000.	9.665	0.16	0.313	0.8423	2.451	0.2517	2.399	418.2
	-60.00	5000.	10.520	0.07	0.328	0.8446	2.498	0.2516	2.338	462.6
1M-11	-70.00	100.	1.794	0.41	0.006	0.8525	2.293	0.2518	2.135	81.9
	-70.00	300.	1.961	0.25	0.023	0.8030	2.302	0.2518	2.650	84.2
	-70.00	500.	2.194	0.45	0.044	0.7496	2.311	0.2518	2.869	87.6
	-70.00	700.	2.574	0.18	0.075	0.7160	2.321	0.2518	2.985	97.6
	-70.00	900.	3.670	0.41	0.135	0.7326	2.330	0.2518	2.929	140.0
	-70.00	1000.	4.729	0.31	0.180	0.7620	2.334	0.2518	2.823	185.0
	-70.00	2000.	7.971	0.19	0.280	0.8258	2.381	0.2517	2.533	332.6
	-70.00	3000.	9.397	0.11	0.309	0.8414	2.428	0.2516	2.421	403.0
	-70.00	4000.	10.440	0.12	0.327	0.8443	2.475	0.2516	2.347	454.9
	-70.00	5000.	11.310	0.04	0.341	0.8465	2.523	0.2515	2.289	501.1
1M-5	-80.00	200.	1.775	0.51	0.016*	0.8192	2.321	0.2518	2.570	78.6
	-80.00	400.	2.008	0.56	0.038*	0.7467	2.330	0.2518	2.880	80.7
	-80.00	600.	2.457	0.63	0.070*	0.7137	2.339	0.2517	2.992	93.7
	-80.00	800.	5.876	0.15	0.228*	0.7855	2.349	0.2517	2.728	234.5
1M-3	-80.00	1000.	7.015	0.20	0.252*	0.8122	2.358	0.2517	2.606	288.0
	-80.00	1500.	8.266	0.12	0.288	0.8294	2.381	0.2516	2.513	345.4
	-80.00	2000.	9.192	0.07	0.304	0.8408	2.404	0.2516	2.437	390.8
	-80.00	3000.	10.490	0.26	0.326	0.8443	2.452	0.2516	2.346	453.1
	-80.00	4000.	11.520	0.33	0.341	0.8470	2.499	0.2515	2.277	505.8
	-80.00	5000.	12.420	0.40	0.354	0.8492	2.548	0.2514	2.220	554.8
1M-10	-100.00	100.	1.550	0.80	0.009*	0.8422	2.364	0.2516	2.401	72.0
	-100.00	200.	1.660	0.43	0.018*	0.7936	2.368	0.2516	2.693	72.6
	-100.00	300.	1.778	0.46	0.031*	0.7437	2.373	0.2516	2.891	72.7
	-100.00	378.	1.945	0.93	0.045*	0.7137	2.378	0.2516	2.992	76.1
	-100.00	435.	9.157	0.14	0.303	0.8406	2.380	0.2516	2.443	385.6

Table P-1 (Continued)

RUN NO.	TEMP. °C	PRESS. PSIA.	FALL TIME SEC.	PERCENT ERROR	DENSITY G/CC	BRED	BCALC X10⁴ CC/SEC²	EQUI DIAMETER CM	LOG(N)	VISCOSITY MICRO-POISE
1M-5	-100.00	1000.	10.320	0.11	0.324	0.8436	2.406	0.2515	2.365	437.4
	-100.00	2000.	11.880	0.13	0.345	0.8475	2.453	0.2515	2.263	511.7
	-100.00	3000.	13.020	0.12	0.359	0.8502	2.500	0.2514	2.193	570.4
	-100.00	4000.	14.050	0.49	0.370	0.8526	2.549	0.2513	2.132	626.7
	-100.00	5000.	14.880	0.00	0.378	0.8545	2.598	0.2513	2.084	675.9
1M-6	-120.00	100.	1.387	0.70	0.009*	0.8310	2.411	0.2514	2.504	64.9
	-120.00	160.	1.464	0.00	0.017*	0.7737	2.415	0.2514	2.777	63.7
	-120.00	300.	12.840	0.42	0.355	0.8494	2.421	0.2514	2.214	545.2
	-120.00	1000.	13.940	0.16	0.366	0.8519	2.454	0.2514	2.151	599.2
	-120.00	2000.	15.220	0.16	0.378	0.8546	2.502	0.2513	2.080	666.1
	-120.00	3000.	16.330	0.16	0.387	0.8569	2.550	0.2512	2.021	727.8
	-120.00	4000.	17.320	0.12	0.395	0.8588	2.599	0.2512	1.971	786.2
	-120.00	5000.	18.290	0.17	0.400	0.8608	2.649	0.2511	1.921	846.5
1M-7	-140.00	70.	1.223	0.67	0.007*	0.8318	2.460	0.2512	2.499	58.5
	-140.00	130.	17.780	0.43	0.390	0.8591	2.463	0.2512	1.965	766.7
	-140.00	420.	18.440	0.47	0.393	0.8602	2.476	0.2512	1.934	799.5
	-140.00	1000.	19.120	0.06	0.398	0.8614	2.503	0.2512	1.904	837.6
	-140.00	2000.	20.590	0.27	0.406	0.8639	2.551	0.2511	1.840	919.1
	-140.00	3000.	21.840	0.30	0.412	0.8660	2.600	0.2510	1.786	993.7
	-140.00	4000.	22.700	0.43	0.419	0.8673	2.650	0.2510	1.752	1051.
	-140.00	5000.	24.070	0.19	0.424	0.8694	2.700	0.2509	1.698	1136.
1M-14	-150.00	100.	21.470	0.09	0.405	0.8651	2.509	0.2511	1.809	944.4
	-150.00	1000.	22.860	0.37	0.413	0.8672	2.552	0.2510	1.755	1022.
	-150.00	2000.	24.370	0.06	0.419	0.8694	2.601	0.2509	1.698	1111.
	-150.00	3000.	25.780	0.22	0.424	0.8714	2.651	0.2509	1.645	1198.
	-150.00	4000.	27.140	0.18	0.430	0.8732	2.701	0.2508	1.599	1285.
	-150.00	5000.	28.470	0.20	0.435	0.8750	2.752	0.2507	1.554	1373.

Table P-1 (Continued)

RUN NO.	TEMP. °C	PRESS. PSIA.	FALL TIME SEC.	PERCENT ERROR	DENSITY G/CC	BRED	BCALC X10⁴ CC/SEC²	EQUI DIAMETER CM	LOG(N$_{Re}$)	VISCOSITY MICRO-POISE
1M-12	-160.00	100.	25.990	0.87	0.421	0.8709	2.509	0.2511	1.659	1144.
	-160.00	1000.	27.490	1.12	0.427	0.8728	2.552	0.2510	1.609	1231.
	-160.00	2000.	29.170	1.02	0.432	0.8750	2.601	0.2509	1.554	1332.
	-160.00	3000.	30.370	0.16	0.436	0.8765	2.651	0.2509	1.515	1413.
	-160.00	4000.	32.000	0.61	0.441	0.8784	2.701	0.2508	1.466	1517.
	-160.00	5000.	33.540	0.56	0.446	0.8801	2.752	0.2507	1.422	1621.
1M-13	-170.00	30.	32.390	0.47	0.436	0.8779	2.530	0.2510	1.478	1441.
	-170.00	100.	32.760	0.77	0.437	0.8783	2.533	0.2510	1.469	1459.
	-170.00	1000.	34.540	0.85	0.441	0.8802	2.577	0.2509	1.419	1566.
	-170.00	2000.	36.410	0.56	0.445	0.8821	2.627	0.2508	1.368	1684.
	-170.00	3000.	38.260	0.41	0.448	0.8840	2.677	0.2508	1.320	1805.
	-170.00	4000.	40.180	0.17	0.452	0.8859	2.727	0.2507	1.273	1932.
	-170.00	5000.	42.160	0.37	0.457	0.8876	2.778	0.2506	1.227	2065.

Table P-2 Viscosity Data of Propane Using No. 1 Falling Cylinder

1P-3	0.00	160.	35.240	0.16	0.529	0.8738	2.137	0.2525	1.585	1267.
	0.00	1000.	37.600	0.11	0.540	0.8759	2.174	0.2524	1.531	1373.
	0.00	2000.	40.160	0.18	0.551	0.8780	2.218	0.2523	1.474	1493.
	0.00	3000.	42.420	0.38	0.561	0.8799	2.263	0.2523	1.427	1606.
	0.00	4000.	44.330	0.12	0.569	0.8814	2.308	0.2522	1.387	1709.
	0.00	5000.	46.140	0.11	0.576	0.8829	2.354	0.2521	1.349	1812.
1P-4	-20.00	150.	42.500	0.13	0.555	0.8796	2.181	0.2523	1.435	1554.
	-20.00	1000.	44.880	0.17	0.564	0.8814	2.219	0.2522	1.388	1667.
	-20.00	2000.	47.440	0.23	0.573	0.8833	2.264	0.2522	1.339	1795.
	-20.00	3000.	49.500	0.09	0.582	0.8848	2.309	0.2521	1.301	1907.
	-20.00	4000.	51.570	0.29	0.589	0.8863	2.355	0.2520	1.262	2023.
	-20.00	5000.	53.630	0.07	0.595	0.8877	2.402	0.2520	1.224	2145.

Table P-2 (Continued)

RUN NO.	TEMP. °C	PRESS. PSIA.	FALL TIME SEC.	PERCENT ERROR	DENSITY G/CC	BRED	BCALC X10^{6} CC/SEC^{2}	EQUI DIAMETER CM	LOG(N$_{Re}$)	VISCOSITY MICRO-POISE
1P-5	-40.00	150.	52.130	0.15	0.578	0.8861	2.226	0.2521	1.267	1942.
	-40.00	1000.	54.570	0.11	0.587	0.8876	2.265	0.2521	1.227	2065.
	-40.00	2000.	57.220	0.18	0.594	0.8893	2.310	0.2520	1.183	2206.
	-40.00	3000.	59.400	0.18	0.602	0.8907	2.356	0.2519	1.148	2331.
	-40.00	4000.	61.600	0.16	0.608	0.8920	2.403	0.2519	1.113	2464.
	-40.00	5000.	63.700	0.11	0.613	0.8933	2.450	0.2518	1.079	2596.
1P-5	-60.00	150.	64.890	0.30	0.602	0.8931	2.272	0.2519	1.086	2463.
	-60.00	1000.	67.210	0.06	0.608	0.8944	2.311	0.2519	1.053	2592.
	-60.00	2000.	70.000	0.11	0.616	0.8958	2.357	0.2518	1.015	2749.
	-60.00	3000.	72.720	0.12	0.622	0.8973	2.404	0.2517	0.978	2910.
	-60.00	4000.	75.130	0.08	0.627	0.8985	2.451	0.2517	0.945	3063.
	-60.00	5000.	77.430	0.13	0.632	0.8997	2.498	0.2516	0.914	3215.
1P-11	-80.00	170.	81.780	0.43	0.624	0.9006	2.320	0.2518	0.892	3168.
	-80.00	1000.	84.240	0.25	0.630	0.9017	2.358	0.2517	0.863	3313.
	-80.00	2000.	87.270	0.29	0.636	0.9030	2.404	0.2516	0.829	3495.
	-80.00	3000.	90.300	0.24	0.641	0.9044	2.452	0.2516	0.794	3686.
	-80.00	4000.	93.240	0.42	0.645	0.9057	2.499	0.2515	0.761	3878.
	-80.00	5000.	95.930	0.16	0.651	0.9068	2.548	0.2514	0.732	4063.
1P-11	-100.00	160.	108.700	0.40	0.646	0.9100	2.366	0.2516	0.650	4300.
	-100.00	1000.	112.440	0.70	0.651	0.9112	2.406	0.2515	0.617	4520.
	-100.00	2000.	116.500	0.56	0.655	0.9126	2.453	0.2515	0.580	4774.
	-100.00	3000.	119.910	0.03	0.660	0.9138	2.500	0.2514	0.550	5004.
	-100.00	4000.	123.880	0.05	0.663	0.9152	2.549	0.2513	0.515	5272.
	-100.00	5000.	127.800	0.12	0.669	0.9163	2.598	0.2513	0.484	5536.

Table P-3 Viscosity Data of Methane and Propane Using No. 2 Falling Cylinder

RUN NO.	TEMP. °C	PRESS. PSIA.	FALL TIME SEC.	PERCENT ERROR	DENSITY G/CC	BRED	BCALC $X10^4$ CC/SEC^2	EQUI DIAMETER CM	LOG(N) $_{Re}$	VISCOSITY MICRO-POISE
2M-1	0.00	880.	3.064	0.15	0.050	0.8021	2.065	0.2526	2.655	116.9
	0.00	1175.	3.332	0.16	0.070	0.7872	2.078	0.2526	2.736	124.7
	0.00	1470.	3.654	0.25	0.091	0.7785	2.091	0.2526	2.777	135.1
	0.00	2060.	4.402	0.26	0.135	0.7761	2.117	0.2525	2.787	161.8
	0.00	2350.	4.800	0.34	0.155	0.7799	2.129	0.2525	2.771	177.0
	0.00	3000.	5.649	0.45	0.194	0.7903	2.158	0.2525	2.721	211.1
	0.00	4000.	6.767	0.22	0.232	0.8059	2.202	0.2524	2.630	259.5
	0.00	5000.	7.644	0.25	0.257	0.8151	2.246	0.2523	2.559	299.7
2M-1	-25.00	880.	2.959	0.65	0.059	0.7821	2.121	0.2524	2.761	112.7
	-25.00	1175.	3.332	0.36	0.086	0.7657	2.133	0.2524	2.830	123.8
	-25.00	1470.	3.844	0.13	0.116	0.7635	2.146	0.2524	2.839	141.8
	-25.00	2060.	4.997	0.19	0.173	0.7779	2.171	0.2524	2.780	186.3
	-25.00	2350.	5.537	0.14	0.195	0.7869	2.182	0.2524	2.738	208.3
	-25.00	3000.	6.543	0.64	0.231	0.8017	2.212	0.2523	2.658	250.9
	-25.00	4000.	7.684	0.32	0.265	0.8141	2.256	0.2523	2.568	301.4
	-25.00	5000.	8.599	0.54	0.286	0.8211	2.301	0.2523	2.494	344.4

Table P-3 (Continued)

RUN NO.	TEMP. °C	PRESS. PSIA.	FALL TIME SEC.	PERCENT ERROR	DENSITY G/CC	BRED	BCALC $X10^4$ CC/SEC^2	EQUI DIAMETER CM	LOG(N) $_{Re}$	VISCOSITY MICRO-POISE
2M-1	-50.00	880.	2.951	0.64	0.078	0.7503	2.174	0.2522	2.888	109.9
	-50.00	1175.	3.715	0.08	0.125	0.7466	2.188	0.2522	2.901	136.3
	-50.00	1470.	4.827	0.15	0.170	0.7741	2.201	0.2522	2.796	181.8
	-50.00	2060.	6.481	0.26	0.234	0.7998	2.228	0.2521	2.669	249.6
	-50.00	2350.	7.080	0.11	0.250	0.8078	2.240	0.2521	2.617	275.2
	-50.00	3000.	8.053	0.19	0.274	0.8173	2.271	0.2520	2.537	318.3
	-50.00	4000.	9.195	0.20	0.298	0.8260	2.317	0.2520	2.449	371.5
	-50.00	5000.	10.079	0.31	0.317	0.8287	2.363	0.2520	2.390	413.7
2M-6	-70.00	1000.	5.050	0.36	0.180	0.7790	2.227	0.2520	2.775	193.1
	-70.00	3000.	9.924	0.62	0.309	0.8283	2.317	0.2518	2.399	400.5
	-70.00	5000.	11.920	0.57	0.341	0.8341	2.410	0.2517	2.267	497.9
2M-6	-120.00	1000.	14.720	0.15	0.366	0.8404	2.343	0.2516	2.127	597.0
	-120.00	3000.	17.060	1.07	0.387	0.8458	2.436	0.2514	2.007	718.2
2P-1	-40.00	1000.	58.440	0.43	0.587	0.8822	2.160	0.2523	1.189	2099.
	-40.00	3000.	63.290	0.31	0.602	0.8856	2.248	0.2521	1.114	2360.
	-40.00	5000.	67.540	0.20	0.613	0.8885	2.339	0.2520	1.049	2617.

Table P-4 Viscosity Data of Methane and Propane Using No. 3 Falling Cylinder

RUN NO.	TEMP. °C	PRESS. PSIA.	FALL TIME SEC.	PERCENT ERROR	DENSITY G/CC	BRED	BCALC $X10^{4}$ CC/SEC^{2}	EQUI DIAMETER CM	LOG(N) $_{Re}$	VISCOSITY MICRO-POISE
3M-1	0.00	880.	4.438	0.76	0.050	0.8773	1.303	0.2545	2.500	116.7
	0.00	1175.	4.842	0.21	0.070	0.8590	1.312	0.2545	2.579	124.6
	0.00	1470.	5.321	0.75	0.091	0.8489	1.322	0.2545	2.618	135.4
	0.00	2060.	6.430	0.52	0.135	0.8473	1.343	0.2544	2.624	163.4
	0.00	2350.	6.995	0.27	0.155	0.8514	1.352	0.2544	2.609	178.6
	0.00	3000.	8.165	0.41	0.194	0.8624	1.372	0.2543	2.565	211.3
	0.00	5000.	10.742	0.50	0.257	0.8915	1.438	0.2542	2.424	294.5
3M-1	-25.00	880.	4.245	0.44	0.059	0.8499	1.347	0.2543	2.614	111.4
	-25.00	1175.	4.812	1.35	0.086	0.8316	1.357	0.2543	2.677	123.4
	-25.00	1470.	5.592	0.22	0.116	0.8314	1.367	0.2543	2.678	142.9
	-25.00	2060.	7.261	0.25	0.173	0.8489	1.386	0.2542	2.618	188.3
	-25.00	2350.	8.035	0.46	0.195	0.8599	1.396	0.2542	2.576	211.0
	-25.00	3000.	9.346	0.21	0.231	0.8752	1.414	0.2541	2.510	249.8
	-25.00	5000.	12.189	0.70	0.286	0.9028	1.481	0.2541	2.347	345.0
3M-1	-50.00	880.	4.225	0.24	0.078	0.8104	1.388	0.2540	2.743	108.3
	-50.00	1175.	5.357	0.27	0.125	0.8088	1.399	0.2540	2.748	135.9
	-50.00	1470.	7.010	0.25	0.170	0.8445	1.408	0.2540	2.634	184.0
	-50.00	2060.	9.238	0.32	0.234	0.8725	1.428	0.2539	2.522	248.4
	-50.00	2350.	10.090	0.19	0.250	0.8836	1.438	0.2539	2.468	275.0
	-50.00	3000.	11.500	0.17	0.274	0.8975	1.456	0.2539	2.386	319.6
	-50.00	5000.	14.220	0.24	0.317	0.9110	1.525	0.2538	2.245	413.5

Table P-4 (Continued)

RUN NO.	TEMP. °C	PRESS. PSIA.	FALL TIME SEC.	PERCENT ERROR	DENSITY G/CC	BRED	BCALC X10^4 CC/SEC^2	EQUI DIAMETER CM	LOG(N$_{Re}$)	VISCOSITY MICRO-POISE
3M-2	-80.00	1000.	10.170	0.14	0.252	0.8845	1.441	0.2538	2.463	278.0
	-80.00	3000.	15.310	0.20	0.326	0.9133	1.509	0.2536	2.197	440.4
	-80.00	5000.	17.840	0.12	0.354	0.9189	1.579	0.2535	2.082	534.6
3M-2	-120.00	1000.	20.850	0.12	0.366	0.9239	1.511	0.2534	1.980	598.8
	-120.00	3000.	24.170	0.41	0.387	0.9300	1.581	0.2533	1.856	725.2
	-120.00	5000.	26.640	0.52	0.400	0.9344	1.653	0.2531	1.766	835.5
3P-3	0.00	200.	54.620	0.32	0.529	0.9527	1.283	0.2545	1.392	1287.
	0.00	1000.	57.900	0.29	0.540	0.9551	1.308	0.2545	1.342	1388.
	0.00	3000.	64.280	0.35	0.561	0.9597	1.372	0.2543	1.249	1610.
	0.00	5000.	69.050	0.25	0.576	0.9631	1.438	0.2542	1.179	1808.
3P-4	-40.00	150.	81.100	0.42	0.578	0.9686	1.346	0.2542	1.066	1998.
	-40.00	1000.	84.020	0.30	0.587	0.9701	1.374	0.2541	1.034	2109.
	-40.00	3000.	90.370	0.26	0.602	0.9736	1.439	0.2540	0.963	2369.
	-40.00	5000.	95.880	0.32	0.613	0.9767	1.507	0.2538	0.900	2629.
3P-4	-80.00	1000.	133.860	0.46	0.630	0.9895	1.441	0.2538	0.638	3532.
	-80.00	5000.	149.320	0.62	0.651	0.9954	1.579	0.2535	0.518	4304.

Appendix Q Experimental Viscosity Data for Mixtures

Table Q-1 Viscosity Data of 22.1 mole% CH_4-77.9 mole% C_3H_8 Using No. 2 Falling Cylinder

RUN NO.	TEMP. °C	PRESS. PSIA.	FALL TIME SEC.	PERCENT ERROR	DENSITY G/CC	BRED	BCALC $X10^4$ CC/SEC^2	EQUI DIAMETER CM	LOG(N_{Re})	VISCOSITY MICRO-POISE
2X1-4	37.78	1000.	19.890	0.62	0.421	0.8457	1.992	0.2530	2.008	674.3
	37.78	2000.	22.800	0.12	0.451	0.8500	2.034	0.2529	1.913	784.0
	37.78	3000.	24.960	0.50	0.467	0.8532	2.076	0.2528	1.841	873.8
	37.78	4000.	26.500	0.32	0.482	0.8552	2.118	0.2527	1.796	943.1
	37.78	5000.	28.130	0.39	0.495	0.8573	2.162	0.2527	1.747	1019.
2X1-1	0.00	815.	28.600	0.20	0.477	0.8580	2.064	0.2526	1.733	997.6
	0.00	1180.	29.410	0.22	0.486	0.8588	2.080	0.2526	1.715	1031.
	0.00	2000.	31.200	0.12	0.500	0.8608	2.114	0.2525	1.670	1108.
	0.00	3000.	33.210	0.06	0.512	0.8631	2.158	0.2525	1.618	1201.
	0.00	4000.	35.030	0.10	0.521	0.8652	2.202	0.2524	1.571	1292.
	0.00	5000.	36.630	0.18	0.530	0.8670	2.246	0.2523	1.531	1375.
2X1-3	0.00	2000.	31.290	0.10	0.500	0.8608	2.114	0.2525	1.670	1108.
	-20.00	815.	34.560	0.11	0.506	0.8645	2.108	0.2524	1.586	1227.
	-20.00	2000.	37.140	0.08	0.525	0.8670	2.159	0.2524	1.531	1344.
	-20.00	3000.	39.070	0.11	0.535	0.8689	2.203	0.2523	1.487	1440.
	-20.00	4000.	40.930	0.10	0.542	0.8709	2.247	0.2522	1.444	1537.
	-20.00	5000.	42.530	0.21	0.549	0.8725	2.292	0.2522	1.408	1628.
2X1-2	-40.00	620.	41.410	0.40	0.529	0.8710	2.143	0.2523	1.442	1492.
	-40.00	1005.	42.030	0.24	0.535	0.8714	2.160	0.2523	1.431	1523.
	-40.00	2000.	43.920	0.08	0.548	0.8730	2.204	0.2522	1.396	1619.
	-40.00	3000.	45.950	0.06	0.556	0.8749	2.248	0.2521	1.355	1725.
	-40.00	4000.	47.770	0.06	0.563	0.8765	2.293	0.2521	1.318	1828.
	-40.00	5000.	50.460	0.16	0.569	0.8788	2.339	0.2520	1.266	1970.

Table Q-1 (Continued)

RUN NO.	TEMP. °C	PRESS. PSIA.	FALL TIME SEC.	PERCENT ERROR	DENSITY G/CC	BRED	BCALC X10^4 CC/SEC^2	EQUI DIAMETER CM	LOG(N$_{Re}$)	VISCOSITY MICRO-POISE
2X1-1	-60.00	420.	49.970	0.24	0.554	0.8777	2.180	0.2521	1.292	1827.
	-60.00	980.	52.210	0.08	0.560	0.8794	2.204	0.2521	1.254	1929.
	-60.00	2000.	54.600	0.12	0.571	0.8811	2.249	0.2520	1.215	2053.
	-60.00	3000.	56.660	0.28	0.577	0.8827	2.294	0.2520	1.180	2172.
	-60.00	4000.	58.740	0.07	0.583	0.8842	2.340	0.2519	1.144	2295.
	-60.00	5000.	60.650	0.17	0.588	0.8857	2.386	0.2518	1.112	2415.
2X1-2	-80.00	345.	63.530	0.28	0.578	0.8865	2.221	0.2520	1.093	2368.
	-80.00	1000.	65.290	0.13	0.585	0.8876	2.250	0.2519	1.069	2461.
	-80.00	2000.	67.900	0.15	0.593	0.8892	2.295	0.2519	1.033	2607.
	-80.00	3000.	70.360	0.17	0.598	0.8908	2.341	0.2518	0.997	2754.
	-80.00	4000.	72.560	0.26	0.605	0.8921	2.387	0.2517	0.968	2892.
	-80.00	5000.	74.890	0.14	0.609	0.8936	2.434	0.2516	0.934	3044.
2X1-1	-100.00	180.	82.970	0.08	0.601	0.8965	2.260	0.2518	0.869	3153.
	-100.00	590.	84.200	0.12	0.605	0.8971	2.278	0.2518	0.856	3222.
	-100.00	2000.	88.510	0.14	0.616	0.8992	2.342	0.2517	0.810	3474.
	-100.00	3000.	91.440	0.20	0.620	0.9007	2.388	0.2516	0.775	3659.
	-100.00	4000.	94.430	0.20	0.625	0.9022	2.435	0.2515	0.743	3851.
	-100.00	5000.	99.300	0.10	0.629	0.9044	2.483	0.2515	0.693	4133.
2X1-2	-120.00	295.	119.010	0.06	0.627	0.9102	2.311	0.2516	0.562	4645.
	-120.00	1350.	123.520	0.30	0.633	0.9119	2.359	0.2516	0.525	4918.
	-120.00	2000.	126.420	0.56	0.637	0.9129	2.389	0.2515	0.503	5094.
	-120.00	3000.	130.300	0.00	0.641	0.9143	2.436	0.2514	0.470	5353.

Table Q-2 Viscosity Data of 50.0 mole% CH_4-50.0 mole% C_3H_8
Using No. 2 Falling Cylinder

RUN NO.	TEMP. °C	PRESS. PSIA.	FALL TIME SEC.	PERCENT ERROR	DENSITY G/CC	BRED	BCALC X10^4 CC/SEC^2	EQUI DIAMETER CM	LOG(N_{Re})	VISCOSITY MICRO-POISE
2X2-7	37.78	1500.	10.170	0.21	0.298	0.8271	2.013	0.2529	2.425	357.0
	37.78	2000.	12.450	0.20	0.338	0.8325	2.034	0.2529	2.303	437.9
	37.78	3000.	15.130	0.04	0.379	0.8381	2.076	0.2528	2.178	538.4
	37.78	4000.	16.910	0.13	0.403	0.8415	2.118	0.2527	2.102	610.8
	37.78	5000.	18.360	0.28	0.420	0.8443	2.162	0.2527	2.041	674.7
2X2-4	0.00	1150.	14.770	0.26	0.354	0.8388	2.078	0.2526	2.164	531.8
	0.00	2000.	18.890	0.28	0.403	0.8459	2.114	0.2525	2.003	684.9
	0.00	3000.	20.650	0.11	0.427	0.8485	2.158	0.2525	1.945	759.6
	0.00	4000.	22.130	0.10	0.445	0.8507	2.202	0.2524	1.895	826.9
	0.00	5000.	23.440	0.20	0.458	0.8527	2.246	0.2523	1.850	890.9
2X2-5	0.00	2000.	18.840	0.45	0.403	0.8458	2.114	0.2525	2.006	683.0
	0.00	3000.	20.620	1.76	0.427	0.8485	2.158	0.2525	1.946	758.4
	0.00	4000.	22.170	2.09	0.445	0.8508	2.202	0.2524	1.894	828.5
	0.00	5000.	23.420	0.16	0.458	0.8527	2.246	0.2523	1.851	890.1
2X2-3	-20.00	2000.	22.490	0.32	0.435	0.8515	2.159	0.2524	1.878	828.2
	-20.00	3000.	24.960	0.26	0.453	0.8551	2.203	0.2523	1.797	935.2
	-20.00	4000.	26.300	0.73	0.467	0.8569	2.247	0.2522	1.758	1002.
	-20.00	5000.	27.450	0.14	0.478	0.8584	2.292	0.2522	1.723	1064.
2X2-3	-40.00	1150.	25.490	0.47	0.444	0.8561	2.166	0.2523	1.775	943.7
	-40.00	2000.	27.200	0.09	0.464	0.8580	2.204	0.2522	1.733	1019.
	-40.00	3000.	28.890	0.04	0.478	0.8601	2.248	0.2521	1.686	1100.
	-40.00	4000.	30.440	0.30	0.490	0.8620	2.293	0.2521	1.644	1180.
	-40.00	5000.	31.800	0.27	0.499	0.8637	2.339	0.2520	1.606	1255.

Table Q-2 (Continued)

RUN NO.	TEMP. °C	PRESS. PSIA.	FALL TIME SEC.	PERCENT ERROR	DENSITY G/CC	BRED	BCALC X10^{4} CC/SEC^{2}	EQUI DIAMETER CM	LOG(N$_{Re}$)	VISCOSITY MICRO-POISE
2X2-2	-60.00	650.	28.430	0.16	0.471	0.8593	2.189	0.2521	1.704	1057.
	-60.00	930.	30.560	0.13	0.476	0.8620	2.201	0.2521	1.643	1143.
	-60.00	2000.	32.400	0.23	0.492	0.8640	2.249	0.2520	1.599	1234.
	-60.00	3000.	34.040	0.14	0.503	0.8658	2.294	0.2520	1.558	1319.
	-60.00	4000.	35.510	0.04	0.512	0.8674	2.340	0.2519	1.521	1401.
	-60.00	5000.	36.910	0.08	0.520	0.8690	2.386	0.2518	1.486	1483.
2X2-5	-60.00	930.	30.470	0.02	0.476	0.8619	2.201	0.2521	1.646	1140.
	-60.00	2000.	32.410	2.18	0.492	0.8640	2.249	0.2520	1.598	1234.
	-60.00	3000.	34.530	1.28	0.503	0.8664	2.294	0.2520	1.545	1339.
2X2-3	-80.00	1000.	39.480	0.14	0.507	0.8711	2.250	0.2519	1.439	1508.
	-80.00	2000.	41.200	0.12	0.518	0.8727	2.295	0.2519	1.403	1601.
	-80.00	3000.	43.040	0.08	0.527	0.8744	2.341	0.2518	1.365	1703.
	-80.00	4000.	44.670	0.11	0.535	0.8759	2.387	0.2517	1.331	1799.
	-80.00	5000.	46.300	0.20	0.541	0.8775	2.434	0.2516	1.296	1900.
2X2-2	-100.00	500.	50.070	0.66	0.532	0.8796	2.274	0.2518	1.248	1932.
	-100.00	1200.	51.440	0.17	0.539	0.8806	2.305	0.2517	1.225	2009.
	-100.00	2100.	53.390	0.19	0.545	0.8822	2.347	0.2517	1.190	2122.
	-100.00	3000.	55.030	0.29	0.550	0.8835	2.388	0.2516	1.160	2224.
	-100.00	4000.	57.010	0.25	0.557	0.8850	2.435	0.2515	1.127	2346.
	-100.00	5000.	58.760	0.14	0.562	0.8864	2.483	0.2515	1.096	2465.
2X2-4	-120.00	290.	69.690	0.32	0.559	0.8918	2.310	0.2516	0.974	2740.
	-120.00	1190.	72.370	0.18	0.564	0.8935	2.352	0.2516	0.937	2897.
	-120.00	2000.	74.400	0.38	0.568	0.8947	2.389	0.2515	0.909	3024.
	-120.00	3000.	77.160	0.21	0.573	0.8963	2.436	0.2514	0.873	3197.
	-120.00	4000.	79.950	0.47	0.578	0.8979	2.484	0.2514	0.838	3377.
	-120.00	5000.	82.360	0.40	0.582	0.8993	2.532	0.2513	0.806	3546.

Table Q-3 Viscosity Data of 75.3 mole% CH_4-24.7 mole% C_3H_8
Using No. 2 Falling Cylinder

RUN NO.	TEMP. °C	PRESS. PSIA.	FALL TIME SEC.	PERCENT ERROR	DENSITY G/CC	BRED	BCALC X10^4 CC/SEC^2	EQUI DIAMETER CM	LOG(N$_{Re}$)	VISCOSITY MICRO-POISE
2X3-2	37.78	1025.	3.706	0.06	0.082	0.7879	1.995	0.2530	2.733	132.7
	37.78	2000.	5.957	0.13	0.193	0.7949	2.034	0.2529	2.697	211.0
	37.78	3000.	8.228	0.12	0.264	0.8168	2.076	0.2528	2.543	297.9
	37.78	4000.	9.860	0.10	0.302	0.8266	2.118	0.2527	2.436	363.4
	37.78	5000.	11.120	0.21	0.326	0.8301	2.162	0.2527	2.358	416.4
2X3-1	0.00	1620.	6.744	0.25	0.237	0.7998	2.095	0.2526	2.669	243.8
	0.00	2000.	8.383	0.23	0.277	0.8170	2.114	0.2525	2.540	307.8
	0.00	3000.	10.750	0.25	0.329	0.8285	2.158	0.2525	2.393	400.8
	0.00	4000.	12.230	0.31	0.356	0.8323	2.202	0.2524	2.308	462.7
	0.00	5000.	13.410	0.38	0.375	0.8352	2.246	0.2523	2.244	515.5
2X3-5	0.00	2000.	8.522	0.23	0.277	0.8185	2.114	0.2525	2.525	313.5
2X3-6	-20.00	1500.	9.273	0.20	0.294	0.8250	2.137	0.2524	2.472	345.5
	-20.00	2000.	10.860	0.73	0.325	0.8292	2.159	0.2524	2.377	406.2
	-20.00	3000.	12.740	0.12	0.364	0.8335	2.203	0.2523	2.283	481.5
	-20.00	4000.	14.230	0.23	0.383	0.8371	2.247	0.2522	2.201	547.0
	-20.00	5000.	15.380	0.22	0.398	0.8397	2.292	0.2522	2.143	601.5
2X3-1	-40.00	1550.	12.990	0.33	0.352	0.8348	2.180	0.2523	2.253	489.0
	-40.00	2000.	13.990	0.51	0.368	0.8369	2.204	0.2522	2.204	530.6
	-40.00	3000.	15.530	0.07	0.393	0.8400	2.248	0.2521	2.136	597.2
	-40.00	4000.	16.810	0.47	0.408	0.8427	2.293	0.2521	2.076	657.6
	-40.00	5000.	17.820	0.15	0.422	0.8446	2.339	0.2520	2.032	708.9

Table Q-3 (Continued)

RUN NO.	TEMP. °C	PRESS. PSIA.	FALL TIME SEC.	PERCENT ERROR	DENSITY G/CC	BRED	BCALC X10⁴ CC/SEC²	EQUI DIAMETER CM	LOG(N$_{Re}$)	VISCOSITY MICRO-POISE
2X3-7	-60.00	1270.	16.590	0.13	0.388	0.8426	2.217	0.2521	2.077	632.5
	-60.00	2000.	17.770	0.91	0.404	0.8447	2.249	0.2520	2.030	684.8
	-60.00	3000.	19.160	0.69	0.421	0.8472	2.294	0.2520	1.975	750.3
	-60.00	4000.	20.150	0.20	0.433	0.8489	2.340	0.2519	1.936	802.8
	-60.00	5000.	21.350	1.28	0.444	0.8510	2.386	0.2518	1.889	865.8
2X3-1	-80.00	910.	20.300	0.34	0.420	0.8491	2.241	0.2519	1.933	778.8
	-80.00	1430.	21.120	0.15	0.430	0.8503	2.265	0.2519	1.905	817.0
	-80.00	2000.	21.970	0.24	0.437	0.8518	2.295	0.2519	1.872	860.2
	-80.00	3000.	23.320	0.13	0.448	0.8539	2.341	0.2518	1.823	929.8
	-80.00	4000.	24.520	0.11	0.458	0.8558	2.387	0.2517	1.781	995.1
	-80.00	5000.	25.490	0.19	0.467	0.8573	2.434	0.2516	1.748	1053.
2X3-5	-80.00	910.	19.980	0.75	0.420	0.8484	2.241	0.2519	1.947	766.0
	-80.00	2000.	22.110	0.55	0.437	0.8520	2.295	0.2519	1.867	866.0
2X3-6	-100.00	1015.	25.850	0.45	0.455	0.8573	2.301	0.2517	1.747	1015.
	-100.00	2000.	27.610	0.36	0.467	0.8597	2.342	0.2517	1.694	1101.
	-100.00	3000.	28.760	0.43	0.474	0.8614	2.388	0.2516	1.657	1168.
	-100.00	4000.	30.190	0.39	0.482	0.8633	2.435	0.2515	1.614	1249.
	-100.00	5000.	31.390	0.51	0.490	0.8648	2.483	0.2515	1.579	1323.
2X3-5	-120.00	340.	34.140	0.49	0.481	0.8672	2.313	0.2516	1.526	1349.
	-120.00	1095.	35.750	0.45	0.488	0.8690	2.348	0.2516	1.486	1433.
	-120.00	2000.	37.020	0.37	0.495	0.8704	2.389	0.2515	1.455	1508.
	-120.00	3000.	38.490	0.33	0.500	0.8721	2.436	0.2514	1.417	1598.
	-120.00	4000.	40.030	0.29	0.506	0.8737	2.484	0.2514	1.380	1694.
	-120.00	5000.	41.410	0.28	0.513	0.8751	2.532	0.2513	1.348	1784.

Table Q-3 (Continued)

RUN NO.	TEMP. °C	PRESS. PSIA.	FALL TIME SEC.	PERCENT ERROR	DENSITY G/CC	BRED	BCALC $X10^4$ CC/SEC^2	EQUI DIAMETER CM	LOG(N_{Re})	VISCOSITY MICRO-POISE
2X3-7	-140.00	290.	48.450	0.31	0.509	0.8801	2.358	0.2514	1.236	1959.
	-140.00	1300.	50.580	0.24	0.516	0.8819	2.405	0.2514	1.197	2084.
	-140.00	2000.	52.370	0.54	0.520	0.8834	2.438	0.2513	1.164	2188.
	-140.00	3000.	54.610	0.18	0.525	0.8852	2.485	0.2513	1.123	2325.
	-140.00	4000.	56.830	0.36	0.530	0.8869	2.533	0.2512	1.084	2466.
	-140.00	5000.	58.920	0.56	0.535	0.8885	2.582	0.2511	1.049	2606.
2X3-5	-150.00	280.	60.350	1.34	0.524	0.8883	2.382	0.2514	1.052	2473.
	-150.00	1000.	63.050	0.33	0.529	0.8901	2.415	0.2513	1.012	2620.
	-150.00	2000.	65.050	0.68	0.533	0.8916	2.462	0.2513	0.980	2755.
	-150.00	3000.	67.610	0.38	0.537	0.8933	2.510	0.2512	0.941	2921.
	-150.00	5000.	74.260	1.52	0.546	0.8974	2.607	0.2510	0.850	3335.

Appendix R

Computer Programs

Flow sheets and computer programs for the following programs appear on the following pages,

Program 510	Calculation of Viscometer constant, Equivalent Diameter and Physical Dimensions of the Viscometer as Functions of Pressure and Temperature
Program 604	Computation of Experimental Viscometer Constant
Program 703	Calculation of Viscosities from Experimentally Determined Fall Time Data

Flow Sheet for Program 510

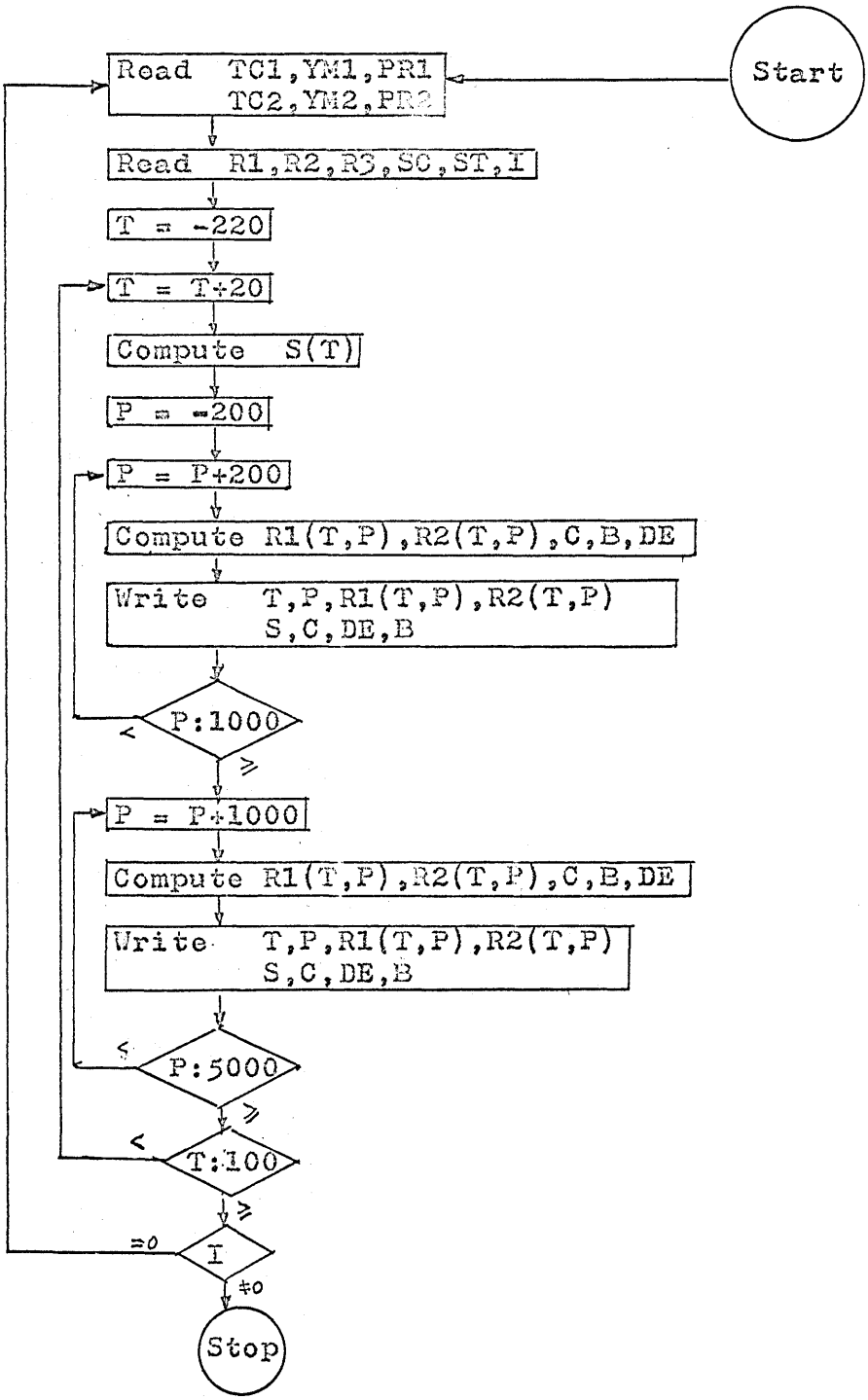

```
C PROGRAM 510
C CALCULATION OF VISCOMETER CONSTANT, EQUIVALENT DIAMETER AND THE
C PHYSICAL DIMENSIONS OF THE VISCOMETER AS A FUNCTION OF PRESSURE
C AND TEMPERATURE
C
C P = PRESSURE(PSIA)
C TC1 = COEFFICIENT OF THERMAL EXPANSION FOR A FALLING CYLINDER(1/C)
C YM1 = YOUNGS MODULUS FOR A FALLING CYLINDER(PSI)
C PR1 = POISSONS RATIO FOR A FALLING CYLINDER
C TC2 = COEFFICIENT OF THERMAL EXPANSION FOR A VISCOMETER TUBE(1/C)
C YM2 = YOUNGS MODULUS FOR FOR A VISCOMETER TUBE(PSI)
C PR2 = POISSONS RATIO FOR A VISCOMETER TUBE
C R1 = OUTER RADIUS OF A FALLING CYLINDER(CM)
C R2 = INNER RADIUS OF A VISCOMETER TUBE(CM)
C C = RATIO OF R1 TO R2
C R3 = OUTER RADIUS OF A VISCOMETER TUBE(CM)
C SC = LENGTH OF A FALLING CYLINDER(CM)
C S = DISTANCE OF FALL (CM)
C ST = S + SC (CM)
C B = CALCULATED VISCOMETER CONSTANT(CM3/SEC2)
C DE = EQUIVALENT DIAMETER(CM)
C THE INPUT DIMENSIONS OF THE VISCOMETER ARE THE VALUES DETERMINED
C          AT 25 C AND 1 ATM
C
      DOUBLE PRECISION TC1,YM1,PR1,TC2,YM2,PR2,R1,R2,R3,S,SC,ST,T,P
     1 R1PT,R2PT,C,C2,B,DE,DLOG,R2T,R3T
    1 READ(5,1000) TC1,YM1,PR1
      WRITE(6,2003) TC1,YM1,PR1
      READ(5,1000) TC2,YM2,PR2
      WRITE(6,2004) TC2,YM2,PR2
```

```
 2 READ(5,1001) R1,R2,R3,SC,ST,I
   WRITE(6,2005) R1,R2,R3,SC,ST
   WRITE(6,2000)
   T=-220.
10 T=T+20.
   S = ST*(1.+TC2*(T-25.)) - SC*(1.+TC1*(T-25.))
   P = -200.
15 P = P+200.
   R1PT=R1*(1.+TC1*(T-25.))*(1.-P*(1.-PR1)/YM1)
   R2T=R2*(1.+TC2*(T-25.))
   R3T=R3*(1.+TC2*(T-25.))
   R2PT=R2T*(1.+(P/YM2)*
  1     ((R3T**2+R2T**2)/(R3T**2-R2T**2)+PR2))
   C = R1PT/R2PT
   C2 = C*C
   B = -(490.*R1PT*R1PT)*
  1      (DLOG(C)+(1.-C2)/(1.+C2))
   DE = -4.*C2*C2*R2PT*(DLOG(C)*(1.+C2)/(1.-C2)+1.)/
  1      ((1.-C)*(1.-C2))
   WRITE(6,2001) T,P,R1PT,R2PT,S ,C,DE,B
   IF(1000.-P) 20,20,15
20 P = P+1000.
   R1PT=R1*(1.+TC1*(T-25.))*(1.-P*(1.-PR1)/YM1)
   R2T=R2*(1.+TC2*(T-25.))
   R3T=R3*(1.+TC2*(T-25.))
   R2PT=R2T*(1.+(P/YM2)*
  1     ((R3T**2+R2T**2)/(R3T**2-R2T**2)+PR2))
   C = R1PT/R2PT
   C2 =.C*C
```

```
      B = -(490.*R1PT*R1PT)*
     1      (DLOG(C)+(1.-C2)/(1.+C2))
      DE = -4.*C2*C2*R2PT*(DLOG(C)*(1.+C2)/(1.-C2)+1.)/
     1      ((1.-C)*(1.-C2))
      WRITE(6,2001) T,P,R1PT,R2PT,S ,C,DE,B
      IF(5000.-P) 30,30,20
   30 IF(100.-T) 40,40,10
   40 WRITE(6,2002)
      IF(I) 50,2,50
   50 CALL EXIT
 1000 FORMAT(1X,3E15.5)
 1001 FORMAT(5F10.0,I2)
 2000 FORMAT(37H VISCOMETER CONSTANT AS FN OF P AND T/
     14X,4HT(C),4X,6HP(PSI),2X,6HR1(CM),2X,6HR2(CM),2X,6HST(CM),3X,
     2  5HR1/R2,4X,9HEQDIA(CM),3X,14HBETA(CM3/SEC2)/)
 2001 FORMAT(1X,F8.2,1X,F8.1,3F8.4,F9.5,2E14.5)
 2002 FORMAT(1H1)
 2003 FORMAT(4X,62HPHYS CONST OF BODY, THERMAL COEF,  YOUNG MODLS,  POIS
     1SON RATIO/21X,3E15.5/)
 2004 FORMAT(4X,62HPHYS CONST OF TUBE, THERMAL COEF,  YOUNG MODLS,  POIS
     1SON RATIO/21X,3E15.5/)
 2005 FORMAT(4X,64HRBODY(CM)  RIN(CM)   ROUT(CM)  LBODY(CM)  L TUBE(CM)
     1           /6F10.5//)
      END
```

Sample input data for Program 510

```
      .23400E-04     .10300E 08     .33300E 00
      .16020E-04     .29000E 08     .26000E 00
  0.39078   0.39878   0.71374     5.331    18.194
```

Flow Sheet for Program 604

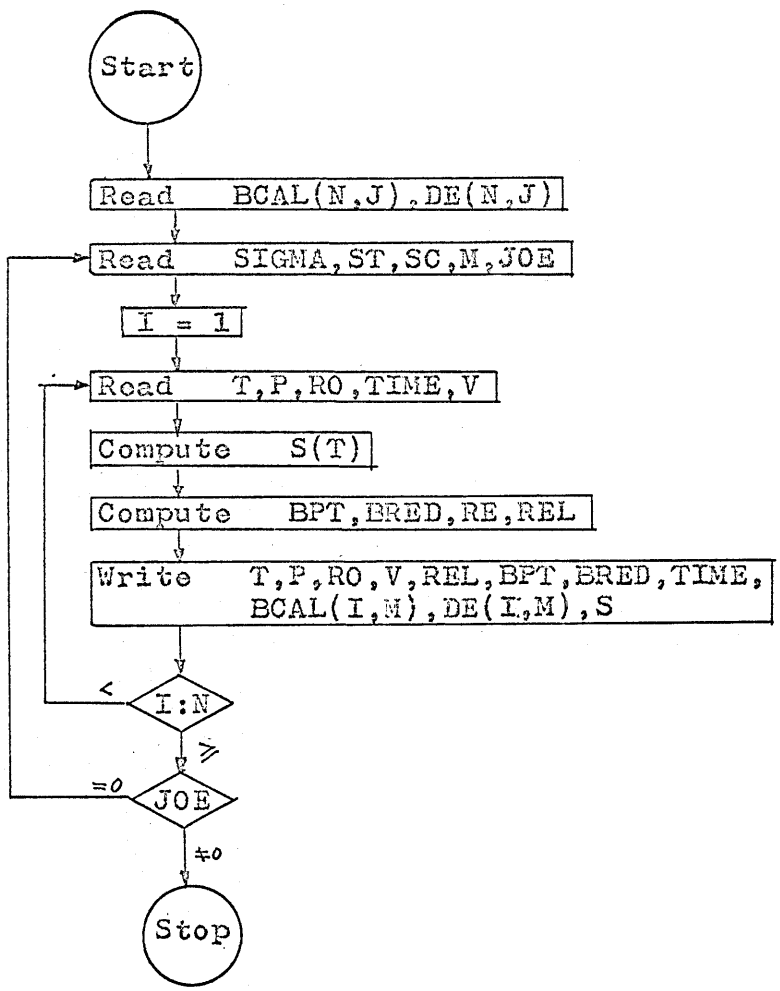

Notes on the input data: BCAL(N,J) and DE(N,J)

(1) The numbers in the first column of matrices BCAL(100,8) and DE(100,8) are temperatures(°C), and those in the second column of matrices are pressures. (psia).

(2) The numbers in the other six columns of matrices represent BCAL's and DE's at different pressure and temperature condition for six falling cylinders having different diameters.

```
C PROGRAM 604
C COMPUTATION OF EXPERIMENTAL VISCOMETER CONSTANT
C
C P = PRESSURE(PSIA)
C T = TEMPERATURE(C)
C RO = DENSITY OF CALIBRATION FLUID (G/CC)
C TIME = TIME OF FALL (SEC)
C V = VISCOSITY OF CALIBRATION FLUID (POISE)
C SIGMA = DENSITY OF A FALLING CYLINDER(G/CC)
C S = DISTANCE OF FALL (CM)
C SC = LENGTH OF A FALLING CYLINDER(CM)
C ST = S + SC(CM)
C DE = EQUIVALENT DIAMETER(CM)
C BPTS=EXPERIMENTAL VISCOMETER CONSTANT(CM3/SEC2)
C BCAL = CALCULATED VISCOMETER CONSTANT(CM3/SEC2)
C BRED = BPTS/BCAL
C RE = REYNOLDS NUMBER
C REL = LOG(RE)
C
      DIMENSION BCAL(100,8),DE(100,8)
      N=1
    2 READ(5,1002)(BCAL(N,J),J=1,8)
      READ(5,1002)(DE(N,J),J=1,8),I
      IF(I)4,3,4
    3 N=N+1
      GO TO 2
    4 DO 10 I=1,N
   10 WRITE(6,2005)(BCAL(I,J),J=1,8)
      DO 12 I=1,N
   12 WRITE(6,2005)(DE(I,J),J=1,8)
      WRITE(6,2004)
      WRITE(6,2000)
```

```
  13 READ(5,1003)SIGMA,ST,SC,M,JOE
     WRITE(6,2001)SIGMA,ST,SC,M
     WRITE(6,2002)
     DO 20 I=1,N
     READ(5,1000)T,P,RO,TIME,V
     S = ST*(1.+.000016*(T-25.)) - SC*(1.+.000023*(T-25.))
     BPTS=S*V/(TIME*(SIGMA-RO))
     BRED=BPTS/BCAL(I,M)
     RE=DE(I,M)*S*RO/(V*TIME)
     REL=(ALOG(RE))/2.3026
     WRITE(7,2003)T,P,RO,V,REL,BPTS,BRED,TIME
  20 WRITE(6,2006)T,P,RO,V,REL,BPTS,BRED,TIME,BCAL(I,M),DE(I,M),S
     WRITE(6,2004)
     IF(JOE)30,13,30
  30 CALL EXIT
1002 FORMAT(F9.4,7F10.4,I1)
1003 FORMAT(3F10.4,2I2)
1000 FORMAT(7F10.4,2I2)
2000 FORMAT(1X,25HCALIBRATION OF VISCOMETER//)
2001 FORMAT(1X,13HD BODY(G/CC)=,F7.4,15H  DISTANCE(CM)=,2F7.3,5X,I2//)
2002 FORMAT(3X,76HT(C)      P(PSIA)   D(G/CC) VS(POISE)  LOGRE   BPT(CM
    13/SEC2)  BPT/BC  SECOND/)
2003 FORMAT(1X,F9.4,F10.1,F10.4,F10.7,F9.3,F11.8,F10.4,F8.3)
2004 FORMAT(1H1)
2005 FORMAT(1X,2F10.3,5F10.7,F9.6)
2006 FORMAT(1X,F9.4,F10.1,F10.4,F10.7,F9.3,F11.8,F10.4,F8.3,F11.8,
    1    2F9.4)
     END
```

Sample input data for Program 604

```
21.1111    200.    2092    1992    1903    1252    1182    1116
21.1111    200.    .2526   .2528   .2530   .2547   .2549   .2551
21.1111   1000.    2128    2025    1938    1275    1203    1140
21.1111   1000.    .2526   .2528   .2530   .2546   .2549   .2550
21.1111   3000.    2216    2110    2021    1339    1263    1198
21.1111   3000.    .2524   .2527   .2528   .2545   .2547   .2549
21.1111   5000.    2305    2199    2103    1402    1327    1258
21.1111   5000.    .2523   .2525   .2527   .2544   .2546   .2548
37.7777    200.    2058    1960    1871    1228    1158    1093
37.7777    200.    .2528   .2530   .2532   .2549   .2551   .2553
37.7777   1000.    2092    1992    1903    1250    1180    1118
37.7777   1000.    .2528   .2530   .2532   .2548   .2550   .2552
37.7777   3000.    2180    2076    1987    1312    1239    1173
37.7777   3000.    .2526   .2528   .2530   .2547   .2549   .2551
37.7777   5000.    2268    2162    2069    1377    1301    1233
37.7777   5000.    .2525   .2527   .2529   .2545   .2548   .2549
```

```
 3.0058   18.194   5.331 3
21.1111    200.    .5000   28.690   .001010
21.1111   1000.    .5110   31.090   .001125
21.1111   3000.    .5380   35.960   .001351
21.1111   5000.    .5530   39.820   .001538
37.7777    300.    .4754   24.660   .000863
37.7777   1000.    .4904   27.000   .000956
37.7777   3000.    .5203   32.220   .001176
37.7777   5000.    .5406   36.060   .001367
```

Flow Sheet for Program 703

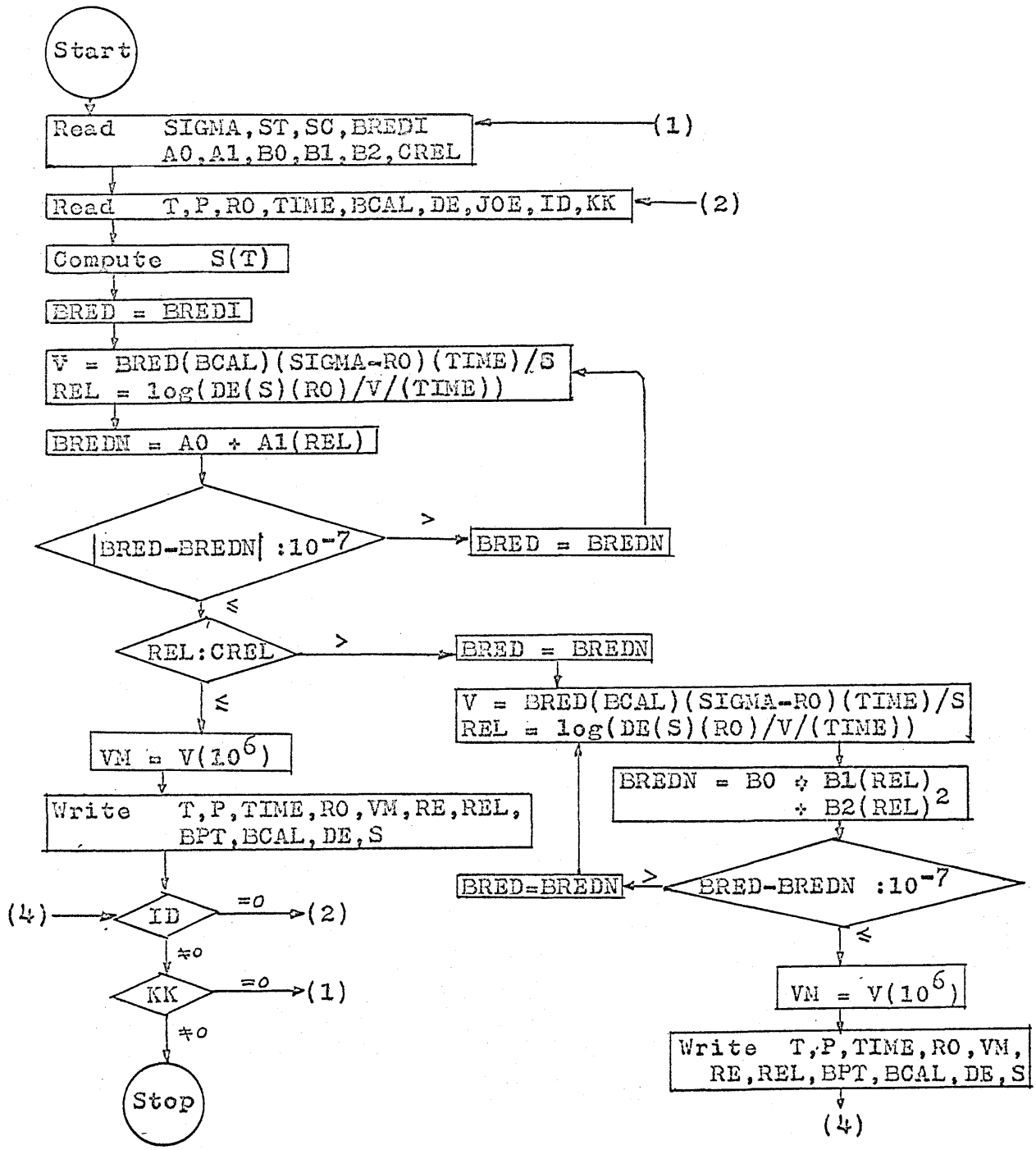

```
C PROGRAM 703
C CALCULATION OF VISCOSITIES FROM EXPERIMENTALLY DETERMINED
C     FALL TIME DATA
C
C P = PRESSURE(PSIA)
C T = TEMPERATURE(C)
C RO = DENSITY OF FLUID(G/CC)
C TIME = TIME OF FALL(SEC)
C VM = VISCOSITY(MICROPOISE)
C SIGMA = DENSITY OF A FALLING CYLINDER(G/CC)
C S = DISTANCE OF FALL(CM)
C SC = LENGTH OF A FALLING CYLINDER(CM)
C ST = S + SC  (CM)
C DE = EQUIVALENT DIAMETER(CM)
C BCAL = CALCULATED VISCOMETER CONSTANT(CM3/SEC2)
C BRED = REDUCED VISCOMETER CONSTANT
C BREDI= INITIAL VALUE OF BRED IN THE TRIAL AND ERROR CALCULATION
C RE = REYNOLDS NUMBER
C REL = LOG(RE)
C CREL = TRANSITION LOG(RE)
C A0,A1,B0,B1,B2  ARE COEFFICIENTS FOR THE VISCOMETER CALIBRATION
C     EQUATIONS
C
    1 READ(5,1000)SIGMA,ST,SC,BREDI
      WRITE(6,1000)SIGMA,ST,SC,BREDI
      READ(5,1000)A0,A1,B0,B1,B2,CREL
      WRITE(6,1000)A0,A1,B0,B1,B2,CREL
   10 READ(5,1000)T,P,RO,TIME,BCAL,DE,JOE,ID,KK
      S = ST*(1.+.000016*(T-25.)) - SC*(1.+.000023*(T-25.))
      BRED=BREDI
   25 BPT=BRED*BCAL
      V=BPT*(SIGMA-RO)*TIME/S
      RE=DE*S*RO/(V*TIME)
      REL=ALOG10(RE)
```

```
      BREDN=A0+A1*REL
      DB=ABS(BRED-BREDN)
      IF(DB-1.0E-07)40,40,30
   30 BRED=BREDN
      GO TO 25
   40 IF(REL-CREL)50,50,60
   50 VM=V*1.0E+6
      WRITE(6,2002)T,P,TIME,RO,VM,RE,REL,BPT,BCAL,DE,S
      WRITE(7,2003) T,P,RO,VM
      IF(JOE) 85,90,85
   60 BRED=BREDN
   65 BPT=BRED*BCAL
      V=BPT*(SIGMA-RO)*TIME/S
      RE=DE*S*RO/(V*TIME)
      REL=ALOG10(RE)
      BREDN=B0+B1*REL+B2*REL**2
      DB=ABS(BRED-BREDN)
      IF(DB-1.0E-07)80,80,70
   70 BRED=BREDN
      GO TO 65
   80 VM=V*1.0E+06
      WRITE(6,2002)T,P,TIME,RO,VM,RE,REL,BPT,BCAL,DE,S
      WRITE(7,2003) T,P,RO,VM
      IF(JOE) 85,90,85
   85 WRITE(6,2004)
   90 IF(ID) 95,10,95
   95 IF(KK) 100,1,100
  100 CALL EXIT
 1000 FORMAT(1X,F9.5,5F10.5,3I2)
 2002 FORMAT(1X,2F7.1,F8.3,F9.4,F10.2,F7.1,F6.3,2E12.4,2F8.4)
 2003 FORMAT(1X,F9.1,F10.0,F10.3,F10.1)
 2004 FORMAT(1H1)
      END
```

Sample input data for Program 703

```
 3.0058    18.194     5.331      .8700
  .9351    -.03870     .3633      .5441     -.1427     2.446
   -60.      500.      .0380     2.209      .2288      .2519
   -60.      800.      .0790     2.707      .2302      .2519
   -60.     1000.      .1220     3.383      .2311      .2519
   -60.     1300.      .1880     4.995      .2325      .2519
   -60.     1600.      .2280     6.078      .2339      .2519
   -60.     2000.      .2560     7.022      .2357      .2518
   -60.     3000.      .2920     8.559      .2404      .2517
   -60.     4000.      .3130     9.665      .2451      .2517
   -60.     5000.      .3280    10.520      .2498      .2516
   -70.      100.      .0062     1.794      .2293      .2518
   -70.      300.      .0228     1.961      .2302      .2518
   -70.      500.      .0440     2.194      .2311      .2518
   -70.      700.      .0750     2.574      .2321      .2518
   -70.      900.      .1350     3.670      .2330      .2518
   -70.     1000.      .1800     4.729      .2334      .2518
   -70.     2000.      .2800     7.971      .2381      .2517
   -70.     3000.      .3090     9.397      .2428      .2516
   -70.     4000.      .3270    10.440      .2475      .2516
   -70.     5000.      .3410    11.310      .2523      .2515
   -80.      200.      .0160     1.775      .2321      .2518
   -80.      400.      .0380     2.008      .2330      .2518
   -80.      600.      .0700     2.457      .2339      .2517
   -80.      800.      .2280     5.876      .2349      .2517
   -80.     1000.      .2520     7.015      .2358      .2517
   -80.     1500.      .2880     8.266      .2381      .2516
   -80.     2000.      .3040     9.192      .2404      .2516
   -80.     3000.      .3260    10.490      .2452      .2516
   -80.     4000.      .3410    11.520      .2499      .2515
   -80.     5000.      .3540    12.420      .2548      .2514
```

Appendix S

Drawings for the Equipment

The following drawings for the equipment appear in the following pages,

Figure S-1 Detailed Drawing of Electrical Lead Assembly

Figure S-2 Detailed Drawing of Falling Cylinder

Figure S-3 Detailed Drawing of the Parts for Low Temperature Differential Pressure Indicator

Figure S-4 High Temperature Differential Pressure Indicator Assembly

Figure S-5 Mass Injection Cylinder Assembly

Figure S-6 Detailed Drawing of the Parts for the Modified Mass Injection Cylinder

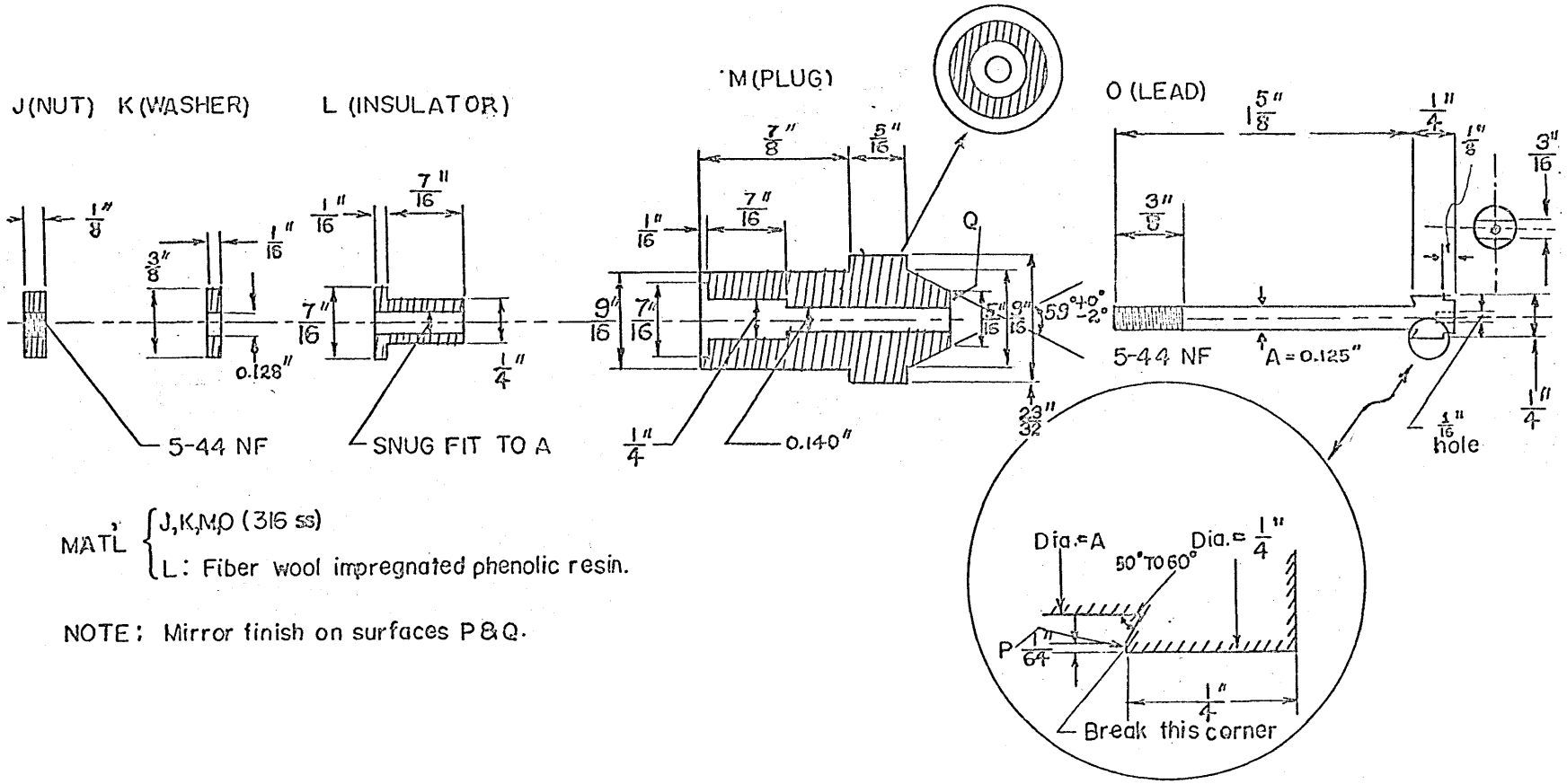

Figure S-1 Detailed Drawing of Electrical Lead Assembly

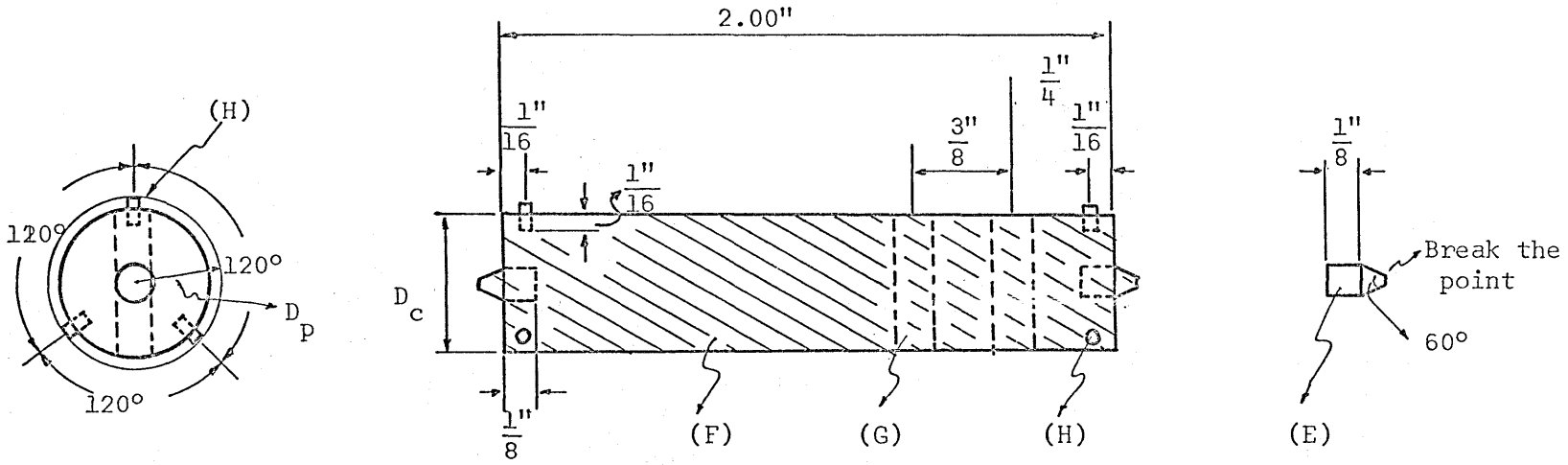

Notes: D_c for each falling cylinder has been specified in P.

(F): Aluminum body (surface is mirror finished)

(G): 0.125" OD mild steel press fit to (F)

(H): 0.026" OD pins press fit to (F)
(D_p is such that the cylinder can fall in the viscometer tube smoothly)

(E): 0.0735" OD stainless steel tip press fit to a flat bottom hole drilled by #49 drill

Figure S-2 Detailed Drawing of Falling Cylinder

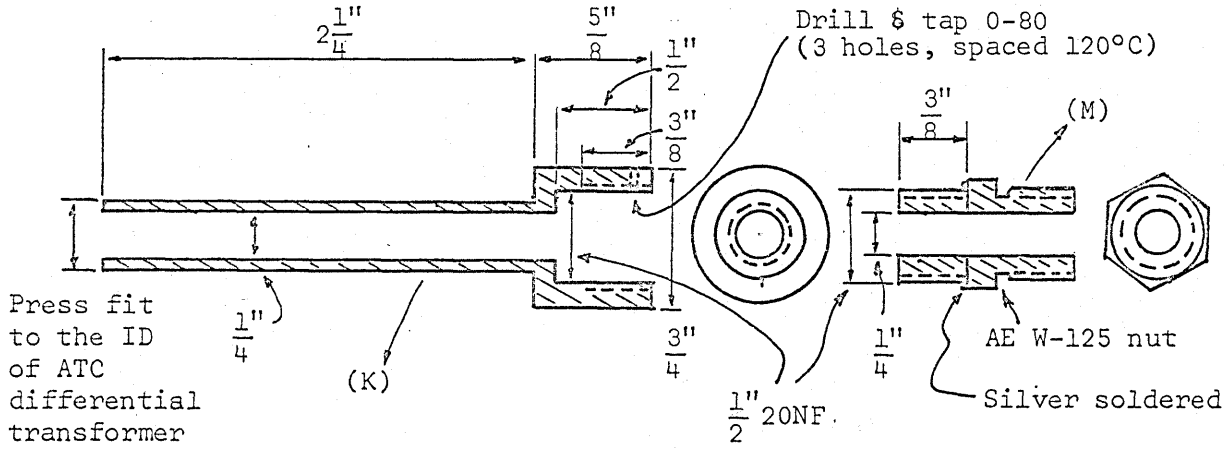

(K) TRANSFORMER HOLDER (M) NUT

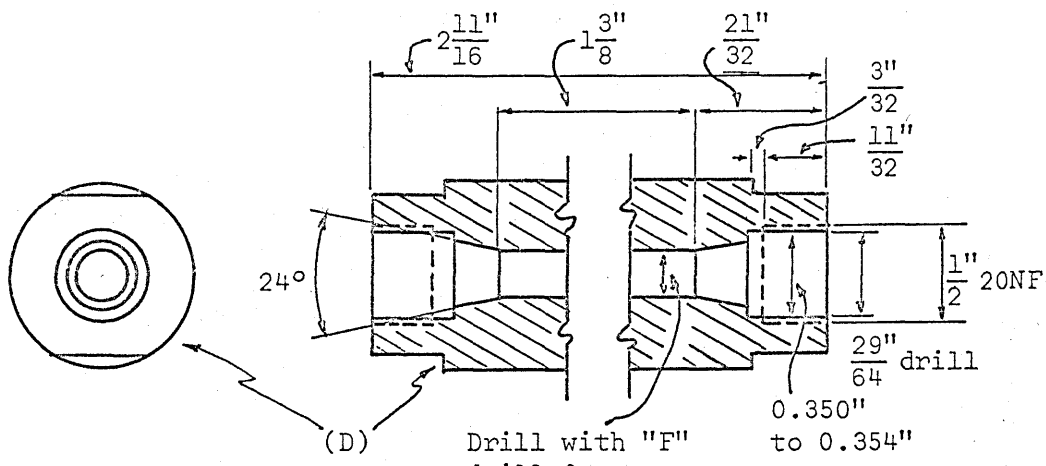

(D) BELLOWS HOUSING

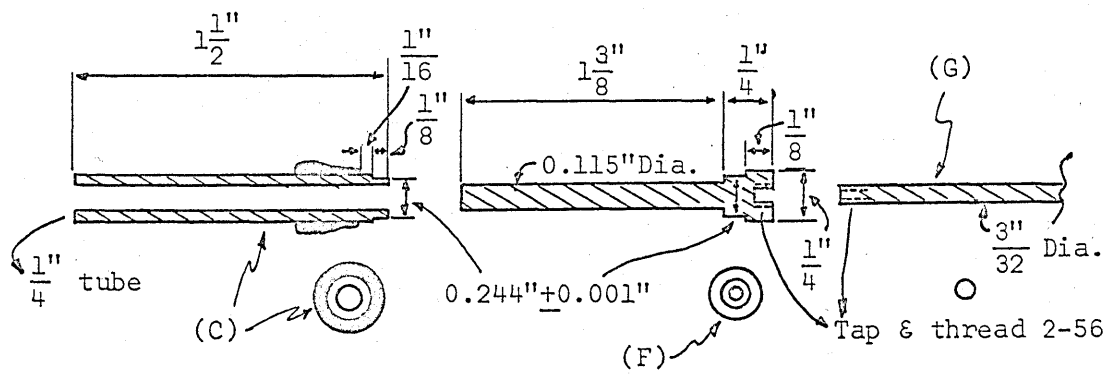

(C) STAINLESS STEEL TUBE (F) MOVABLE END CAP (G) EXTENSION ROD

Note: Except for (K) which is made of brass, all the other parts are fabricated from 316 stainless steel.

Figure S-3 Detailed Drawing of the Parts for Low Temperature Differential Pressure Indicator

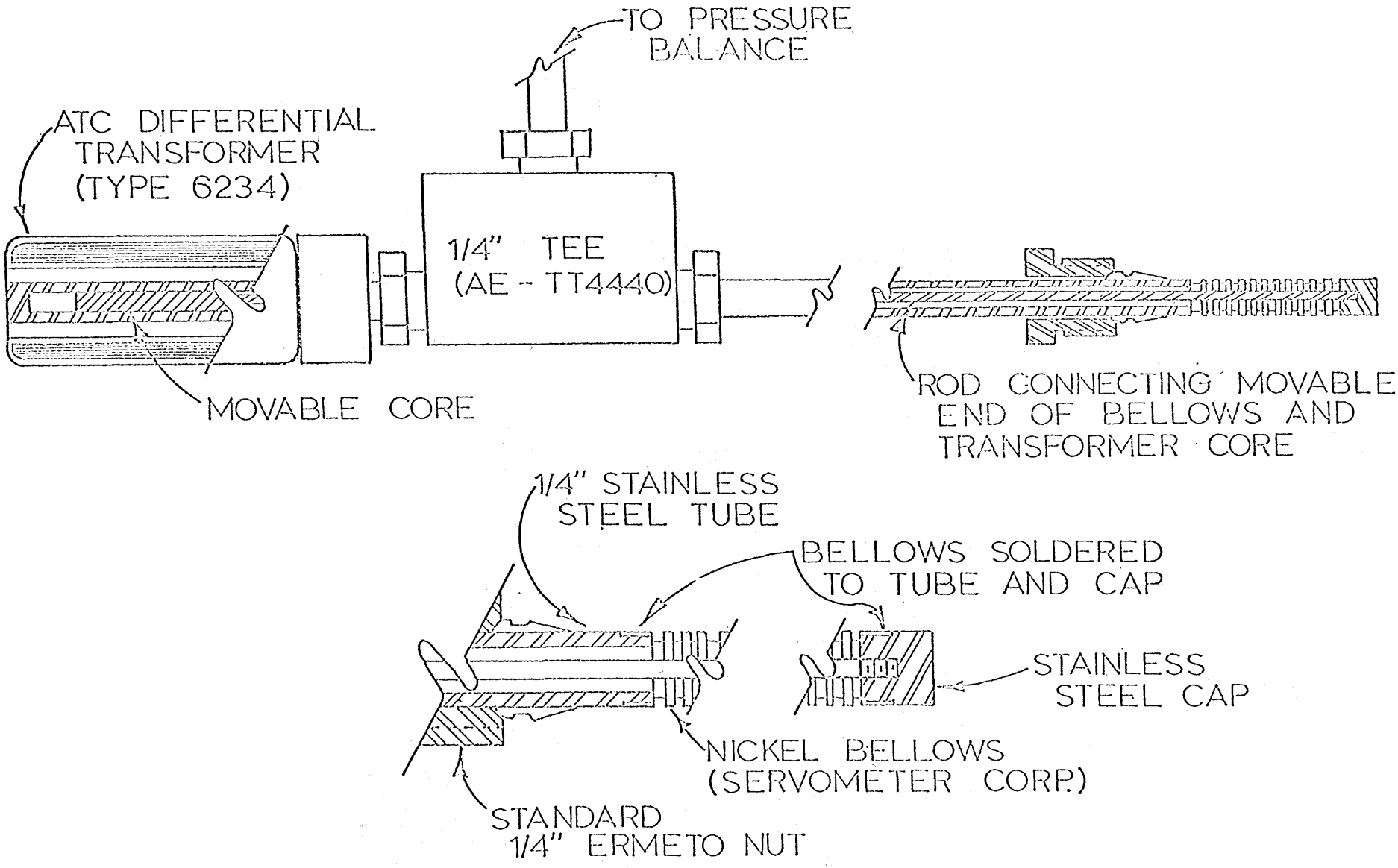

Figure S-4 High Temperature Differential Pressure Indicator Assembly

NOTES: (1) Working pressure: 12,000 psia at -10°F to 400°F.
(2) Hydraulic pressure test: 18,000 psia.
(3) The size of O-ring for the end plugs & the piston is No. 214.
(4) The assembly was constructed from 300 series stainless steel except for the piston which was made of brass.
(5) The packings for stuffing box are 1/16" thick and have OD of 0.248". The ID for ss packings is 0.128", while that for teflon packings is 0.122". These packings fit in the 1/4" bore of the stuffing box.

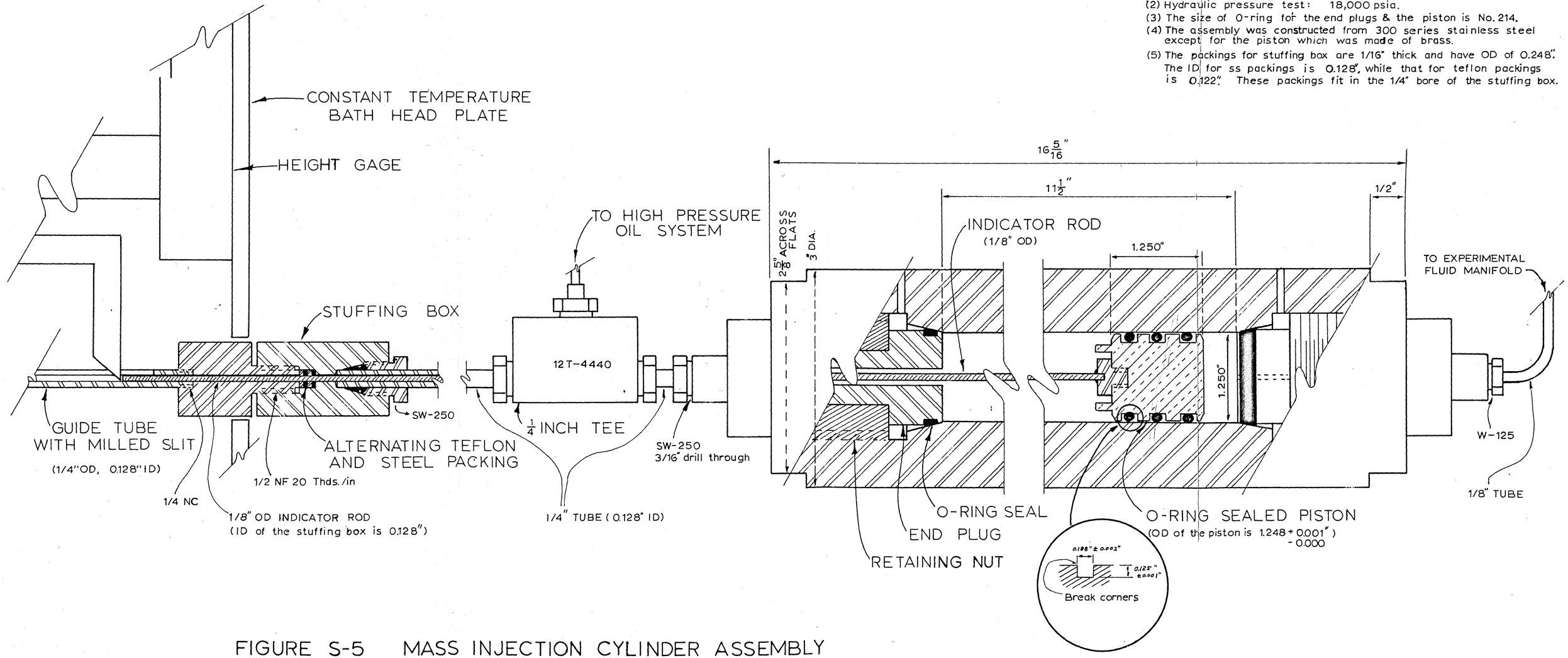

FIGURE S-5 MASS INJECTION CYLINDER ASSEMBLY

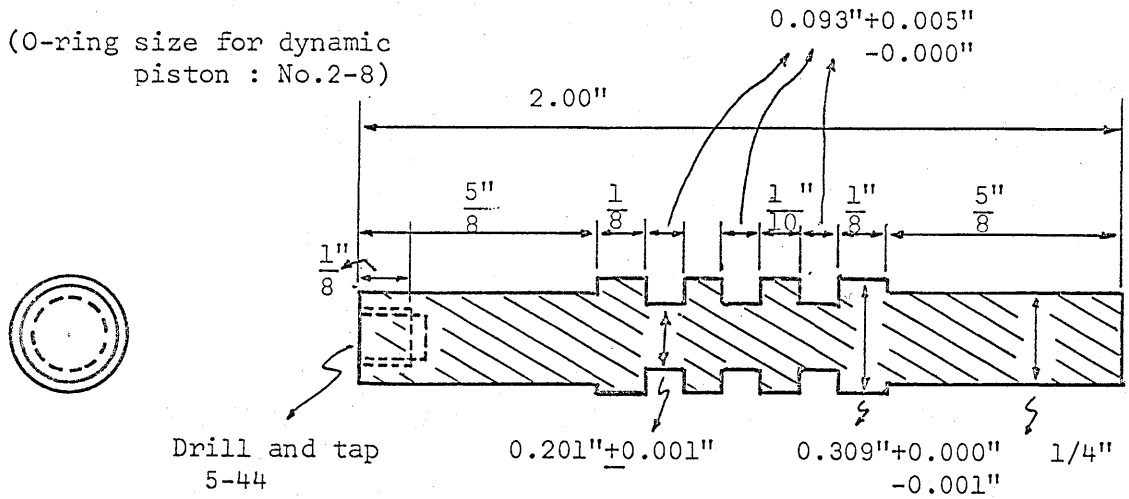

DYNAMIC O-RING SEALED PISTON

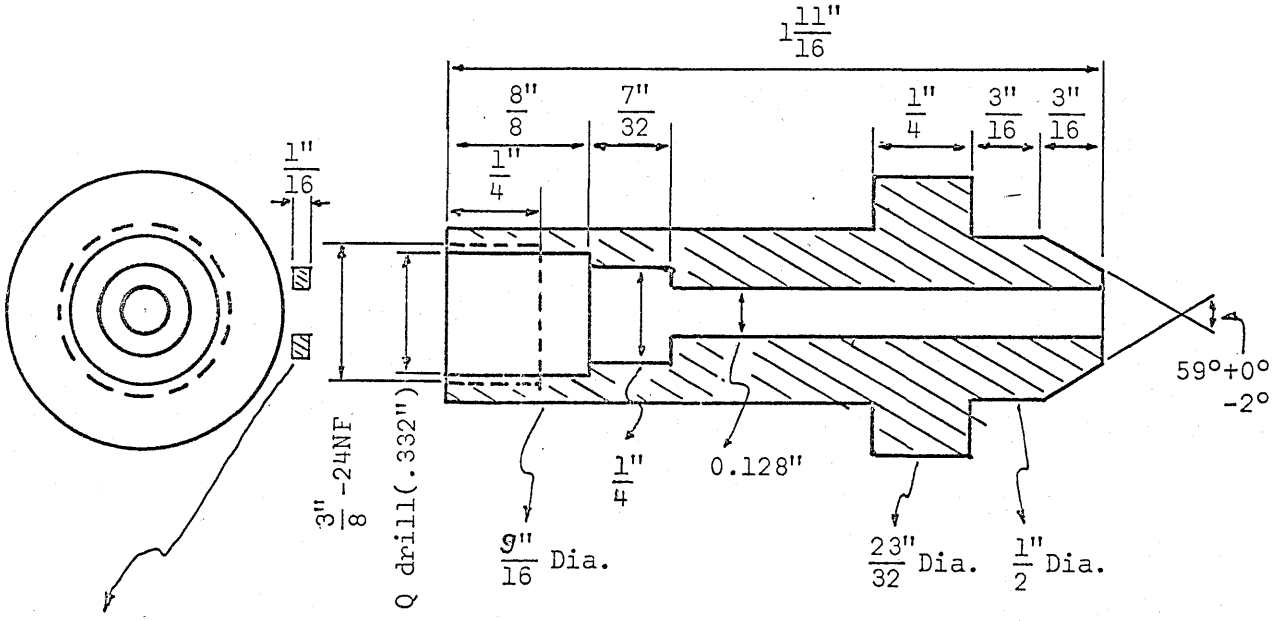

STUFFING BOX MODIFIED FROM AUTOCLAVE ENGINEERS' PLUS(Cat.No. CPX-90)

Figure S-6 Detailed Drawing of the Parts for the Modified Mass Injection Cylinder

Appendix T

Atmospheric Pressure Viscosities of Methane, Propane and Their Mixtures

Temp. °C.	Mole % Methane				
	0.0	22.1	50.0	75.3	100.0
0	73	77	84	91	101
-20	68	72	78	86	95
-40	62	66	72	79	89
-60	57	61	67	74	83
-80	51	55	60	67	76
-100	45	49	55	62	71
-120	40	44	49	56	64
-140	34	38	43	50	58
-150	31	35	40	47	55
-160	29	--	--	--	52
-170	--	--	--	--	49

Notes: (1) Viscosity data of methane are from Table VI-1.
(2) Viscosity data of propane were calculated from Sutherland equation (24).
(3) Viscosity data of mixtures were calculated from Equation (VII-2).

Appendix U

Physical Constants for Methane, Propane and the Mixtures of Methane and Propane used in the Correlations

	Mole % Methane				
	0.0	22.1	50.0	75.3	100.
Molecular weight	44.09	37.90	30.07	22.97	16.04
Critical temperature, T_c (°K)	370.	352.	319.	273.	191.
Critical pressure, P_c (psia)	617.	629.	645.	659.	673.
Critical density, ρ_c (g/cc)	0.220	0.213	0.201	0.185	0.162
Critical viscosity, μ_c (microp)	232	216	195	177	159
Atmospheric pressure viscosity at T_c, μ_{c_0} (microp)	100	--	--	--	76
ξ $(= T_c^{1/6}/(M^{1/2}P_c^{2/3}))$	0.0334	0.0354	0.0377	0.0415	0.0464

Notes: (1) The critical temperatures, pressures and densities for methane and propane are from Rossini, et al.(65).

(2) The critical temperatures for the mixtures are from Reamer, et al.(62).

(3) The critical pressures for the mixtures are the molar average values of those of the pure components.

(4) The critical densities for the mixtures were calculated(57) by,
$$\rho_{cm} = \sum_i^2 M_i X_i / \sum_i^2 X_i V_{ci}$$

(5) The critical viscosity for methane is from Uyehara and Watson (77) and that for propane is from Starling, et al.(72). while those for mixtures are the molar average values of those of pure components.

(6) The atmospheric viscosity at critical temperature was interpolated from the data shown in Appendix T.

(7) ξ's for pure components are available in the paper of Jossi, et al.(38).

(8) ξ's for mixtures were calculated by the method suggested by Dean and Stiel(21).